New Parameters for Beyond-Planar Graphs

Dissertation

der Mathematisch-Naturwissenschaftlichen Fakultät
der Eberhard Karls Universität Tübingen
zur Erlangung des Grades eines
Doktors der Naturwissenschaften
(Dr. rer. nat)

vorgelegt von
Thomas Schneck (M.Sc.)
aus Sindelfingen

Tübingen
2020

Gedruckt mit Genehmigung der Mathematisch-Naturwissenschaftlichen Fakultät der Eberhard Karls Universität Tübingen.

Tag der mündlichen Qualifikation:	19.10.2020
Stellvertretender Dekan:	Prof. Dr. József Fortágh
1. Berichterstatter:	Prof. Dr. Michael Kaufmann
2. Berichterstatter:	Prof. Dr. Klaus-Jörn Lange

Acknowledgements

Firstly, I would like to express my deepest gratitude to my supervisor Professor Michael Kaufmann, for the continuous guidance throughout my Ph.D study, the proof-reading of my Ph.D thesis, and very helpful comments to improve it.

I also would like to pay my special regards to my second adviser Professor Klaus-Jörn Lange, for reviewing my Ph.D thesis and being a member of my committee.

Moreover, I want to sincerely thank Professor Torsten Grust and Professor Andreas Geiger for being members of my committee, especially in this CORONA-influenced time.

I wish to whole-heartedly thank the current and former members of our team in Tübingen: Patrizio Angelini, Michalis Bekos, Henry Förster, Niklas Heinsohn, Axel Kuckuk, Maximilian Pfister and Lena Schlipf, for the great cooperation in research and teaching.

I would also like to thank all who worked with me on diverse research projects, especially Philipp Kindermann, Tamara Mchedlidze, and Antonios Symvonis, for working together on the few-segments which led to a publication in GD 2019, and Fabrizio Frati and Giordano Da Lozzo, for starting to work together with Henry and me on the 2-layer graphs during our visit in Rome.

Finally, I want to thank my family for supporting me during the process of writing this thesis and in my life in general.

Abstract

In der Geschichte der Graphtheorie sind Parameter nicht wegzudenken. Sie stellen wichtige Indikatoren für die Eigenschaften von Graphen und Graphzeichnungen dar. Außerdem sind sie oft ein Hauptkriterium für die Klassifikation von Graphen und für deren visuelle Wahrnehmung. In dieser Arbeit zeigen wir neue Resultate für die folgenden Graphparameter:

- Die Segmentkomplexität von Bäumen;
- die Zugehörigkeit von Graphen mit beschränktem Knotengrad zu bestimmten Graphklassen;
- die Zugehörigkeit von vollständigen und vollständig bipartiten Graphen zu bestimmten Graphklassen;
- die Kreuzungszahl von Graphen;
- die maximale Anzahl an Kanten in outer-gap-planaren Graphen und in bipartiten gap-planaren Graphen mit bestimmten Eigenschaften;
- die maximale Anzahl an Kanten in 2-Layer Graphen, sowie Beziehungen zwischen verschiedenen 2-Layer Graphklassen und Charakterisierungen für vollständige bipartite 2-Layer Graphen.

Abstract

Parameters for graphs appear frequently throughout the history of research in this field. They represent very important measures for the properties of graphs and graph drawings, and are often a main criterion for their classification and their aesthetic perception. In this direction, we provide new results for the following graph parameters:

– The segment complexity of trees;

– the membership of graphs of bounded vertex degree to certain graph classes;

– the maximal complete and complete bipartite graphs contained in certain graph classes beyond-planarity;

– the crossing number of graphs;

– edge densities for outer-gap-planar graphs and for bipartite gap-planar graphs with certain properties;

– edge densities and inclusion relationships for 2-layer graphs, as well as characterizations for complete bipartite graphs in the 2-layer setting.

Contents

Chapter 1

Introduction

The start of graph theory dates back to the 18th century, when Leonhard Euler published a paper which is considered as the first one in this field: His paper about the – nowadays – very famous Seven Bridges of Königsberg [37, 68]. Thereby he asked the question if all seven bridges of Königsberg[1] can be traversed exactly once; see Fig. 1.1 for an illustration. In fact, this problem can be stated in terms of graphs: The three land masses are represented by vertices and the bridges between them by edges; then the task is to find a path that contains every edge exactly once, a so-called Eulerian Path. In general, an Eulerian Path in a connected graph G exists if and only if exactly zero or two vertices in G have odd degree [68,85], where the degree of a vertex is the number of its neighbors. So, already in the early days of graph theory, parameters played an important role, in this case vertex degrees of a graph.

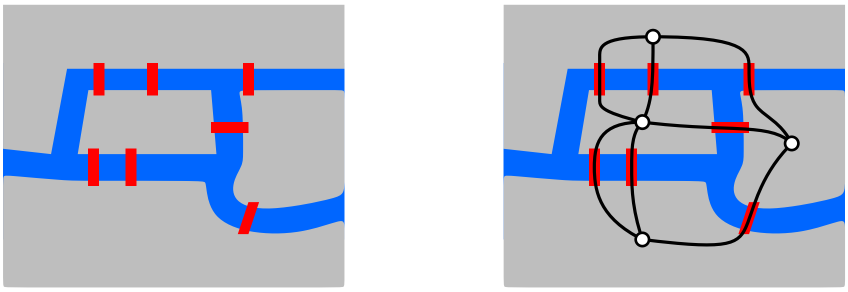

(a) (b)

Fig. 1.1: (a) The bridges of Königsberg. (b) The graph corresponding to the bridges of Königsberg.

The very same Leonhard Euler also discovered the relation between geometric entities in a crossing-free drawing of a connected graph, namely the formula $n-m+f=2$ for the number of vertices n, the number of edges m, and the number of faces[2] f [121]. A well-known consequence of this formula is an upper bound of $3n-6$ edges for planar graphs. For a collection of graphs with certain properties – a

[1]Today: Kaliningrad in Russia.
[2]A faces in a drawing is a region bounded by edges.

so-called graph class –, the edge density, i. e. the (tight) upper bound on the number of edges, usually is one of the first parameters that is searched for.[3] It provides a fast indicator for the affiliation of a graph to a certain graph class; namely, the compliance of the edge density is necessary for a graph to belong to a graph class.

Another famous historic problem of graph theory, which reaches back to 1852, is the one of coloring a map such that neighboring regions have different colors [104]; an example is depicted in Fig. 1.2. Thereby Francis Guthrie conjectured that four colors are always sufficient to solve this task. Early proofs for Guthrie's conjecture turned out to be incorrect [134]. On the other hand, in 1890 Heawood was able to show the five color theorem: Every map can be colored with at most five colors, such that neighboring regions receive different colors [83]. Surprisingly it took until 1976 and the assistance of a computer to prove the original four color theorem [20, 21].

The minimal number of colors needed to color the vertices of a graph such that adjacent vertices have different colors is called the chromatic number and represents a parameter for a graph class. Since any planar map is equivalent to a planar graph, where the regions correspond to vertices and two vertices are connected by an edge if the corresponding regions have a common border, the four color theorem states that the chromatic number of a planar graph is 4.

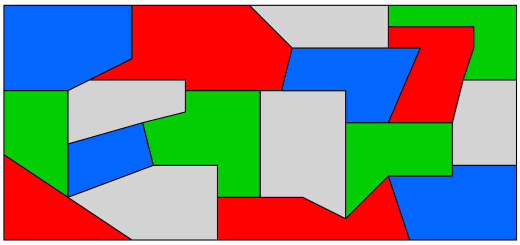

Fig. 1.2: Example for a map coloring with 4 colors, such that no two neighboring regions have the same color.

These historic examples already indicate the importance of parameters in graph theoretical questions. In general, such parameters help to understand better the structure, the properties, the benefits, and the limitations of graphs and graph classes. E. g. the number of crossings is an important measure for the aesthetic quality of a graph [117] and hence it is beneficial to draw graphs planar; on the other hand, the class of planar graphs is very restricted, since its members have not more than $3n-6$ edges, and, due to this fact, one may encounter a non-planar graph with high probability.

[3] For an overview of known edge densities see [61].

To overcome some disadvantages of planar graphs, other graph classes were defined. One of them is the class of k-planar graphs, where each edge is allowed to have at most k crossings [2, 40, 106, 108, 122]. This class plays the major role when proving lower bounds on the number of crossings for arbitrary drawings. Namely, the known upper bounds on the number of edges for k-planar graphs, where $k \leq 4$ [3, 106, 108, 122], are the key ingredient for showing the well-known Crossing Lemma [3,7,67,102], which in turn also provides an upper bound on the number of edges in k-planar graphs for $k > 4$ [3, 14]. Here parameters are used to derive other parameters, all of which are valuable for graph theory and graph drawing in their own right.

Compared to planar graphs, k-planar graphs have the advantage that, given a graph, a value k can be chosen such that this specific graph is k-planar. The downside is that drawings, where edges have many crossing, are not perceived very well. To this end, beside the k-planar graphs, several other graph classes were introduced; refer e g. to [5, 9, 30, 93, 140]. Since these classes allow edge crossings, they are called graphs beyond-planarity or beyond-planar graphs.

In order to decide to which classes a graph belongs to, or in which way a graph may be drawn such that its aesthetics are beneficial for the viewer, it helps to know many parameters for a graph class. In this spirit, we provide important parameters for several graph classes beyond-planarity.

We start by introducing notations and definitions for graph theory and graph drawing in Chapter 2.

Chapter 3 is dedicated to the so-called segment complexity. Thereby a segment consists of one or more consecutive edges, all of which are drawn as a straight-line segment in the plane. The goal is the minimize the number of segments used. In this way, edges may be easier to follow by the law of continuation of the Gestalt principles of perception [98], and the aesthetics may be influenced positively [96]. We specialize on the improvement of a result by Hültenschmidt et al. [89], who recently provided an algorithm to draw a tree on a grid with $\frac{3}{4}n$ segments and $\mathcal{O}(n^{3.58})$ area; more precisely, we improve the area bound to $n \times n$, while still using $\frac{3}{4}n$ segments. More details and references to previous works for this and the following chapters can be found in the introductory parts of the corresponding chapters.

In Chapter 4 the parameter "vertex degrees" is considered. Namely, we study graphs where the maximal vertex degree is bounded by a constant c (so-called graphs of maximum degree c, or short, graphs of degree c), and decide if graphs with this property always belong to certain graph classes or not. To answer this question in the positive, one usually needs to find an algorithm for drawing all graphs of degree c according to the rules in the considered graph class. On the other hand, this question can be answered in the negative if a graph of degree c is known that does not belong to a certain graph class. However, since for small values of c graphs of degree c are very sparse, it is usually not easy to construct such graphs and, in general, leads to large case analyses which often require some kind of graph enumeration.

Note that graph enumeration dates back to 1857, when the famous British mathematician Arthur Cayley consider the enumeration of trees [49]. Other important contributors to this field are for example Frank Harary [79, 81], Howard Redfield [119, 120] and George Pólya [114]. Nowadays there also exist various databases for graphs with certain properties [46, 110, 129], which can be accessed online (see e. g. `https://hog.grinvin.org/` which is presented in [46]).

We address an aspect of the enumeration issue in Chapter 5, where we provide an algorithm to enumerate all complete and complete bipartite graphs for certain graph classes. Thereby a graph with n vertices is complete if there is an edge between every pair of vertices; we denote complete graphs by K_n. A graph is bipartite if its edges can be partitioned in two disjoint sets, such that there are only edges between vertices of these two sets. A bipartite graph is complete if every vertex of the first set is connected to every vertex of the second set; we denote complete bipartite graphs by $K_{a,b}$, where a and b are the sizes of the two vertex sets. For the considered graph class, the goal of our enumeration is to find the largest n, such that K_n belongs to it, while K_{n+1} does not. Similarly, for bipartite graphs, we aim at finding the largest graphs $K_{a,b}$ that belong to a certain graph class.

A complete subgraph in a graph G is also denoted by a clique. The problem of finding the largest clique arises e. g. in questions regarding (social) networks [80,103], or when determining lower bounds for the chromatic number. Hence, the knowledge of complete graphs provides a valuable contribution to these fields. The same holds true for complete bipartite graphs, since bipartite graphs appear in many situations, from trees over (social) networks [26,138] and chemistry [51] to scheduling tasks [55, 90, 135], just to name some.

As already mentioned, the number of crossings in a drawing is an important measure for its aesthetic qualities [116]. Moreover it has many applications e. g. in combinatorial geometry [105, 107, 133] and Very Large-Scale Integration design [35,101,102]. So the lower bound on the number of crossings for each drawing of a graph, described by the Crossing Lemma [3,7,67,102], is an important parameter in graph drawing. In Chapter 6, we generalize the well-known Crossing Lemma to a Meta Theorem. More precisely, we show that the number of crossings in a graph G with properties $\mathcal{P}$ (such a property is e. g. "bipartite") is lower bounded by $c\frac{m^3}{n^2}$. Thereby n and m are the number of vertices and edges of G, and c is a constant that depends on the maximal number of edges in k-planar graphs (for small values of k) with properties $\mathcal{P}$. Moreover, from our Meta Crossing Theorem we deduce Meta Theorems for edge density bounds of k-planar and k-gap-planar graphs (where the graphs also have properties $\mathcal{P}$). Finally we show how to apply the Meta Theorems to outer-k-planar graphs and to bipartite k-gap-planar graphs, and also provide some additional edge density results for 1-gap-planar graphs.

A special drawing paradigm for a bipartite graph is the drawing of its vertices on several parallel lines. This approach and a corresponding drawing algorithm was first introduced by Sugiyama [131] and is beneficial for the perception of bipartite graphs. Various subsequent works considered the crossing minimization of layered graphs [65, 91, 136]. In Chapter 7 we focus on graphs that can be drawn on two parallel lines, such that the edges are represented by monotonic curves between them (so-called 2-layer graph). This drawing style is also one of the main parts in Sugiyama's drawing algorithm and has recently been studied for RAC-graphs [56] and fan-planar graphs [38]. We provide upper bounds on the number of edges for several graph classes, apply the generalized Crossing Lemma of Chapter 6 to 2-layer k-planar graphs, and study the relationships between different 2-layer graph classes.

Finally we summarize our findings in Chapter 8.

Chapter 2

Definitions

In this chapter we introduce vocabulary of graph theory and graph drawing that is used throughout this work.

2.1 Graphs and Drawings

A *graph* $G = (V, E)$ consists of a set of *vertices* V and a set of *edges* $E \subseteq V \times V$, where $e \in E$ is a tuple of vertices, that is $e = (u, v)$ for some $u, v \in V$; thereby the vertices u and v are called *end vertices* of e. The vertex set V is also denoted by $V(G)$ or V_G, and the edge set by $E(G)$ or E_G.

The graph G is called a *directed* graph if (u, v) and (v, u) are considered to be different, otherwise G is called *undirected*[1]. Throughout this work, we study only undirected graphs and just call them “graphs”, omitting the word “undirected”.

A graph is *simple* if it has at most one edge between each pair of vertices (“no parallel edges”) and no self-loops, i. e. E contains no edge (u, u) for some vertex $u \in V$. Otherwise G is called *multi-graph*. Observe that a simple graph with n vertices has at most $\frac{1}{2}n(n-1)$ edges.

For an edge $e = (u, v) \in E$ we say that v is a *neighbor* of u, v is *connected* to u, or v is *adjacent* to u; further we call u (and v) *incident* to e. Two edges are *adjacent* if they share a common end vertex. The *degree* $\deg(v)$ of a vertex $v \in V$ is the number of vertices adjacent to it.

A *drawing* Γ of a graph in the plane $\mathbb{R}^2$ is defined as follows: Every vertex $v \in V$ is mapped to a point p_v in the plane; every edge $e = (u, v)$ is drawn as a Jordan curve J_e connecting the points p_u and p_v in the plane. In the following we refer to p_v simply by v and to J_e by e.

[1] In the literature, the notation $e = \{u, v\}$ is often used for undirected edges.

A drawing is called *simple*[2], if no edge crosses itself (referred to as “self-crossing”), and each pair of distinct edges have at most one point in common; i. e. they have either one single crossing or one single common endpoint.

An edge that does not cross any other edge is called *crossing-free* or *planar*. The drawing Γ is *planar* if all its edges are planar; the graph G is *planar* if a planar drawing for G exists. In a planar drawing, each area delimited by edges is a *face*; the edges delimiting a face f are *incident* to f. Note that each edge is incident to two (not necessarily distinct) faces. We call the unbounded face the *outer face* of Γ (refer to Fig. 2.1a).

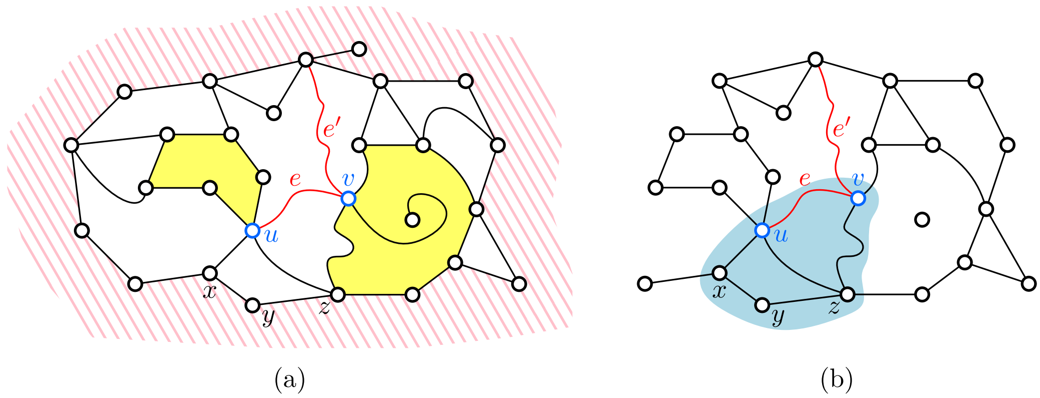

Fig. 2.1: (a) A drawing Γ of a graph. The vertices u and v are adjacent, as well as the edges e and e'. The vertices u and v are incident to e. The two yellow regions are examples for faces in Γ. The outer face of Γ is indicated by the bright red area. (b) A subdrawing of Γ. The highlighted blue part illustrates an induced subdrawing of $\{u, v, x, y, z\}$.

A *subgraph* $H = (V_H, E_H)$ of G is a graph with $V_H \subseteq V$ and $E_H \subseteq E$ such that $E_H \subseteq V_H \times V_H$. For $V' \subseteq V$, the *induced subgraph* $G[V']$ is the subgraph H of G with $V_H = V'$ and $E_H = \{(u, v) \in E \mid u \in V' \text{ and } v \in V'\}$. A *subdrawing* Γ_H of Γ is the part of the drawing Γ that consists of vertices V_H and edges E_H for some subgraph H of G. An *induced subdrawing* $\Gamma[V']$ is a subdrawing for an induced subgraph $G[H']$ (for an illustration see Fig. 2.1b).

If H is a subgraph of G, we call G an *augmentation* of H; similarly, we call Γ an *augmentation* of Γ' if Γ' is a subdrawing of Γ.

A *matching* is a set of edges $E' \subseteq E$, such that no two edges of E' share a common end vertex. Two edges $e_1, e_2 \in E$ are *independent* if the set $\{e_1, e_2\}$ is a matching, or, in other words if e_1 and e_2 are not adjacent.

In a graph $G = (V, E)$, we call $p = (v_0, v_1, \ldots, v_t)$ a *path* of length t if $(v_{i-1}, v_i) \in E$ for all $1 \leq i \leq t$. Note that a single vertex is a path of length 0, and a single edge

[2]In the literature, “simple drawings” are also called “good drawings”, see e. g. [97].

is a path of length 1. For $t \geq 1$ the tuple $c = (v_1, \dots, v_t, v_1)$ is a *cycle* of size t if $(v_1, \dots, v_t)$ is a path of length $t-1$, and additionally $(v_t, v_1) \in E$.

Let $n = |V|$ be the number of vertices in G. A *Hamiltonian cycle* is a cycle $c = (v_1, \dots, v_n, v_1)$, such that the vertices $v_1, \dots, v_n$ are pairwise distinct; that is, cycle c contains all vertices of G. The graph G is called *Hamiltonian* if it contains a Hamiltonian cycle.

We call G *connected* if for every pair $u, v \in V$ there exists a path p between u and v; e. g. a Hamiltonian graph is connected. Otherwise G is *disconnected*. A *connected component* of G is an induced subgraph $G[V']$ of G such that $G[V']$ is connected, and for every vertex $v \in V \setminus V'$ (if any) the subgraph $G[V' \cup \{v\}]$ is disconnected (for an illustration of connected components refer to Fig. 2.2). In other words: In a connected component of G, every pair of vertices is connected by a path.

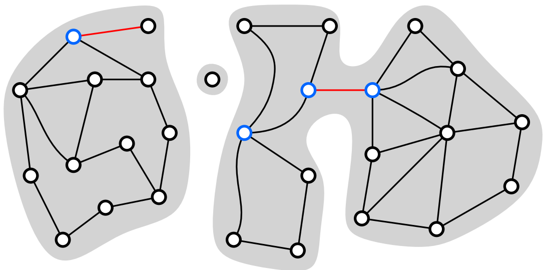

Fig. 2.2: Illustration of the connected components (gray) of a graph. The cut vertices are blue and the bridges are red.

The graph G is called *biconnected* (or 2-connected) if $G[V \setminus \{v\}]$ is connected for every vertex $v \in V$. More generally, G is *k-connected* if $G[V \setminus \{v_1, \dots, v_k\}]$ is connected for every $\{v_1, \dots, v_k\} \subseteq V$.

Let $H = (V_H, E_H)$ be a connected component of a graph G. Then $v \in V_H$ is a *cut vertex* of G if $H[V_H \setminus \{v\}]$ is disconnected. An edge $e \in E_H$ is called a *bridge* in G if $H \setminus \{e\}$ is disconnected. Note that biconnected graphs have neither cut vertices nor bridges.

2.2 Special Types of Graphs

Usually it is (almost) impossible to derive algorithms or certain parameters for general graphs. However, if we impose more restrictions on graphs, that is, if we consider graphs with special properties, it becomes possible to do so. In the following we give some classes of graphs which are defined solely on the graph itself, in contrast to Secs. 2.3 and 2.7, where the existence of certain drawings indicate that a graph belongs to a class.

We already know paths and cycles. The two terms induce the classes of *path-graphs* and *cycle-graphs*, which consist of graphs that are paths, and graphs that are cycles, respectively.

A well studied class of graphs are the so-called trees. Thereby a *tree* is a connected graph which contains no cycle (illustrated in Fig. 2.3a). On the other hand, if a graph is disconnected and has no cycles, then it is called a *forest*. In this case the connected components are trees. Since a path-graph contains no cycles, it belongs to the class of trees.

The definition for a *pseudo-tree* is very similar to the one of a tree. The only difference is that in a pseudo-tree at most one cycle is allowed (see e. g. Fig. 2.3b). So the trees and the cycle-graphs form subclasses of the class of pseudo-trees. Corresponding to a forest for trees, a *pseudo-forest* is a graph such that all its components are pseudo-trees.

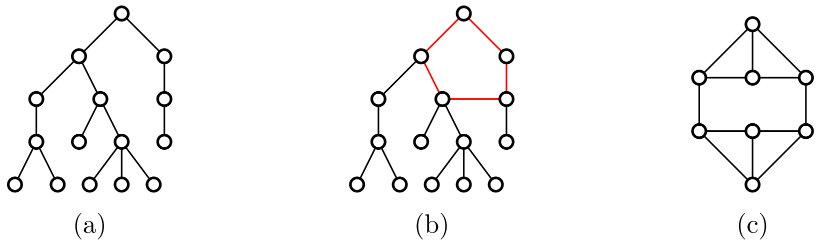

Fig. 2.3: Drawings for: (a) A tree; (b) a pseudo-tree (the cycle is red); (c) a 3-regular graph.

For some $d \geq 0$, we call a graph *d-regular* if each of its vertices has degree d. For example, a 0-regular graph consists of a set of vertices and no edges, a 1-regular graph is a matching, and a 2-regular graph consists of a set of cycles. The 3-regular graphs are also called *cubic graphs* (illustrated in Fig. 2.3c).

A simple $(n-1)$-regular graph is called *complete*; that is, in a complete graph each pair of distinct vertices is connected by exactly one edge. We denote complete graphs with n vertices by K_n (see Fig. 2.4a for an illustration of K_3 and K_4). Note that the number of edges in a d-regular graph is $\frac{1}{2}dn$, and hence, a complete graph has exactly $\frac{1}{2}n(n-1)$ edges. For $n = 3$ a complete graph is also called a *triangle*.

For a graph G, consider an induced subgraph H with k vertices. A complete subgraph H is also called a *clique of size k* or a *k-clique*. On the other hand, if H is 0-regular (that is, there are no edges between its vertices), then H is an *independent set of size k* (for an illustration see Fig. 2.4b). The size of the largest clique in G, referred to as *clique number*, is denoted by $\omega(G)$, and the size of a maximal independent set is denoted by $\alpha(G)$. It is not difficult to observe that $\omega(G) = \alpha(\overline{G})$, where $\overline{G} = (V, \{(u,v) \in V^2 \mid u \neq v \text{ and } (u,v) \notin E\})$ is the *complement* of G.

For example the real world problem of finding k mutually friends in social networks translates into the problem of finding a k-clique in a graph.[3]

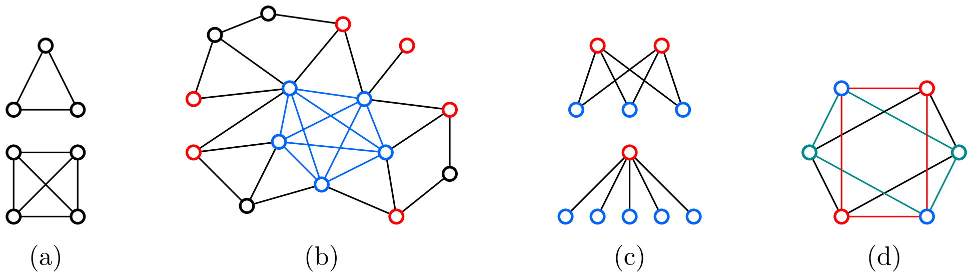

Fig. 2.4: (a) The complete graphs K_3 and K_4. (b) A graph with a 5-clique (blue) and an independent set of size 6 (red). (c) The complete bipartite graph $K_{2,3}$ and the star $K_{1,5}$; the two independent parts are indicated by different colors. (d) The complete 3-partite graph $K_{2,2,2}$.

A graph $G = (V, E)$ is *bipartite* if V can be split into two disjoint sets $U, W \subseteq V$, such that $E \subseteq \{(u, w) \mid u \in U \text{ and } w \in W\}$. In particular, there are no edges between two vertices of U, and no edges between two vertices of W; hence, U and W are independent sets. When considering bipartite graphs, we refer to U and W as the *independent parts* or *independent sets* of G. Allocation problems are a typical example for a field where bipartite graphs appear, e. g. in the assignment of teachers to classes, where the set of all teachers and the set of all classes are the two independent parts.

Graph G is called *complete bipartite* if $E = \{(u, w) \mid u \in U \text{ and } w \in W\}$. A complete bipartite graph with $a = |U|$ and $b = |W|$ has exactly $a \cdot b$ edges and is denoted by $K_{a,b}$. Complete bipartite graphs $K_{1,b}$ are called *stars* (see Fig. 2.4c). An important characterization of bipartite graphs is the following (see e. g. [27]): A graph is bipartite if and only if all its cycles have even length.

Bipartite graphs are generalized by the so-called *k-partite (multipartite)* graphs, where V can be split into k disjoint independent sets $U_1, \ldots, U_k$. For 3-partite graph also the term *tripartite* is commonly used. If G has the maximal number of edges, i. e. there is an edge (u_i, u_j) in G for every $u_i \in U_i$ and $u_j \in U_j$ where $i \neq j$, then G is *complete k-partite*. A complete k-partite graph with $a_i = |U_i|$ has exactly $a_1 a_2 \cdots a_k$ edges and is denoted by $K_{a_1,\ldots,a_k}$.

[3] Note that most variants of the clique problem are $\mathcal{NP}$-hard.

2.3 Special Types of Drawings

Recall from school that a *(straight) line* is a curve whose coordinate points (x, y) satisfy $y = ax + b$ for some constants $a, b \in \mathbb{R}$. Further, a *segment* is a part of a line such that $y = ax + b$ holds for $x \in [\ell, r]$, where $\ell, r \in \mathbb{R}$ are constants. In a *straight-line drawing* Γ, every edge is represented by a segment (for example, the drawing in Fig. 2.4b represents a straight-line drawing). On the other hand, if every edge consists of at most $(k + 1)$ segments, such that consecutive segments have different slopes, then Γ is called a *k-bend drawing* (illustrated in Fig. 2.5a).

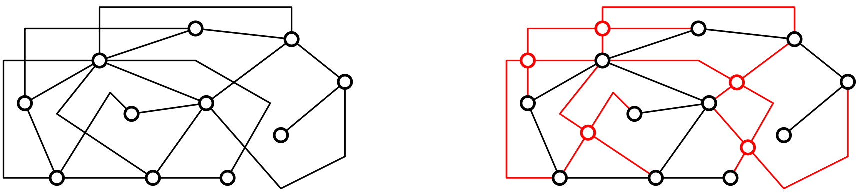

(a) (b)

Fig. 2.5: (a) A 2-bend drawing Γ. (b) The planarization Γ_p of drawing Γ from Fig. 2.5a. Real vertices and edges that are also in Γ are black. Dummy vertices and edges incident to them are red.

Let Γ be a non-planar drawing. The *planarization* Γ_p of Γ is defined as follows (see also Fig. 2.5b):

- The vertices of Γ_p are the vertices of Γ together with the crossing points of Γ. A crossing point is called a *dummy vertex* or a *crossing (vertex)*; a vertex of Γ is called a *real vertex*.
- The edges of Γ_p are the planar edges of Γ, as well as the planar edge parts between real vertices and dummy vertices, and the planar edge parts between two dummy vertices in Γ_p.

The *faces* in Γ are defined as the faces of the planarization Γ_p; the outer face of Γ is the outer face of Γ_p.

An *outerplanar drawing* is a planar drawing where all vertices lie on the boundary of the outer face (see Fig. 2.6a). For a non-planar drawing Γ we say that Γ is outerplanar if the corresponding planarization Γ_p is outerplanar. A graph is outerplanar if it has an outerplanar drawing.

A *2-layer drawing* is a drawing where all vertices are placed on two parallel lines (usually the lines are horizontally); the edges are usually drawn as straight lines between vertices of the two layers[4] (see Fig. 2.6b). Thus a 2-layer drawing is necessarily bipartite. Note that all vertices of a 2-layer drawing are on the outer face, hence such a drawing is outerplanar.

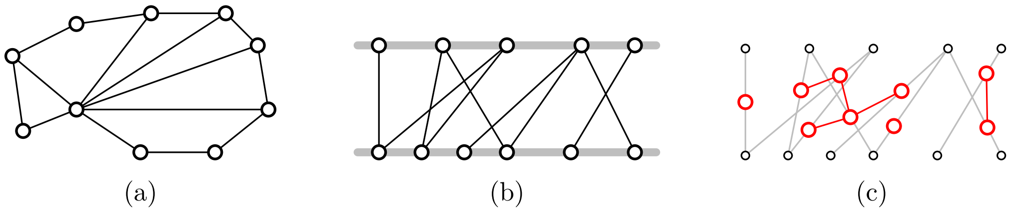

Fig. 2.6: (a) An outerplanar drawing. (b) A 2-layer drawing Γ. (c) A drawing of the crossing graph $X(\Gamma)$ in red, where Γ is the drawing in Fig. 2.6b.

We conclude this section by three special types of graphs, which, in fact, are not drawings, but defined by drawings.

For a drawing Γ, the *crossing graph* $X = X(\Gamma) = (V_X, E_X)$ consists of the following vertices and edges (refer also to Fig. 2.6c):

- The vertices V_X of X are the edges E of Γ, that is, $V_X = E$;
- if two edges $e_1, e_2 \in E$ cross each other in Γ, then (e_1, e_2) is an edge in X, that is, $(e_1, e_2) \in E_X$ if and only if e_1 and e_2 cross in Γ.

The second type of graphs we want to introduce are the permutation graphs. Permutation graphs were first introduced in [70, 113] and defined as follows. Let $\pi = (\pi_1, \ldots, \pi_N)$ be a permutation of the set $\{1, \ldots, N\}$ for some $N \geq 1$, that is $\pi(i) = \pi_i$ for $i = 1, \ldots, N$, and $\{\pi_1, \ldots, \pi_N\} = \{1, \ldots, N\}$. Further let Γ_π be the drawing consisting of line segments L_i with endpoints $(i, 1)$ and $(\pi_i, 0)$, where $1 \leq i \leq N$. Then the *permutation graph* $G_\pi = (V_\pi, E_\pi)$ is defined as the crossing graph of Γ_π: the vertex set is $V_\pi = \{L_1, \ldots, L_N\}$, and, for $i \neq j$, the edge (L_i, L_j) belongs to E_π if and only if L_i and L_j cross in Γ_π. Figure 2.7 shows an example for a permutation graph with $N = 6$ vertices.

The last graph type we introduce in this section is the so-called dual graph of a planar drawing Γ. The *dual graph* $D = D(\Gamma) = (V_D, E_D)$ is defined as follows (for an illustration see Fig. 2.8):

- The vertices V_D of D are the faces of Γ;
- for every edge (u, v) in Γ there is an edge (f_1, f_2) in V_E, where f_1 and f_2 are the two (not necessarily distinct) faces incident to (u, v).

[4]For horizontal layers, it suffices to assume that the edges are y-monotonic curves between the two layers; otherwise the edges are monotonic with respect to the direction perpendicular to the two lines.

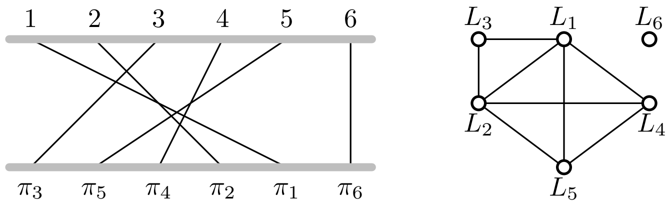

Fig. 2.7: Left: A drawing Γ_π, where the permutation is given by $\pi = (5, 4, 1, 3, 2, 6)$. The lines L_i are numbered according to the order of the end point $(i, 1)$ (top line). Right: The corresponding permutation graph.

Note that $D(\Gamma)$ is in general not a simple graph, since it may contain self-loops and multiple edges. If Γ is not planar, we define the dual graph of Γ as the dual graph of the planarization of Γ.

(a) (b)

Fig. 2.8: (a) A drawing and (b) an illustration of its corresponding dual graph.

2.4 Embeddings

A single graph can be represented by infinitely many drawings, even by drawings that have the same properties. For example, all drawings of Fig. 2.9 are planar drawings of the same graph. However, in the drawing of Fig. 2.9d, the vertex v_3 belongs to a different face as in the other three drawings and hence the order of the vertices around v_2 is different; namely, the vertices in clockwise order are v_1, v_6, v_5, v_3, while the corresponding order in the other drawings is v_1, v_3, v_6, v_5. This gives rise to the following definition.

A *rotation system* is the order in which incident edges appear around each vertex in a drawing Γ. Further, a *coarse embedding* of a graph G is an equivalence class which contains all drawings of G that have the same rotation system, and where each edge is crossed by the same edges. In this sense the drawings of Figs. 2.9a to 2.9c are all representatives of the same coarse embedding, while Fig. 2.9d represents another coarse embedding of the same graph.

We define a *(fine) embedding* by the drawings that belong to the same equivalence class: Let Γ_1 and Γ_2 be two drawings of a graph G that represent the same coarse

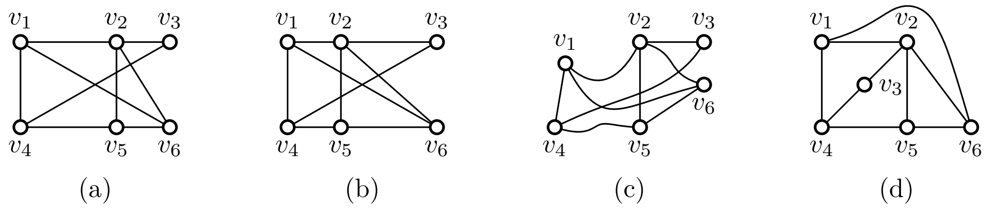

Fig. 2.9: Several drawings of the same graph. The non-planar drawings in (a), (b) and (c) represent the same coarse embedding; in contrast, the drawing in (d) is planar, yielding a different coarse embedding.

embedding. Then Γ_1 and Γ_2 are representatives of the same (fine) embedding if for every edge $e \in G$ the order of the edges that cross e is the same in Γ_1 and Γ_2. If this is the case, Γ_1 and Γ_2 are called *equivalent* (e. g. the drawings in Fig. 2.9a and Fig. 2.9c are equivalent). Note that, in the planarizations of equivalent drawings Γ_1 and Γ_2, the order of incident edges around each (dummy and real) vertex is the same; hence two drawings are equivalent if and only if their planarizations have the same rotation system.[5]

Each equivalence class for coarse embeddings might contain several equivalence classes regarding fine embeddings. Therefore two drawings that are not equivalent (regarding fine embeddings) can represent the same coarse embedding; refer to Fig. 2.10 for an example.

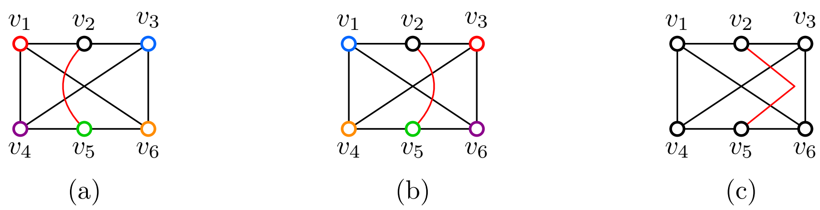

Fig. 2.10: Several drawings of the same graph. In (a) and (b) the edge (v_2, v_5) is crossed by the same two edges, but in a different order, hence the drawings are not equivalent. On the other hand, the drawings in (b) and (c) are equivalent. Although the drawings of (a) and (b) are not equivalent, they are isomorphic, as the mapping indicated by the vertex colors show.

In the following we consider only fine embeddings (if not stated otherwise) and call them just embeddings. Further, for an embedding D with drawing Γ, we call the planarization of Γ *a planarization* of D. An embedding is *simple* if one of its representative drawings is simple (which implies that all drawings representing the considered embedding are simple by the definition of a fine embedding).

Let D_1 and D_2 be embeddings of the same connected graph G. Then D_1 and D_2 are *isomorphic* if there exists a bijective mapping f of their vertices such that

[5]For a planar drawing, fine and coarse embeddings coincide, since all its edges are crossing-free.

$D_1' = D_2$, where D_1' is the embedding obtained by applying f to the vertex set of D_1. Two drawings Γ_1 and Γ_2 are *isomorphic* if the embeddings they represent are isomorphic; that is, if and only if the planarizations of Γ_1 and Γ_2 are equivalent after relabeling vertices, edges, and faces of Γ_1. If no such relabeling exists, then Γ_1 and Γ_2 are called *non-isomorphic*. For example, the drawings in Figs. 2.10a and 2.10b, which are not equivalent, are isomorphic; the corresponding mapping is indicated by the different colors of the vertices.

2.5 The Crossing Number

Let $cr(\Gamma)$ be the number of crossings in a drawing Γ of G. Then the *crossing number* $cr(G)$ of G is the minimal value of $cr(\Gamma)$ over all drawings Γ of G, that is,

$$cr(G) := \min\{cr(\Gamma) \mid \Gamma \text{ is a drawing of } G\}.$$

For complete graphs K_n the bound

$$cr(K_n) \leq \frac{1}{4} \cdot \left\lfloor \frac{n}{2} \right\rfloor \cdot \left\lfloor \frac{n-1}{2} \right\rfloor \cdot \left\lfloor \frac{n-2}{2} \right\rfloor \cdot \left\lfloor \frac{n-3}{2} \right\rfloor$$

holds [75], while for complete bipartite graphs $K_{a,b}$ the upper bound

$$cr(K_{a,b}) \leq \left\lfloor \frac{a}{2} \right\rfloor \cdot \left\lfloor \frac{a-1}{2} \right\rfloor \cdot \left\lfloor \frac{b}{2} \right\rfloor \cdot \left\lfloor \frac{b-1}{2} \right\rfloor$$

is known [139]. The conjecture is that these bounds are tight, that is, the inequalities are conjectured to be in fact equalities. This was proven for some special cases, but is still open in the general case [74, 75, 123].

Regarding general graphs, the lower bound for the crossing number is $c\frac{m^3}{n^2}$, where c is a constant [67]. Currently the best value for c is $\frac{1}{29}$ [3].

2.6 The Chromatic Number

Let $G = (V, E)$ be a graph, $t \geq 1$ a positive integer and $c_1, \ldots, c_t$ colors. A *(vertex) coloring* of G is a mapping $\mathbf{c} : V \longrightarrow \{c_1, \ldots, c_t\}$, such that adjacent vertices are mapped to different colors; that is, $\mathbf{c}(u) \neq \mathbf{c}(v)$ for each $(u, v) \in E$ (see Fig. 2.11 for an illustration).

If the mapping $\mathbf{c}$ is surjective, i. e. if $\mathbf{c}^{-1}(c_j) \neq \emptyset$ for every j (at least one vertex has color j), then $\mathbf{c}$ is called a *t-coloring* and G is called *t-colorable*. The *(vertex)*

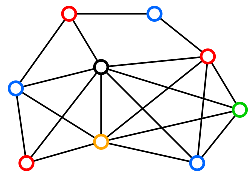

Fig. 2.11: A coloring of a graph with 5 different colors.

chromatic number $\chi = \chi(G)$ of G is the minimal number of colors needed in any coloring of G. One observation is that a graph is bipartite if and only if it has chromatic number $\chi = 2$ [27]; this implies e. g. that every tree and every cycle-graph with a cycle of even length is 2-colorable. Another important observation is that, for every graph G, the clique number $\omega(G)$ is a lower bound for $\chi(G)$.

Corresponding to a vertex coloring, an *edge coloring* is usually defined as a mapping $\mathbf{c} : E \longrightarrow \{c_1, \ldots, c_t\}$, such that adjacent edges are mapped to different colors. The *edge chromatic number* $\chi_e = \chi_e(G)$ of G is the minimal number of colors needed in any edge coloring of G.

However, the concept of an edge coloring can be transformed into a vertex coloring by the following construction: Let $G' = (V', E')$, where $V' := E$ and $(e_1, e_2) \in E'$ if and only if e_1 and e_2 have a common endpoint in G. Then an edge coloring of G corresponds to a vertex coloring of G'. For this reason edge colorings are usually not considered in the literature.

We want to use the term "edge coloring" for a different situation. Let Γ be a drawing of G. For us, an *edge coloring* is a mapping $\mathbf{c} : E \longrightarrow \{c_1, \ldots, c_t\}$, such that $\mathbf{c}(e_1) \neq \mathbf{c}(e_2)$ if e_1 and e_2 cross in Γ. That is, an edge coloring corresponds to a vertex coloring in the crossing graph X of Γ, and the edge chromatic number of Γ corresponds the the chromatic number of X.

We conclude this section with a class of graphs that are defined by the chromatic number and the clique number. Namely, a graph G is called *perfect* if its chromatic number χ equals its clique number ω. Examples for perfect graphs are complete graphs (for $G = K_n$ we have obviously $\omega(G) = n = \chi(G)$), bipartite graphs (where $\omega = \chi = 2$), and permutation graphs [70].

2.7 Graph Classes

Recall that a drawing Γ is planar if it has no crossings, and a graph G is planar if a planar drawing of G exists. A planar drawing Γ is *maximal* if no edge can be added to Γ without violating planarity; in this case Γ is called a *triangulation*, since all its faces are bounded by exactly three edges (see e. g. Fig. 2.12).

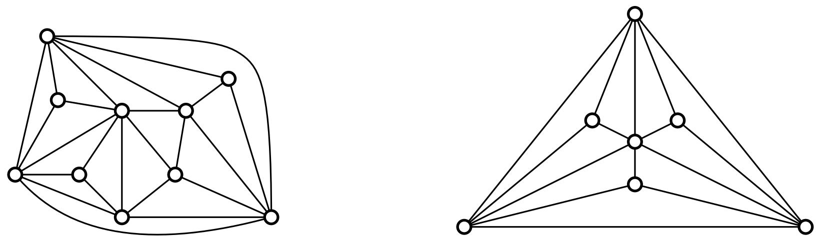

(a) (b)

Fig. 2.12: Two triangulations. The triangulation in (b) is a straight-line drawing.

As a consequence of Euler's formula[6], a maximal planar drawing Γ has $3n - 6$ edges, where n is the number of vertices of Γ. Thus, the number of edges in planar graphs is upper bounded by $3n - 6$ and, since every triangulation reaches this upper bound, it is a tight upper bound. We refer to the maximal number of edges in a class of graphs also as *edge density* of this class.

Apart from the class of planar graphs, there exist many more interesting graph classes. In the following we explain some of them, namely the ones which we study in this work, together with their edge density bounds. In contrast to planar graphs, these classes allow a graph to have crossings, and are hence "more than planar", or "graph classes beyond planarity"; see e. g. [61, 87].

We start with a natural generalization of planar graphs. For $k \geq 1$ a drawing is called *k-planar* [2, 40, 106, 108, 122] if each of its edges has at most k crossings; a graph is k-planar if it has a k-planar drawing[7]; refer to Fig. 2.13a. The general edge density for k-planar graphs is $3.81\sqrt{k}n$ [3]. However, for $k \leq 4$ there exist better upper bounds on the number of edges, namely $4n-8$ edges for 1-planar graphs [122], $5n - 10$ edges for 2-planar graphs [108], $\frac{11}{2}n - 11$ edges for 3-planar graphs [106], and $6n - 12$ edges for 4-planar graphs [3].

For the definition of the next two graph classes, assume that Γ contains two pairs of crossing edges $E_1 := \{(u_1, u_2), (v_1, v_2)\}$ and $E_2 := \{(w_1, w_2), (z_1, z_2)\}$. Let $V' := \{u_1, u_2, v_1, v_2\} \cap \{w_1, w_2, z_1, z_2\}$ be the set of their common endpoints. A drawing is *IC-planar* [9, 141] (IC is short for "independent crossing") if V' is empty (refer to Fig. 2.13b), and *NIC-planar* [140] (NIC is short for "nearly independent crossing"), if V' contains at most one vertex (refer to Fig. 2.13c). In other words, no two pairs of crossing edges share an end vertex in an IC-planar drawing; two pairs of crossing edges share at most one end vertex in NIC-planar drawings. By definition, every IC-planar drawing is NIC-planar, while every NIC-planar drawing is 1-planar.

[6]Euler's formula states that $n - m + f = 2$ holds in connected planar drawings, where n, m and f are the numbers of vertices, edges and faces, respectively; refer e. g. to [121].

[7]Note that we always declare a graph as belonging to a certain graph class by the existence of a drawing with corresponding properties.

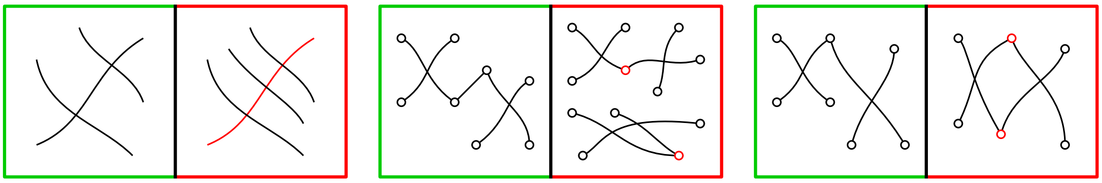

(a) 2-planar (b) IC-planar (c) NIC-planar

Fig. 2.13: Allowed (green box) and forbidden (red box) configurations in (a) 2-planar drawings; the red edge has 3 crossings, which violates 2-planarity. (b) IC-planar drawings; the red vertices are shared by two pairs of crossing edges. (c) NIC-planar drawings; the two red vertices are shared by the same pair of crossing edges.

The maximal number of edges in IC- and NIC-planar graphs is $\frac{13}{4}n - 6$ [141] and $\frac{18}{5}n - \frac{36}{5}$ [140], respectively.

For $k \geq 3$, a drawing is called *k-quasi-planar* [4, 5, 71] if it contains no k mutually crossing edges; refer to Fig. 2.14a. It is known that 3-quasi-planar graphs, also referred to as quasi-planar graphs, have an edge density of $\frac{13}{2}n - 20$ [4].

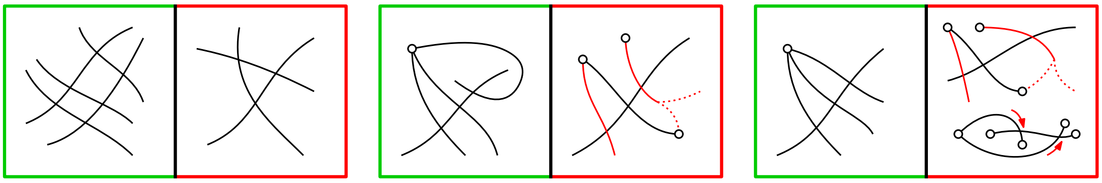

(a) quasi-planar (b) fan-crossing (c) fan-planar

Fig. 2.14: Allowed (green box) and forbidden (red box) configurations in (a) quasi-planar drawings. (b) fan-crossing drawings; the red edges are independent. (c) fan-planar drawings; the red edges are independent; the red arrows indicate a crossing of an edge from different sides.

A *fan* is a set of edges which are all incident to the same vertex. Recall that two edges are independent if they share no common endpoint. We say that a drawing Γ is *fan-crossing* [43, 44] if each edge in Γ crosses no two independent edges, i. e. an edge in Γ may either be planar, or cross a single edge, or cross a fan; refer to Fig. 2.14b.

If for every edge, that is crossed by more than one edge, it also holds that the crossings are from the same “side”, then Γ is *fan-planar* [32, 38, 39, 93]; refer to Fig. 2.14c. Although the fan-planar graphs are a subclass of the class of fan-crossing graphs, both classes have the same tight edge density of $5n - 10$ [43, 93].

In a sense complementary to the fan-crossing graphs are the fan-crossing free graphs. Thereby a drawing is *fan-crossing free* [44, 50] if no edge crosses a fan, that is, every edge may only cross independent edges; refer to Fig. 2.15a. The maximal number of edges in fan-crossing free graphs is $4n - 8$ [50].

Let C be the set of crossings of a drawing Γ with edge set E. For $k \geq 1$, we call a drawing Γ *k-gap-planar* [30] if a mapping $f : C \longrightarrow E$ exists, such that the inverse image $f^{-1}(e)$ of every $e \in E$ contains at most k crossings; that is, each crossing is mapped to an edge such that each edge has at most k crossings mapped to it; refer to Fig. 2.15b. We call the crossings that are mapped to an edge also *gaps* and draw them as gaps in Γ to enhance the readability of Γ. The edge density of 1-gap-planar graphs – often just called gap-planar graphs – is known to be $5n - 10$ [30].

Bae et al. [30] showed that a drawing Γ is k-gap-planar if and only if the number of edges in every induced subgraph $\Gamma[E']$, where $E' \subseteq E$, contains at most $k|E'|$ crossings. Moreover, they observed that a graph is k-gap-planar, if and only if it allows a drawing whose crossing graph can be covered by at most k pseudoforests. For gap-planar graphs this means that a graph is gap-planar, if and only if it allows a drawing whose crossing graph is a pseudoforest.

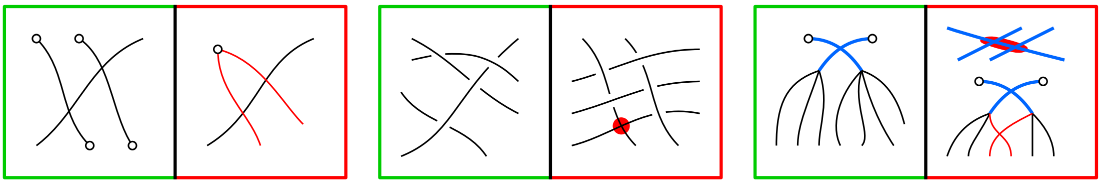

(a) fan-crossing free (b) gap-planar (c) fanbundle-planar

Fig. 2.15: Allowed (green box) and forbidden (red box) configurations in (a) fan-crossing free drawings; the red edges are not independent. (b) gap-planar drawings; two crossings are mapped to one of the edges, since there are only five edges but six crossings. (c) fanbundle-planar drawings.

The next class we consider is the one of k-fanbundle-planar graphs [13] (if $k = 1$, we say just "fanbundle-planar graphs"). Similar to a fan, a *(fan)bundle* is a set of edges incident to the same vertex. The difference of both concepts is the way how they are drawn. While in a fan each edge is still drawn individually, this is not the case for a bundle. Namely, every edge $e = (u, v)$ of a *1-sided k-fanbundle-planar* drawing consists of two parts (see also Figs. 2.15c and 2.16a):

- The bundle B_u, which belongs to one of the vertices u or v, say u (called *origin* of B_u), and may be shared with several other edges incident to u. Bundle B_u is drawn as a segment starting in u and ending in a point t_u, the so-called *terminal* of B_u. It is allowed that B_u crosses at most k other bundles with an origin different from u.
- The non-bundle part of e, which is drawn crossing-free between t_u and v; this part is also called planar part of e.

The number of edges in 1-sided fanbundle-planar graphs is $\frac{13}{3}n - \frac{26}{3}$ [13], which is a tight bound.

The *2-sided k-fanbundle-planar* drawings are defined accordingly; the only difference to 1-sided k-fanbundle-planar drawings is, that every edge $e = (u, v)$ consists of three parts: bundles B_u and B_v with origins u and v, respectively, and a planar part between the terminals of B_u and B_v. Here the known edge density bound is $8.6n - 15.6$ [13]. The lower bound construction in [13] provides a drawing with only $7n - 18$ edges, so the bound is not tight.

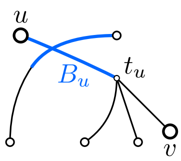

(a)

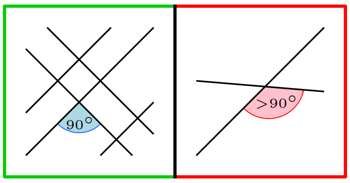

(b) RAC

Fig. 2.16: (a) Illustration for a bundle B_u with origin u and terminal t_u. (b) Allowed (green box) and forbidden (red box) configurations in RAC drawings.

We conclude with the so-called *RAC (right-angle crossing)* drawings [59, 60, 64], where edges are drawn straight-line and may only cross at right angles; refer to Fig. 2.16b. For RAC graphs the edge density is $4n - 10$ [59]. Compared with the other graph classes introduced in this section, RAC graphs are different, because their drawings have straight-line edges by definition, while this is not necessarily the case for the other graph classes.

Chapter 3

Drawing a Tree with Few Segments

One measure for the quality of a graph drawing is the number of simple geometric entities used in it, the so-called *visual complexity* [127]. For a straight-line drawing Γ of a graph, the visual complexity is the number of segments in Γ, referred to as *segment complexity*, where one segment consists of a path in Γ, i. e. each segment may consist of several edges. This approach can be attributed to the *Gestalt principles of perception* [98], which are laws describing how the mind typically perceives and organizes a scene with several objects in it. Thereby edges grouped together to a segment may be easier to follow by the law of continuation, and drawings with fewer segments might hence improve the perceptual processing of them. Also aesthetics may be influenced in a positive way by reducing the number of segments in a drawing, as a recent user study suggested [96].

Results regarding the segment complexity stem e. g. from Durocher and Mondal [63], who provided an algorithm to draw a triangulation with $\frac{7}{3}n - \mathcal{O}(1)$ segments, and from Dujmović et al. [62], who proved upper and lower bounds for the number of segments in several graph classes. In particular they showed that every tree can be drawn with $\frac{\vartheta}{2}$ segments, where ϑ is the number of odd-degree vertices; moreover, this bound is tight, that is, there exists trees which need $\frac{\vartheta}{2}$ segments. Another result in this direction is by Hültenschmidt et al. [89]. Recently they presented an algorithm to draw a tree on a grid with $\frac{3}{4}n$ segments and $\mathcal{O}(n^{3.58})$ area. In this chapter[1] we improve their area bound to $n \times n$, while retaining the number of segments.

[1]The results of this chapter are part of the conference paper “Drawing planar graphs with few segments on a polynomial grid” [95].

3.1 Preliminaries

Let $T = (V, E)$ be a tree and Γ a drawing of T. A *segment* in Γ is a (maximal) path $p = (v_1, v_2, \ldots, v_t)$, such that all vertices of p, lie on the same straight line. As already mentioned, the segment complexity of Γ is the number of segments in Γ. A *grid drawing* is a drawing Γ, such that all its vertices lie on grid points $(x, y) \in \mathbb{Z} \times \mathbb{Z}$. For convenience, we set $-(x, y) := (-x, -y)$.

3.2 How to Draw T with few Segments on a Grid

In the following we describe an algorithm to draw the tree T with at most $\frac{3n}{4} - 1$ segments on an $n \times n$ grid. Our algorithm runs in $\mathcal{O}(n)$ time. To this end, let α be the number of leaves of T, and β the number of degree-2 vertices of T.

If T is a path, it can be drawn with one segment and $n \times 1$ area. In the following we assume that T is not a path, that is, T has a vertex of degree larger than 2. We choose such a vertex as root of our tree T.

Contraction of degree-2 vertices. We create another tree T' by contracting all degree-2 vertices of T (refer to Figs. 3.1a and 3.1b). The new tree T' has $n - \beta$ vertices and still α leaves. For a degree-2 vertex $u \in T$ we say that u *belongs* to v if v is the first descendent of u in T with a degree different from 2 (refer to Fig. 3.1a). Note that the running time for this step is $\mathcal{O}(n)$, since each vertex of T must be considered only once.

Removing leaves. We create a new tree T'' by removing all leaves from T'. The tree T'' has $n - \beta - \alpha$ vertices. (see Fig. 3.1c). The running time to do so is $\mathcal{O}(n - \beta) = \mathcal{O}(n)$.

Before describing the next steps of our algorithm, we explain the main idea. We draw T'' with $n - \beta - \alpha$ segments, that is, each edge of T'' is one segment. Then we add the α leaves such that a leaf either extends a segment of T'', or every pair of leaves belong to one segment. Thus we need at most $\frac{\alpha}{2}$ additional segments, yielding at most $n - \beta - \frac{\alpha}{2}$ segments for T'. Observe that more than half of the vertices of T' are leaves, i. e. $\alpha > \frac{n-\beta}{2}$, since T' has no degree-2 vertices; this implies an upper bound of $\frac{3}{4}(n - \beta) \leq \frac{3}{4}n$ segments for T'. Finally we re-insert the degree-2 vertices without increasing the number of segments.

We use the following definitions in our algorithm. For a vertex v of T'' we denote the subtree of T rooted at v by T_v and the number of vertices of T_v by n_v. Our goal is to draw T_v inside a polygon $\mathbf{P}_v$, where $\mathbf{P}_v$ has the dimensions ℓ_v, r_v, t_v, b_v and h_v

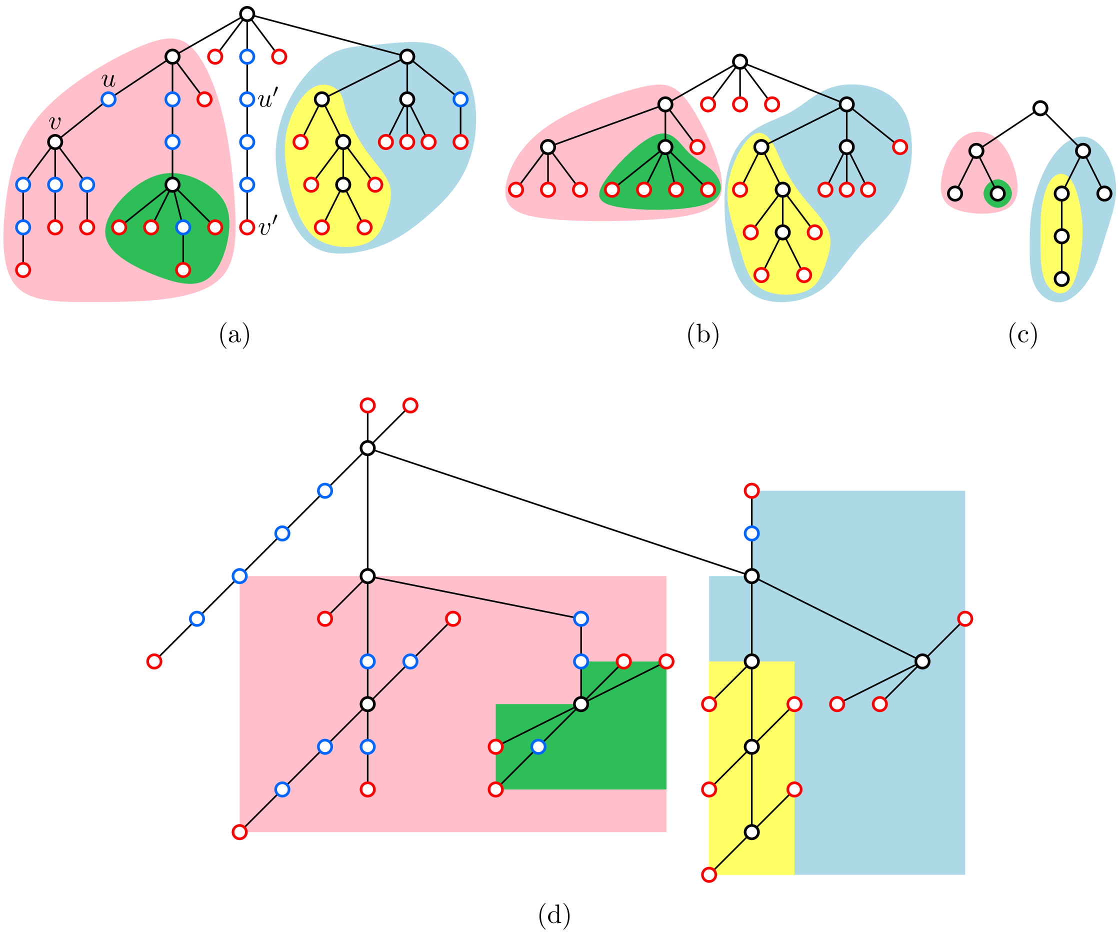

Fig. 3.1: (a) A tree T. Degree-2 vertices are blue and leaves are red. Vertex u belongs to v and vertex u' belongs to v'. (b) The tree T', where all degree-2 vertices from T are contracted. (c) The tree T'', where all leaves from T' are removed. (d) The drawing our algorithm produces.

as indicated in Fig. 3.2a. We create the drawing of T_v recursively (using a pre-order walk), while maintaining the following two properties:

Property 1: No vertex of T_v is placed to the top left of v;

Property 2: the polygon $\mathbf{P}_v$ has area $n_v \times n_v$.

If v is a leaf of T'', we place it at (relative) position $s = (0, 0)$ and both properties are clearly fulfilled. Otherwise we assume that $v_1, \ldots, v_k$ are the children of v in T'', and that each subtree $T_i := T_{v_i}$ is drawn inside a polygon $\mathbf{P}_i$ with dimensions ℓ_i, r_i, t_i, b_i and h_i such that Properties 1 and 2 hold. Again, let $s = (0, 0)$ be the (relative) position of v; further, for a vertex $u \in T_v$, let $s + (x(u), y(u))$ be its coordinates with respect to v. For each vertex v, we save the dimensions of the corresponding polygon and the number of degree-2 vertices belonging to v; further, we save the position of v relative to its parent, in order to guarantee a linear running time for our algorithm.

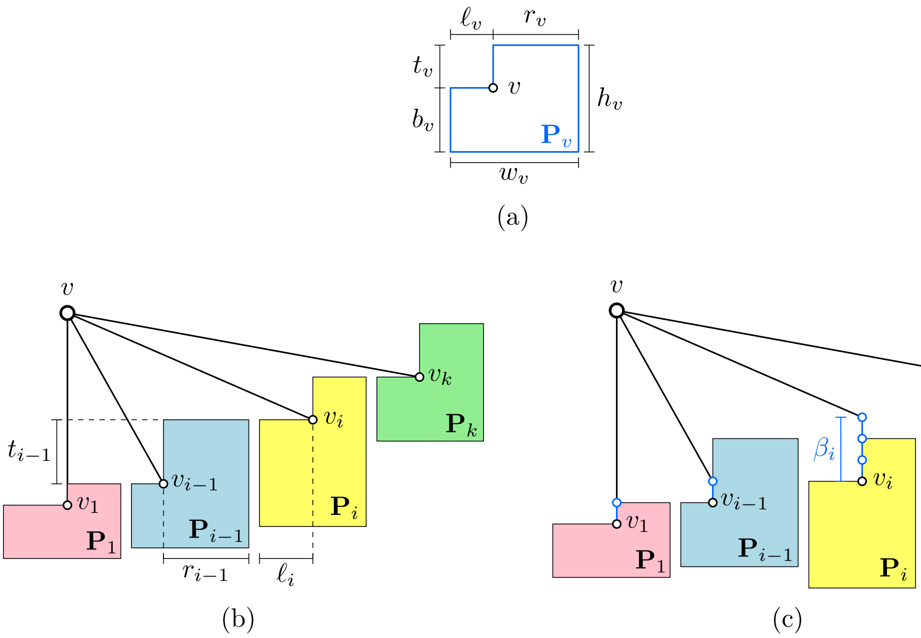

Fig. 3.2: (a) The polygon $\mathbf{P}_v$ and its dimensions. (b) The drawing of T_v after Step 1. (c) The drawing of T_v after Step 2.

Step 1. We place v_1 directly below v, and we place each polygon $\mathbf{P}_i$, where $i \geq 2$ to the right of $\mathbf{P}_{i-1}$, such that v_i is aligned with the top boundary of $\mathbf{P}_{i-1}$ (refer to Fig. 3.2b). That is, the position of v_1 is $s - (0, 1 + \sum_{i=1}^{k} t_i)$, and for $i \geq 2$ the position of vertex v_i is $(x(v_{i-1}) + r_{i-1} + \ell_i + 1, y(v_{i-1}) + t_{i-1})$. By Property 2 the total width and height of this drawing is at most $\sum_{i=1}^{k} n_i$, where n_i is the number of vertices in subtree T_i.

Step 2. Let β_i be the number of degree-2 vertices belonging to v_i. We move each polygon $\mathbf{P}_i$ down by β_i and place the degree-2 vertices that belong to v_i directly above v_i, that is, at positions $(x(v_i), y(v_i)+1), \ldots, (x(v_i), y(v_i)+\beta_i)$ (for an illustration see Fig. 3.2c). This does not change any edge incident to v and the polygons $\mathbf{P}_1, \ldots, \mathbf{P}_k$ are still disjoint, since they are only moved down. Therefore the drawing is still planar. The width of the drawing remains $\sum_{i=1}^{k} n_i$, and the height increases at most by $\max(\beta_1, \ldots, \beta_k) \leq \sum_{i=1}^{k} \beta_i$, so the height is now at most $\sum_{i=1}^{k}(n_i + \beta_i)$.

Step 3. If v has no leaf-children in T' then continue with the next vertex (which is either a sibling of v, or the parent of v, or no vertex at all). Otherwise let $u_1, \ldots, u_a$ be the leaf-children of v in T' and $\gamma_1, \ldots, \gamma_a$ the number of degree-2 vertices belonging to them. We assume without loss of generality $\gamma_1 \geq \gamma_2 \geq \cdots \geq \gamma_a$.[2] Further let C_v

[2]We stress that this ordering can be done in time $\mathcal{O}(a)$, e. g. by using CountingSort [52, 128].

be the subtree of T_v induced by v, $u_1, \dots, u_a$ and the degree-2 vertices belonging to $u_1, \dots, u_a$.

First suppose that a is even, say $a = 2j$ for some $j > 0$. We place the leaves alternating to the bottom-left and top-right of v, such that

- u_{2i-1}, v and u_{2i} lie on a segment with slope $\frac{1}{i}$ for each $i = 1, \dots, j$, and
- the degree-2 vertices belonging to u_{2i-1} and u_{2i} can be placed on this segment.

To this end, vertex u_{2i-1} is placed at coordinate $s - ((\gamma_{2i-1} + 1) \cdot i, \gamma_{2i-1} + 1)$ and u_{2i} at coordinate $s + ((\gamma_{2i} + 1) \cdot i, \gamma_{2i} + 1)$. The γ_{2i-1} degree-2 vertices belonging to u_{2i-1} are placed at coordinates

$$s - (i, 1), s - (2i, 2), s - (3i, 3), \dots, s - (\gamma_{2i-1} \cdot i, \gamma_{2i-1}),$$

while the γ_{2i} degree-2 vertices belonging to u_{2i} are placed at coordinates

$$s + (i, 1), s + (2i, 2), s + (3i, 3), \dots, s + (\gamma_{2i-1} \cdot i, \gamma_{2i-1})$$

(refer to Fig. 3.3a).

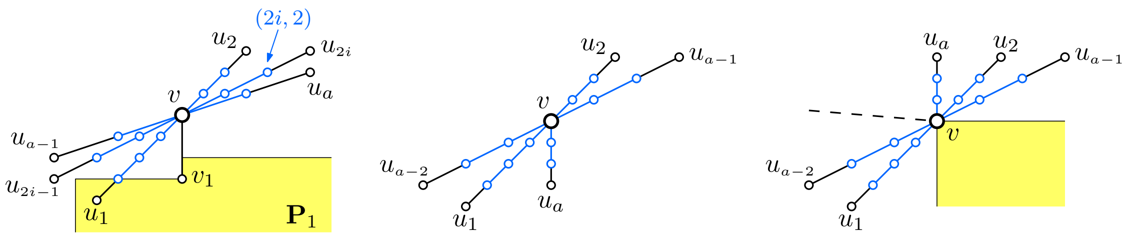

(a) (b) (c)

Fig. 3.3: The placing of $u_1, \dots, u_a$ and their degree-2 vertices. (a) a is even. (b) a is odd and v is a leaf in T''. (c) a is odd and neither is v the first child of its parent, nor belongs a degree-2 vertex to v.

Now suppose that a is odd. In this case we apply the procedure described above for the leaves $u_1, \dots, u_{a-1}$. The rules for placing u_a are the following.

- If v is a leaf in T'', we place u_a below v at coordinate $s - (0, \gamma_a + 1)$ (see e.g. Fig. 3.3b).
- If v is not a leaf in T'', and no degree-2 vertex belongs to v, and v is not the first child of its parent in T'' (i.e. no edge leaves v vertically above), then we place u_a directly above v at coordinate $s + (0, \gamma_a + 1)$. In this case, edge (v, u_a) shares a segment with (v, v'), where v' is v_1 or a degree-2 vertex belonging to v_1 (see e.g. Fig. 3.3c).
- Otherwise u_a is placed like every other vertex with odd index, that is, at coordinate $s - ((\gamma_a + 1) \cdot i, \gamma_a + 1)$.

Step 4. By construction, no segment drawn in Step 3 crosses $\mathbf{P}_2, \dots, \mathbf{P}_k$. However, there might be an intersection with $\mathbf{P}_1$; refer to the segment between u_1 and u_2 in Fig. 3.3a. If this is the case, we move $\mathbf{P}_1$ down until the crossing disappears.

With Steps 1-4 we have created a drawing of T_v in a polygon $\mathbf{P}_v$ such that Property 1 hold. We show that $\mathbf{P}_v$ also satisfies Property 2, that is $\mathbf{P}_v$ has area $n_v \times n_v$.

We have already seen that after Step 2, i. e. before C_v was drawn, the width of the drawing of T_v is $\sum_{i=1}^{k} n_i$ and the height is at most $\sum_{i=1}^{k}(n_i + \beta_i)$. Now we analyze the width and height of C_v in our drawing after Steps 3 and 4. To this end, let $\gamma^L = \sum_{i=1}^{\lceil \frac{a}{2} \rceil} \gamma_{2i-1}$ be the number of degree-2 vertices of C_v which are drawn to the left of v, and $\gamma^R = \sum_{i=1}^{\lfloor \frac{a}{2} \rfloor} \gamma_{2i}$ the number of degree-2 vertices of C_v which are drawn to the right of v. Further let $\gamma = \gamma^L + \gamma^R$.

Since $\gamma_1 \geq \gamma_2 \geq \dots \geq \gamma_a$ and since u_i is placed at y-coordinate $s \pm (\gamma_i + 1)$, the vertices with the lowest and highest y-coordinate are u_1 and u_2, respectively. This yields

- a height of $1 + \gamma = 1 + a + \gamma$ for C_v if v has no leaf-children in T', that is $a = 0$;
- a height of $2 + \gamma_1 = 1 + a + \gamma$ for C_v if v has exactly one leaf-child in T', that is $a = 1$ and $\gamma = \gamma_1$;
- a height of $3 + \gamma_1 + \gamma_2 \leq 1 + a + \gamma$ for C_v if v has more than one leaf-child in T', that is $a \geq 2$ and $\gamma \geq \gamma_1 + \gamma_2$.

In every case the height of C_v is at most $1 + a + \gamma$.

To analyze the width of C_v, consider the leftmost vertex $u_{2\ell-1}$ and the rightmost vertex u_{2r} among the vertices $u_1, \dots, u_a$. Since $u_{2\ell-1}$ has x-coordinate $s-(\gamma_{2\ell-1}+1)\cdot\ell$ and u_{2r} has x-coordinate $s + (\gamma_{2r} + 1) \cdot r$, the width of C_v is

$$w(C_v) := 1 + (\gamma_{2\ell-1} + 1) \cdot \ell + (\gamma_{2r} + 1) \cdot r = 1 + \gamma_{2\ell-1}\ell + \ell + \gamma_{2r}r + r.$$

Observe that the order $\gamma_1 \geq \gamma_2 \geq \dots \geq \gamma_a$ implies

$$\gamma^L = \sum_{i=1}^{\lceil \frac{a}{2} \rceil} \gamma_{2i-1} \geq \sum_{i=1}^{\ell} \gamma_{2i-1} \geq \ell \cdot \gamma_{2\ell-1}$$

and

$$\gamma^R = \sum_{i=1}^{\lfloor \frac{a}{2} \rfloor} \gamma_{2i} \geq \sum_{i=1}^{r} \gamma_{2i} \geq r \cdot \gamma_{2r}.$$

Hence we have

$$w(C_v) \le 1 + \ell + r + \gamma^L + \gamma^R \le 1 + 2\max(\ell, r) + \gamma \le 1 + a + \gamma.$$

So in Step 3 the width of the drawing of T_v increases by at most $1 + a + \gamma$, while the height increases by at most $\frac{1}{2}(a+\gamma)$ (only the part above v increases the height). In Step 4 the drawing of T_1 is moved down if it is crossed by the segment between u_1 and v. Because $y(u_1) > y(v_1)$ implies that there is no such crossing, it suffices to move T_1 down by $|y(u_1)| \le \frac{1}{2}(a + \gamma)$. Together with Step 3, the height increases at most by $1 + a + \gamma$. So the width is at most

$$\sum_{i=1}^{k} n_i + 1 + a + \gamma \le 1 + \sum_{i=1}^{r}(n_i + \beta_i) + a + \gamma = n_v,$$

and the height is at most

$$\sum_{i=1}^{k}(n_i + \beta_i) + 1 + a + \gamma \le 1 + \sum_{i=1}^{r}(n_i + \beta_i) + a + \gamma = n_v.$$

This complies with Property 2.

In the following we show that T has at most $\frac{3}{4}n - 1$ segments. To this end let r be the root of T. Further, for a vertex $v \in T'' \setminus \{r\}$ let p_v be the parent of v in T'', P_v the path between v and p_v in T, and e_v the edge incident to p_v on P_v (see Fig. 3.4). Let $T_v^+ := T_v \cup P_v$, further let n_v^+ be the number of vertices in T_v^+, and let s_v be the number of segments in the drawing of T_v^+. For the number of segments in $T_i^+ = T_{v_i}^+$ we set $s_i := s_{v_i}$.

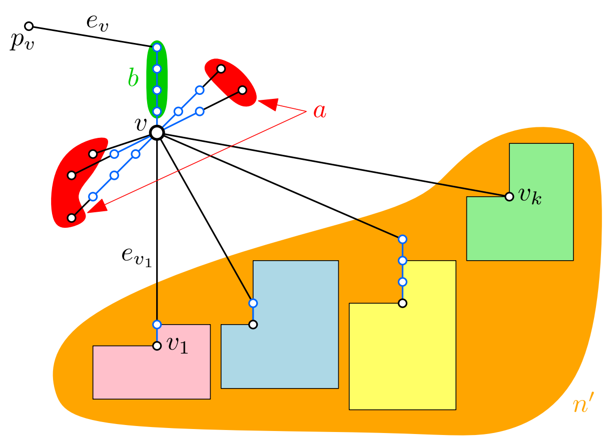

Fig. 3.4: Illustration for the tree T_v^+.

Lemma 3.1. *If e_v is drawn vertically, then $s_v \leq \frac{3n_v^+-1}{4}$, otherwise $s_v \leq \frac{3}{4}n_v^+$.*

Proof. We prove the lemma by induction on the height of T''. Assume that the bound on the number of segments holds for all children of v in T'' (the base of the induction will be proved in the first two cases of the case analysis below). Recall that $v_1, \dots, v_k$ are the children of v in T'' and $u_1, \dots, u_a$ are the leaf-children of v in T'. Let b be the number of degree-2 vertices belonging to v and $n' := \sum_{i=1}^{k} n_i^+$. Then

$$n_v^+ = n' + a + \gamma + b + 1 \geq n' + a + b + 1$$

(refer to Fig. 3.4). By induction we have $s_1 \leq \frac{3n_1^+-1}{4}$ (recall that e_{v_1} is drawn vertically) and $s_i \leq \frac{3}{4}n_i^+$ for $i = 2, \dots, k$. This yields

$$\sum_{i=1}^{k} s_i \leq \frac{3n_1^+-1}{4} + \sum_{i=1}^{k} \frac{3}{4}n_i^+ = \frac{3n'-1}{4}.$$

In the following we analyze the number of segments for C_v and P_v with a case analysis.

v is a leaf in T$''$ and b = 0. Since v is a leaf in T'' we have $n' = 0$ and v has at least two children in T; so $n_v^+ \geq n' + a + b + 1 = a + 1$ and $a \geq 2$. Also $b = 0$ implies that the path P_v consists only of the edge e_v.

- If a is even, we draw C_v with $\frac{a}{2}$ segments, and the edge e_v with one additional segment. Thus

$$s_v \leq \frac{a}{2} + 1 \leq \frac{n_v^+ - 1}{2} + 1 = \frac{3n_v^+ - n_v^+ + 2}{4} \leq \frac{3n_v^+ - 1}{4}$$

  since $n_v^+ \geq 3$.

- If a is odd, we have $a \geq 3$ and $n_v^+ \geq 4$. The leaves $u_1, \dots, u_{a-1}$ (together with the degree-2 vertices belonging to them) are drawn with $\frac{1}{2}(a-1)$ segments. If e_v is vertical, it shares a segment with u_a, yielding

$$s_v \leq \frac{a-1}{2} + 1 \leq \frac{n_v^+ - 2}{2} + 1 = \frac{3n_v^+ - n_v^+}{4} \leq \frac{3n_v^+ - 4}{4} = \frac{3}{4}n_v^+ - 1.$$

  Otherwise, that is if e_v is not vertical, we have one more segment and obtain $s_v \leq \frac{3}{4}n_v^+$.

v is a leaf in T″ and b > 0. We still have $n' = 0$ and $a \geq 2$, which implies $n_v^+ \geq n' + a + b + 1 = a + b + 1 \geq a + 2 \geq 4$. But now the path P_v consists of more than one edge.

- If a is even, we draw C_v with $\frac{a}{2}$ segments. Moreover, if e_v is vertical, the edge e_v and the degree-2 vertices belonging to v lie on a common vertical segment. We obtain

$$s_v \leq \frac{a}{2} + 1 \leq \frac{n_v^+ - 2}{2} + 1 = \frac{n_v^+}{2} = \frac{3n_v^+ - n_v^+}{4} \leq \frac{3}{4}n_v^+ - 1.$$

  On the other hand, if e_v is not vertical, the degree-2 vertices belonging to v and the edge e_v belong to two different segments; hence $s_v \leq \frac{3}{4}n_v^+$.

- If a is odd, then we draw $u_1, \ldots, u_{a-1}$ with $\frac{1}{2}(a-1)$ segments, and u_a on a vertical segment together with the degree-2 vertices belonging to v. If e_v is also vertical, we obtain

$$s_v \leq \frac{a-1}{2} + 1 \leq \frac{n_v^+ - 3}{2} + 1 = \frac{n_v^+ - 1}{2} \leq \frac{n_v^+}{2} \leq \frac{3}{4}n_v^+ - 1,$$

  otherwise we need one more segment for e_v and obtain $s_v \leq \frac{3}{4}n_v^+$.

v is not a leaf in T″ and b = 0. Then we have $n_v^+ \geq n' + a + b + 1 = n' + a + 1$.

- Let a be even. Then C_v is drawn with $\frac{a}{2}$ segments (if $a = 0$ then C_v is drawn with $\frac{a}{2} = 0$ segments). If e_v is vertical, then it shares a segment with e_{v_1} and we have

$$s_v \leq \frac{3n' - 1}{4} + \frac{a}{2} = \frac{3n' + 2a - 1}{4} \leq \frac{3(n_v^+ - a - 1) + 2a - 1}{4}$$
$$= \frac{3n_v^+ - a - 4}{4} \leq \frac{3}{4}n_v^+ - 1.$$

  On the other hand, if e_v is not vertical, we need an additional segment, hence $s_v \leq \frac{3}{4}n_v^+$.

- Let a be odd. Then we use $\frac{1}{2}(a-1)$ segments for $u_1, \ldots, u_{a-1}$. If e_v is vertical, then it shares a segment with e_{v_1}, but we have an additional segment for u_a. On the other hand, if e_v is not vertical, then we need an additional segment for e_v, but u_a is drawn above v and shares a segment with e_{v_1}. Hence, in every case we have

$$s_v \leq \frac{3n' - 1}{4} + 1 \leq \frac{3(n_v^+ - a - 1) + 3}{4} = \frac{3n_v^+ - 3a}{4} \leq \frac{3n_v^+ - 3}{4}.$$

v is not a leaf in T″ and b > 0. In this case we have $n_v^+ \geq n'+a+b+1 \geq n'+a+2$.

- If a is even, we draw $u_1, \ldots, u_a$ with $\frac{1}{2}a$ segments. The edges of P_v share a vertical segment with e_{v_1} and we use at most one additional segment for e_v; hence

$$s_v \leq \frac{3n'-1}{4} + \frac{a}{2} + 1 = \frac{3n'+2a+3}{4} \leq \frac{3(n_v^+ - a - 2) + 2a + 3}{4}$$
$$= \frac{3n_v^+ - a - 3}{4} \leq \frac{3n_v^+ - 3}{4}.$$

- Let a be odd. We draw $u_1, \ldots, u_a$ with $\frac{1}{2}(a+1)$ segments. Since the edges of P_v share a segment with e_{v_1}, they don't need an additional segment. So, if e_v is vertical (and hence shares also a segment with e_{v_1}), we obtain

$$s_v \leq \frac{3n'-1}{4} + \frac{a+1}{2} \leq \frac{3(n_v^+ - a - 2) + 2a + 1}{4} = \frac{3n_v^+ - a - 5}{4} \leq \frac{3n_v^+ - 5}{4}.$$

 If e_v is not vertical we need one more segment and have $s_v \leq \frac{3}{4}n_v^+$. □

We use Lemma 3.1 to give a bound for the total number of segments in the drawing of T.

Lemma 3.2. *For $n \geq 3$, our algorithm draws T with at most $\frac{3}{4}n - 1$ segments.*

Proof. We use the same notation as in Lemma 3.1.

If T is a path with length $n \geq 3$, then the bound clearly holds.

If T is no path and T'' consists of one vertex v, that is, $T = C_v$ and $b = 0$ (in this case T is a star or the subdivision of a star), we have $\frac{1}{2}a \leq \frac{1}{2}(n-1) \leq \frac{3}{4}n - 1$ segments if a is even, and also $\frac{1}{2}(a+1) \leq \frac{1}{2}n \leq \frac{3}{4}n - 1$ segments if a is odd (note that $n \geq 4$ when a is odd and T is not a path).

Otherwise T'' consists of more than one vertex. Let r be the root of T'' and $v_1, \ldots, v_k$ be the children of r. By Lemma 3.1, in the drawing of T, the subtrees $T_1^+, \ldots, T_k^+$ contribute at most $\frac{1}{4}(3n'-1)$ segments, where $n' = \sum_{i=1}^k n_i^+$. Let $u_1, \ldots, u_a$ be the leaf-children of r in T'. If a is even, we draw them with $\frac{1}{2}a$ segments; otherwise, we draw $u_1, \ldots, u_{a-1}$ with $\frac{1}{2}(a-1) < \frac{1}{2}a$ segments, and align u_a with the vertical segment of v_1. Also observe that the relation $n \geq n' + a + 1$ holds. Hence, the number of segments in our drawing is upper bounded by

$$\frac{3n'-1}{4} + \frac{1}{2}a = \frac{3n'-1+2a}{4} \leq \frac{3n-3a-3-1+2a}{4} = \frac{3n-a-4}{4} \leq \frac{3}{4}n - 1. \quad \square$$

Since all steps of our algorithm can be executed in linear time, we obtain the following theorem.

Theorem 3.3. *Any tree with $n \geq 3$ vertices can be drawn planar on an $n \times n$ grid with $\frac{3}{4}n - 1$ segments in time $\mathcal{O}(n)$.*

3.3 Conclusions and Open Problems

We provided a linear-time algorithm that calculates a grid-drawing of a tree using at most $\frac{3}{4}n - 1$ segments in an area of $n \times n$. With that we improved the $\mathcal{O}(n^{3.58})$ area of Hültenschmidt et al. [89] to $\mathcal{O}(n^2)$. However, we were not able to construct a corresponding lower bound example, that is, a family of trees on n vertices such that these trees all need $n \times n$ area. Hence, the question remains open, if a tree can be drawn with the same number of segments on a grid smaller than $\mathcal{O}(n^2)$.

Chapter 4

Graphs of Low Degree

We call a graph G *of degree* d if d is an upper bound on the vertex degrees for G. In this chapter we establish lower and upper bounds for the values of d, such that every graph of degree d belongs to a certain graph class beyond planarity. More precisely, for a graph class $\mathcal{C}$, we aim at determining a value d_ℓ such that every degree-d graph with $d \leq d_\ell$ belongs to $\mathcal{C}$, as well as a value d_u such that there exists a graph of degree d_u that does not fulfill the properties of class $\mathcal{C}$. By definition the inequality $d_\ell < d_u$ holds. Ideally, we have $d_\ell + 1 = d_u$ for a class $\mathcal{C}$.

An easy observation is that every graph of degree 2 can be drawn in a planar way and therefore belongs to every graph class beyond planarity. So the lower bound d_ℓ is at least 2, independent of the beyond-planarity graph class.

For deriving an upper bound d_u there exists a standard technique: By using the maximum edge density it is possible to find complete or complete bipartite graphs not belonging to the considered graph class. However, since graphs of low degree are very sparse (in fact, graphs of degree $d \leq 5$ are even sparser than planar graphs), this technique fails in our case or gives lower and upper bounds that are far from tight.

Other than in this work, which is based on a publication in [15], graphs of low degree were already considered in several papers. Thereby a long-standing open question was if all graphs of degree 3 belong to the class of RAC-graphs [18, 59], [60, Problem 6], [61, Problem 8]. Argyriou et al. [23] answered this question in the positive for degree-3 graphs that are additionally Hamiltonian, and Angelini et al. [18] for graphs of degree 3 that are allowed to have one bend per edge. In contrast to these results, Didimo et al. [58] showed that not all graphs of degree 4 are RAC. More precisely, the 4-regular complete bipartite graph $K_{4,4}$ does not allow a RAC drawing. Since $K_{4,4}$ is Hamiltonian, we obtain $d_\ell = 3$ and $d_u = 4$ for the class of Hamiltonian RAC graphs by combining the two results of Argyriou et al. [58] and Didimo et al. [58].

Regarding the quasi-planar graphs, Alam et al. made two observations [8]:

(1) Every graph $G = (V, E)$ of degree 4 is quasi-planar: The edges E of a degree-4 graph can be decomposed into two disjoint sets E_1 and E_2 such that planar drawings Γ_1 and Γ_2 of $G_1 = (V, E_1)$ and $G_2 = (V, E_2)$, respectively, exist, where Γ_1 and Γ_2 use the same point set to draw the vertices of V. Since in the stacked drawing Γ of Γ_1 and Γ_2 (which is a drawing for G), the edges of E_1 can only cross the edges of E_2 and vice versa, there are no three mutually crossing edges in Γ (refer also to Fig. 4.1). Thus, the drawing Γ is quasi-planar. This yields a lower bound of $d_\ell = 4$ for the class of quasi-planar graphs.

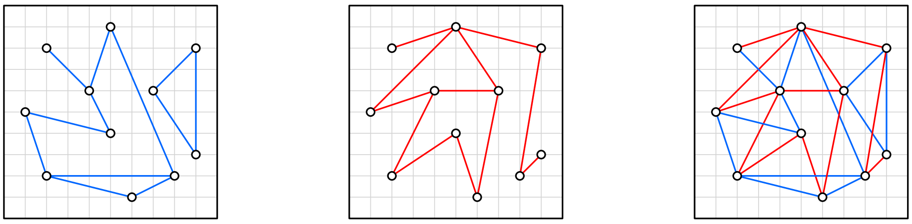

(a) (b) (c)

Fig. 4.1: Illustration for stacking two drawings using the same point set. (a) and (b) show two planar drawings Γ_1 and Γ_2 for graphs $G_1 = (V, E_1)$ and $G_2 = (V, E_2)$. (c) shows the stacked quasi-planar drawing of Γ_1 and Γ_2 for the graph $G = (V, E_1 \cup E_2)$.

(2) Graphs of degree 3 that can be decomposed into a matching and a set of cycles (the bipartite 3-regular graphs are an example for graphs having this property), are quasi-planar and fan-crossing free at the same time. We remark that RAC graphs are quasi-planar and fan-crossing free, so quasi-planarity and the fan-crossing free property are two necessary conditions for a graph to be RAC.

We contribute to this discussion by studying various graph classes and showing lower and upper bounds for the maximum degree d of graphs belonging to those classes. Table 4.1 gives an overview of our results and the state of the art.

4.1 The Classes of k-Gap-Planar Graphs

First we consider the class of k-gap-planar graphs. Recall that a drawing Γ of a graph G is k-gap-planar if there is a mapping f from the crossings to the edges, such that the inverse image $f(e)$ of an edge contains at most k crossings (in other words: each edge gets at most k crossings assigned to it). Also recall that every graph of degree 2 is planar and therefore k-gap-planar. We show that d_ℓ cannot be larger than 2 by showing that $d_u = 3$ for k-gap-planar graphs. In doing so we obtain tight bounds for this class of graphs. In fact, we will even prove a stronger result in Thm. 4.1.

Table 4.1: The largest known value d_ℓ such that all graphs of degree $d \leq d_\ell$ belong to the indicated graph class $\mathcal{C}$, and the smallest value d_u where a graph is known that does not belong to $\mathcal{C}$.

graph class $\mathcal{C}$	d_ℓ		d_u	
k-planar Hamiltonian bipartite	2		3	(CCC_n, Cor. 4.2)
fan-planar Hamiltonian bipartite	2		3	(CCC_n, Cor. 4.3)
k-gap-planar Hamiltonian bipartite	2		3	(CCC_n, Thm. 4.1)
quasi-planar	4	[8]	10	(K_{11}, ref. [4])
RAC (0-bend)	2		4	($K_{4,4}$, ref. [58])
RAC (0-bend) Hamiltonian	3	[22]	4	($K_{4,4}$, ref. [58])
RAC 1-bend	3	[18]	9	(K_{10}, ref. [10])
RAC 2-bends	6	[18]	148	(K_{149}, ref. [24])
fan-crossing free	3	(Thm. 4.4)	5	($K_{5,5}$, Thm. 4.5)

For our proof we need the following theorem by Bae et al. [30]:

Let Γ be a drawing of a graph $G = (V, E)$. The drawing Γ is k-gap-planar if and only if for each set $E' \subseteq E$ the subdrawing $\Gamma[E']$ contains at most $k \cdot |E'|$ crossings.

Since every drawing of a graph G has at least $cr(G)$ crossings, the theorem by Bae et al. has the following implication: If $cr(G) > k|E|$ then no drawing Γ of G is k-gap-planar and by definition G is not k-gap-planar in this case. We use this fact to prove the next theorem.

Theorem 4.1. *For every $k \geq 1$, there exist infinitely many bipartite Hamiltonian 3-regular graphs that are not k-gap-planar.*

Proof. In order to prove the theorem, we need some definitions.

Harary [78] introduced the so-called *hypercube graph* $Q_n = (V_n, E_n)$ as follows: The vertex set V_n consists of 2^n vertices; each vertex is denoted by a unique distinct n-digit binary number. Two vertices v and w are connected by an edge in E_n if and only if the binary representations of v and w differ in a single digit; see Figs. 4.2a and 4.2b for an illustration. Clearly each vertex is adjacent to exactly n other vertices of V_n; therefore the graph Q_n is n-regular.

Starting from Q_n we obtain the so-called *cube-connected cycles* CCC_n [115] as follows: Each vertex v of Q_n is replaced with a cycle $v_1, \ldots, v_n$ of length n. Let $e_1, \ldots, e_n$ be the edges incident to v in Q_n. Then the edge e_i is attached to v_i; for an illustration see Fig. 4.2c. Note that each vertex in CCC_n has exactly 3 neighbors; thus, the graph CCC_n is 3-regular.

Since Q_n has 2^n vertices, the number of vertices in CCC_n is $n2^n$, and since CCC_n is a 3-regular graph, the sum of the vertex degrees in CCC_n is $3n2^n$, which implies a number of $3n2^{n-1}$ edges for CCC_n.

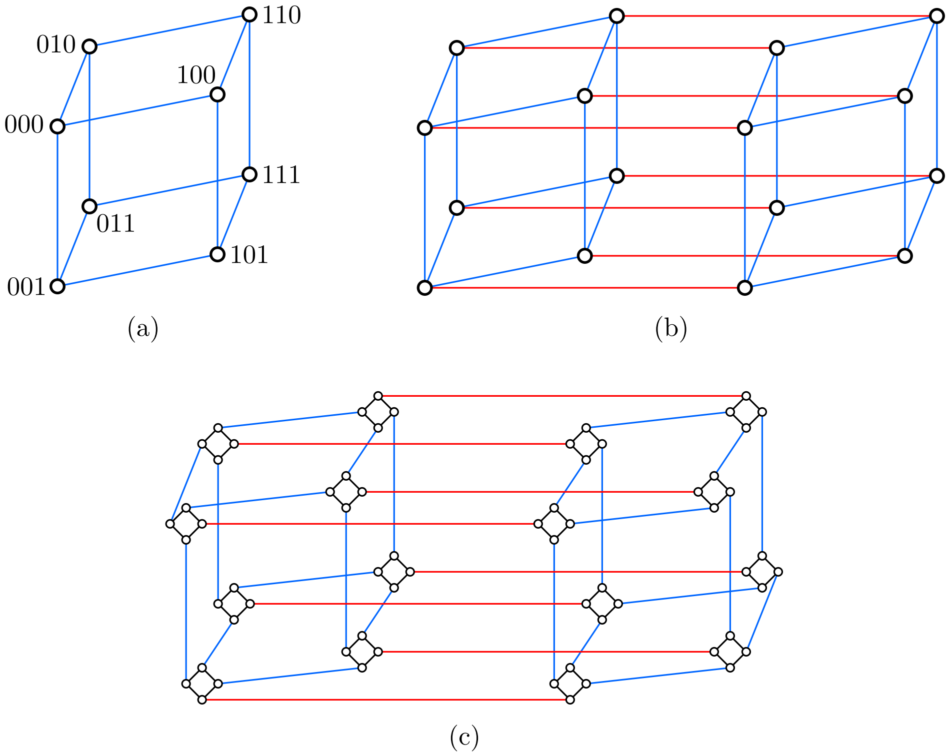

Fig. 4.2: (a) Illustration of Q_3, in which each vertex is labeled by a distinct 3-digit binary number. (b) Illustration of Q_4. The graph Q_4 is created by connecting two duplicates of Q_3 as depicted by the red edges. (c) Illustration of CCC_4, in which each vertex of Q_4 is replaced by a cycle of length 4 (see black edges). The 4 edges incident to each vertex in Q_4 are distributed such that each vertex of the corresponding cycle in CCC_4 is incident to exactly one of them.

According to Sýkora and Vrtó [132] the crossing number[1] $cr(CCC_n)$ of CCC_n is lower bounded by

$$\frac{1}{20}4^n - (9n+1)2^{n-1}.$$

It is easy to see that for each $k \geq 1$ there exist infinitely many n such that

$$\frac{2}{3n \cdot 20}2^n - \frac{9n+1}{3n} > k.$$

For infinite many values of n this yields

$$cr(CCC_n) \geq \frac{1}{20}4^n - (9n+1)2^{n-1} > k \cdot 3n2^{n-1} = k|E|.$$

[1] Recall that the crossing number $cr(G)$ of a graph G describes the minimal number of edge crossing that an arbitrary drawing of G has.

To complete our proof we show that CCC_n is bipartite and Hamiltonian for infinite many n. Hsu et al. [88] derived the exact length of cycles occurring in the graph CCC_n: If $L(n)$ denotes the set of all possible lengths of cycles in CCC_n, then

$$L(n) = \{n\} \cup \{i \mid i \text{ is even, } 8 \leq i \leq n+5, \text{ and } i \neq 10\} \cup \{i \mid n+6 \leq i \leq n2^n\}$$

if n is odd, and

$$L(n) = \{n\} \cup \{i \mid i \text{ is even, } 8 \leq i \leq n2^n, \text{ and } i \neq 10\}$$

if n is even and $n \geq 6$. Since CCC_n has $n2^n$ vertices and a cycle of length $n2^n$, the graph CCC_n is Hamiltonian for $n \geq 6$. Further, since a graph is bipartite if and only if it contains cycles of even length exclusively, the cube-connected cycles CCC_n is bipartite for $n \geq 6$ and n even. □

We conclude this section by noting that, since degree-4 graphs are quasi-planar, Thm. 4.1 gives an alternative proof (to the proof of Bae [30]) that there exist quasi-planar graphs which are not k-gap-planar for any fixed k.

4.2 The Class of k-Planar Graphs

Recall that a graph is k-planar if it can be drawn such that each edge has at most k crossings. Similar to the k-gap-planar graphs, we show that d_ℓ cannot be larger than 2 by showing that $d_u = 3$ for the class of k-planar graphs. This result is an easy consequence of Thm. 4.1 and a result by Bae [30].

Corollary 4.2. *For every $k \geq 1$, there exist infinitely many bipartite Hamiltonian 3-regular graphs that are not k-planar.*

Proof. Bae [30] showed that the class of $(2k)$-planar graphs are a subclass of the k-gap-planar graphs. Since there are infinitely many bipartite Hamiltonian 3-regular graphs not belonging to the class of k-gap-planar graphs by Thm. 4.1, we obtain that these graphs also do not belong to the class of k'-planar graphs for each $k' \leq 2k$. □

We observe that Cor. 4.2 can also be obtained by considering the average number of crossings per edge: Since we have $cr(CCC_n) \geq \frac{1}{20}4^n - (9n+1)2^{n-1}$ [132], the average number of crossings per edge in CCC_n is:

$$\frac{2 \cdot cr(CCC_n)}{|E(CCC_n)|} > 2 \cdot \frac{(1/20) \cdot 4^n - (9n+1) \cdot 2^{n-1}}{3n \cdot 2^{n-1}} = \frac{1}{10} \cdot \frac{4^n}{3n \cdot 2^{n-1}} - \frac{(9n+1) \cdot 2^n}{3n \cdot 2^{n-1}} = \frac{1}{15} \cdot \frac{2^n}{n} - 6 - \frac{2}{3n}.$$

Since this is a lower bound for the average number of crossings, the graph CCC_n contains an edge that is crossed by at least

$$\left\lceil \frac{1}{15}\frac{2^n}{n} - 6 - \frac{2}{2n} \right\rceil$$

edges. So, for a fixed $k \geq 1$, the graph CCC_n is not k-planar for every n satisfying the inequality

$$k < \left\lceil \frac{1}{15}\frac{2^n}{n} - 6 - \frac{2}{2n} \right\rceil .$$

4.3 The class of fan-planar graphs

Recall that a graph is fan-planar if an edge does not cross two independent edges. First we observe the following for a drawing Γ of a 3-regular fan-planar graph $G = (V, E)$: Since an edge $e \in E$ can cross at most a complete fan in Γ, that is all edges incident to a vertex $v \in V$, and the degree of v is 3, we conclude that Γ is also 3-planar. As a consequence, a 3-regular graph that is not 3-planar cannot be fan-planar. Applying Cor. 4.2 for $k = 3$ we obtain the following corollary, which implies a value of $d_u = 3$ for the class of fan-planar graphs.

Corollary 4.3. *There exist infinitely many 3-regular bipartite Hamiltonian graphs that are not fan-planar.*

4.4 The Class of Fan-Crossing Free Graphs

This section is dedicated to the fan-crossing free graphs. We recall that a graph is fan-crossing free if no edge crosses a fan, i. e. each edge is only allowed to cross independent edges. We prove that $d_\ell = 3$ and $d_u = 5$, leaving only open the question if all graphs of degree 4 are fan-crossing free.

4.4.1 An algorithm to draw a degree-3 graph fan-crossing free

As already mentioned before, Alam et al. [8] observed that every degree-3 graph which can be decomposed into a matching and a set of cycles, is simultaneously fan-crossing free and quasi-planar. However, Alam et al. did not give a concrete algorithm to produce such a drawing. Instead they are referring to a paper by Argyriou et al. [22], whose drawing algorithm for degree-3 Hamiltonian RAC graphs creates in fact quasi-planar and fan-crossing free graphs. But it is not obvious how to adjust this algorithm in order to work for general graphs of degree 3.

So we developed our own algorithm for drawing a degree-3 graph in a fan-crossing free style, and thereby showing that $d_\ell = 3$.

Algorithm. Let $G = (V, E)$ be a graph of degree 3. We assume that G is connected (otherwise we can draw each component independently). If G has at least one bridge $e = (v, w)$, consider the components G_1 and G_2 of $G \setminus \{e\}$. Let Γ_1 and Γ_2 be fan-crossing free drawings of G_1 and G_2, respectively. Then we can change Γ_1 and Γ_2 such that v and w are on the outer face of Γ_1 and Γ_2 (see also Fig. 4.3) and both drawings are still fan-crossing free, and re-insert the bridge e in a planar way.

Another observation is that graphs of degree 2 are planar and therefore fan-crossing free. Thus, we assume in the following that G is a connected bridgeless graph that contains a vertex of degree 3. Since G has no bridge, there is no degree-1 vertex in G.

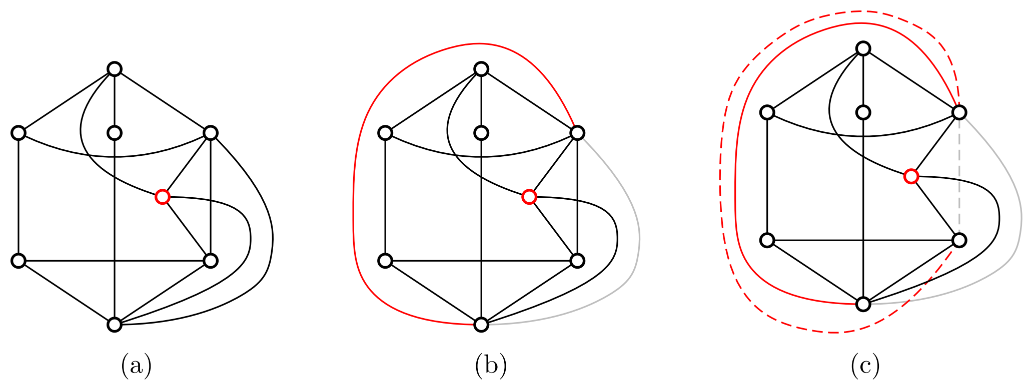

Fig. 4.3: (a) A drawing of an arbitrary graph G. Suppose the red vertex must be on the outer face. (b) and (c) show how to achieve this by rerouting two edges. In (b) the solid gray edge is rerouted to the solid red edge. In (c) the dashed gray edge is rerouted to the dashed red edge. The result is another drawing of graph G such that the red vertex is placed on the outer face.

In a preprocessing step, we perform the following operation: While there is a degree-2 vertex v with neighbors u and w in the graph, we remove v together with its incident edges (v, u) and (v, w) and insert the edge (u, w). Note that this operation does not change the degree of u and w, but might create multiple edges.

Let $G' = (V', E')$ be the graph obtained after executing the preprocessing step. Then G' is a 3-regular, bridgeless multigraph. By Petersen's theorem [111] there is a perfect matching $M \subseteq E'$ in G'. Since G' is 3-regular, the set $C := E' \setminus M$ consists of cycles, i. e. $C = C_1 \cup C_2 \cup \cdots \cup C_k$, where $C_1, \ldots, C_k \subseteq C$ are disjoint cycles. For $i = 1, \ldots, k$, let $C_i = (v_{i,1}, \ldots, v_{i,\alpha_i}, v_{i,1})$.

Let $\mathcal{U}$ be the unit circle in the plane $\mathbb{R}^2$. Recall that the unit circle is the set of points with distance one to the origin $(0, 0)$ of $\mathbb{R}^2$. Starting at position $(0, 1)$ with vertex $v_{1,1}$, we put the vertices $v_{1,1}, v_{1,2}, \ldots, v_{1,\alpha_1}, v_{2,1}, \ldots, v_{k,\alpha_k}$ of $C_1, \ldots, C_k$

on the unit circle (clockwise or counter-clockwise) such that consecutive vertices are equidistant. For $i = 1, \dots, k$ and $j = 1, \dots, \alpha_i - 1$, the edge $(v_{i,j}, v_{i,j+1})$ is drawn by following $\mathcal{U}$. The edge $(v_{i,1}, v_{i,\alpha_i})$ is drawn as a half-circle outside of the unit disc (see black edges in Fig. 4.4). Then the edges of C are drawn in a planar way and no edge of C is drawn in the interior of $\mathcal{U}$.

Further, we draw each edge $e = (v_{i,j}, v_{i',j'}) \in M$, where $i, i' = 1, \dots, k$, $j = 1, \dots, \alpha_i$ and $j' = 1, \dots, \alpha_{i'}$, by connecting $v_{i,j}$ and $v_{i',j'}$ using a straight line (see blue edges in Fig. 4.4). In doing so we ensure that edges belonging to M are drawn in the interior of $\mathcal{U}$. Thus, edges from M and C do not intersect each other. Different edges from M might cross, but since each vertex of G' is incident to at most one edge of M, all edges in M are independent and therefore no edge of M is part of a fan-crossing.

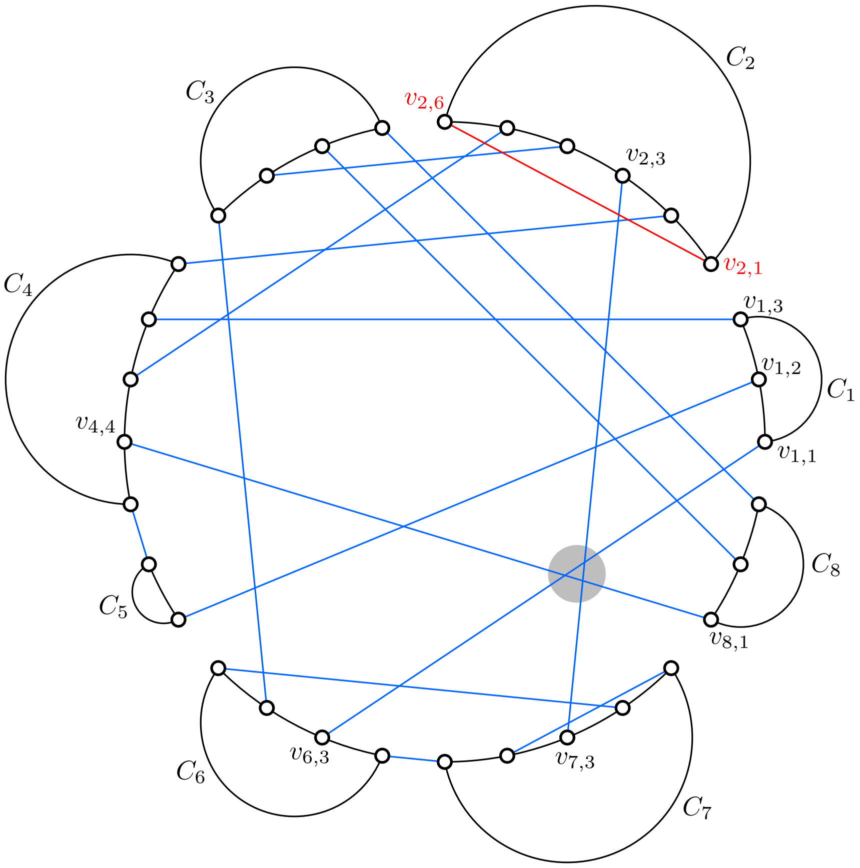

Fig. 4.4: A fan-crossing free drawing for a 3-regular graph, using our algorithm. The edges belonging to the cycles $C_1, \dots, C_k$ are black, and the matching edges are blue, except one: The red edge shows a matching edge that is a second version of another edge, namely the black edge $(v_{2,1}, v_{2,6})$ belonging to the cycle C_2.

At this point we have a closer look what happens with multiple edges. Suppose there are vertices v and w that have a multiple edge (v, w). We consider different cases:

(1) Edge (v, w) appears four more times. Then we would have $\deg(v), \deg(w) \geq 4$, which is not possible.

(2) Edge (v, w) appears three times. Since the degree of v and w is three and G' is connected, the whole graph G' consists of v, w and the three versions of (v, w). One version (v, w) belongs to M, the other two belong to C. This configuration is drawable as described above.

(3) Edge (v, w) appears twice and both versions belong to M. This is clearly not possible, since M is a matching.

(4) Edge (v, w) appears twice and both versions belong to C. In this case one cycle of C consists of v and w only. This can be drawn as described above (see black edges of cycle C_5 in Fig. 4.4).

(5) Edge (v, w) appears twice and one version belongs to M, the other to C. Say $e_1 \in C$ and $e_2 \in M$. The vertices and edges can be drawn as described above. Thereby the vertices v and w belong to a cycle of length at least 3 and are placed either consecutively on $\mathcal{U}$, or at the extremal positions of the cycle they belong to (see the cycle C_2 in Fig. 4.4).

So, in fact, our drawing algorithm for G' works also for multiple edges.

Let Γ' be the drawing we constructed so far for the graph G'. In the final step our goal is to extend Γ' in order to obtain a drawing Γ of G. That is, we want to re-insert the degree-2 vertices into Γ' such that the resulting drawing is still fan-crossing free. We re-insert these vertices in the reversed order as we have removed them. Suppose v is a degree-2 vertex that has been removed in some preprocessing step. Let u and w be the neighbors of v before the removal. Then we also removed the edges (v, u) and (v, w), but added the edge (u, w). We re-insert v now by subdividing the edge (u, w) such that between the subdivision vertex v and the vertex u there is no crossing. Then the edge (v, u) is planar, while the edge (v, w) has the same crossings as the edge (u, w) before the subdivision. This implies that the drawing is still fan-crossing free after re-inserting v.

The drawing algorithm described above yields the following theorem.

Theorem 4.4. *Every graph of degree 3 is fan-crossing free.*

Given a degree-3 graph, our algorithm produces a fan-crossing free drawing, using a decomposition into a matching and a set of cycles. Since Alam et al. [8] observed that every degree-3 graph which can be decomposed into a matching and a set of cycles, is simultaneously fan-crossing free and quasi-planar, a natural question is if our algorithm also produces a drawing that is not only fan-crossing free but also quasi-planar. However, the answer to this is negative, as Fig. 4.4 shows: The highlighted gray area indicates three mutually crossing edges, namely the edges $(v_{1,1}, v_{6,3})$, $(v_{2,3}, v_{7,3})$ and $(v_{4,4}, v_{8,1})$ (in fact, there can be found several triples of mutually crossing edges in Fig. 4.4).

4.4.2 A degree-5 graph that is not fan-crossing free

As we have seen, every graph of degree 3 is fan-crossing free. However, this is not true for all graphs of degree 5. To prove this, we consider the complete bipartite graph $K_{5,5}$. We show not only that it is not fan-crossing free, but even give a characterization of the bipartite fan-crossing free graphs in general. Note that such characterizations also exist for other graph class, see e. g. [53, 58].

Theorem 4.5. *The complete bipartite graph $K_{a,b}$, with $a \leq b$, is fan-crossing free if and only if*

(i) $a \in \{1, 2\}$, *or*

(ii) $a \in \{3, 4\}$ *and* $b \leq 6$.

In particular, $K_{5,5}$ is not fan-crossing free.

We prove the theorem in several steps. Lemma 4.6 shows the sufficiency of Conditions i and ii in Thm. 4.5.

Lemma 4.6.

(i) The graph $K_{2,b}$ is fan-crossing free.

(ii) The graph $K_{4,6}$ is fan-crossing free.

Proof. Since the graph $K_{2,b}$ is planar for every positive integer b, it is clearly fan-crossing free. Moreover, Fig. 4.5 shows a fan-crossing free drawing of the graph $K_{4,6}$. The statement follows. □

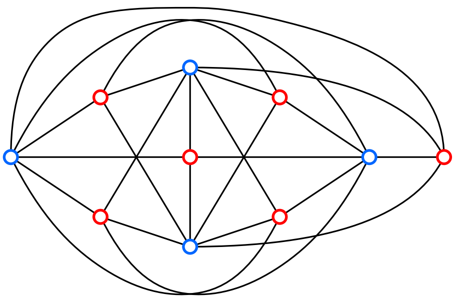

Fig. 4.5: A fan-crossing free drawing of $K_{4,6}$.

To prove the necessity of Conditions i and ii in Thm. 4.5, we show in the following that neither of the two graphs $K_{5,5}$ and $K_{3,7}$ allow a fan-crossing free drawing. Thereby we assume simplicity of the drawings. During the proof we consider various complete bipartite subgraphs of $K_{5,5}$ and $K_{3,7}$. For such a graph $K_{a,b}$ we denote the two independent parts by $U = \{u_1, \ldots, u_a\}$ and $W = \{w_1, \ldots, w_b\}$, respectively.

We start by considering the common subgraph $K_{2,2}$ of $K_{5,5}$ and $K_{3,7}$. There are two different simple embeddings for $K_{2,2}$. Figure 4.6 shows drawings for these embeddings. Since the graph $K_{3,5}$ is a subgraph of both, graph $K_{5,5}$ as well as $K_{3,7}$, the next lemma states that it is not necessary to consider both embeddings of $K_{2,2}$.

(a) (b)

Fig. 4.6: Drawings for the two simple embeddings of $K_{2,2}$. Note that the drawing in (a) has no crossings, while the drawing in (b) has exactly one crossing.

Lemma 4.7. *Let $\Gamma_{3,5}$ be a fan-crossing free drawing of $K_{3,5}$. There is a $K_{2,2}$-subgraph of $K_{3,5}$ whose edges do not cross each other in $\Gamma_{3,5}$.*

Proof. Let H be the $K_{2,2}$-subgraph induced by u_1, u_2, w_1, w_2 and Γ_H the drawing of H in $\Gamma_{3,5}$. If no two edges of Γ_H cross each other, the statement follows immediately. So we assume that there is at least one pair of crossing edges in Γ_H. Simplicity implies that only the edge pairs (u_1, w_2) and (u_2, w_1), or (u_1, w_1) and (u_2, w_2), can cross each other in Γ_H. Also by simplicity, it is not possible that both these pairs cross each other; see Fig. 4.7 for an illustration. Thus, we can assume that exactly one of these two edge pairs cross, say the pair (u_1, w_2) and (u_2, w_1). Figure 4.8a shows this configuration.

Now we consider another vertex $w_3 \in W$ of $\Gamma_{3,5}$ and determine in which of the regions depicted in Fig. 4.8a it may be placed.

First we consider the case in which w_3 is in the region R_1 (see Fig. 4.8b). For the edges incident to w_3 the following hold:

- Since adjacent edges are not allowed to cross, the edge (u_1, w_3) can cross neither (u_1, w_1) nor (u_1, w_2). For the same reason the edges (u_1, w_3) and (u_2, w_3) cannot cross.

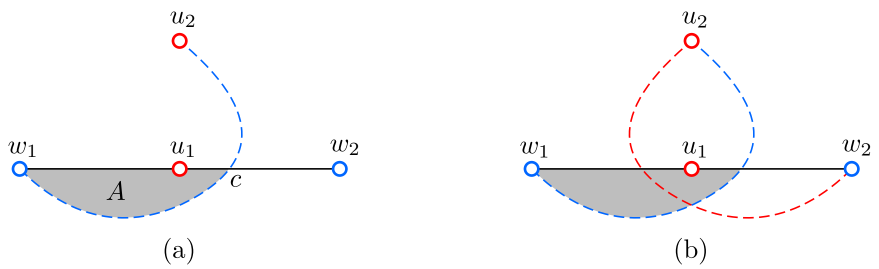

Fig. 4.7: (a) If (u_2, w_1) crosses (u_1, w_2) at a point c, then the cycle (w_1, u_1, c, w_1) encloses an area A. (b) If additionally (u_1, w_1) and (u_2, w_2) cross, then the edge (u_2, w_2) "enters" A at one point. In order to "leave" this area again, the condition of simplicity is violated: Either the edge (u_1, w_1) is crossed twice by (u_2, w_2), or (u_2, w_2) is crossing the adjacent edge (u_2, w_1).

- If the edge (u_1, w_3) would cross (u_2, w_1), it also would have to cross (u_2, w_2) in order to connect u_1 and w_3. But then (u_1, w_3) would cross a fan incident to u_2. So (u_1, w_3) cannot cross (u_2, w_1).
- Further, the edge (u_1, w_3) cannot cross the remaining edge (u_2, w_2), since otherwise it would have to cross a fan incident to u_2, too.

As a consequence, the edge (u_1, w_3) cannot cross any edge of H. Because of symmetry the same is also true for the edge (u_2, w_3). This implies that there are even two $K_{2,2}$-subgraphs in $\Gamma_{3,5}$ whose edges do not cross each other: the subgraph induced by the vertices u_1, u_2, w_3, w_1, and the subgraph induced by u_1, u_2, w_3, w_2.

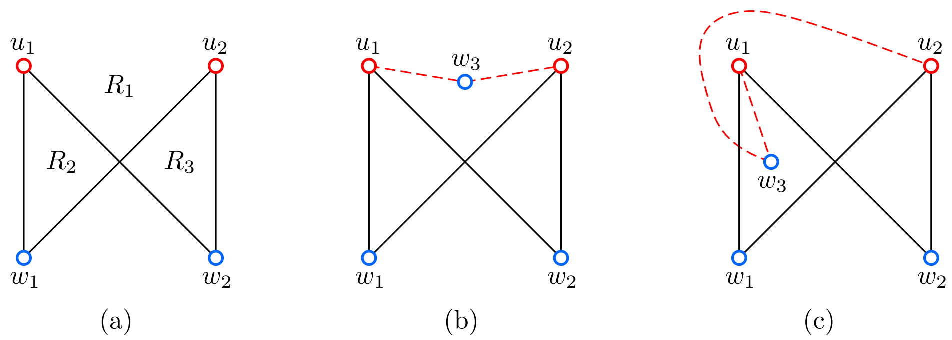

Fig. 4.8: (a) A drawing of the only embedding of H in which (u_1, w_2) and (u_2, w_1) cross each other. (b) Vertex w_3 is placed in the region R_1. The edges (u_1, w_3) and (u_2, w_3) (red edges) are crossing-free. (c) Vertex w_3 is placed in the region R_2. The edge (u_1, w_3) is crossing-free; the edge (u_2, w_3) crosses (u_1, w_1).

Finally we consider the case in which w_3 lies in region R_2 (see Fig. 4.8c). The case in which w_3 lies in R_3 is symmetric. Again we argue about the edges:

- Since adjacent edges do not cross, the edge (u_1, w_3) has no crossing with (u_1, w_1), (u_1, w_2) and (u_2, w_3).
- For the same reason the edge (u_2, w_3) has no crossing with (u_2, w_1) and (u_2, w_2).

– Further, the edge (u_1, w_3) cannot cross the edge (u_2, w_1), as otherwise (u_2, w_1) would be crossed by a fan, namely the fan (u_1, w_2), (u_1, w_3) anchored at u_1.

– The edge (u_2, w_3) cannot cross the edge (u_1, w_2) for the same reason.

Hence, the edge (u_1, w_3) has no crossing at all and the only possible crossing for (u_2, w_3) is a crossing with (u_1, w_1) (see Fig. 4.8c). However, in this specific case there is a $K_{2,2}$-subgraph with non-crossing edges: the graph induced by the vertices u_1, u_2, w_2, w_3. The statement of the lemma follows. □

Like in the proof of Lemma 4.7, let H be the graph induced by the vertices u_1, u_2, w_1, w_2. According to Lemma 4.7, we may assume in the following that in any fan-crossing free drawing of the graphs $K_{3,7}$ or $K_{5,5}$, respectively, the subgraph H is drawn in such a way that no two of its edges cross each other. Let Γ_H be such a drawing of H.

In the next step we insert successively the vertices w_3, w_4, and w_5 into the planar drawing of H. This is an intermediate step in reaching our final goal: We want to try to create all non-isomorphic fan-crossing free embeddings of $K_{5,5}$ and $K_{3,7}$, and – by finding no such embeddings – show that the graphs $K_{5,5}$ and $K_{3,7}$ are not fan-crossing free. In the following, we give representative drawings for the created embedding, rather than describing the embedding itself. Moreover, in an abuse of notation we use the word "embedding" and "drawing" as synonyms in the remainder of this chapter.

4.4.2.1 Adding vertex w_3

In this section we want to determine the set $\mathcal{D}_{2,3}$ of all non-isomorphic fan-crossing free embeddings that can be obtained when inserting vertex w_3 together with the edges (u_1, w_3) and (u_2, w_3) into Γ_H. Recall that each drawing $D \in \mathcal{D}_{2,3}$ must be simple, so edge (u_1, w_3) may cross neither of the edges (u_1, w_1), (u_1, w_2), and (u_2, w_3). Further, the edge (u_1, w_3) is not allowed to cross both edges (u_2, w_1) and (u_2, w_2) because the drawing D is fan-crossing free. However, edge (u_1, w_3) can have a crossing with at most one of the edges (u_2, w_1) and (u_2, w_2).

Similarly, we observe that the second "new" edge (u_2, w_3) is not allowed to cross one of the edges (u_2, w_1), (u_2, w_2), and (u_1, w_3); it can possibly cross one of edges (u_1, w_1) and (u_1, w_2), but not both.

Using these restrictions on (u_1, w_3) and (u_2, w_3), we obtain the fan-crossing free drawings that are listed in Fig. 4.9 when adding w_3, (u_1, w_3) and (u_2, w_3) to Γ_H.

However, many drawings in Fig. 4.9 are isomorphic, namely:

- Figs. 4.9a and 4.9j;
- Figs. 4.9b, 4.9d, 4.9f, 4.9h, 4.9k, 4.9m, 4.9n and 4.9p;
- Figs. 4.9c, 4.9e, 4.9g, 4.9i, 4.9l and 4.9o;

Given some different isomorphic embeddings we only need to consider one of them, since from all such embeddings we would obtain the same embeddings while inserting more vertices. Thus we only need to consider three different configurations; we will consider the ones from Figs. 4.9a to 4.9c, and denote them by D_1, D_2 and D_3, respectively.

4.4.2.2 Adding vertex w_4.

Let $\mathcal{D}_{2,4}$ be the set of all non-isomorphic fan-crossing free embeddings that can be obtained when inserting vertex w_4 together with the edges (u_1, w_4) and (u_2, w_4) into each of the drawings from $\mathcal{D}_{2,3} = \{D_1, D_2, D_3\}$. We consider the three different drawings separately and give restrictions on the configurations in each case.

For the drawing D_1 (see Fig. 4.9a and, for the reader's convenience, also Fig. 4.10a) we have the following:

- By simplicity, the edge (u_1, w_4) is not allowed to cross one of the edges (u_1, w_1), (u_1, w_2), (u_1, w_3) and (u_2, w_4);
- the edge (u_1, w_4) can cross at most one of the edges (u_2, w_1), (u_2, w_2) or (u_2, w_3) because of the fan-crossing free property;
- also by simplicity, the edge (u_2, w_4) is not allowed to cross (u_2, w_1), (u_2, w_2), (u_2, w_3) and (u_1, w_4);
- the fan-crossing freeness implies that (u_2, w_4) may cross at most one of the edges (u_1, w_1), (u_1, w_2) or (u_1, w_3).

These conditions yield the three non-isomorphic drawings depicted in Fig. 4.10.

Using simplicity and the fan-crossing free property also for D_2 (see Fig. 4.9b and also Fig. 4.11a), we obtain:

- the edge (u_1, w_4) cannot cross (u_1, w_1), (u_1, w_2), (u_1, w_3), (u_2, w_4) and (u_2, w_1);
- it is allowed to cross at most one of (u_2, w_2) and (u_2, w_3);
- the edge (u_2, w_4) cannot cross any of the edges (u_2, w_1), (u_2, w_2), (u_2, w_3), (u_1, w_4), and (u_1, w_3);
- it is allowed to cross at most one of the two edges (u_1, w_1) and (u_1, w_2).

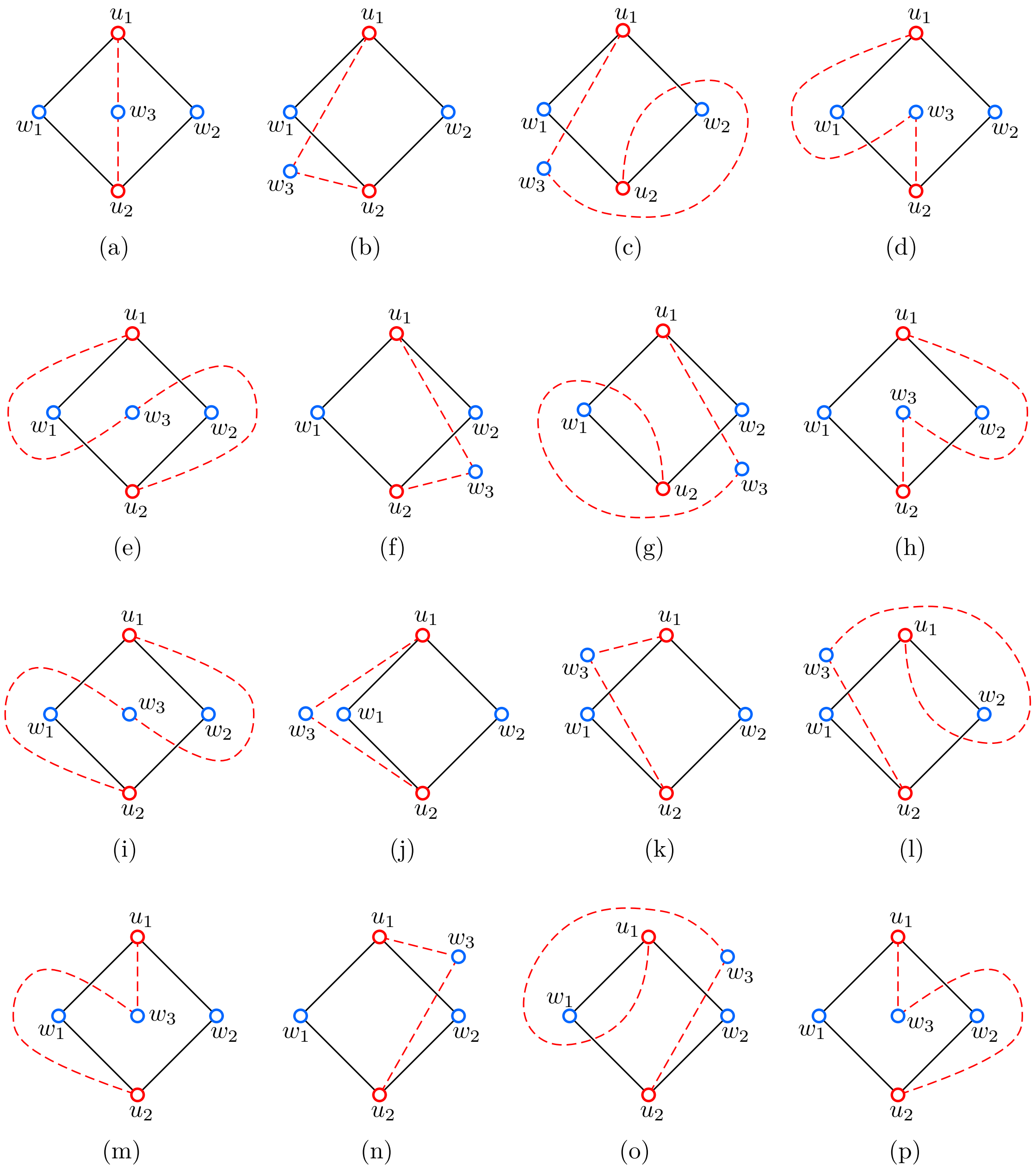

Fig. 4.9: All cases that preserve the fan-crossing free property when adding a third node w_3 (red) to the drawing Γ_H of $K_{2,2}$. The dashed red edges indicate the newly added edges.

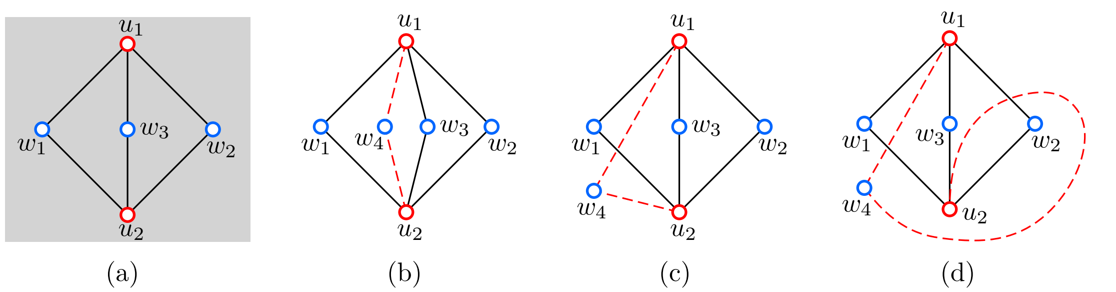

Fig. 4.10: (a) Drawing D_1. (b)–(d) All non-isomorphic drawings that preserve the fan-crossing free property when adding a fourth node w_4 to drawing D_1.

The seven non-isomorphic drawings we obtain by respecting these restrictions are shown in Fig. 4.11.

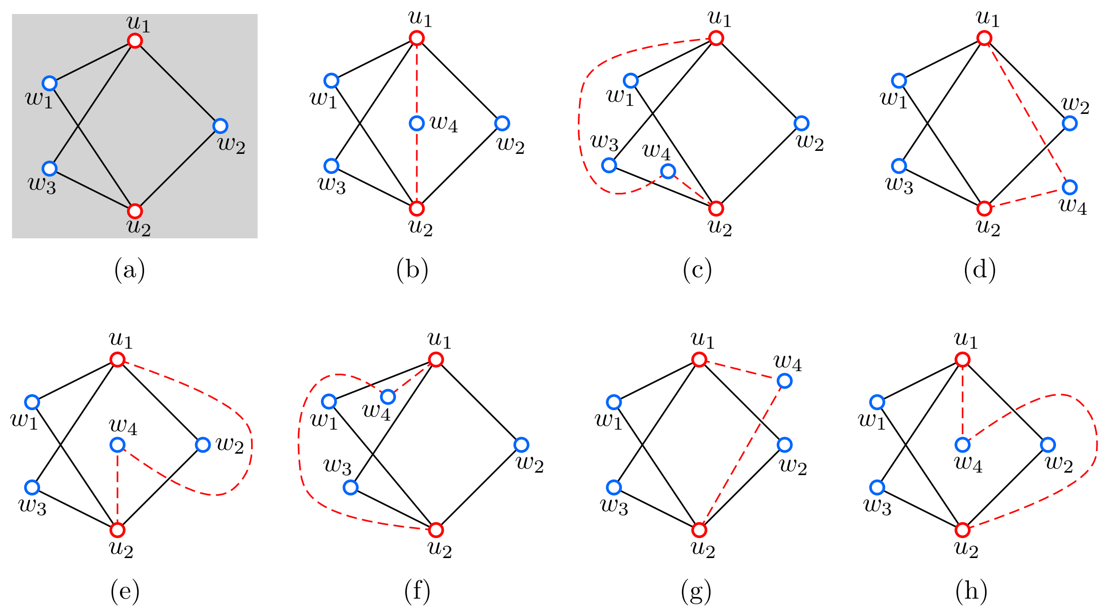

Fig. 4.11: (a) Drawing D_2. (b)–(h) All non-isomorphic drawings that preserve the fan-crossing free property, when adding a fourth node w_4 into D_2.

Finally, we have the following restrictions when considering D_3 (see Figs. 4.9c and 4.12a):

- since the edge (u_1, w_4) is not allowed to cross any of (u_1, w_1), (u_1, w_2), (u_1, w_3), (u_2, w_4), (u_2, w_1) and (u_2, w_3), the only edge it can actually cross is the edge (u_2, w_2);
- the edge (u_2, w_4) can also cross only one edge, namely the edge (u_1, w_1), since it is not allowed to cross (u_2, w_1), (u_2, w_2), (u_2, w_3), (u_1, w_4), (u_1, w_2) and (u_1, w_3).

Using these conditions we obtain only one non-isomorphic drawing when inserting w_4, (u_1, w_4) and (u_2, w_4) into D_3: the drawing in Fig. 4.12.

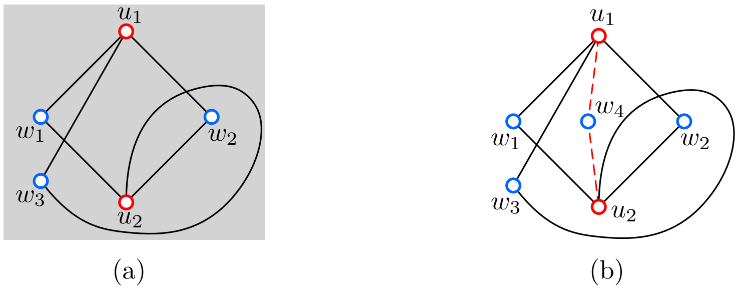

Fig. 4.12: (a) Drawing D_3. (b) The only drawing that preserves the fan-crossing free property, when adding a fourth node w_4 to D_3.

Comparing the drawings from Figs. 4.10, 4.11 and 4.12b, we observe that the following figures represent isomorphic embeddings:

- Figs. 4.10c and 4.11b;
- Figs. 4.10d, 4.11c, 4.11f and 4.12b;
- Figs. 4.11d and 4.11g;
- Figs. 4.11e and 4.11h.

So, in the following, it is sufficient to consider the five non-isomorphic configurations from Figs. 4.10b to 4.10d, 4.11d and 4.11e. Let the drawings in these figures be denoted by D'_1, D'_2, D'_3, D'_4 and D'_5, respectively. Thus, the set of non-isomorphic drawings is here $\mathcal{D}_{2,4} = \{D'_1, D'_2, D'_3, D'_4, D'_5\}$.

4.4.2.3 Adding vertex w_5.

Similarly to the last section, by $\mathcal{D}_{2,5}$ we denote the set of all non-isomorphic fan-crossing free embeddings that can be obtained by inserting vertex w_5, and edges (u_1, w_5) and (u_2, w_5) into each of the drawings from $\mathcal{D}_{2,4}$ in all possible ways.

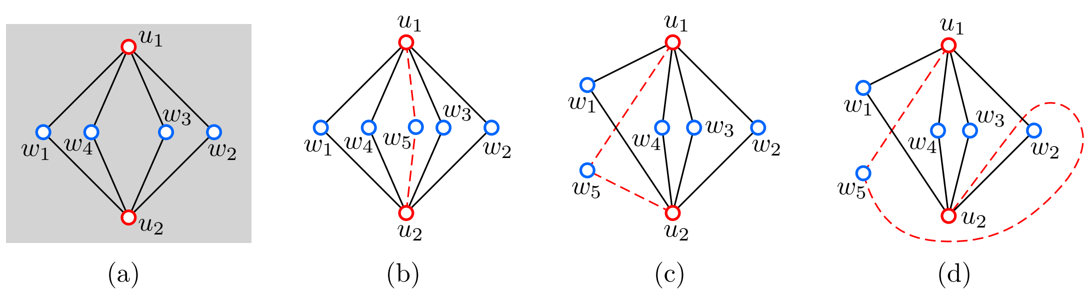

Fig. 4.13: (a) Drawing D'_1. (b)–(d) All non-isomorphic drawings that preserve the fan-crossing free property when adding a fifth node w_5 (together with its incident edges (u_1, w_5) and (u_2, w_5)) to the drawing D'_1.

First consider D'_1 (depicted in Figs. 4.10b and 4.13a). We observe the following:

– The edge (u_1, w_5) may not cross any of the edges (u_1, w_1), (u_1, w_2), (u_1, w_3), (u_1, w_4) and (u_2, w_5);

– it may cross at most one of the edges (u_2, w_1), (u_2, w_2), (u_2, w_3) and (u_2, w_4);

– the edge (u_2, w_5) is not allowed to cross any of the edges (u_2, w_1), (u_2, w_2), (u_2, w_3), (u_2, w_4) and (u_1, w_5);

– while it can cross at most one of the edges (u_1, w_1), (u_1, w_2), (u_1, w_3) and (u_1, w_4).

These restrictions yield the three non-isomorphic drawings shown in Fig. 4.13.

The restrictions for inserting w_5 into D'_2 (see Figs. 4.10c and 4.14a) are as follows:

– the edge (u_1, w_5) cannot cross any of (u_1, w_1), (u_1, w_2), (u_1, w_3), (u_1, w_4), (u_2, w_5) and (u_2, w_1);

– it is allowed to cross at most one of the edges (u_2, w_2), (u_2, w_3) and (u_2, w_4).

– the edge (u_2, w_5) cannot cross any of (u_2, w_1), (u_2, w_2), (u_2, w_3), (u_2, w_4), (u_1, w_5) and (u_1, w_4);

– it may cross at most one of the edges (u_1, w_1), (u_1, w_2) and (u_1, w_3).

Taking these restrictions into account, we obtain the 12 (not necessarily non-isomorphic) drawings shown in Fig. 4.14.

In the next step we consider the drawing D'_3 (see Figs. 4.10d and 4.15a):

– the edge (u_1, w_5) is not allowed to cross any of the edges (u_1, w_1), (u_1, w_2), (u_1, w_3), (u_1, w_4), (u_2, w_5), (u_2, w_1) and (u_2, w_4);

– it is allowed to cross at most one of the edges (u_2, w_2) and (u_2, w_3);

– the edge (u_2, w_5) cannot cross any of (u_2, w_1), (u_2, w_2), (u_2, w_3), (u_2, w_4), (u_1, w_5), (u_1, w_4) and (u_1, w_2);

– however, it can cross at most one of the edges (u_1, w_1) and (u_1, w_3).

These restrictions yield the drawings given in Fig. 4.15.

The drawing D'_4 (see Figs. 4.11d and 4.16a) gives us the following restrictions:

– the edge (u_1, w_5) is not allowed to cross any of (u_1, w_1), (u_1, w_2), (u_1, w_3), (u_1, w_4), (u_2, w_5), (u_2, w_1) and (u_2, w_2);

– it may cross at most one of (u_2, w_3) and (u_2, w_4);

– the edge (u_2, w_5) is not allowed to cross any of (u_2, w_1), (u_2, w_2), (u_2, w_3), (u_2, w_4), (u_1, w_5), (u_1, w_3) and (u_1, w_4);

– but it may cross at most one of the edges (u_1, w_1) and (u_1, w_2).

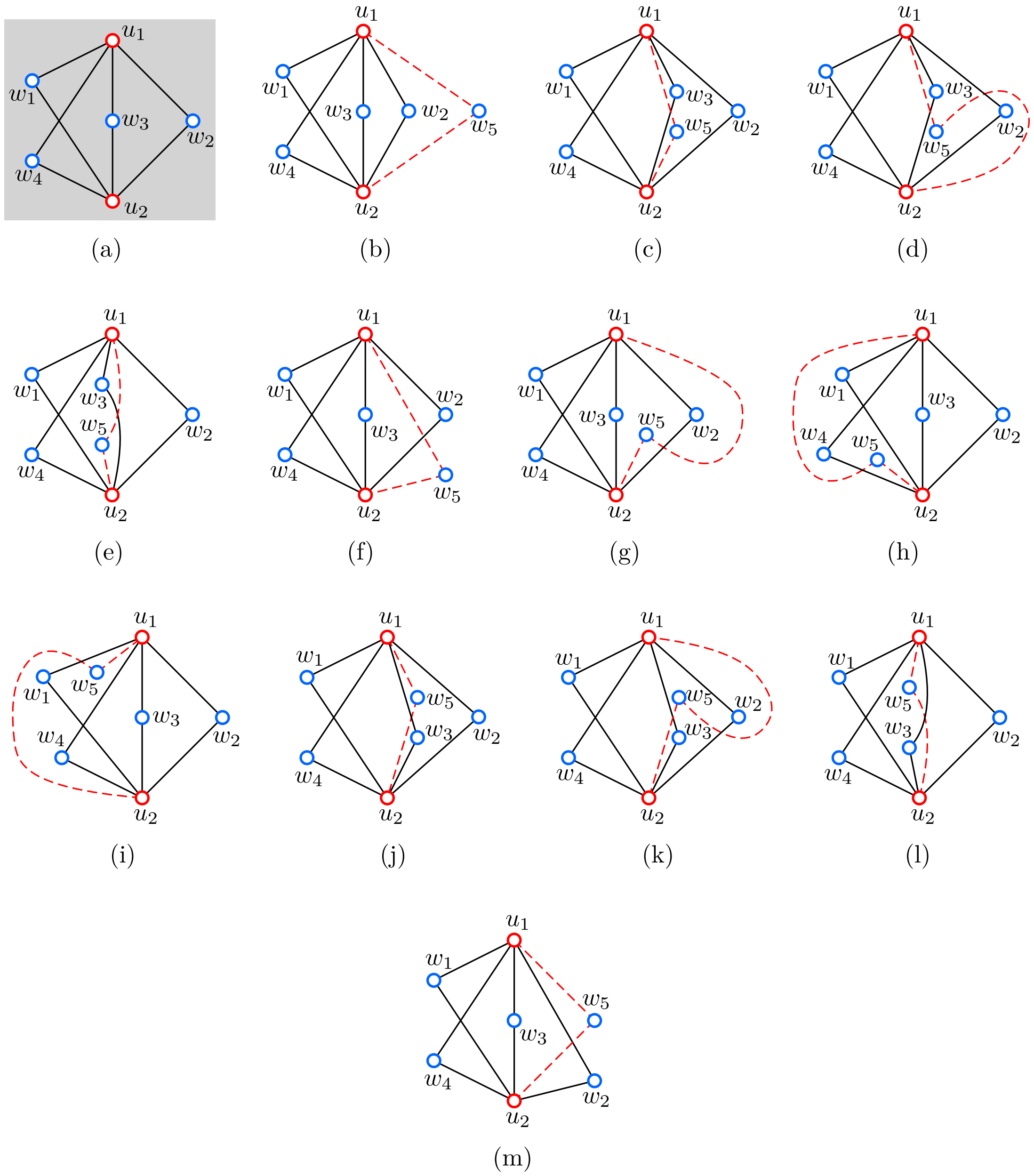

Fig. 4.14: (a) Drawing D_2'. (b)–(m) All drawings that preserve the fan-crossing free property, when adding w_5 to D_2'.

Using these restrictions we obtain the drawings shown in Fig. 4.16.

In the last step we consider the drawing D_5' (see Figs. 4.11e and 4.17a). The restrictions are in this case:

– the edge (u_1, w_5) is not allowed to cross any of the edges (u_1, w_1), (u_1, w_2), (u_1, w_3), (u_1, w_4), (u_2, w_5), (u_2, w_1) and (u_2, w_2);

– however, it is allowed to cross at most one of the edges (u_2, w_3) and (u_2, w_4);

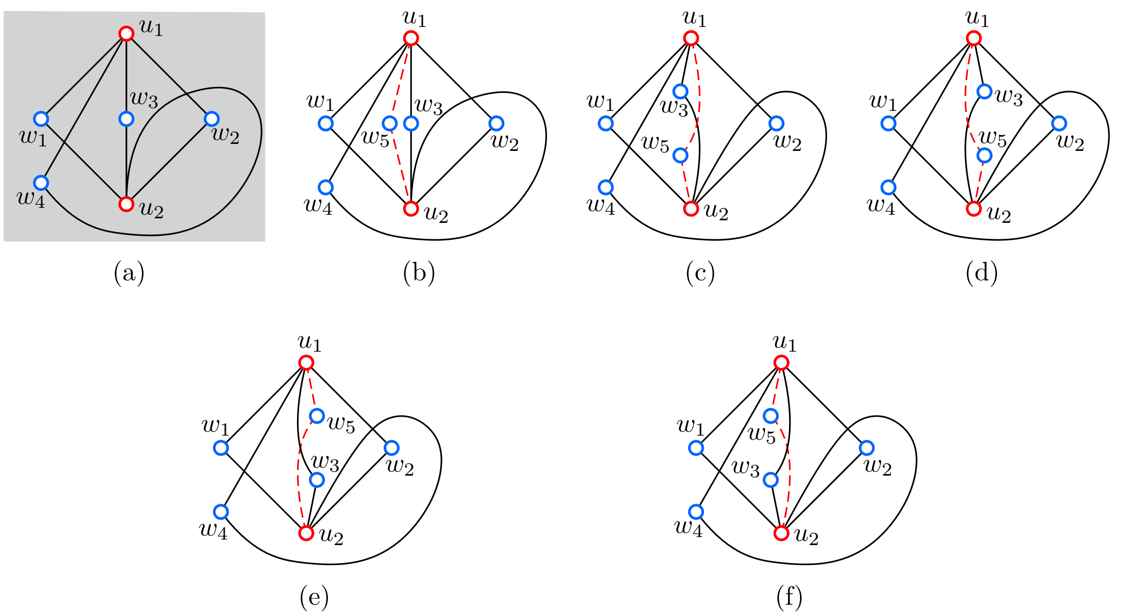

Fig. 4.15: (a) Drawing D_3'. (b)–(f) All fan-crossing free drawings we obtain by adding vertex w_5 to drawing D_3'.

– the edge (u_2, w_5) cannot cross any of (u_2, w_1), (u_2, w_2), (u_2, w_3), (u_2, w_4), (u_1, w_5), (u_1, w_3) and (u_1, w_4);

– it may cross at most one of the edges (u_1, w_1) and (u_1, w_2).

Minding these restrictions, we obtain the drawings depicted in Fig. 4.17.

Finally, by comparing the drawings from Figs. 4.13 to 4.17, we observe that the following figures represent isomorphic embeddings:

(1) Figs. 4.13c and 4.14b;

(2) Figs. 4.13d, 4.14h, 4.14i and 4.15b;

(3) Figs. 4.14c, 4.14j and 4.16c;

(4) Figs. 4.14d, 4.14k, 4.15d, 4.15e, 4.16d to 4.16g, 4.17e and 4.17g;

(5) Figs. 4.14e, 4.14g, 4.14l, 4.17b and 4.17c;

(6) Figs. 4.14f, 4.14m and 4.16b;

(7) Figs. 4.15f, 4.17d, 4.17f and 4.17g. In fact, these embeddings are isomorphic to the embeddings listed in Point 4.

Note that the drawing shown in Fig. 4.13b is not isomorphic to any other drawing and therefor has to be considered further. Therefore we have to consider seven non-isomorphic embeddings in the future: The ones given in Figs. 4.13b to 4.13d and 4.14c to 4.14f. We denote these drawings by Γ_1 to Γ_7, and thus have $\mathcal{D}_{2,5} = \{\Gamma_1, \Gamma_2, \Gamma_3, \Gamma_4, \Gamma_5, \Gamma_6, \Gamma_7\}$. For the reader's convenience these drawings

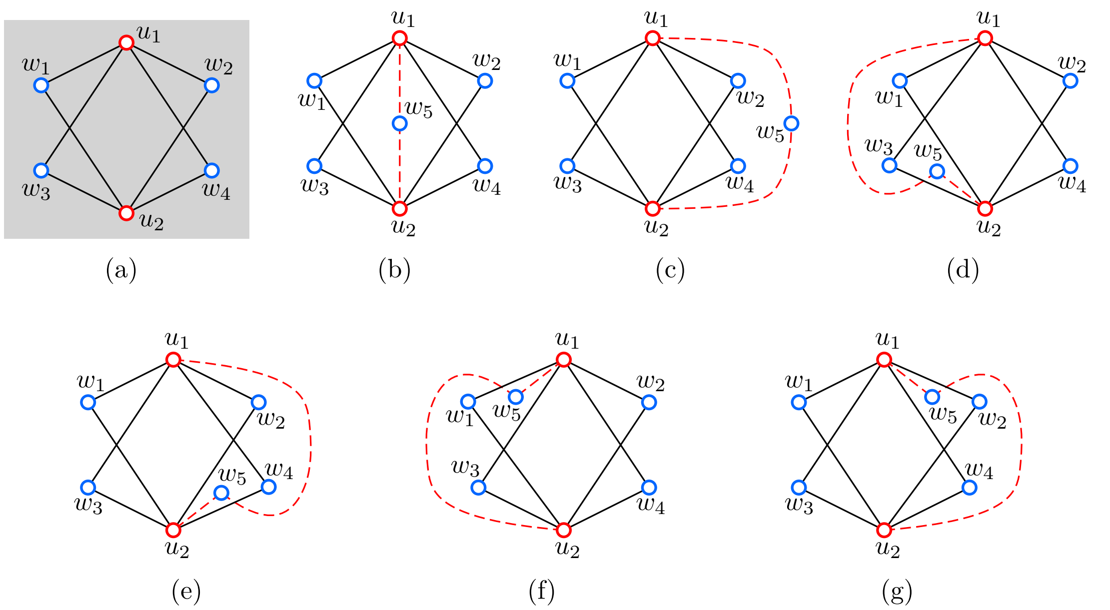

Fig. 4.16: (a) Drawing D'_4. (b)–(g) All drawings that preserve the fan-crossing free property when adding vertex w_5 to D'_4.

are shown again in Fig. 4.18. Summarizing our results so far, we have shown the following lemma.

Lemma 4.8. *There are exactly seven simple non-isomorphic fan-crossing free embeddings of* $K_{2,5}$*, namely the embeddings in* $\mathcal{D}_{2,5}$*.*

Recall that our goal is to show that neither of the two graphs $K_{3,7}$ and $K_{5,5}$ is fan-crossing free. By Lemma 4.8, it suffices to show the following:

(1) It is not possible to add the remaining vertices u_3, u_4 and u_5 to a drawing of $\mathcal{D}_{2,5}$ without violating the fan-crossing free property. This will show that $K_{5,5}$ is not fan-crossing free.

(2) It is not possible to add the remaining vertices u_3, w_6 and w_7 to a drawing of $\mathcal{D}_{2,5}$ without violating the fan-crossing free property. This will show that $K_{3,7}$ is not fan-crossing free.

We will consider both graphs separately. Before we do so, we introduce two lemmas that are useful in the further proof.

4.4.2.4 Lemmas for the proof

We start by observe the following: Given a drawing Γ with vertices $u_1, \ldots, u_a \in U$ and $w_1, \ldots, w_{b-1} \in W$ (thereby U and W and the corresponding vertices are swappable). In order to respect simplicity and fan-crossing freeness, the insertion of

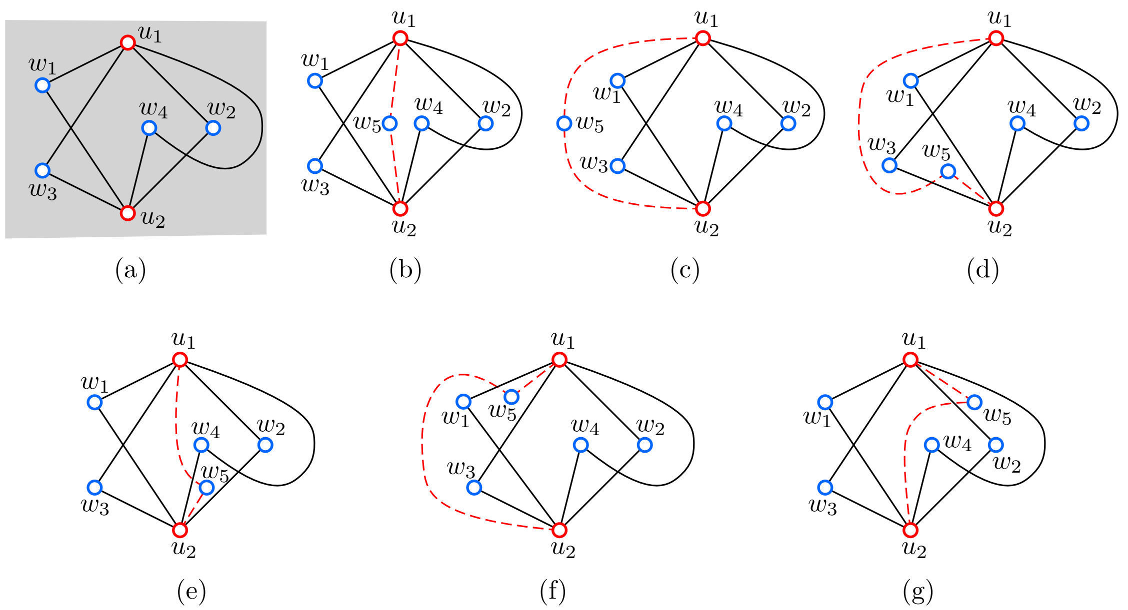

Fig. 4.17: (a) Drawing D'_5. (b)–(g) All fan-crossing free drawings we obtain when adding w_5 to D'_5.

w_b is subject to some restrictions. Namely, there are some regions (where a region is a face in the planarization of Γ) in which vertex w_b cannot be inserted without violating simplicity or fan-crossing freeness for an edge (u_i, w_b) incident to a certain vertex u_i. We call such a region *blocked* for w_b with respect to u_i. Further, the *range* of vertex u_i regarding w_b is the union of all regions that are not blocked for w_b. The *common range* with respect to w_b of two or more vertices from U is the intersection of the ranges for these vertices. Note that if the common range is empty, then it is not possible to place w_b in Γ.

The first lemma points out such a configuration, in which a specific region of a drawing is blocked for another vertex from U. This configuration is illustrated in Fig. 4.19a.

Lemma 4.9 (Triangle Lemma)**.** *Let Γ be a fan-crossing free drawing of $K_{a,b}$ with $a \geq 3$ and $b \geq 5$. Suppose there is a region R of Γ bounded by an edge (u_1, w_i) and by two crossing edges (u_1, w_j), (u_2, w_i), with $1 \leq i, j \leq 5$. If at least four vertices of W lie outside of the region R, there is no vertex $u_h \in U$, where $3 \leq h \leq a$, inside R.*

Stating the Triangle Lemma in terms of blocked regions, we have that R is blocked for u_h with respect to some vertex $w_i \in W$.

Proof. Suppose for a contradiction that R contains a vertex $u_h \in U$, with $3 \leq h \leq a$, and at least four vertices of W lie outside of R. Let $e_1, \ldots, e_4$ be edges between u_h and four different vertices which are positioned outside of R. Then each of $e_1, \ldots, e_4$

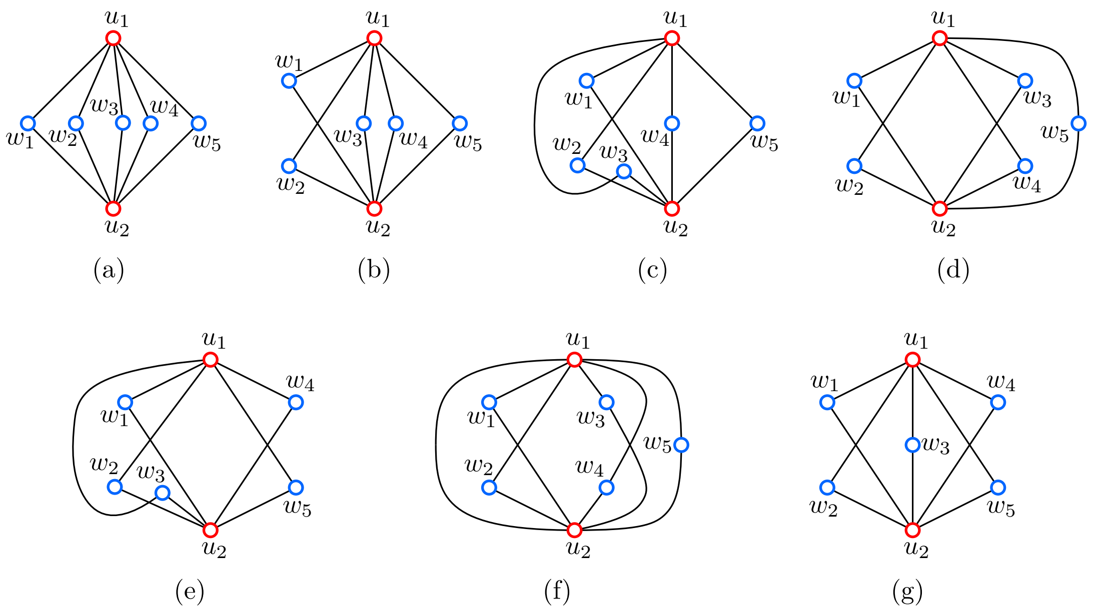

Fig. 4.18: All topologically different drawings of the subgraph $K_{2,5}$ that are fan-crossing free. Note that the nodes are relabeled in comparison to the Figures above.

crosses at least one of the three edges bounding R. By the pigeonhole principle, at least one of these three bounding edges must be crossed by two (or more) edges of e_1, e_2, e_3 and e_4. However, this would violate the fan-crossing free property of Γ, a contradiction. □

The second lemma considers another configuration, in which we can say something about the number of vertices in certain regions. An illustration for this configuration can be found in Figs. 4.19b and 4.19c.

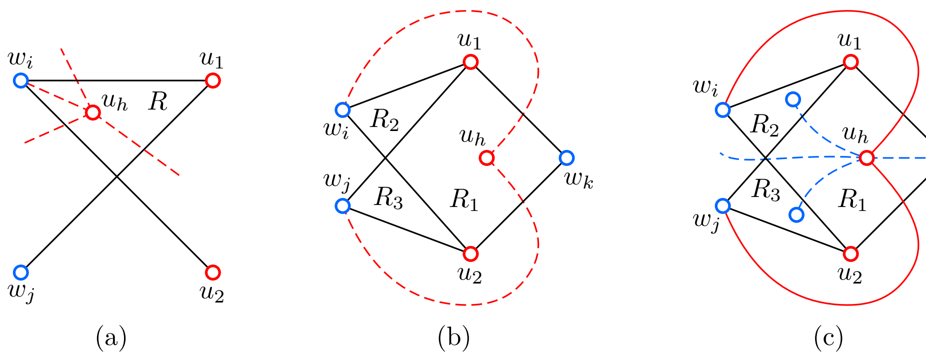

Fig. 4.19: (a) Illustration for the configuration of the Triangle Lemma (Lemma 4.9). (b) and (c) are illustrations for the configurations of the Beetle Lemma (Lemma 4.10).

Lemma 4.10 (Beetle Lemma). *Let Γ be a fan-crossing free drawing of $K_{a,b}$ with $a \geq 3$ and $b \geq 5$ and let $1 \leq i, j, k \leq 5$. Suppose there is a region R_1 that does not contain the vertices w_i and w_j and is bounded by two edges (u_1, w_k) and (u_2, w_k), and by two edges (u_1, w_j) and (u_2, w_i) that cross each other. Further suppose that there is a region R_2 bounded by the edges (u_1, w_i) and edge (u_1, w_j), and a region R_3 bounded by the edges (u_2, w_j) and (u_2, w_i). Then the following holds:*

(i) At most one vertex $u_h \in U$ is placed in R_1, where $3 \leq h \leq a$.

(ii) If a vertex u_h is placed in R_1, the edge (u_h, w_i) crosses (u_1, w_k) and the edge (u_h, w_j) crosses (u_2, w_k).

(iii) Further, if a vertex u_h is placed in R_1, at most two vertices of $W \setminus \{w_i, w_j, w_k\}$ are placed outside R_1; one of these vertices lies in R_2 and the other in R_3.

Proof. Suppose that a vertex u_h, with $3 \leq h \leq a$, is placed in the region R_1.

First we claim that (u_h, w_i) and (u_h, w_j) cross the edges (u_1, w_k) and (u_2, w_k), respectively; see Fig. 4.19b. Observe that edge (u_h, w_i) cannot cross (u_1, w_j), since such a crossing would create a fan-crossing, namely (u_1, w_j) would be crossed by the fan $\{(w_i, u_h), (w_i, u_2)\}$. Further, the edge (u_h, w_i) is not allowed to cross (u_2, w_i), since then it would have to cross edge (u_2, w_j) as well; however, this would be a fan-crossing. Because of symmetry, the edge (u_h, w_j) also crosses neither (u_1, w_j) nor (u_2, w_i). If both edges (u_h, w_i) and (u_h, w_j) would cross (u_1, w_k), the drawing Γ would contain a fan-crossing; so this constellation is not possible, as well as a crossing of (u_2, w_k) by both edges (u_h, w_i) and (u_h, w_j). Thus, there are two possible crossing configurations for the edges (u_h, w_i) and (u_h, w_j): Either (u_h, w_i) crosses (u_1, w_k) and (u_h, w_j) crosses (u_2, w_k), or (u_h, w_i) crosses (u_2, w_k) and (u_h, w_j) crosses (u_1, w_k). But in fact, the latter constellation is impossible: if (u_h, w_i) crosses (u_2, w_k), and (u_h, w_j) crosses (u_1, w_k), then (u_h, w_i) and (u_h, w_j) cross each other, which violates simplicity. The claim follows.

Now it is easy to see that another vertex $u_z \in U$, with $z \in \{3, \ldots, a\} \setminus \{h\}$ cannot be placed in R_1: For such a vertex the same "rules" would hold as for u_h and its edges. So the edge (u_z, w_i) would need to cross (u_1, w_k), creating a fan-crossing between (u_1, w_k) and $\{(w_i, u_h), (w_i, u_z)\}$. So the first statement of the lemma follows.

To prove the second statement, we assume that u_h is placed in R_1, and as a consequence edge (u_h, w_i) crosses (u_1, w_k) and edge (u_h, w_j) crosses (u_2, w_k). We consider the placement of a vertex $w_x \in W \setminus \{w_i, w_j, w_k\}$ in Γ outside of the region R_1 (for an illustration see Fig. 4.19c). Suppose that w_x is also outside of R_2 and R_3. In this case, by the fan-crossing free property, the edge (u_h, w_x) crosses both edges (u_1, w_j) and (u_2, w_i); therefore it is (again by the fan-crossing property) not possible to place any other vertex of $W \setminus \{w_i, w_j, w_k, w_x\}$ outside of R_1. Finally, if w_x is placed in R_2, the edge (u_h, w_x) can be drawn such that it crosses only the single edge (u_1, w_j); in doing so, we still have the option to place an additional vertex $w_y \in W \setminus \{w_i, w_j, w_k, w_x\}$ in the region R_3 and draw the edge (u_h, w_y) by crossing (u_2, w_i). We conclude by noting that if both edges, (u_h, w_x) as well as (u_h, w_y), are present in Γ, there cannot be another vertex of W outside the region R_1 without violating fan-crossing freeness. □

In the following we call the vertices w_i and w_j in Lemma 4.10 the *eyes* of the beetle, the vertex w_k the *tail*, the vertices u_1 and u_2 *legs*, the region R_1 *shell*, and for a vertex u_h placed in R_1 we call (u_h, w_i) and (u_h, w_j) *wings* of the beetle.

The next corollary is a direct consequence of Lemma 4.10.

Corollary 4.11 (Empty-Shell Corollary). *Let $1 \leq i, j, k, \ell \leq 5$ pairwise distinct. Suppose a drawing Γ fulfills the requirements of the Beetle Lemma for legs u_1, u_2, eyes w_i, w_j, tail w_k and shell R_1. Further suppose that Γ also fulfills the requirements of the Beetle Lemma for legs u_1, u_2, eyes w_i, w_j, tail w_ℓ and shell R'_1. Then there is no vertex $u_h \in U$ in the common region $R^\star_1 = R_1 \cap R'_1$ of R_1 and R'_1.*

Proof. Suppose there is a vertex $u_h \in U$ in $R^\star_1$ (for an illustration see Fig. 4.20). By Property ii of the Beetle Lemma, the wing (u_h, w_i) crosses both edges (u_1, w_k) and (u_1, w_ℓ). This violates the fan-crossing free property of Γ. The statement follows. □

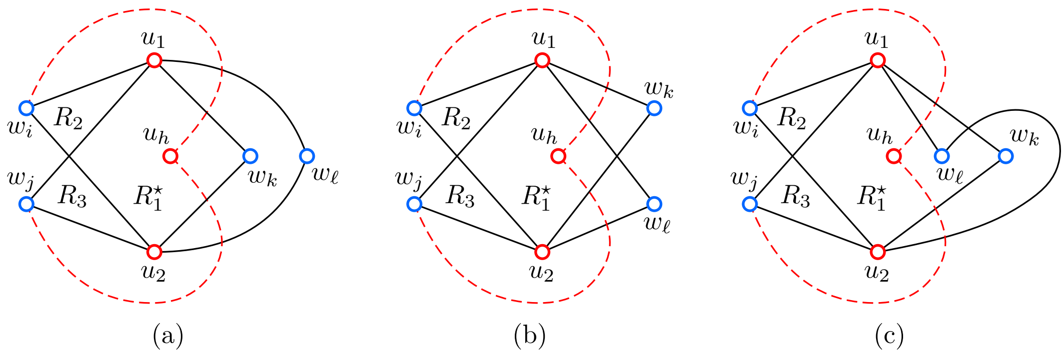

Fig. 4.20: Illustration for Cor. 4.11.

In the reminder of this chapter we exploit the Triangle Lemma, the Beetle Lemma, the Empty-Shell Corollary, as well as the observation from the beginning of blocked regions and the range of a certain vertex.

4.4.2.5 The graph $K_{5,5}$ is not fan-crossing free

In this section we continue with the proof of Thm. 4.5; namely we show the following lemma.

Lemma 4.12. *None of the seven drawings $\Gamma_1, \dots, \Gamma_7$ of $K_{2,5}$ can be extended to a drawing of $K_{5,5}$.*

Proof. We prove the statement by looking at each of the seven fan-crossing free drawings $\Gamma_1, \dots, \Gamma_7$ of $K_{2,5}$, and by arguing why none of them can be extended to a fan-crossing free drawing of $K_{5,5}$.

The drawing Γ_1. There are five regions in Γ_1. We denote these regions by $R_1, \dots, R_5$, as depicted in Fig. 4.21a. Since all these regions are topologically equivalent, it suffices to consider the placement of u_3 in only one of them, say R_1.

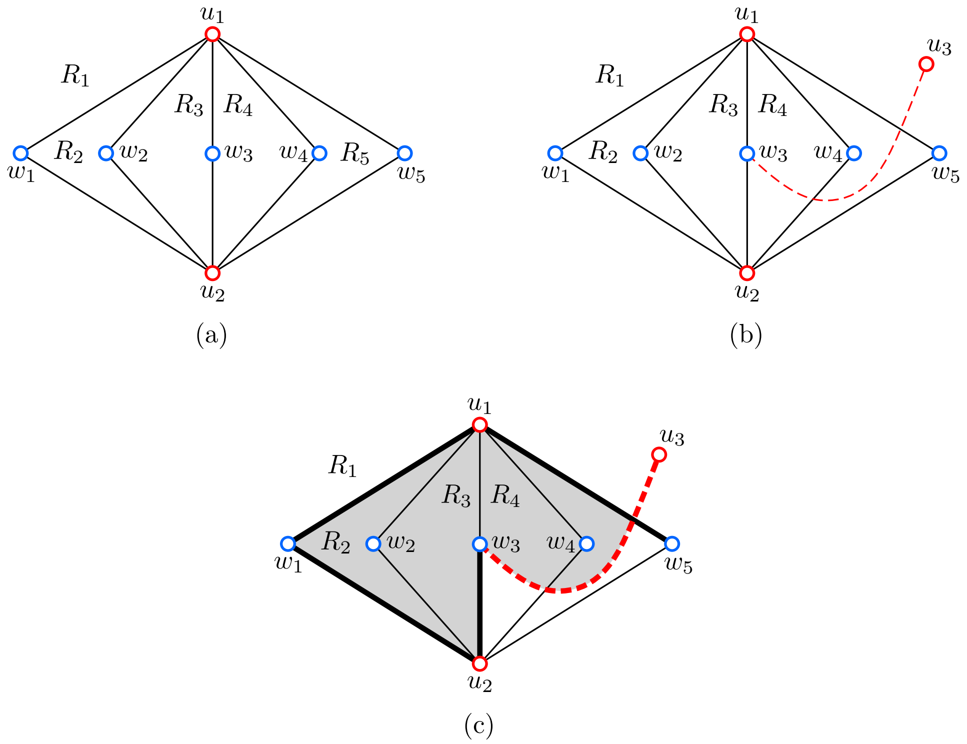

Fig. 4.21: (a) The regions in Γ_1. (b) The dashed red line represents the edge (u_3, w_3). (c) The range of w_3 with respect to u_3 is highlighted in gray. The bold edges indicate the boundary of the range.

In order to draw the edge (u_3, w_3) in a fan-crossing free way, it is necessary to cross exactly one edge incident to u_1 and exactly one edge incident to u_2; without loss of generality we assume that (u_1, w_5) and (u_2, w_4) are these edges (see the dashed red edge in Fig. 4.21b for an illustration). With this configuration we observe the following: The edge (u_3, w_4) may not cross (u_1, w_5) (otherwise the fan-crossing free property is violated), and it may not cross (u_3, w_3) (because of simplicity). Further, it cannot cross a fan. Thus, the region R_1 is not in the range of w_3 regarding u_3 (see also Fig. 4.21c).

So we have shown that it is not even possible to extend Γ_1 to a fan-crossing free drawing of $K_{3,5}$.

The drawing Γ_2. There are six regions in Γ_2, which we denote by $R_1, \ldots, R_6$ as shown in Fig. 4.22a.

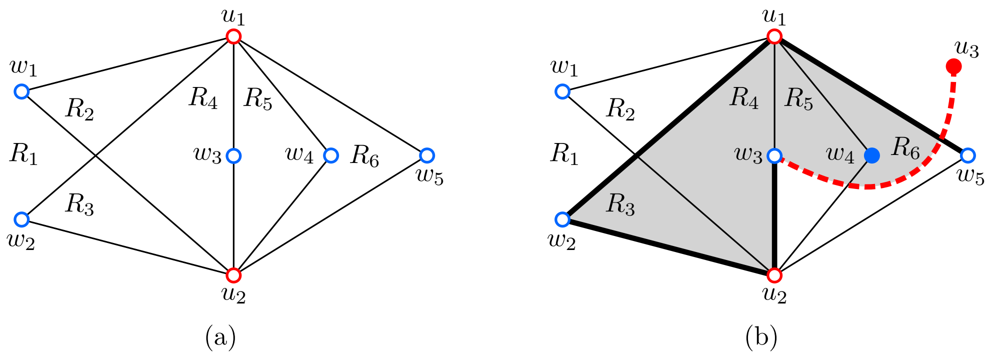

Fig. 4.22: (a) The regions in Γ_2. (b) Vertex u_3 is placed in region R_1 and the edge (u_3, w_3) (dashed red) crosses (u_1, w_5) and (u_2, w_4). It is not possible to connect u_3 and w_4 (filled vertices) without violating simplicity or fan-crossing freeness. In order to satisfy the fan-crossing free condition for the edge (u_3, w_4), this edge may not "leave" the gray area.

First we observe that the following configurations are impossible:

- The vertices u_3, u_4, u_5 cannot lie in the regions R_2 or R_3 by the Triangle Lemma;
- the vertices u_3, u_4, u_5 cannot be in the regions R_4 or R_5 by the Empty-Shell Corollary Cor. 4.11;
- at most one of vertices u_3, u_4, u_5 can lie in region R_6 by Property i of the Beetle Lemma.

By the previous analysis, at least two vertices, say u_3 and u_4, are placed in region R_1. At most one of the two edges (u_3, w_3) and (u_4, w_3) can cross the edge pair (u_1, w_2) and (u_2, w_1). This implies that at least one of these edges has to cross the pair (u_1, w_4) and (u_2, w_5), or the pair (u_1, w_5) and (u_2, w_4). We assume w. l. o. g that (u_3, w_3) crosses (u_1, w_5) and (u_2, w_4) (see the dashed red edge in Fig. 4.22b). But then it is no longer possible to draw the edge (u_3, w_4) without violating simplicity or the fan-crossing free property: Region R_1, where u_3 is located, is not in the range of w_4 regarding u_3 (for an illustration see the gray area in Fig. 4.22b). Namely, by simplicity the edge (u_3, w_4) cannot cross (u_3, w_3); since crossing (u_1, w_5) would create a fan-crossing, this is also not possible; in fact, the edge (u_3, w_4) is allowed to cross (u_1, w_3) and (u_2, w_1), nevertheless it cannot cross any of the edges (u_1, w_2), (u_2, w_3) and (u_2, w_2) (see the thick black edges in Fig. 4.22b).

The arguments above imply that Γ_2 cannot be extended to a fan-crossing free drawing of $K_{5,5}$.

The drawing Γ_3. There are seven regions in Γ_3, which we denote by $R_1, \ldots, R_7$ as shown in Fig. 4.23a.

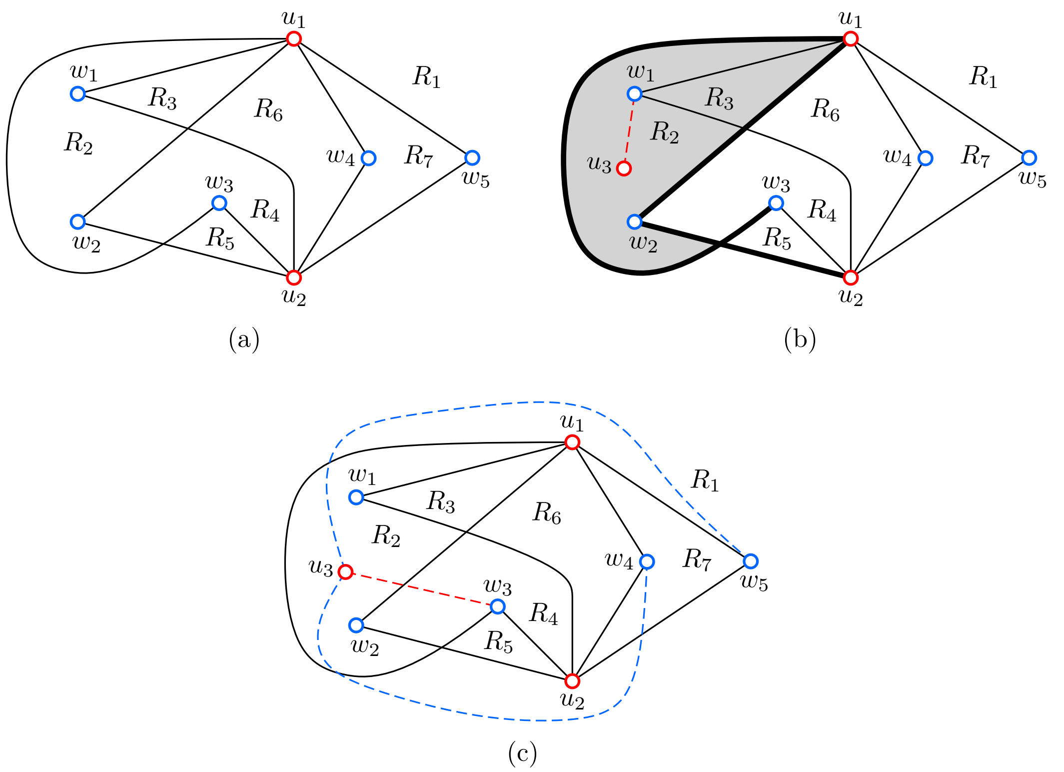

Fig. 4.23: (a) The regions in Γ_3. (b) The area $A = R_2 \cup R_3$ in gray. A vertex u_3 and the edge (u_3, w_1) (dashed red) must be in this area. (c) The dashed blue lines indicate the two edges (u_3, w_4) and (u_3, w_5) that are not drawable without fan-crossings when adding vertex u_3 in R_2.

Again we observe some implications of the Triangle Lemma, the Beetle Lemma, and the Empty-Shell Corollary:

- the Triangle Lemma implies that none of the vertices u_3, u_4, u_5 can be in R_3 or in R_5;
- none of the vertices u_3, u_4, u_5 can be in R_6 by the Empty-Shell Corollary;
- also by the Empty-Shell Corollary, none of the vertices u_3, u_4, u_5 can lie in R_1, where w_2 and w_3 are the eyes of both beetles, vertex w_4 and w_5, respectively, are the tails of the beetles, and R_1 is the intersection of the two shells of the beetles;

– the vertices u_3, u_4, u_5 cannot lie in region R_7 by Property ii of the Beetle Lemma: if u_i is placed in R_7 for $3 \leq i \leq 5$, the edge (u_1, w_3) would be crossed by the fan $\{(u_i, w_1), (u_i, w_2)\}$.

Thus, the vertices u_3, u_4, u_5 can only be placed in the regions R_2 and R_5.

Now consider the edges $(u_3, w_1), (u_4, w_1)$ and (u_5, w_1). None of these edges can cross (u_1, w_2), since this would create a fan-crossing. Further the fan-crossing free property implies that only one of these edges can cross the edge (u_1, w_3), and only one of them can cross (u_2, w_2). Since w_1 lies in an area $A = R_2 \cup R_3$ delimited by $(u_1, w_2), (u_1, w_3)$ and (u_2, w_2) (see gray area in Fig. 4.23b), at least one of of the edges $(u_3, w_1), (u_4, w_1)$ and (u_5, w_1) must be entirely in A. Consequently, one of the vertices u_3, u_4, u_5 must be in A, say u_3, and since u_3 cannot be in R_3 it must lie in R_2.

Then the edge (u_3, w_3) can neither cross (u_1, w_3), nor (u_2, w_2), nor the pair of edges (u_1, w_1) and (u_1, w_2), nor the pair (w_1, u_1) and (w_1, u_2). This implies that the edge (u_3, w_3) must cross (u_1, w_2) (see dashed red edge in Fig. 4.23c). Further we note that the edges (u_3, w_4) and (u_3, w_5) can cross neither (u_3, w_3) (this would violate simplicity) nor (u_1, w_2) (this would violate the fan-crossing free property). So both edges (u_3, w_4) and (u_3, w_5) have to cross (u_1, w_3) (see the dashed blue edges in Fig. 4.23c). However, this configuration has a fan-crossing and is therefore also not possible.

Hence, the drawing Γ_3 cannot be extended to a fan-crossing free drawing of $K_{5,5}$.

The drawing Γ_4. There are seven regions in Γ_4, which we denote by $R_1, \ldots, R_7$ as shown in Fig. 4.24.

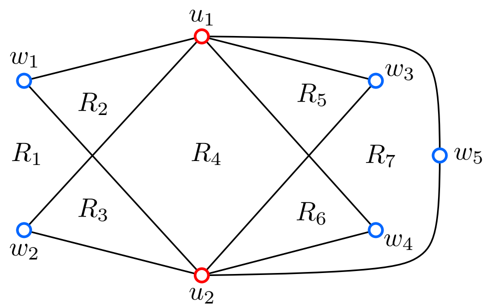

Fig. 4.24: The seven regions in Γ_4.

For Γ_4 we have the following consequence of the Beetle Lemma, Property i: At most one of the vertices u_3, u_4, u_5 can be in $R_4 \cup R_5 \cup R_6 \cup R_7$, and at most one of them can be in $R_1 \cup R_2 \cup R_3 \cup R_4$. We obtain immediately that not all the three vertices u_3, u_4, u_5 and their incident edges can be placed in Γ_4 such that the resulting drawing is a fan-crossing free drawing of $K_{5,5}$.

The drawing Γ_5**.** In Γ_5 we have eight regions, which we denote by $R_1, \ldots, R_8$ as shown in Fig. 4.25.

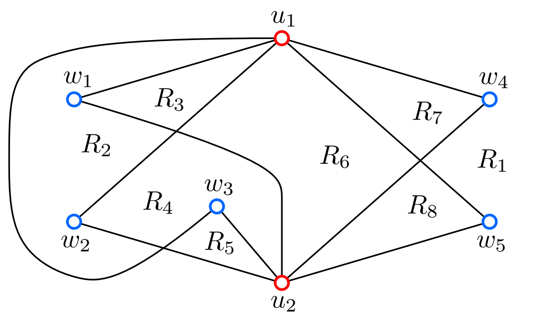

Fig. 4.25: The eight regions in Γ_5.

The Triangle Lemma 4.9 and the Empty-Shell Corollary 4.11 imply the following:

- According to the Triangle Lemma, none of the vertices u_3, u_4, u_5 can lie in R_3, R_5, R_7, R_8;
- the vertices u_3, u_4 and u_5 can be neither in R_4 nor in R_6 by the Empty-Shell Corollary;
- also none of the vertices u_3, u_4 and u_5 can be in region R_1, again by the Empty-Shell Corollary (note that the eyes of the two beetles are w_2 and w_3, the tails are w_4 and w_5, respectively, the shells are $R_1 \cup R_8$ and $R_1 \cup R_7$, respectively).

So all vertices u_3, u_4, u_5 must be in the region R_2, but this is not possible: According to the Beetle Lemma, Property ii, at most one of the vertices u_3, u_4 and u_5 can be in R_2.

This shows that the drawing Γ_5 cannot be extended to a fan-crossing free drawing of the bipartite graph $K_{5,5}$.

The drawing Γ_6**.** There are seven regions in the drawing Γ_6, which are denoted by $R_1, \ldots, R_7$ as depicted in Fig. 4.26.

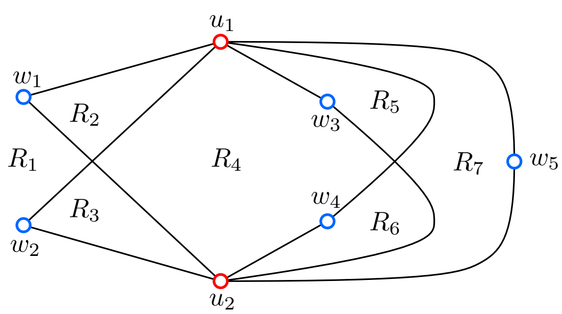

Fig. 4.26: The regions in Γ_6.

We observe the following:

– None of the vertices u_3, u_4, u_5 can lie in any of the regions R_2, R_3, R_5, R_6 by the Triangle Lemma;

– further, none of the vertices u_3, u_4, u_5 can be placed in R_1, R_4 or R_7 by the Empty-Shell Corollary.

Hence, the drawing Γ_6 cannot be extended to a fan-crossing free drawing of $K_{5,5}$.

The drawing Γ_7. Finally we consider drawing Γ_7. There are seven regions which we denote by $R_1, \ldots, R_7$ as shown in Fig. 4.27a.

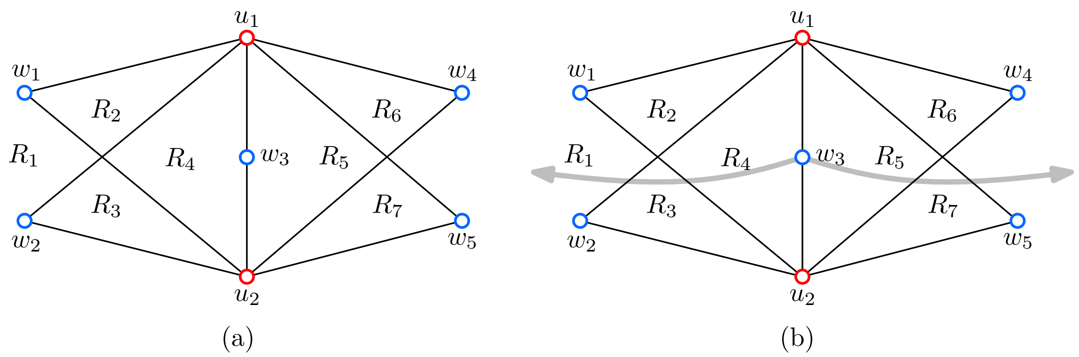

Fig. 4.27: (a) The regions of Γ_7. (b) The only two ways to connect w_3 to u_3, u_4 and u_5 in R_1.

The implications from the Lemmas and the Corollary of Sec. 4.4.2.4 for Γ_7 are:

– None of the vertices u_3, u_4, u_5 can be placed in any of the regions R_2, R_3, R_6, R_7 by the Triangle Lemma;

– none of the vertices u_3, u_4, u_5 can be placed in R_4 or R_5 by the Empty-Shell Corollary.

Thus, all of the vertices u_3, u_4, u_5 must be in region R_1. In order to not violate the fan-crossing free property, every edge connecting one of u_3, u_4 or u_5 with w_3 can cross neither both edges (u_1, w_2) and (u_1, w_1), nor both edges (u_2, w_1) and (u_2, w_2), nor both edges (u_1, w_5) and (u_1, w_4), nor both edges (u_2, w_4) and (u_2, w_5). Therefore each of the edges (u_3, w_3), (u_4, w_3) and (u_5, w_3) must cross either the edge pair (u_1, w_2) and (u_2, w_1), or the edge pair (u_1, w_5) and (u_2, w_4) (see Fig. 4.27b). By the pigeon principle, one of the two edge pairs is crossed by two of the edges (u_3, w_3), (u_4, w_3) and (u_5, w_3) – a violation of the fan-crossing free property.

Consequently, the drawing Γ_7 can also not be extended to a fan-crossing free drawing of the bipartite graph $K_{5,5}$.

Since it is not possible to extend one of the drawings $\Gamma_1, \ldots, \Gamma_7$ to a fan-crossing free drawing of $K_{5,5}$, this graph is not fan-crossing free. □

4.4.2.6 The graph $K_{3,7}$ is not fan-crossing free

Finally we complete the proof of Thm. 4.5 by showing the following lemma.

Lemma 4.13. *None of the seven drawings $\Gamma_1, \ldots, \Gamma_7$ of the graph $K_{2,5}$ can be extended to a drawing of $K_{3,7}$.*

Proof. We follow the same approach as in Sec. 4.4.2.5 and try to insert the vertices u_3, w_6 and w_7 into each of the seven drawings $\Gamma_1, \ldots, \Gamma_7$.

The drawing Γ_1. In Sec. 4.4.2.5 we already proved that it is not possible to insert vertex u_3 into Γ_1 (see Fig. 4.21a which is shown again in Fig. 4.28 for the readers convenience) without violating fan-crossing freeness. Hence, Γ_1 cannot be extended to a fan-crossing free drawing of $K_{3,5}$.

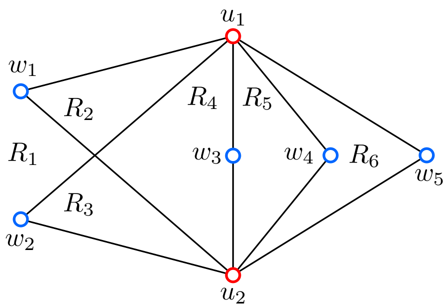

Fig. 4.28: The drawing Γ_1.

The drawing Γ_2. We denote the six regions $R_1, \ldots, R_6$ of Γ_2 as in Fig. 4.22a. For the readers convenience this figure is also shown in Fig. 4.29a.

As we have already seen in the previous section, the following configurations for u_3 are not possible:

– The vertex u_3 cannot lie in the regions R_2 or R_3 by the Triangle Lemma;

– it can also not be in the regions R_4 or R_5 by the Empty-Shell Corollary.

Thus, the vertex u_3 must be in one of the regions R_1 or R_6.

First, we consider the case where u_3 is placed in the region R_1. With the same argumentation as in the corresponding case of Sec. 4.4.2.5 for $K_{5,5}$, the edge (u_3, w_3) cannot be drawn through the regions R_5 and R_6. The only way to draw (u_3, w_3) is by crossing both edges (u_1, w_2) and (u_2, w_1). Further, the edge (u_3, w_4) must cross either (u_1, w_5) or (u_2, w_5) in order to satisfy the fan-crossing free property. We assume without loss of generality that (u_3, w_4) crosses (u_1, w_5). For an illustration of this configuration see Fig. 4.29b. Note that the two regions R_1 and R_6 are subdivided by (u_3, w_3) and (u_3, w_4). In the following, two of these subdivided regions are important

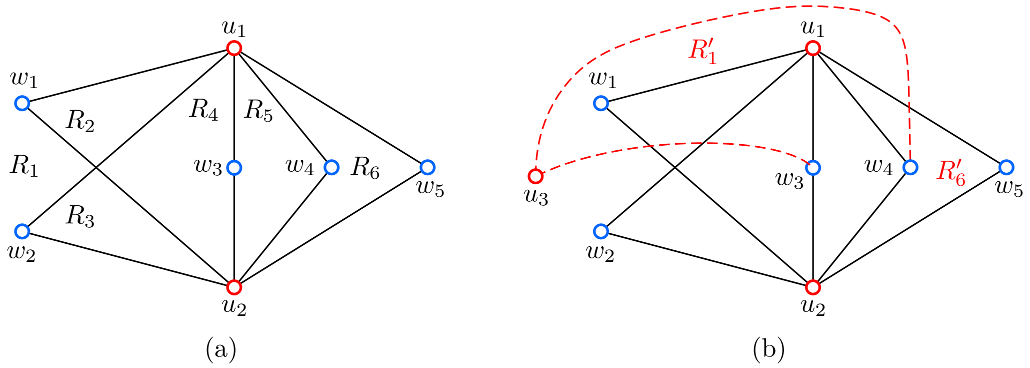

Fig. 4.29: (a) The six regions of Γ_2. (b) Vertex u_3 is placed in region R_1. The edge (u_3, w_3) crosses both edges (u_1, w_2) and (u_2, w_1), and edge (u_3, w_4) crosses (u_1, w_5). After inserting the two edges, some of the regions $R_1, \ldots, R_6$ are subdivided; the red labels denote such subdivisions.

for us, namely the region R'_1, which is bounded by (u_1, w_1), (u_1, w_5), (u_3, w_3) and (u_3, w_4), and the region R'_6, which is bounded by (u_1, w_5), (u_2, w_4), (u_2, w_5) and (u_4, w_4).

In the next steps we prove that placing u_3 in R_1 does not lead to a valid fan-crossing free drawing of $K_{3,7}$. To this end we try to put the vertex $w_6 \in V_2$ into the drawing shown in Fig. 4.29b.

(1) The vertex w_6 cannot be placed in region R_2, and for symmetry reasons also not in R_3: For a contradiction suppose it is in R_2. Neither of the edges (u_2, w_6) and (u_3, w_6) can cross (u_1, w_2) or (u_2, w_1), since this would create a fan-crossing or violate simplicity. Thus, both edges (u_2, w_6) and (u_3, w_6) must cross (u_1, w_1), which yields a fan-crossing – a contradiction.

(2) Further, placing vertex w_6 in one of the regions R_4 and R_5 is not possible: Due to simplicity an edge incident to u_3 (dashed red edges in Fig. 4.30a) may not be crossed by (u_3, w_6). To avoid a fan-crossing where the fan is anchored at u_3, the edge (u_3, w_6) can cross neither of the edges (u_1, w_2), (u_2, w_1) or (u_1, w_5) (thick black edges in Fig. 4.30a). The last option is the one where (u_3, w_6) crosses (u_2, w_5) and (u_2, w_4) – a fan anchored at u_2 (green edges in Fig. 4.30a). So indeed w_6 cannot be placed in R_4 or R_5.

(3) Now we assume that w_6 is in the region R_6. Then, by the observations above, the edge (u_3, w_6) crosses (u_2, w_5) and w_6 lies in the region R'_6 (see Fig. 4.30b). Using similar arguments, we obtain that edge (u_1, w_6) has to cross (u_2, w_4). Consider now the placement of vertex w_7. Note that all the arguments above for w_6 also apply to w_7, implying that w_7 has to be in region R'_6 or R_1. But also by the arguments above, if w_7 is placed in R'_6, then the edge (u_3, w_7) would have to cross (u_2, w_5), yielding a fan-crossing. Consequently, vertex w_7 is placed in R_1. For

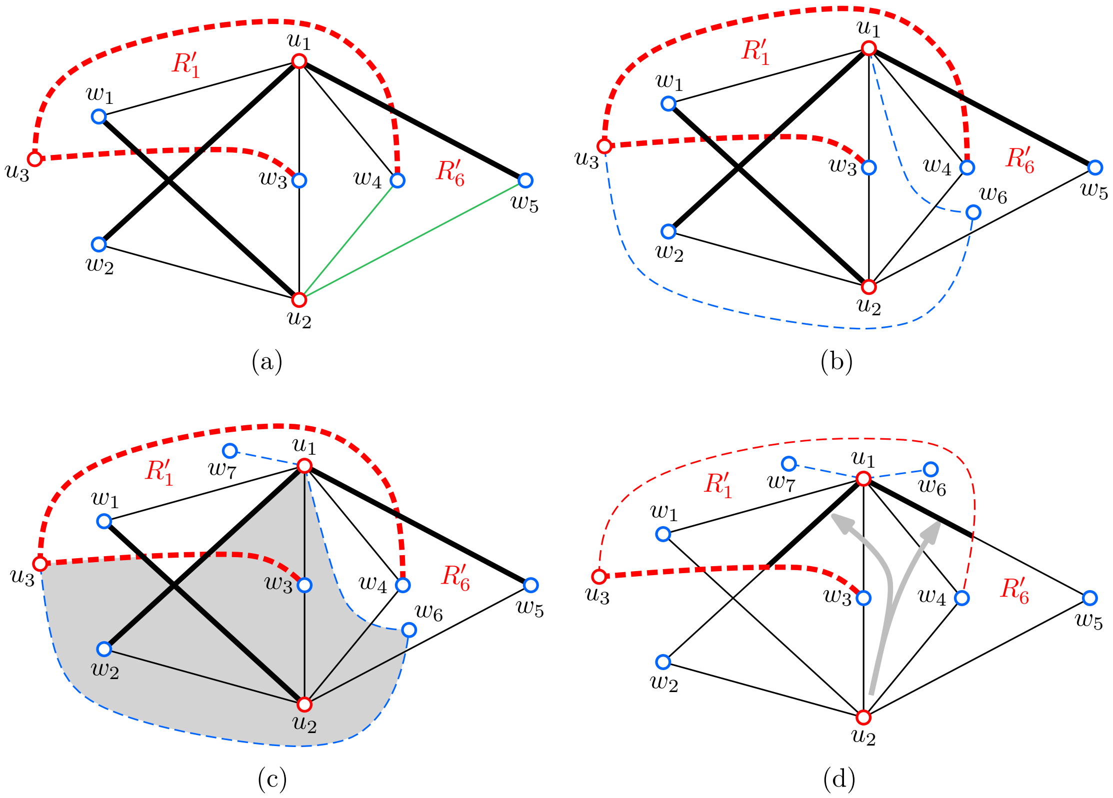

Fig. 4.30: Vertex u_3 is placed in region R_1 of Γ_2. (a) In a simple fan-crossing free drawing neither the thick red and black edges can be crossed by (u_3, w_6), nor the green fan. (b) Vertex w_6 is placed in the region R'_6. Edge (u_3, w_6) crosses (u_2, w_5), and edge (u_1, w_6) crosses (u_2, w_4). (c) Vertex w_7 has to be placed in region R'_1: The thick red and black edges are not allowed to be crossed by (u_1, w_7). The gray area is the range of u_2 regarding w_7. (d) Vertices w_6 and w_7 are in the region R'_1. The thick edges are non-crossable edges for (u_2, w_6) and (u_2, w_7).

the edge (u_1, w_7) we observe the following, again because of the fan-crossing free property: It can cross neither the edge (u_3, w_3), nor (u_3, w_4), nor (u_2, w_4), nor the pair (u_2, w_3) and (u_2, w_1) (see Fig. 4.30c). This implies that w_7 must be placed in R_1'. However, in this case the edge (u_2, w_7) yields inevitably a fan-crossing: The region R_1' is not in the range of u_2 with respect to w_7. So we are not able to obtain a simple fan-crossing free drawing of $K_{3,7}$ when placing w_6 in region R_6.

(4) To complete the case where u_3 is placed in R_1, it remains to consider the placement of vertex w_6 in the region R_1. First we observe that the dashed red, the blue and the bold black edges in Fig. 4.30a are not crossable by (u_1, w_6). Therefore w_6 must be in region R_1'.

By the arguments of the previous case the vertex w_7 cannot be in R_6, and therefore must be also in R_1. Moreover, by the same arguments as for w_6, vertex w_7 is placed in R_1'. We conclude by observing that the edges (u_2, w_6) and (u_2, w_7) can cross neither (u_3, w_3), nor the fan $\{(u_1, w_3), (u_1, w_2)\}$, nor the fan $\{(u_1, w_4), (u_1, w_5)\}$ (see also Fig. 4.30d). This implies that both, (u_2, w_6) and (u_2, w_7), have to cross (u_3, w_4), violating the fan-crossing free property.

From this case analysis, we conclude that placing u_3 in region R_1 yields no valid simple crossing-free drawing of $K_{3,7}$.

In the last part of the proof for the drawing Γ_2 we consider the case in which u_3 is placed in region R_6. By Property i of the Beetle Lemma, the edges (u_3, w_1) and (u_3, w_2) cross the edges (u_1, w_5) and (u_2, w_5), respectively (for an illustration see Fig. 4.31a). Due to the fan-crossing free property, edge (u_3, w_3) crosses either (u_1, w_4) or (u_2, w_4). We assume without loss of generality that (u_3, w_3) crosses (u_1, w_4). By simplicity and the fan-crossing free property, any other edge incident to u_3 can cross neither (u_1, w_4), nor (u_1, w_5), nor (u_2, w_5), nor (u_3, w_3) (more generally, no edge incident to u_3), nor the fan $\{(u_2, w_3), (u_2, w_4)\}$. So the edge (u_3, w_4) must be drawn without crossings, and both vertices w_6 and w_7 must be placed in R_5 or R_6. Again the regions R_5 and R_6 are subdivided. The important regions are denoted as follows:

– Region R_5' is delimited by the edges (u_1, w_4), (u_2, w_3), (u_2, w_4), and (u_3, w_3);

– region R_6' is delimited by the edges (u_1, w_4), (u_2, w_4), (u_2, w_5), and (u_3, w_2);

We note that the restrictions on edges incident to u_3 (see arguments above) imply that, if one of the vertices w_6 or w_7 is placed in R_5, it must be placed in R_5'. Further, Fig. 4.31b shows the range of u_1 regarding w_6 (and w_7), implying that there are only two regions where w_6 or w_7 might be: The region R_5' or region R_6'. In the following we discuss each of the options.

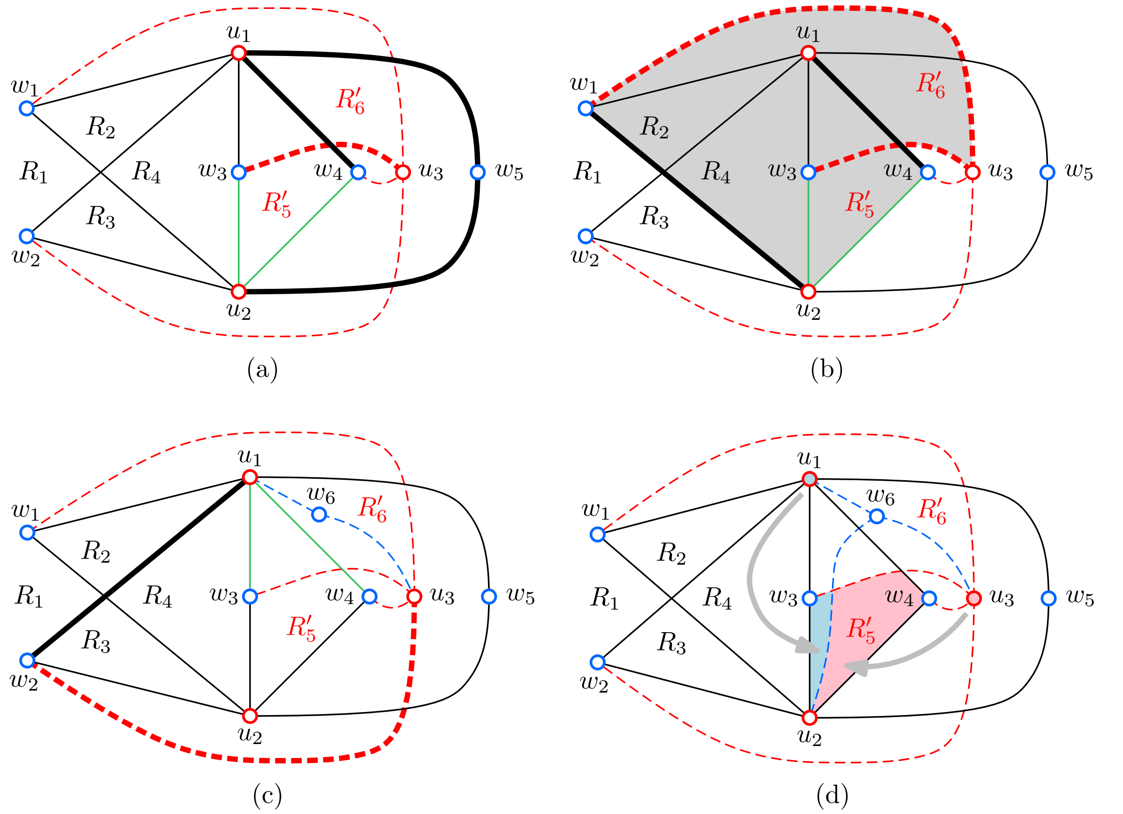

Fig. 4.31: The vertex u_3 is placed in region R_6 of Γ_2. (a) The edge (u_3, w_1) crosses (u_1, w_5), edge (u_3, w_2) crosses (u_2, w_5) and edge (u_3, w_3) crosses (u_1, w_4). Another edge incident to u_3 is not allowed to cross the bold black and red edges or the green fan. Important subregions of R_5 and R_6 are colored in red. (b) Another edge incident to u_1 is not allowed to cross the bold black and red edges or the green fan. The gray area shows the range of u_1 regarding w_6. (c) Vertex w_6 is placed in R'_6. (d) Edge (u_2, w_6) crosses (u_3, w_3). Vertex w_7 must be placed in R'_5. It should be placed in the blue area to satisfy fan-crossing freeness for (u_1, w_7), but it should be placed in the red area to satisfy fan-crossing freeness for (u_3, w_7).

(1) First we assume that w_6 is in R'_6 (see Fig. 4.31c). Since neither of the edges (u_1, w_6) and (u_3, w_6) is allowed to cross any of (u_1, w_4), (u_1, w_5), (u_3, w_1) and (u_3, w_3) (otherwise fan-crossing freeness is violated), the only way to insert (u_1, w_6) and (u_3, w_6) into the drawing is to draw them entirely in the region R'_6. Further we observe that the edge (u_2, w_6) can cross neither (u_1, w_2), nor (u_3, w_2), nor the fan $\{(u_3, w_3), (u_3, w_4)\}$, nor the fan $\{(u_1, w_3), (u_1, w_4)\}$; the only way to draw (u_2, w_6) is by crossing (u_1, w_4) and (u_3, w_3). Since the same arguments also apply to vertex w_7, it cannot be placed in region R'_6: If we would place it in R'_6 as well, then the edge (u_3, w_4) would be crossed by the fan $\{(u_2, w_6), (u_2, w_7)\}$. As a consequence, vertex w_7 is placed in R'_5. However, adding the edges (u_1, w_7) and (u_3, w_7) to the drawing yields a fan-crossing. Either the edge (u_1, w_7) crosses the

fan $\{(u_2, w_3), (u_2, w_6)\}$ or the edge (u_3, w_7) crosses the fan $\{(u_2, w_4), (u_2, w_6)\}$; refer also to Fig. 4.31d, which shows valid placements of w_7 regarding the edge (u_1, w_7) (bright blue area), and valid placements of w_7 regarding the edge (u_3, w_7), respectively (bright red area). So it is not possible to place w_6 (or w_7) in R'_6.

(2) It remains to consider the placement of w_6 and w_7 in region R'_5.

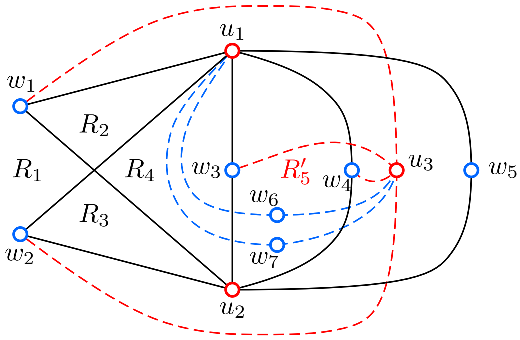

Fig. 4.32: Both vertices w_6 and w_7 are placed in region R'_5 of Γ_2, yielding two fan-crossings.

From the discussion before (see i. e. Figs. 4.31a and 4.31b), both edges (u_1, w_6) and (u_1, w_7) must cross (u_2, w_3), and both edges (u_3, w_6) and (u_3, w_7) must cross (u_2, w_4) (see Fig. 4.32). Since this violates the fan-crossing free property, there is no valid drawing when w_6 and w_7 are placed in region R'_5.

We conclude that Γ_2 cannot be extended to a fan-crossing free drawing of $K_{3,7}$.

The drawing Γ_3. As in the previous section, we denote the seven regions of Γ_3 by $R_1, \ldots, R_7$ as in Fig. 4.23a. For the readers convenience this figure is shown again in Fig. 4.33a.

In the previous section we have already observed the following: The vertex u_3 can be neither in R_3 or R_5 (Triangle Lemma), nor in R_1 or R_6 (Empty-Shell Corollary), nor in R_7 (Property ii of the Beetle Lemma). Consequently, vertex u_3 must be placed in one of the regions R_2 or R_4.

We observe that none of the vertices w_6 and w_7 may be placed in R_4 or R_5, since they are blocked for u_1 by (u_1, w_2), (u_2, w_1) and (u_2, w_2) regarding w_6 (for an illustration see Fig. 4.33b). An immediate implication of this observation is, that u_3 cannot lie in R_4: If it would be in this region, then w_6 needs to be in R_4 or R_5 by the Triangle Lemma, which is not possible.

A similar observation is that none of the vertices w_6 and w_7 may be placed in R_2 or R_3, since (u_1, w_2), (u_1, w_3) and (u_2, w_2) represent an impenetrable barrier for edges

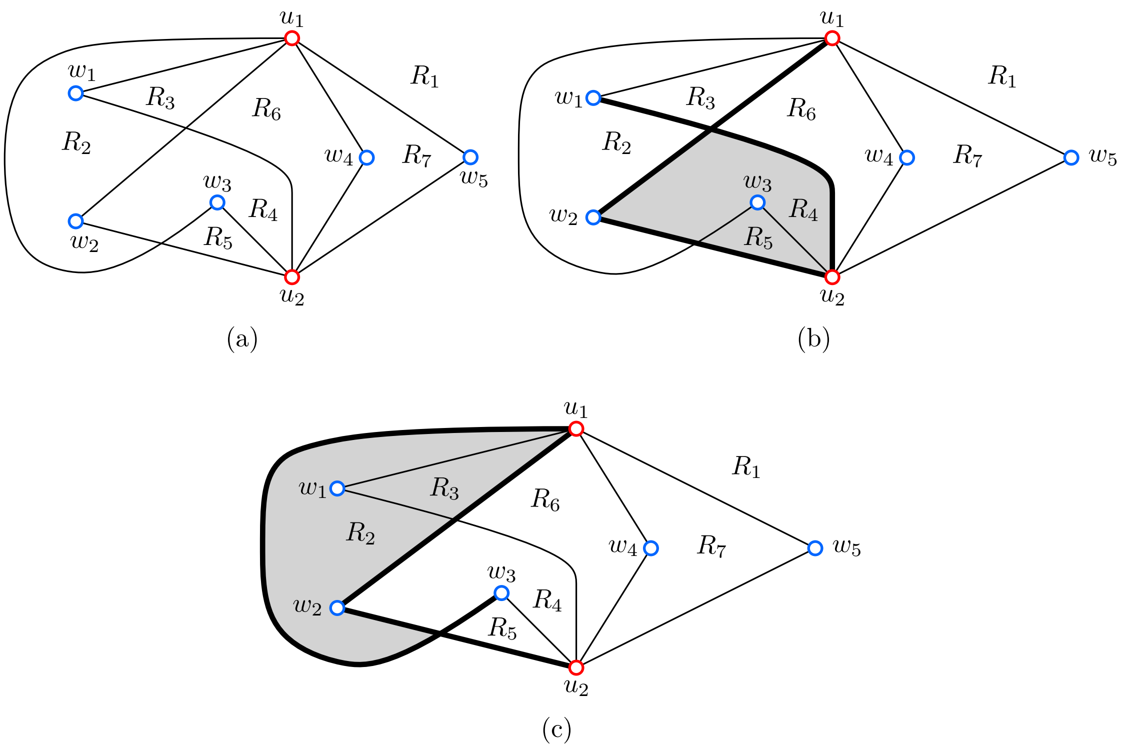

Fig. 4.33: (a) The seven regions of Γ_3. (b) The bold edges show a barrier for any edge incident to vertex u_1; so the vertices w_6 and w_7 cannot be in the gray area. (c) Here the bold edges represent a barrier for any edge incident to vertex u_2; so the vertices w_6 and w_7 cannot be in the gray area.

incident to u_2 (for an illustration refer to Fig. 4.33c). Thus, u_3 can also not lie in R_2 as a consequence of the Triangle Lemma.

Our case analysis proves that Γ_3 cannot be extended to a fan-crossing free drawing of $K_{3,7}$.

The drawing Γ_4. Recall that this drawing has seven regions $R_1, \ldots, R_7$ as shown in Fig. 4.34a (and Fig. 4.24). Further recall that vertex u_3 cannot be in any of the regions R_2, R_3, R_5 and R_6 (Triangle Lemma), and not in the region R_4 (Empty-Shell Corollary). So we have only to consider the case where u_3 is in R_7 (the case where u_3 is placed in R_1 is symmetric).

To this end we assume that u_3 is lying in R_7. Then, by the Beetle Lemma 4.10, the wing (u_3, w_1) crosses (u_1, w_5), and the wing (u_3, w_2) crosses (u_1, w_2) (see Fig. 4.34b). Because of simplicity and fan-crossing freeness, all three edges (u_3, w_3), (u_3, w_4) and (u_3, w_5) must be crossing-free.

We determine the range of u_1 regarding w_6 (and w_7) as follows: Simplicity prevents any crossing with another edge incident to u_1; the fan-crossing free property prevents a crossing with (u_2, w_1), (u_2, w_3), (u_3, w_1), and the fan $\{(u_3, w_3), (u_3, w_4)\}$. Thus,

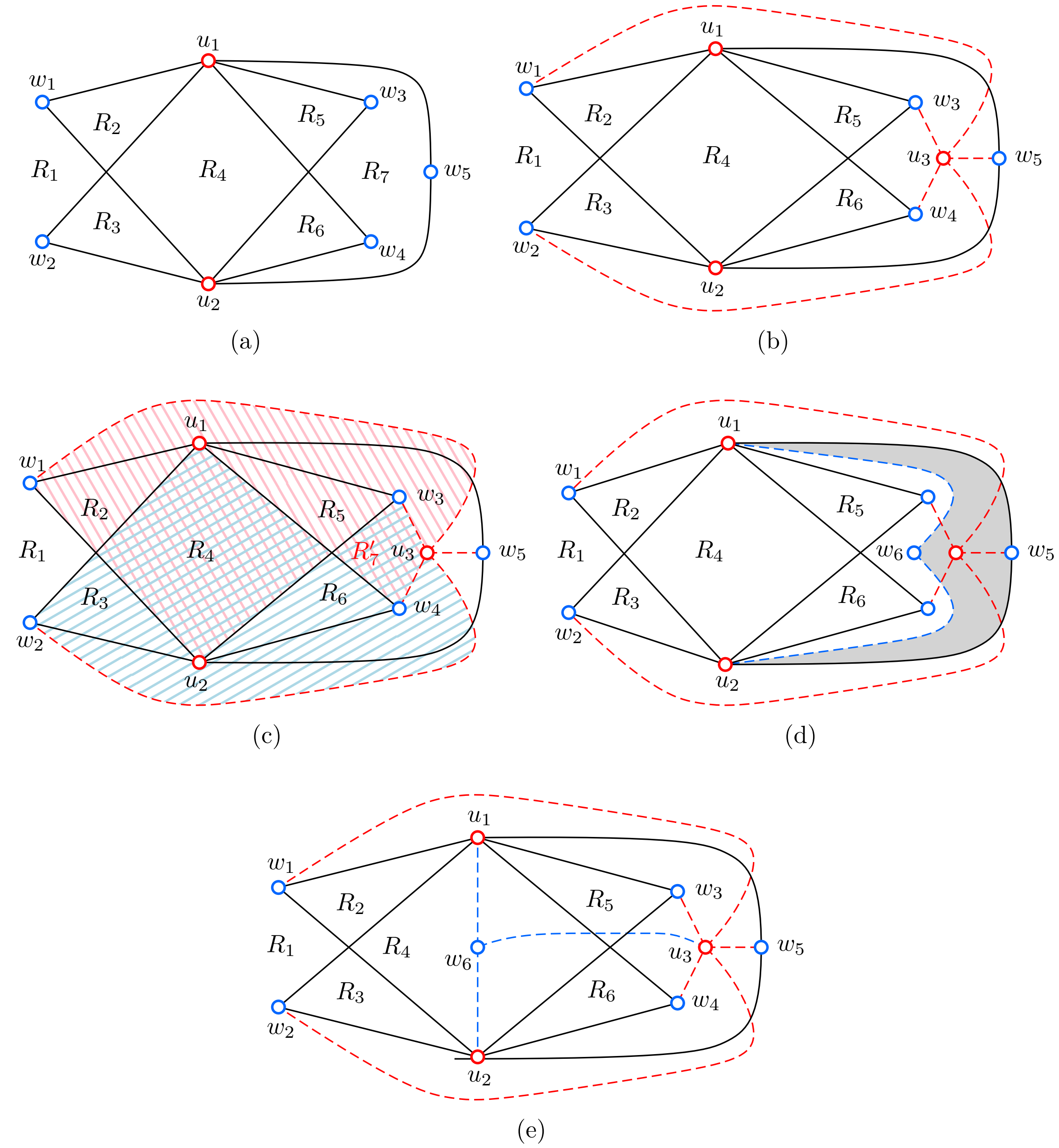

Fig. 4.34: (a) The seven regions in Γ_4. (b) Vertex u_3 is in region R_7; the red edges show the (topologically) only way to draw $(u_3, w_1), \ldots, (u_3, w_5)$. (c) The range of u_1 (bright red) and u_2 (bright blue) regarding w_6. The common range is $R_4 \cup R'_7$ (bright red and blue). (d) Vertex w_6 is placed in R'_7. (e) Vertex w_6 is placed in R_4.

the range of u_1 regarding w_6 contains the regions R_2, R_4, R_5 and parts of R_1 and R_7. The range of u_2 regarding w_6 is symmetric to the range of u_1 regarding w_6 and therefore contains the regions R_3, R_4, R_6 and parts of R_1 and R_7. Both ranges are illustrated in Fig. 4.34c, as well as the common range consisting of R_4 and a part of R_7, which we denote by R'_7. Consequently, both vertices w_6 and w_7 must be in one of the regions R_4 or R'_7. We consider the cases separately.

(1) First assume that w_6 is placed in R'_7. Then simplicity and fan-crossing freeness implies that (u_1, w_6) crosses (u_3, w_3), and (u_2, w_6) crosses (u_3, w_4) (see Fig. 4.34d). If w_7 would also be in R'_7, then, by symmetry, the edge (u_1, w_7) would cross (u_3, w_3), yielding a fan-crossing. So w_7 must be in R_4. But in this case the edge (u_3, w_7) is not realizable: The range of u_3 is the area delimited by $(u_1, w_5), (u_1, w_6), (u_2, w_5)$ and (u_2, w_6) (see gray area in Fig. 4.34d).

(2) The analysis above shows that both vertices w_6 and w_7 must be in R_4. Since the edge (u_3, w_6) can cross neither (u_1, w_5), nor (u_2, w_5), nor the fan $\{(u_1, w_3), (u_1, w_4)\}$, nor the fan $\{(u_2, w_3), (u_2, w_4)\}$, it has to cross (u_1, w_4) and (u_2, w_3) (as illustrated in Fig. 4.34e). But, as the same is true for (u_3, w_7), inserting (u_3, w_7) would create a fan-crossing. This rules out the last case.

We conclude that the drawing Γ_4 cannot be extended to a fan-crossing free drawing of $K_{3,7}$.

The drawing Γ_5. Figure 4.35a shows the eight regions $R_1, \ldots, R_8$ of Γ_5 again (see also Fig. 4.25 in Sec. 4.4.2.5). As already proved in Sec. 4.4.2.5, the vertex u_3 cannot be in any of the regions R_3, R_5, R_7 and R_8 by the Triangle Lemma, and it cannot be in the regions R_1, R_2, R_4 and R_6 by the Empty-Shell Corollary.

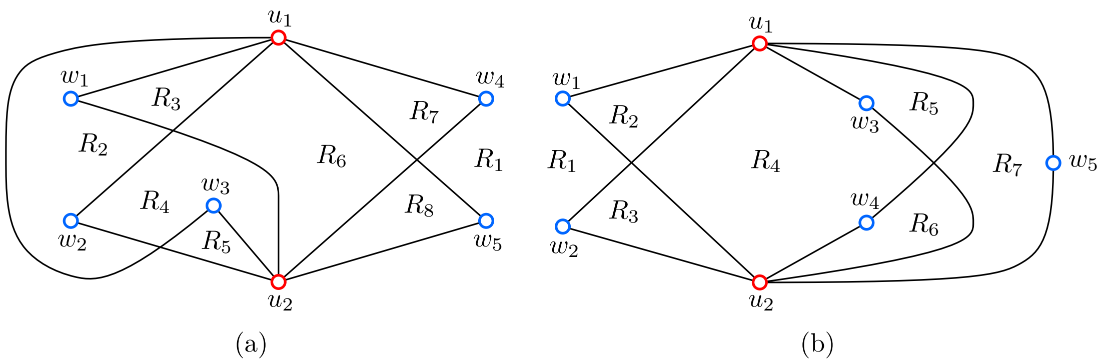

Fig. 4.35: (a) The eight regions in Γ_5. (b) The eight regions in Γ_6.

Thus, the drawing Γ_5 cannot be extended to a fan-crossing free drawing of $K_{3,7}$.

The drawing Γ_6. In Γ_6, we have the seven regions $R_1, \ldots, R_7$ as illustrated in Fig. 4.26 and, for the readers convenience, also in Fig. 4.35b. In Sec. 4.4.2.5 we proved already that the vertex u_3 can lie neither in R_2, R_3, R_5, R_6 (Triangle Lemma), nor in R_1, R_4, R_7 (Empty-Shell Corollary). Therefore we can directly conclude that the drawing Γ_5 cannot be extended to a fan-crossing free drawing of $K_{3,7}$.

The drawing Γ_7. The seven regions $R_1, \ldots, R_7$ of Γ_7 are shown again in Fig. 4.36a (see also Fig. 4.27a). We have already seen in Sec. 4.4.2.5 that the vertex u_3 cannot be positioned in any of the regions R_2, R_3, R_6 and R_7 (Triangle Lemma), and in any of the regions R_4 and R_5 (Empty-Shell Corollary). It remains to consider the case where u_3 is placed in region R_1.

In this case the edge (u_3, w_3) can be drawn in two ways without introducing fan-crossings: It crosses either both edges (u_1, w_2) and (u_2, w_1), or both edges (u_1, w_5) and (u_1, w_4). We assume without loss of generality that (u_3, w_3) crosses (u_1, w_2) and (u_2, w_1). Then, by simplicity and fan-crossing freeness, each of the edges (u_3, w_1), (u_3, w_2), (u_3, w_4) and (u_3, w_5) must be crossing-free (for an illustration see Fig. 4.36b).

Now we consider w_6 and w_7. First we observe that R_2, R_3 and R_4 are not in the range of u_3 with respect to w_6 (or w_7). Of the remaining regions, the region R_7 and parts of region R_1 are not in the range of u_1, and R_6 and parts of region R_1 are not in the range of u_2, regarding w_6 (see also Fig. 4.36c). This implies that w_6 (and w_7) are in R_5 or the region of R_1 that is delimited by $(u_1, w_5), (u_2, w_4), (u_3, w_4)$ and (u_3, w_5), in the following denoted by R'_1.

(1) First assume that w_6 is placed in R'_1. Then it is necessary for the edge (u_1, w_6) to cross (u_3, w_4) and for the edge (u_2, w_6) to cross (u_3, w_5) (by simplicity and the fan-crossing free property). If w_7 would also be in R'_1, then (u_1, w_7) must also cross (u_3, w_4), yielding a fan-crossing. Hence, there is only one vertex in R'_1, and vertex w_7 lies in R_5 (see Fig. 4.36d for an illustration of this situation). But now the region R_5 is not in the range of u_3 (regarding w_7) anymore (the range of u_3 is the non-gray area in Fig. 4.36d). This rules out the case in which $w_6 \in V_2$ is in R_1.

(2) Finally we consider the case in which w_6 and w_7 are both in R_5. There is only one way to realize the edge (u_3, w_6) such that the resulting drawing is fan-crossing free: This edge must cross (u_1, w_5) and (u_2, w_4) (see Fig. 4.36e). Since the same holds for (u_3, w_7) as well, the edge (u_1, w_5) is crossing the fan $\{(u_3, w_6), (u_3, w_7)\}$. Thus, the last case is ruled out.

We conclude that Γ_7 cannot be extended to a fan-crossing free drawing of $K_{3,7}$. □

Combining the results from Lemma 4.6, Lemma 4.8, Lemma 4.12, and Lemma 4.13, the statement of Thm. 4.5 follows.

4.4.2.7 A note on the simplicity assumption

The assumption that a graph is simple, i. e. no adjacent edges cross each other, no edge crosses itself, and each pair of edges crosses at most once, is very common, see e. g. Kleitman [97], or Pach and Tóth [108]. In fact, for some graph classes it

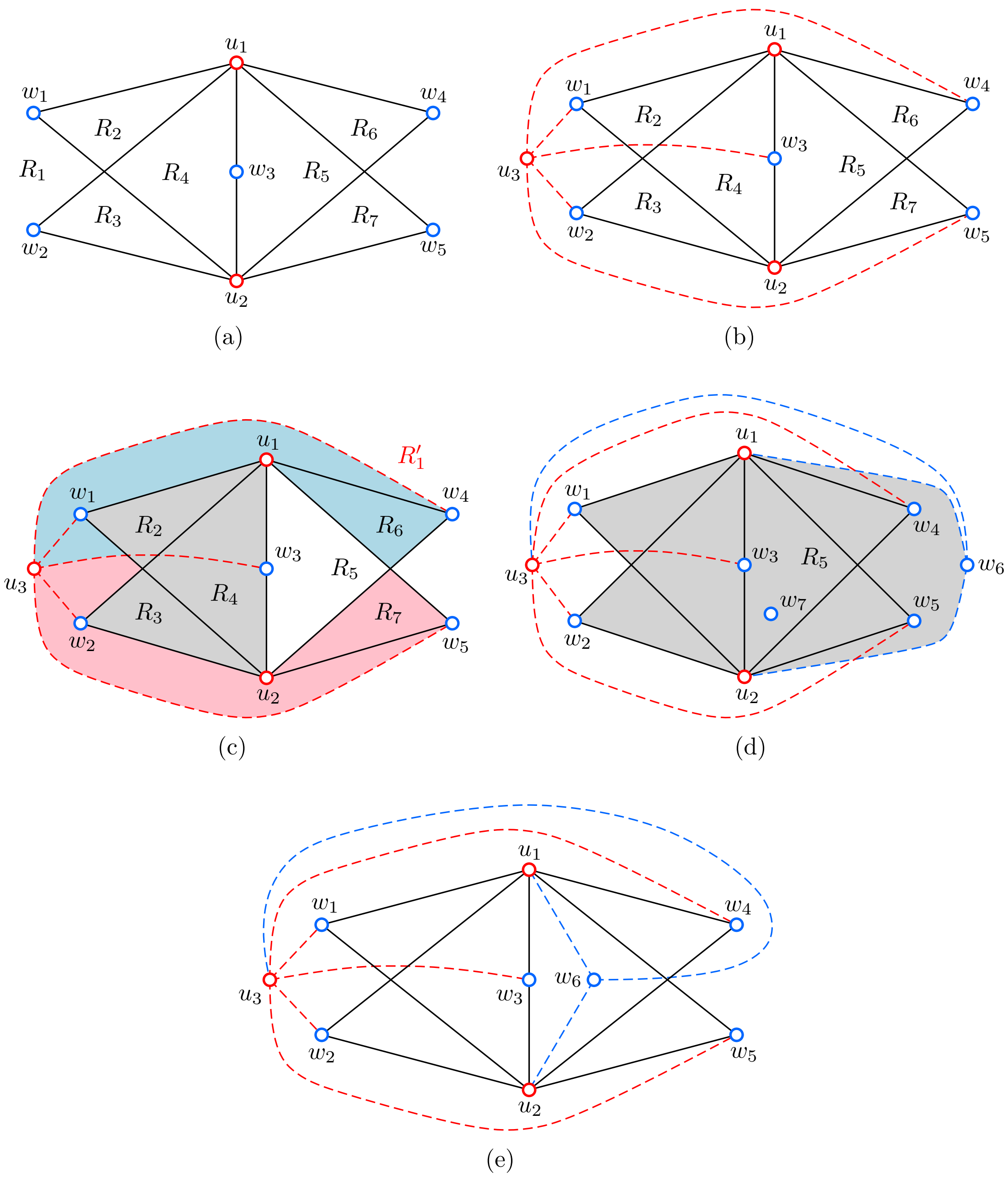

Fig. 4.36: (a) The seven regions in Γ_7. (b) Vertex u_3 is in R_1. (c) The ranges of u_1, u_2 and u_3 regarding w_6 and w_7: The gray area is not in the range of u_3, the bright red area is not in the range of u_1, and the bright blue area is not in the range of u_2. (d) Vertex w_6 is in R'_1. (e) Vertex w_6 is placed in R_5.

is known that this assumption is no constraint in the following sense: If there is a non-simple drawing of a graph G belonging to a certain graph class $\mathcal{C}$, then this drawing can be changed such that it is simple and still belongs to $\mathcal{C}$. Examples for such classes are the k-planar graphs for $k \leq 3$, see [122] and [106]. However, there exist also classes where this is not true. Such an example are the 4-planar graphs, see Schaefer [125]. Another prominent example is the class of quasi-planar graphs. Ackerman [4] showed that the upper bound on the edge density for simple quasi-planar graphs is $6.5n - 20$, while it is $8n - 20$ for non-simple quasi-planar graphs. Moreover, he constructed a family of non-simple quasi-planar graphs that exceed the bound of $6.5n - 20$ edges, showing that the class of simple quasi-planar graphs is a proper subclass of the non-simple quasi-planar graphs.

An easy observation is that each self-crossing can be avoided – no matter which graph class is considered (possibly with the exception of future graph classes that are defined in a very strange way, not complying to the common definitions nowadays). If there is a self-crossing $e = (v_1, v_2)$ for two vertices v_1, v_2 in a drawing Γ, the loop caused by it can be erased in order to obtain an edge that is non-self-crossing; namely, e can be replaced by the edge consisting of the arc of e from v_1 to the crossing, joined with the arc of e from v_2 to the crossing (see Fig. 4.37a for an illustration). Note that this does not introduce any new crossings, and for some edges (including e) even reduces the number of crossings; thus Γ still belongs to the same graph class as it belonged to before redrawing e.

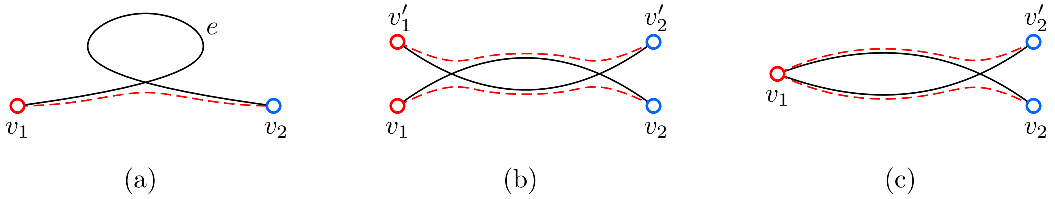

Fig. 4.37: (a) A self-crossing edge. It can be replaced by the dashed red edge. (b) Two edges that cross each other twice, where the area between the two crossings (called “lens”) is empty. The red edges indicate how this configuration can be resolved. (c) Adjacent edges that cross, such that the lens they form (from the common vertex to the crossing point) is empty; the red edges show how to resolve this configuration.

In general, it is also possible to eliminate empty lenses. Thereby a lens is defined as follows:

(a) Given two edges $e = (v_1, v_2)$ and $e' = (v_1', v_2')$ that cross each other twice. Let c_1 and c_2 be the crossing points, e_{c_1,c_2} the part of e between c_1 and c_2, and e'_{c_1,c_2} the part of e' between c_1 and c_2. Then a lens is the area enclosed by e_{c_1,c_2} and e'_{c_1,c_2}.

(b) Given two adjacent edges $e = (v_1, v_2)$ and $e' = (v_1, v_2')$ that cross each other. Let c_2 be the crossing point, e_{v_1,c_2} the part of e between v_1 and c_2, and e'_{v_1,c_2} the part of e' between v_1 and c_2. Then a lens is the area enclosed by e_{v_1,c_2} and e'_{v_1,c_2}.

The dashed red edges in Figs. 4.37b and 4.37c show how to eliminate lenses if they are empty. Since the lenses are empty, the crossing configuration for edges not equal to e or e' does not change, while the number of crossing for e and e' is reduced by one, which also does not affect the graph class Γ belongs to.

While empty lenses always can be avoided, the discussion above shows that the same is not true for non-empty lenses. However, in the case of a fan-crossing free complete bipartite graph $K_{a,b}$, where $b \geq a$, $a \geq 4$ and $b \geq 5$, there can in fact be no non-empty lenses.

To see this we consider two different cases. Like before, let $U = \{u_1, \ldots, u_a\}$ and $W = \{w_1, \ldots, w_b\}$ be the two independent parts for $K_{a,b}$ and Γ a drawing of $K_{a,b}$ (or a drawing of a subgraph of $K_{a,b}$).

Adjacent edges cannot cross. Suppose to the contrary that there is a crossing c of two adjacent edges $e = (u_1, w_1)$ and $e' = (u_1, w_2)$. Then $e_{u_1,c}$ and $e'_{u_1,c}$ enclose a region R (see Fig. 4.38a). As already discussed, if this region does not contain a vertex, then e and e' can be rerouted such that this region vanishes. So let us assume that there is a vertex in R.

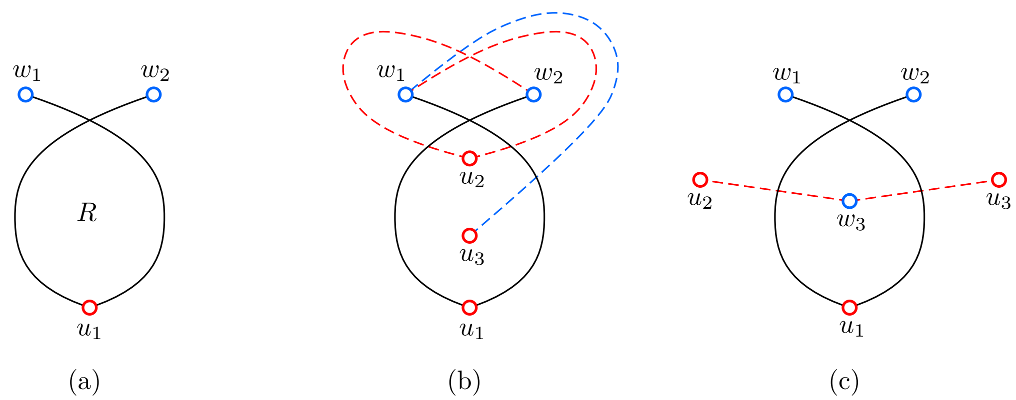

Fig. 4.38: (a) Adjacent edges that cross each other with enclosed area R. (b) A node $u_2 \in U$ is in R. (c) A node $w_3 \in W$ is in R.

First we consider the case, where a vertex $u_2 \in U$ is in R. Then the edge (u_2, w_1) cannot cross (u_1, w_2) since this would create a fan-crossing; for the same reason the edge (u_2, w_2) is not allowed to cross (u_1, w_1). This yields crossings of (u_2, w_1) with (u_1, w_1), and of (u_2, w_2) with (u_1, w_2) (see dashed red edges in Fig. 4.38b). The vertex u_2 has edges to all nodes in W, so there must be at least edges (u_2, w_3), (u_2, w_4) and (u_2, w_5) in Γ. Fan-crossing freeness disallows these edges to cross (u_1, w_1) or

(u_1, w_2), implying that w_3, w_4 and w_5 are placed in region R. Now consider u_3, which has edges to w_3, w_4 and w_5. Since at most two of these edges can cross (u_1, w_1) or (u_1, w_2), vertex u_3 must also be in R. But then it is impossible to draw the edge (u_3, w_1) without a fan-crossing (see dashed blue edge in Fig. 4.38b). So, in this case there is no valid fan-crossing free drawing of $K_{a,b}$.[2]

Now consider the case where a vertex $w_3 \in W$ is in R (see Fig. 4.38c). Then at most one of the edges $(u_2, w_3), (u_3, w_3)$ and (u_4, w_3) is allowed to cross (u_1, w_1), and at most one of them can cross (u_1, w_2). Thus, at least one of the vertices u_2, u_3, u_4 must be in R. But we already ruled out this case.[3] So adjacent edges indeed cannot cross each other.

Two distinct edges cannot cross twice. Assume that there are two distinct edges $e = (u_1, w_1)$ and $e' = (u_2, w_2)$ in $K_{a,b}$, that cross each other twice.

First we assume that the lens enclosed by e and e' does not contain any of the vertices u_1, u_2, w_1, w_2 (see Fig. 4.39a). Since the lens is not empty, it contains a vertex v, either belonging to U or to W, say to W (the other case is symmetric). The edge (u_1, v) cannot cross e', since this would create a fan-crossing (see dashed red edge in Fig. 4.39a). But it can also not cross e, since this would create a configuration with crossing adjacent edges (see dashed gray edge in Fig. 4.39a).

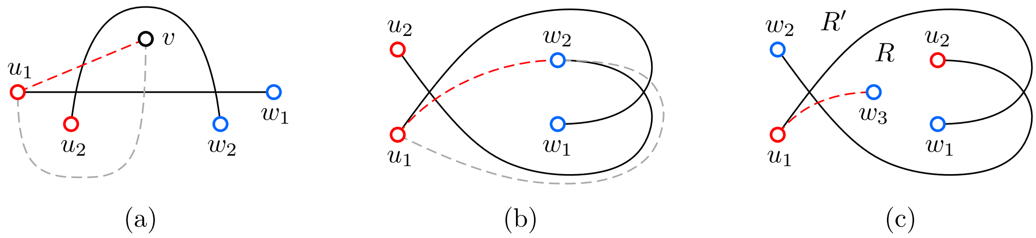

Fig. 4.39: (a) Edges that cross each other twice with empty lens. (b) Two edges that cross each other twice, where two vertices of W are in the lens. (c) Two edges that cross each other twice, where one vertex of U and one vertex of W is in the lens.

Next we assume that the lens enclosed by e and e' contains w_1 and w_2 (see Fig. 4.39b). This configuration is not possible, since the edge (u_1, w_2) crosses (u_2, w_2) (see dashed red edge in Fig. 4.39b), or it crosses (u_1, w_1) (see dashed gray edge in Fig. 4.39b), yielding a fan-crossing.

Finally assume that the lens R enclosed by e and e' contains u_2 and w_1. Note that R' in Fig. 4.39c is also a lens, this one contains u_1 and w_2, and note also that considering R' instead of R is a symmetric case. So we can assume without loss of generality that R contains another vertex $w_3 \in W$. The edge (u_1, w_3) cannot

[2]Note that this argument only works for $|U| \geq 3$ and $|W| \geq 5$.
[3]Note that for this argument we need $|U| \geq 4$ and, from the first case, $|W| \geq 5$.

cross (u_1, w_1) by the discussion above, and hence has to cross (u_2, w_2) (red edge in Fig. 4.39c), yielding a fan-crossing. This rules out the last case.

These arguments show the following: If there is a non-simple fan-crossing free drawing of $K_{a,b}$ for $b \geq a$, where $a \geq 4$ and $b \geq 5$, then there is also a simple fan-crossing free drawing for $K_{a,b}$. Conversely, since there is no such drawing for the bipartite graphs $K_{5,5}$ and $K_{4,7}$ that is simple, there is also no such drawing when abandoning the simplicity assumption. However, as the arguments above need the assumption $|U| \geq 4$ and $|W| \geq 5$, we cannot conclude the same for the graph $K_{3,7}$, but we believe it also holds for this graph and that it can be proven by a more detailed case analysis.

4.5 Conclusions and Open Problems

For some graph classes we answered the question if all graphs of a certain degree d belong to it or not. In the case of k-planar, k-gap-planar and fan-planar graphs we were able to give tight bounds, even for the more restrictive case of Hamiltonian bipartite graphs. However, for various graph classes there are still gaps between the lower and upper bounds of d (see Table 4.1). In particular, the long-standing question if all degree-3 graphs are RAC is still open. Since fan-crossing freeness and quasi-planarity are necessary conditions for a graph to be RAC, and all graphs of degree 3 are fan-crossing free and quasi-planar, there is hope to find an algorithm to draw such graphs with right angle crossings. If the claim by Alam et al. [8], that all degree-3 graphs have a drawing that is fan-crossing free and quasi-planar at the same time, turns out to be true, then this would be another important step towards showing that all degree-3 graphs are RAC.

Another interesting question arising from our results is whether degree-4 graphs are fan-crossing free. More general, we pose as future goals to narrow down the gaps for the graph classes presented in Table 4.1, namely for quasi-planar, RAC 1-bend, and RAC 2-bend graphs. The upper bounds d_u in the table are derived from the known upper bounds on the maximum edge density of graphs in these classes [4, 10, 24]. So the hope is to find some low-degree graphs not belonging to these classes using direct arguments, like we did for the fan-crossing free graphs.

Chapter 5

Enumeration of Drawings for Complete and Complete Bipartite Graphs

In order to find graphs of low degree that are not fan-crossing free, we proved a characterization for the class of bipartite fan-crossing free graphs in Thm. 4.5. Such characterizations are not only interesting in the low-degree setting, but also of interest in itself, since the size of the largest complete or complete bipartite graph is a common measure to understand the extent of a specific graph class [30, 42, 53, 58]. Moreover, it has implications for different areas of graph theory and graph drawing and has been studied in related fields, refer e.g. to [25, 41, 47, 66, 69, 82, 130]. One such example is the chromatic number [76], which is lower bounded by the largest n such that K_n is contained in the considered graph class.

In this chapter, which is based on our conference paper "Efficient Generation of Different Topological Representations of Graphs Beyond-Planarity" [16], we study different graph classes, aiming at giving an algorithm to characterize complete and complete bipartite graphs.[1]

5.1 Preliminaries

In the following we give definitions that are relevant for the current chapter. Moreover, in this section we discuss the state of the art regarding characterizations of complete and complete bipartite graphs.

[1] Our paper was also invited to a special issue of the Journal of Graph Algorithms and Applications (JGAA), dedicated to selected papers from "Graph Drawing and Network Visualization 2019" (GD 2019). Thus, an extended version appeared in JGAA [17].

5.1.1 Definitions

We focus our studies on simple graphs, i. e. graphs without self-loops or multi-edges, and on simple drawings, that is drawings where each edge pair has at most one point in common.[2]

For a drawing D of a graph $G = (V, E)$, we denote the planarization[3] of D by Γ_D. If we have a set of drawings $D_1, \dots, D_k$ for some $k \in \mathbb{N}$, we also denote the planarization of D_i $(1 \leq i \leq k)$ by Γ_i instead of Γ_{D_i}. Recall that the planarization of a drawing is obtained by replacing each of its crossings with a dummy vertex. In the following we refer to these dummy vertices also as *crossing vertices*, while the original vertices are called *real vertices*.

Let $V = \{u_1, \dots, u_n\}$ be the vertices for a complete graph K_n, while we assume that for a complete bipartite graph $K_{a,b}$ the vertices are given by the two disjoint independent sets $U = \{u_1, \dots, u_a\}$ and $W = \{w_1, \dots, w_b\}$.

In the following we consider graphs belonging to certain graph classes. To this end we denote a graph class by $\mathcal{C}$. If the drawing of a graph respects the restrictions of $\mathcal{C}$, we say the drawing is $\mathcal{C}$-drawable. Recall the following graph classes beyond-planarity:

– k-planar graphs, in which each edge may be crossed by at most k other edges;

– fan-planar graphs, in which each edge can cross only a fan and edges of the fan must cross from the same "side" [32, 38, 39, 93];

– fan-crossing free graphs, in which no edge is allowed to cross a fan [45, 50];

– gap-planar graphs, in which each crossing is assigned to one of the two crossing edges, such that each edge receives at most one crossing assigned to it [30];

– RAC graphs, in which edges are only allowed to cross at right angles [59, 60, 64];

– the IC-planar graphs, in which no two pairs of crossing edges share a vertex (referred to as independent crossings) [9, 141];

– the NIC-planar graphs, in which no two pairs of crossing edges share more than one vertex (referred to as nearly independent crossings) [140];

– and finally the fan-crossing graphs [43, 44], which are defined like fan-planar graphs, except that edges of a fan are allowed to cross from different sides.

[2]Note that the simplicity assumption may be not without loss of generality for some of the graph classes; e.g., for the quasi-planar graphs [4]. We refer also to Sec. 4.4.2.7, which contains a short discussion about this assumption.

[3]For the detailed definitions we refer to Chapter 2.

5.1.2 Known results

For some of the aforementioned classes, characterizations for complete or complete bipartite graphs are already known.

One of these classes is the class of 1-planar graphs, where Czap and Hudák [53] proved that K_n belongs to it if and only if $n \leq 6$, while $K_{a,b}$, with $a \leq b$, is 1-planar if and only if $a \leq 2$, or $a = 3$ and $b \leq 6$, or $a = b = 4$.

For the IC-planar, NIC-planar and RAC graphs, the complete graph K_n belongs to any of these classes if and only if $n \leq 5$ [59, 140, 141]. Moreover, the graph $K_{a,b}$, with $a \leq b$, is IC-planar if and only if $a \leq 2$, or $a = b = 3$ [140], and NIC-planar or RAC if and only if $a \leq 2$, or $a = 3$ and $b \leq 4$ [58, 140].

However, when considering quasi-planar graphs, gap-planar graphs, and fan-crossing free graphs, there exist only characterizations for complete graphs in the literature. Namely K_n is quasi-planar if and only if $n \leq 10$ [4, 42], gap-planar if and only if $n \leq 8$ [30], and fan-crossing free if and only if $n \leq 6$ [50, 53].

As already mentioned, we were able to provide the characterization for fan-crossing free complete bipartite graphs, refer to Thm. 4.5. More details about the state of the art and our findings are collected in Tables 5.1 and 5.2.

5.1.3 Techniques

We note that, while it suffices to find a certificate drawing for showing that a certain graph belongs to a specific graph class, it is in general more difficult to show that a graph is *not* part of a graph class, since one needs to argue that there exist no drawing at all which respects the constraints of the class.

A main technique to prove the latter is by using the edge density for the considered graph class (density bounds for several graph classes are also provided in Tables 5.1 and 5.2). For example, the 1-planar and fan-crossing free graphs have an edge density of $4n - 8$ edges [50, 108], yielding that the complete graph K_7 is in neither of the two classes.[4]

Nevertheless, this technique fails in most cases. E. g. for the class of 2-planar graphs, the edge density of $5n - 10$ only ensures that K_9 does not belong to this class, while it provides no answer to the question if K_8 is also 2-planar or not. In regard to the complete bipartite graphs, the limitations of this approach are even more evident, due to the fact that they are sparser than the complete graphs.

[4]In greater detail: The graph K_7 has 21 edges, while 1-planar and fan-crossing free graphs with 7 vertices allow only for $4 \cdot 7 - 8 = 20$ edges.

Table 5.1: Known results and our findings for complete graphs. For each class, we present the largest complete graph that belong to this class (col. "$\in$"), and the smallest one that does not (col. "$\notin$").

Class	Density	Ref.	$\in$	Ref.	$\notin$	Ref.
IC-planar	$\frac{13}{4}n - 6$	[141]	K_5	[64, Fig.5]	K_6	[141, Prp.2.1]
NIC-planar	$\frac{18}{5}n - \frac{36}{5}$	[140]	K_5	[140, Thm.7]	K_6	[140, Thm.7]
1-planar	$4n - 8$	[122]	K_6	[53, Fig.1]	K_7	[108, Thm.1]
2-planar	$5n - 10$	[108]	K_7	[39, Fig.7]	K_8	Char. 5.3
3-planar	$\frac{11}{2}n - 11$	[106]	K_8	Char. 5.3	K_9	Char. 5.3
4-planar	$6n - 12$	[3]	K_9	Char. 5.3	K_{10}	Char. 5.3
5-planar	$< 8.52n$	[3]	K_9	Char. 5.3	K_{10}	Char. 5.3
6-planar	$< 9.34n$	[3]	K_{10}	Fig. 5.7c	K_{20}	[3]
fan-planar fan-crossing	$5n - 10$	[93]	K_7	[39, Fig.7]	K_8	Char. 5.8
fan-crossing free	$4n - 8$	[50]	K_6	[53, Fig.1]	K_7	[50, Thm.1]
gap-planar	$5n - 10$	[30]	K_8	[30, Fig.7]	K_9	[30, Thm.23]
RAC	$4n - 10$	[59]	K_5	[64, Fig.5]	K_6	[59, Thm.1]
quasi-planar	$\frac{13}{2}n - 20$	[4]	K_{10}	[42, Fig.1]	K_{11}	[4, Thm.5]

Another technique to obtain the desired characterizations takes the crossings into account. More precisely, the minimum number of crossings required by *any* drawing of a certain graph G (as derived by, e.g., the Crossing Lemma [3, 6, 7, 102, 106] or closed formulas [75, 139]) is compared to the maximum number of crossings allowed in the considered graph class $\mathcal{C}$. If the former number exceeds the latter, the graph G cannot be part of $\mathcal{C}$. However, to make good use of this technique, graph classes must impose such restrictions (like e. g. gap-planar and 1-planar graphs [29, 53]), and these restrictions should yield tight bounds.

Since it is in general not easy or presumably impossible to find combinatorial arguments while proving characterizations for certain complete or complete bipartite graphs, often a large case analysis is needed (refer to the proofs in Sec. 4.4.2 and [58]). We noticed that a characterization for the complete bipartite 2-planar graphs [94] could be derived in a similar manner as the corresponding one for fan-crossing free graphs. This was our motivation to develop a systematic method to find complete and complete bipartite graphs belonging to a certain graph class beyond-planarity,

Table 5.2: Known results and our findings for complete bipartite graphs. For each class, we present the largest complete bipartite graphs that belong to this class (col. "$\in$"), and the smallest ones that do not (col. "$\notin$"). Color gray indicates weaker results that follow from other entries. A star behind the density indicates that it is the same bound as in the general case, since no density tailored for the bipartite case is known.

Class	Density	Ref.	$\in$	Ref.	$\notin$	Ref.
IC-planar	$\frac{9}{4}n - 4$	[14]	$K_{3,3}$	[140, Cor.19]	$K_{3,4}$	[140, Cor.19]
NIC-planar	$\frac{5}{2}n - 5$	[14]	$K_{3,4}$	[140, Thm.9]	$K_{3,5}$	[140, Thm.9]
			$K_{3,4}$		$K_{4,4}$	[140, Thm.9]
1-planar	$3n - 8$	[54]	$K_{3,6}$	[53, Fig.2]	$K_{3,7}$	[53, Lem.4.2]
			$K_{4,4}$	[53, Fig.3]	$K_{4,5}$	[53, Lem.4.3]
2-planar	$\frac{7}{2} - 7$	[14]	$K_{3,10}$	[13, Lem.1]	$K_{3,11}$	[13, Lem.1]
			$K_{4,6}$	Char. 5.4	$K_{4,7}$	Char. 5.4
			$K_{4,5}$		$K_{5,5}$	Char. 5.4 [94]
3-planar	$< 5.21n$	[14]	$K_{3,14}$	[13, Lem.1]	$K_{3,15}$	[13, Lem.1]
			$K_{4,9}$	Char. 5.5	$K_{4,10}$	Char. 5.5
			$K_{5,6}$	Char. 5.5	$K_{5,7}$	Char. 5.5
			$K_{5,6}$		$K_{6,6}$	Char. 5.5
4-planar	$6n - 12$*	[3]	$K_{3,18}$	[13, Lem.1]	$K_{3,19}$	[13, Lem.1]
			$K_{4,11}$	Obs. 5.6	$K_{4,19}$	
			$K_{5,8}$	Obs. 5.6	$K_{5,19}$	
			$K_{6,6}$	Obs. 5.6	$K_{6,19}$	
5-planar	$< 6.72n$	[14]	$K_{3,22}$	[13, Lem.1]	$K_{3,23}$	[13, Lem.1]
			$K_{4,11}$		$K_{4,23}$	
			$K_{5,8}$		$K_{5,23}$	
			$K_{6,7}$	Obs. 5.7	$K_{6,23}$	
fan-planar fan-crossing	$4n - 12$	[14]	$K_{4,n}$	[93, Fig.3]	$K_{5,5}$	Char. 5.9
fan-crossing free	$4n - 8$*	[50]	$K_{3,6}$		$K_{3,7}$	Char. 5.11
			$K_{4,6}$	Char. 5.11	$K_{4,7}$	
			$K_{4,5}$		$K_{5,5}$	Char. 5.11
gap-planar	$5n - 10$*	[30]	$K_{3,12}$	[30, Fig.7]	$K_{3,14}$	[29, Thm.1]
			$K_{4,8}$	[30, Fig.9]	$K_{4,9}$	Obs. 5.13
			$K_{5,6}$	[30, Fig.9]	$K_{5,7}$	[30]
			$K_{5,6}$		$K_{6,6}$	[29, Thm.1]
RAC	$3n - 7$	[14]	$K_{3,4}$	[58, Fig.4]	$K_{3,5}$	[58, Thm.2]
			$K_{3,4}$		$K_{4,4}$	[58, Thm.2]
quasi-planar	$\frac{13}{2}n - 20$*	[4]	$K_{4,n}$	[93, Fig.3]	–	
			$K_{5,18}$	Obs. 5.15	?	
			$K_{6,10}$	Obs. 5.15	?	
			$K_{7,7}$	Obs. 5.15	$K_{7,52}$	[4, Thm.5]

or, alternatively, for proving that there exists no drawing for a specific graph K_n or $K_{a,b}$, respectively.

5.2 Our Contribution

The case analyses for the proofs that the bipartite graph $K_{5,5}$ is neither fan-crossing free (Thm. 4.5) nor 2-planar [94] use the same technique of considering all possible drawings and discarding isomorphic drawings regularly. This caused us to ask the question if the proofs can be automated and generalized, such that the automation also works for other graph classes. We were able to answer this question in the positive for topological graph classes, while it does not extend to the geometric ones (such as the class of RAC graphs). Moreover, our technique is tailored for complete and complete bipartite graphs, since we highly exploit the symmetry of such graphs.

Our algorithm consists of two main steps, which are applied in turns. The first one is the generation of all possible embeddings that can be obtained by inserting a vertex into a given complete (bipartite) graph, while respecting the constraints of the graph class considered. The second step is the elimination of isomorphic graphs, which generally discards a large number of them and thus reduces the search space extremely.

We will describe our algorithm in detail and start with the isomorphic test, which is not only applicable to drawings of complete or complete bipartite graphs, but even to drawings of general connected graphs.[5]

5.3 Testing for Isomorphism

Let D_1 and D_2 be embeddings of a connected graph G with planarizations Γ_1 and Γ_2 respectively. Recall that D_1 and D_2 are isomorphic if Γ_1 and Γ_2 can be transformed into each other by relabeling (dummy and real) vertices, edges, and faces of Γ_1.

We remark that a weaker definition of isomorphism is used in several works (see, e.g., [1, 73, 118]) that generate simple drawings of complete graphs. More precisely, the drawings D_1 and D_2 are called *weakly isomorphic* [99], if there is an incidence preserving bijection between their vertices and edges, such that two edges cross in D_1 if and only if they do in D_2. Figure 5.1 shows that both terms are not the same,

[5]We remark that the isomorphic test can also be adjusted to non-connected graphs. However, since we only consider connected graphs and the number of possible configurations to check is higher in non-connected graphs, we focus only on the connected case.

as two graphs that are weakly isomorphic might differ in the order in which their edges cross [72]; refer also to the discussion in Sec. 2.4.

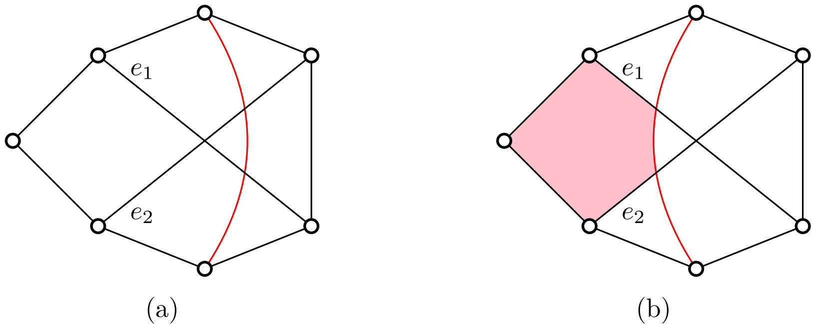

Fig. 5.1: The drawings in (a) and (b) are weakly isomorphic, but not isomorphic, since the planarization of drawing (b) has a face of size 5 (area colored in red), while the planarization of drawing (a) has no such face. Note that the order of e_1 and e_2 along the red edge is different in both drawings.

Further, two simple drawings of a complete graph are weakly isomorphic if and only if they have the same rotation system[6] [72, 109]. So, in order to find all simple drawings that are not weakly isomorphic, it suffices to find all rotation systems that yield a simple drawing [100]. Since this property is only true for complete graphs [1], and regarding complete bipartite graphs only partial results are known in the literature [48], we followed another approach.

Our first observation is that the number of each, the dummy vertices, the real vertices, the edges and the faces, must be the same in Γ_1 and in Γ_2. Apart from this easy observation, at first sight testing for isomorphism seems to be a difficult task, since one could think that it is necessary to try all the possible mappings for the vertices of Γ_1. Doing so would lead to a number of $n!$ different mappings, where n is the number of real and dummy vertices in Γ_1 (and by the observation before in Γ_2, as well) – alone to assign the vertices of Γ_1 and Γ_2 to each other. However, it is not necessary to run such an extraordinarily large test, as we will see soon. To this end we introduce the so-called *valid bijective mapping*. Thereby a bijective mapping[7] between vertices, crossings, edges, and faces of Γ_1 and Γ_2 is *valid* if and only if the following two properties hold:

[6]Recall that a rotation system describes the cyclic order of edges around each vertex.

[7]The word “bijective” implicitly implies that the number of crossings, real vertices, edges and faces is the same for both planarizations. It also implies that crossings and real vertices in Γ_1 are mapped to the same type of vertices in Γ_2.

Prop. 1 If an edge (v_1, w_1) of Γ_1 is mapped to an edge (v_2, w_2) of Γ_2, and v_1 is mapped to v_2, then w_1 is mapped to w_2 (see Fig. 5.2a).

Prop. 2 If a face f_1 of Γ_1 is mapped to a face f_2 of Γ_2, and an edge e_1 incident to f_1 is mapped to an edge e_2 incident to f_2, then the predecessor (successor) of e_1 is mapped to the predecessor (successor) of e_2 when walking along the boundary of f_1 in counter-clockwise direction and along the boundary of f_2 in clockwise or counter-clockwise direction (see Fig. 5.2b). Also, the face incident to the other side of e_1 is mapped to the face incident to the other side of e_2 (see Fig. 5.2c).

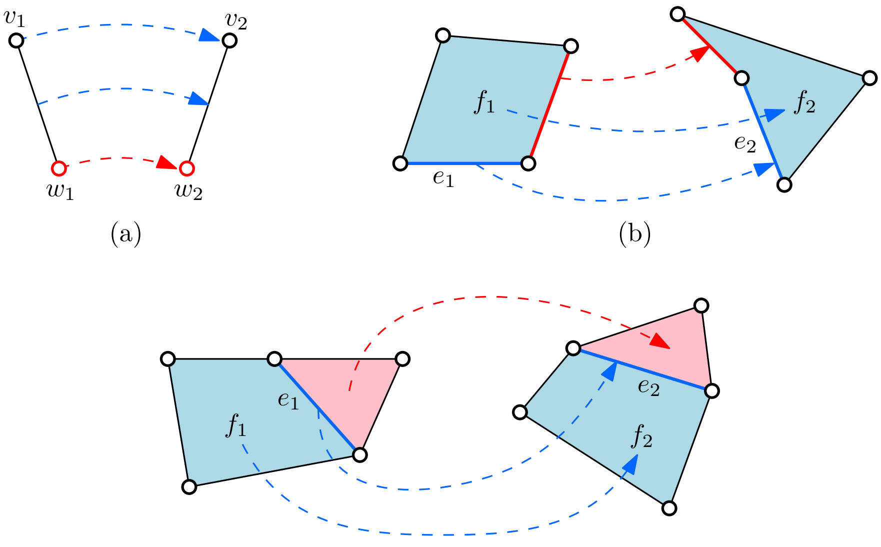

Fig. 5.2: Illustration of the properties for a valid bijective mapping. (a) If v_1 and (v_1, w_1) are mapped to v_2 and (v_2, w_2), respectively (blue arrows), then w_1 is mapped to w_2 (red arrow). (b) If e_1 and f_1 are mapped to e_2 and f_2, respectively (blue arrows), then the successor of e_1 is mapped to the successor of e_2 (red arrow). (c) If e_1 and f_1 are mapped to e_2 and f_2, respectively (blue arrows), then the face on the other side of e_1 is mapped to the face on the other side of e_2 (red arrow).

Clearly these Properties are sufficient for D_1 and D_2 to be isomorphic. Next we argue that they are also necessary.

To this end, suppose that D_1 and D_2 are isomorphic. Then Γ_1 can be transformed into Γ_2 by relabeling the vertices, edges, and faces of Γ_1, that is, there is a bijective mapping φ between the vertices, edges, and faces of Γ_1 and Γ_2.

If φ maps some vertex v_1 of Γ_1 to a vertex v_2 in Γ_2, then φ necessarily maps one of the edges incident to v_1 to one of the edges incident to v_2, since φ transforms Γ_1 into Γ_2. For the same reason, the order of the edges around v_1 must be the same as the order of the edges around v_2, namely, if $e_1, e_2, \ldots, e_\delta$ are the edges around v_1

in clockwise order, where δ is the degree of v_1, then $\varphi(e_1), \varphi(e_2), \ldots, \varphi(e_\delta)$ are the edges around $v_2 = \varphi(v_1)$ in clockwise or counterclockwise order. Moreover, the face f_i whose boundary contains both edges e_i and e_{i+1} (where $1 \leq i \leq \delta$ and $\delta + 1$ is identified with 1), must be mapped to the face whose boundary contains both edges $\varphi(e_i)$ and $\varphi(e_{i+1})$. This implies the second condition of Property 2.

Suppose now that φ maps an edge (v_1, w_1) of Γ_1 to an edge (v_2, w_2) of Γ_2, and v_1 to v_2. Again, since φ transforms Γ_1 into Γ_2, it must map w_1 to w_2. So Property 1 holds.

Finally, we claim that the first condition of Property 2 is also true for φ by a similar argument as above: If $\varphi(f_1) = f_2$ for faces f_1 and f_2 in Γ_1 and Γ_2, respectively, the mapping φ must be such that the order of the edges along the boundaries of f_1 and f_2 is preserved; that is, if $e_1, e_2, \ldots, e_\delta$ appear in this (clockwise) order along the boundary of f_1 (where δ is the degree of f_1), then $\varphi(e_1), \varphi(e_2), \ldots, \varphi(e_\delta)$ are the edges along f_2 in clockwise or counterclockwise order.

So Properties 1 and 2 are indeed necessary for D_1 and D_2 to be isomorphic and we obtain the following lemma.

Lemma 5.1. *Two drawings D_1 and D_2 of the same graph G are isomorphic if and only if there is a valid bijective mapping between their planarizations Γ_1 and Γ_2.*

Algorithm. Next we describe an algorithm that tests if D_1 and D_2 are isomorphic. More precisely, we test if there is a valid bijective mapping between Γ_1 and Γ_2.

(1) First we select an edge $e_1 = (v_1, w_1)$ in Γ_1. This is our base edge. Let $e_2 = (v_2, w_2)$ be an edge in Γ_2 whose end vertices are compatible with the ones of e_1 (i. e., both vertices v_1 and v_2 are real vertices or crossings, and the same holds for w_1 and w_2). Let f_1 be the face of Γ_1 that is on the left side of e_1 when walking along e_1 from v_1 to w_1. Further let f_2 be one of the two faces that are incident to e_2 in Γ_2, say f_2 is the face on the left side of e_2 when walking along e_2 from v_2 to w_2.

We bijectively map edge e_1 to e_2, (real or crossing) vertex v_1 to v_2, vertex w_1 to w_2 (these three mappings complies with Property 1), and face f_1 to f_2. We call this mapping a *base mapping*. The idea of the main step of our algorithm is to try to extend this base mapping to a valid bijection between Γ_1 and Γ_2. Note that the case when f_2 is on the right side of e_2 is symmetric and is part of another base mapping. Further note that we consider the edge (w_2, v_2) as different from $e_2 = (v_2, w_2)$, so (w_2, v_2) gives rise to two additional base mappings (see Fig. 5.3 for an illustration of the four different cases that an edge of Γ_2 generates).

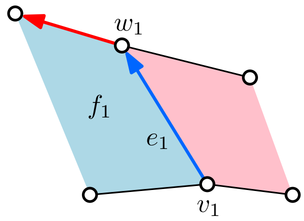

(a)

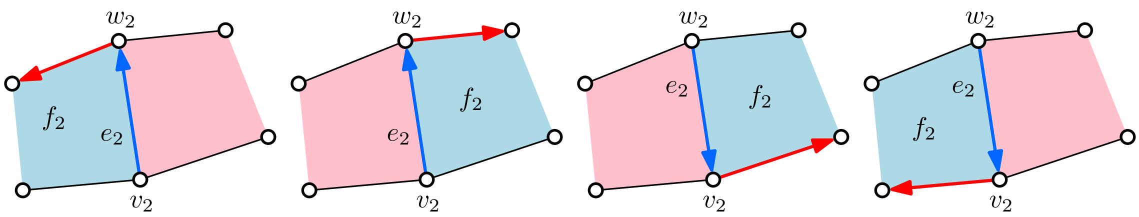

(b) (c) (d) (e)

Fig. 5.3: The four different base mappings a single edge e_2 of Γ_2 can be part of. The colors indicate which edges and faces are mapped to each other. For the edges, only the mapping of the successor of base edge e_1 to the successor of e_2 is shown (red arrows). (a) A partial drawing of Γ_1. (b)–(e) Partial drawings of Γ_2; each figure shows one of the four possible base mappings in which edge e_2 is involved.

(2) In order to extend the base mapping, it is necessary for f_1 and f_2 to have the same degree δ. If not, we can discard the current base mapping immediately. Otherwise we walk simultaneously in counter-clockwise direction along the boundaries of f_1 and f_2, starting at e_1 and e_2 respectively.[8] To meet the requirements of Property 2, for each $i = 1, \ldots, \delta$, we bijectively map the i-th vertex of f_1 to the i-th vertex of f_2, and the i-th edge of f_1 to the i-th edge of f_2.[9] (See also Fig. 5.3, where, in each drawing, the blue arrow represent the first edge on the boundaries of f_1 and f_2, respectively, and the red arrow represent the second edge.)

We discard the current base mapping if a crossing is mapped to a real vertex, or if the degrees of two mapped vertices are different, since in this case Property 1 or Property 2 is violated.

(3) In the next step we consider the two maximal connected subdrawings Γ_1' and Γ_2' of Γ_1 and Γ_2, respectively, such that each edge of Γ_1' and Γ_2' has at least one face incident to it that is already mapped.

If $\Gamma_1' = \Gamma_1$ and $\Gamma_2' = \Gamma_2$, we were able to extend the base mapping to a valid bijection. Otherwise, there is an edge e_1' in Γ_1' that is incident to only one

[8]When f_2 is on the right side of e_2, we walk along the boundary of f_2 in clockwise direction.

[9]Note that, if we were successful, all the edges mapped so far have at least one face incident to it that is already mapped (namely the faces f_1 and f_2, respectively); so this gives us the base of Step 3.

mapped face f_1', and another face $f_1^\star$ which is not mapped yet. Let e_2' be the edge of Γ_2' that is mapped to e_1'. The edge e_2' must be incident to a face f_2' that is mapped to f_1' and to a face $f_2^\star$ that is not mapped yet (otherwise we would have discarded the current base mapping already in a step before, since Property 2 would have been violated). Then, by Property 2, we are forced to map $f_1^\star$ to $f_2^\star$.

We continue by applying the procedure described in Step 1 to $f_1^\star$ and $f_2^\star$, that is, we walk along the boundaries of $f_1^\star$ and $f_2^\star$ simultaneously, while ensuring that the mapping remains valid. Here the direction of the boundary walk for $f_2^\star$ is given by the known mapping of the endpoints of e_1' to the endpoints of e_2'.

If this procedure can be performed successfully, we obtain two subdrawings Γ_1'' and Γ_2'' of Γ_1 and Γ_2, respectively, such that $\Gamma_1' \subseteq \Gamma_1''$, $\Gamma_2' \subseteq \Gamma_2''$, and each edge of Γ_1'' and Γ_2'' has at least one face incident to it that is already mapped. Therefore we can recursively apply Step 3 to Γ_1'' and Γ_2''. As the number of faces in Γ_1 is finite, this process will eventually terminate – either with a valid bijective mapping or with discarding the current base mapping.

(4) If the base mapping can be extended, the drawings D_1 and D_2 are isomorphic. Otherwise we start with Step 1 again, using a different base mapping. If none of the base mappings can be extended, then D_1 and D_2 are not isomorphic.

Observe that, if we fix a base mapping, all other assignments between vertices, edges and faces of Γ_1 and Γ_2 are forced by Properties 1 and 2. Thus, the number of tests depend on the number of different base mappings, or more precisely on the number of edges of Γ_2. However, we can reduce the number of base mappings we have to consider: We count the number of edges of Γ_1 and Γ_2 whose endpoints are both real vertices, whose endpoints are both crossing vertices, and whose endpoints consists of one real vertex and one crossing vertex. If the drawings D_1 and D_2 are isomorphic, these numbers must clearly be the same for both drawings Γ_1 and Γ_2. If this is the case, we choose as base edge an edge of the type with the smallest positive number of occurrences, since it suffices to consider base mappings only restricted to one of the three types of edges.

We conclude this section by mentioning that in the worst case we still have to consider all $|E(\Gamma_2)|$ edges, which gives rise to $4 \cdot |E(\Gamma_2)|$ base mappings. But in general it will be a much smaller number, in most cases less than one third of the aforementioned number.

5.4 Insertion Procedure

In this section we describe how to insert a vertex and its incident edges into a drawing, such that simplicity and the restrictions of a graph class $\mathcal{C}$ are respected.

5.4.1 Pathways

We start with the basic definitions used in our algorithm.

Let $\overline{G} = (\overline{V}, \overline{E})$ be a graph, $G = (V, E)$ a subgraph of $\overline{G}$ which belongs to class $\mathcal{C}$, D a $\mathcal{C}$-drawing of G, and $\Gamma = \Gamma(D)$ its planarization.

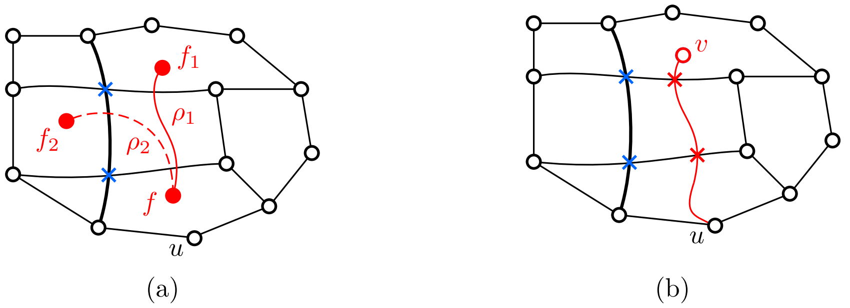

Fig. 5.4: (a) Two pathways ρ_1 (solid red) and ρ_2 (dashed red) for u of length 2, with destinations f_1 and f_2 (the crosses indicate dummy vertices of Γ). For the class of 2-planar graphs, ρ_1 is valid, while ρ_2 is not valid, since in its presence the bold drawn edge has three crossings. (b) An augmentation of Γ by edge (u, v), using the valid pathway ρ_1.

Let Γ_d be the dual of Γ, vertex u a vertex of Γ and f a face incident to u. Then a *half-pathway* for u is a path in Γ_d starting from f and ending at some face f' in Γ (note that $f' = f$ is allowed). We call f' the *destination* of the half-pathway (see Fig. 5.4 for an illustration). The *length* of a half-pathway is the number of edges in this path. A half-pathway ρ for u is called *valid* with respect to class $\mathcal{C}$ if Γ can be augmented such that:

(i) a vertex $v \in \overline{V} \setminus V$ is placed in the interior of the destination of ρ,

(ii) edge (u, v) is drawn as a curve from u to v in such a way that this curve only crosses the edges dual to the edges in ρ, in the same order, and

(iii) drawing edge (u, v) in D with the same curve as in Γ, results in a simple $\mathcal{C}$-drawing.

Given two vertices $u, v \in V$ and an edge $(u, v) \in \overline{E} \setminus E$, we define a *pathway* for (u, v) as a half-pathway for u, whose destination is a face incident to v. Analogously to a valid half-pathway, a pathway ρ is called *valid* for (u, v) with respect to $\mathcal{C}$, if Γ can be augmented such that:

(i) edge (u, v) is drawn as a curve from u to v such that it only crosses the edges dual to the edges in ρ, in the same order, and

(ii) drawing edge (u, v) in D with the same curve as in Γ, results in a simple $\mathcal{C}$-drawing.

So the only difference between a valid pathway and a valid half-pathway is that v does not need to be placed in Γ, since it is already part of it.

5.4.2 Insertion algorithm

By means of half-pathways and pathways we describe our algorithm for inserting a vertex $v \in \overline{V} \setminus V$ (together with its edges) into D, given a certain graph class $\mathcal{C}$ (also refer to Alg. 1). To this end let $u_1, \dots, u_k$ be the neighbors of v in G.

Algorithm 1: Insertion Algorithm

Input: A vertex v, a drawing D, and a class $\mathcal{C}$
Output: All non-isomorphic drawings that contain v, belong to $\mathcal{C}$, and have D as a subdrawing.

INSERT(*Vertex:* v, *Drawing:* D, *Class:* $\mathcal{C}$)

$u_1, \dots, u_k \leftarrow$ the neighbors of v in G;
$\mathcal{S}_1, \mathcal{S}_2 \leftarrow \emptyset$;
foreach *valid half-pathway* ρ *for* u_1 *in* D **do**
  /* choose a face for v and connect it to u_1 */
  Add to $\mathcal{S}_1$ the drawing obtained by inserting an edge (following ρ) and a new vertex v (in the destination of ρ) into D;
end
for $i = 2, \dots, k$ **do**
  /* connect v to all its other neighbors */
  foreach *drawing* D' *in* $\mathcal{S}_1$ **do**
    foreach *valid pathway* ρ *for* (v, u_i) *in* D' **do**
      Add to $\mathcal{S}_2$ the drawing obtained by inserting an edge (following ρ) into D';
    end
  end
  $\mathcal{S}_1 \leftarrow \mathcal{S}_2$;
  $\mathcal{S}_2 \leftarrow \emptyset$;
end
return $\mathcal{S}_1$

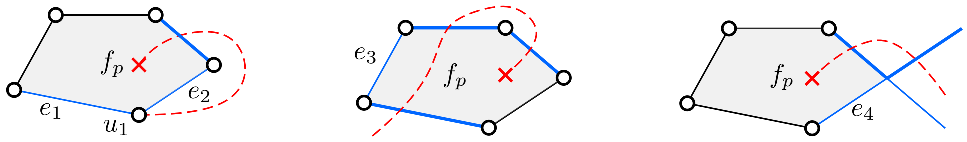

Fig. 5.5: The prohibited edges (blue) for a half-pathway (red dashed) that ends in a face f_p. The thick blue edges are prohibited, because they are crossed by the half-pathway. In (a) edges e_1 and e_2 are prohibited, since they are incident to u_1. In (b) edge e_3 is prohibited, since, in order to cross this edge, the half-pathway would make a self-crossing. In (c) edge e_4 is prohibited, since it is part of a crossed edge.

First we compute all possible valid half-pathways for u_1 in Γ with respect to $\mathcal{C}$. For each such half-pathway we construct a $\mathcal{C}$-drawing by augmenting D with the edge (u_1, v) (see Line 3 of Alg. 1).

We compute these valid half-pathways (and also the valid pathways) recursively. Note that, in order to be valid, a half-pathway must violate neither simplicity nor the restrictions of class $\mathcal{C}$. So there are some edges in Γ, which we call *prohibited* edges, that a valid half-pathway is not allowed to cross (see Fig. 5.5). While creating the half-pathways we maintain a list of prohibited edges for each half-pathway, ensuring the validity of it.

In the base of the recursion, we determine all valid half-pathways for u_1 of length zero. In other words, for each face f that is incident to vertex u_1, we create a half-pathway starting at f with its destination also at f. Such a half-pathway (which is clearly valid) corresponds to placing the vertex v in f and drawing edge (v, u_1) crossing-free (we refer to Fig. 5.6 for an example). For each such half-pathway the list of prohibited edges is initialized with all edges of Γ corresponding to edges of D that are incident to u_1.

Now assume that we have already computed all valid half-pathways of some length $i \geq 0$ in Γ. We show how to compute all valid half-pathways for u_1 of length $i + 1$ (if any). On that account we consider a valid half-pathway ρ of length i. Let f_ρ be its destination and ℓ its list of prohibited edges. Every non-prohibited edge e on the boundary of f_ρ yields a new half-pathway ρ_e of length $i + 1$, composed of ρ followed by the edge that is dual to e in Γ. For ρ_e we create the list ℓ_e of prohibited edges by first copying ℓ. Then we add to ℓ_e all edges of Γ that correspond to the same edge of G as e (see Fig. 5.5c) to guarantee simplicity, as well as the edges of Γ that cannot be further crossed due to the restrictions of class $\mathcal{C}$. Note that the list of prohibited edges will increase at least by one, because e is admitted into ℓ_e. So this process will finally terminate, since the number of edges of Γ is bounded.

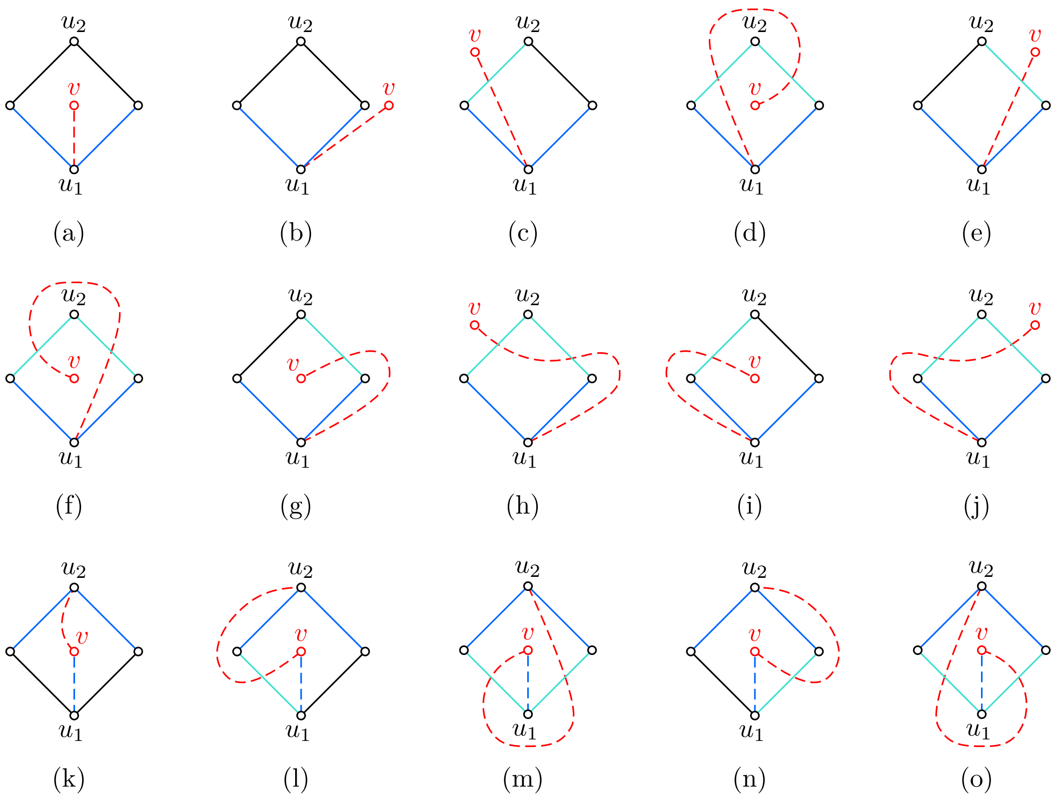

Fig. 5.6: An example for the insertion of a vertex v into a crossing-free 4-cycle, such that v is connected to two vertices u_1 and u_2. In each drawing, the dashed red edge is the newly inserted edge; the blue edges are prohibited; the turquoise edges are the edges that are marked as prohibited while computing the half-pathway that corresponds to the red edge. Figures 5.6a to 5.6j illustrate all possible ways for drawing edge (v, u_1). Figures 5.6k to 5.6o illustrate all possible ways for inserting edge (v, u_2) into the drawing of Fig. 5.6a. Note that among the drawings that contain edge (v, u_2), the drawings of Figs. 5.6l and 5.6n are isomorphic, as well as the drawings Figs. 5.6m and 5.6o. Moreover, all drawings illustrated here are legal for the topological graph classes mentioned at the beginning of this chapter (in Sec. 5.1.1), except for the class of 1-planar graphs.

As already outlined before, for each valid half-pathway ρ we obtain a new (intermediate) drawing by inserting (u_1, v) into Γ following ρ and by inserting v into the destination of ρ (see Line 4 of Alg. 1).

In order to get a $\mathcal{C}$-drawing for $G[V \cup \{v\}]$, it remains to insert the edges $(u_2, v), \ldots, (u_k, v)$ into each of these (intermediate) drawings, again in all possible ways (see Lines 6 to 13 of Alg. 1). The insertion process for these edges is mostly the same as the one for (u_1, v) described above, with one difference: Instead of valid *half-pathways*, we search for valid *pathways* for each edge (v, u_i), $2 \leq i \leq k$, that is, we only consider pathways starting in a face incident to v and ending in a face incident to u_i.

During this procedure, it may happen that we encounter an edge (v, u_i) such that there is no valid pathway at all (for none of the intermediate drawings). In this case Γ cannot be extended to a simple $\mathcal{C}$-drawing of $G[V \cup \{v\}]$ and we can report this fact. Otherwise, we compute all simple $\mathcal{C}$-drawings of $G[V \cup \{v\}]$ and can use them for further computations in the general procedure, see the following section.

5.5 Generation Procedure

Using the algorithms from Secs. 5.3 and 5.4, we are now able to formulate an algorithm to calculate all simple non-isomorphic $\mathcal{C}$-drawings of a complete or a complete bipartite graph G for some topological graph class $\mathcal{C}$.[10] We describe our algorithm in a recursive way. Thereby a set $\mathcal{S}$ is computed, which contains all non-isomorphic simple $\mathcal{C}$-drawings of G (if any). For an outline of the main steps of our algorithm we refer to Alg. 2.

Recall that the insertion procedure in Sec. 5.4 and the isomorphic test in Sec. 5.3 are both defined on planarizations of drawings. For this reason, with a slight abuse of terminology, we assume in the following (sometimes implicitly) that $\mathcal{S}$ contains the planarizations of the drawings of G.

We distinguish two cases for the base of the recursion (see Line 10 of Alg. 2):

- If we consider complete graphs, then the base of the recursion is a cycle of length 3, that is $G = K_3$. In this case the set $\mathcal{S}$ only contains a single drawing,

[10] We remark that our approach can also be applied to graphs that are neither complete nor complete bipartite. However, in this case the number of non-isomorphic drawings increases drastically, and thus the running time, up to the point that it is not possible to execute our algorithm within appropriate time. We give more details about the effect of the isomorphic test in Sec. 5.8.

Algorithm 2: Enumeration Algorithm

Input: A complete (bipartite) graph G and a graph class $\mathcal{C}$ beyond planarity.
Output: All non-isomorphic drawings of G that are certificates that G belongs to $\mathcal{C}$.

ENUMERATE(*Graph* G)
1 **if** $G \notin \{K_3, K_{2,2}\}$ **then**
2     $v \leftarrow$ a vertex of G;
3     $\mathcal{S}' \leftarrow$ ENUMERATE($G \setminus \{v\}$);
4     $\mathcal{S} \leftarrow \emptyset$;
5   **foreach** *drawing* D *in* $\mathcal{S}'$ **do**
        /* Add v and its edges to D in all possible ways respecting $\mathcal{C}$ */
6         $\mathcal{S} \leftarrow \mathcal{S} \cup$ INSERT($v, \Gamma, \mathcal{C}$);
7   **end**
8   Remove drawings from $\mathcal{S}$ that are isomorphic to other ones in $\mathcal{S}$;
9 **else**
    /* G is the complete graph K_3 or the complete bipartite graph $K_{2,2}$ */
10     $\mathcal{S} \leftarrow$ all non isomorphic drawings of G;
11 **end**
12 **return** $\mathcal{S}$;

namely a planar drawing of K_3, since all other drawings are isomorphic to this one or non-simple.

- If we consider complete bipartite graphs, then the base of the recursion is a cycle of length 4, that is $G = K_{2,2}$. In this case the set $\mathcal{S}$ contains two drawings, namely a planar drawing and one with a crossing between two non-adjacent edges.

In the recursive step we consider a vertex v of G (see Line 2 of Alg. 2). Note that the vertex v can be chosen arbitrarily for complete graphs; for a complete bipartite graph $K_{a,b}$ the running time may differ, depending to which of the two independent parts of $K_{a,b}$ the vertex v belongs to. We refer to the discussion in Sec. 5.8.

We recursively compute a set $\mathcal{S}'$ which contains all non-isomorphic simple $\mathcal{C}$-drawings of $G[V \setminus \{v\}]$ (refer to Line 3 of Alg. 2). If $\mathcal{S}'$ is empty, graph G does not belong to class $\mathcal{C}$. So we may assume w. l. o. g that $\mathcal{S}' \neq \emptyset$. For each drawing $D \in \mathcal{S}'$, our algorithm reports all simple $\mathcal{C}$-drawings of G with D as subdrawing, by means of the procedure described in Sec. 5.4 (see Alg. 1). All these drawings are saved in a set $\mathcal{S}$ that is initially empty (Line 6 of Alg. 2). In the final step we ensure that $\mathcal{S}$ only contains non-isomorphic drawings (see Line 8 of Alg. 2), using the procedure described in Sec. 5.3.

We summarize our results in the following theorem.

Theorem 5.2. *Let G be a complete (or a complete bipartite) graph and let $\mathcal{C}$ be a beyond-planarity class of topological graphs. Then G belongs to $\mathcal{C}$ if and only if our algorithm returns a drawing of G.*
In particular, if $G \in \mathcal{C}$, our algorithm returns ***all*** *non-isomorphic drawings for G.*

5.6 Data Structure

In this section we give a brief high-level introduction in the data structure we used in our implementation.

The requirement for saving a planarization Γ of a drawing D for a connected graph G is the following: The data structure should be such that it is possible to implement the insertion of a new vertex and new edges easily. It turned out to be a good choice to use a so-called doubly-connected edge list (see e. g. Berg et al.[34, Section 2.2]). The doubly-connected edge list consists of collections of (real and crossing) vertices, faces, and so-called half-edges. Thereby each (undirected) edge (u, v) of Γ is represented by two directed half-edges, one with source u and target v, the other with source v and target u. The most important details for these data types are as follows:

- A vertex v contains a pointer to one of its incident half-edges; this half-edge must have v as its source. Further v contains a variable, indicating whether v is a crossing or a real vertex. It is not necessary for our algorithm, but beneficial for drawing the planarization, to create a field for the vertex coordinate.
- A face f contains a pointer to one of the half-edges on its boundary.
- A half-edge $e = (u, v)$, where u is the source of e and v the target, contains several pointers:
  - a pointer to the source u;
  - a pointer to the target v;
  - a pointer to its twin half-edges, that is the edge with source v and target u;
  - a pointer to the face f_e “left” of e;
  - a pointer to the successor of e, that is the edge (with source v) following e when walking along the boundary of f_e;
  - a pointer to the predecessor of e, that is the edge (with target u) that has e as successor when walking along the boundary of f_e.

Note that, since Γ is connected, all elements are defined in such a way that it is possible to traverse the whole planarization starting at an arbitrary element. In particular, the boundary of a face and the edges around a vertex can be traversed easily. Thus, it is not difficult to obtain the prohibited edges mentioned in Sec. 5.4. Further, inserting vertices and its incident edges is just a matter of creating new vertices, edges and faces, and of changing pointers. So our main requirement is fulfilled. Since it is easy to traverse the planarization, and such a simultaneous traversal is the main part of our isomorphic test, the doubly-connected edge list also supports the second part of Alg. 2 in an efficient way.

Apart from the doubly-connected edge list, no special data structures are needed. All other steps of the algorithm could be executed using basic structures like lists, sets, etc.

We close this section by mentioning one important issue. It might not be practicable to keep all the data in main memory, since the number of different non-isomorphic drawings is too large for this strategy in most of the cases.[11] We accommodated this fact by saving only a small number of the drawings in main memory, while saving them on hard disc if a certain number was reached.

5.7 Proof of Concept – Applications

We implemented the algorithm described in Sec. 5.5 for some topological graph classes $\mathcal{C}$.[12] In this section we use our implementation to test if there exist simple $\mathcal{C}$-drawings for certain complete or complete bipartite graphs. Further we give corresponding characterizations – if possible – and describe how our results are positioned within the literature (see also Tables 5.1 and 5.2). We refer to the smallest instances reported as negative by our algorithm (or by other means) as upper bounds for $\mathcal{C}$. Likewise, lower bounds are instances reported as positive, i. e., our algorithm found a drawing which certifies that a particular graph belongs to class $\mathcal{C}$.

Our implementation is available to the community in the following repository:

`https://github.com/beyond-planarity/complete-graphs`

In the following we discuss our findings for various classes of beyond-planar graphs.

[11] We will list statistics of our calculations in Sec. 5.8.

[12] We chose graph classes where we hoped to obtain results in reasonable time; refer also to the discussion in Sec. 5.8.

5.7.1 The class of k-planar graphs

Recall that k-planar graphs are such that each edge may be crossed at most k times.

Regarding the complete 1-planar graphs, we already mentioned that Czap and Hudák [53] showed that K_n is 1-planar if and only if $n \leq 6$. Further, it was already known that K_9 is not 2-planar, since every 2-planar graph has at most $5n - 10$ edges [108], while K_7 belongs to the class of 2-planar graphs (see Fig. 7 in [39]). However, the question if K_8 is a 2-planar graph was still open. We were able to answer this question with our implementation by reporting that K_8 is not 2-planar.

For complete 3-, 4-, and 5-planar graphs, a similar edge-density argument can be applied as for the 2-planar graphs [3, 106] (for the densities of these classes we refer to Table 5.1), proving that K_{10}, K_{11}, and K_{19} are not 3-, 4-, and 5-planar, respectively. Again we could improve these upper bounds with our implementation, by concluding that even K_9 is not 3-planar, while K_{10} is neither 4- nor 5-planar. Moreover, our algorithm provided a 3-planar drawing of K_8 (see Fig. 5.7a), and a 4-planar (which is of course also 5-planar) drawing of K_9 (see Fig. 5.7b), while we constructed a 6-planar drawing of K_{10} (see Fig. 5.7c) by adding one extra vertex inside the red colored triangle in the 4-planar drawing of K_9 in Fig. 5.7b.[13]

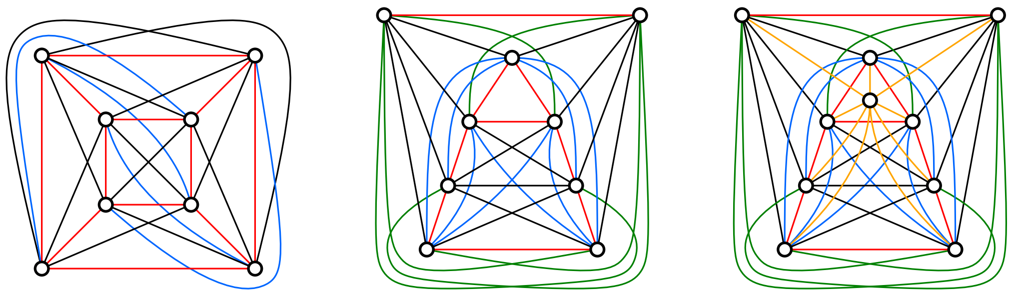

(a) (b) (c)

Fig. 5.7: (a) A 3-planar drawing of K_8. (b) A 4-planar drawing of K_9. (c) A 6-planar drawing of K_{10}.

We summarize these results in the following characterization.

Characterization 5.3. *For $k \in \{1, 2, 3, 4\}$, the complete graph K_n is k-planar if and only if $n \leq 5 + k$. Also, K_n is 5-planar if and only if $n \leq 9$.*

A consequence of the fact that K_8 is 3-planar is that the chromatic number of 3-planar graphs is at least 8. Similarly, the chromatic number of 4- and 5-planar graphs is lower bounded by 9, and the one of 6-planar graphs by 10.

[13]Density arguments imply that K_{20} is not 6-planar.

Another result from our experiments is that K_6 has a unique 1-planar drawing (up to isomorphism), the graph K_7 has only two 2-planar drawings, K_8 has three 3-planar drawings, while K_9 has 35 drawings that are 4-planar. The number of 5-planar drawings for K_9 is drastically larger, namely there are 29,939 of them. More statistics regarding complete and complete bipartite graphs can be found in Sec. 5.8.

With a slight modification of our algorithm we were even able to determine an edge-exact bound when aiming to draw complete graphs. More precisely, it is possible to insert into the maximal $\mathcal{C}$-drawable complete graph another vertex together with some edges incident to it. We could determine how many edges can be added such that the resulting graph still belongs to class $\mathcal{C}$. For 1-planar graphs, one can add three more edges to K_6, as the 1-planar drawing in Fig. 5.8a shows, while we concluded (by trying all possibilities using our implementation) that it is not possible to add to K_6 one vertex together with four incident edges, such that the resulting drawing is still 1-planar. The corresponding maximal numbers of edges that can be added for the other complete graphs considered above are as follows. The graph K_7 enriched with one vertex and 5 edges incident to it is still 2-planar (see Fig. 5.8b for a certificate drawing). The graph K_8 plus a vertex together with 5 incident edges is 3-planar (see Fig. 5.8c). Regarding 4-planarity, one may add a vertex and 3 incident edges to K_9 without losing this property (see Fig. 5.8d), while K_{10} minus one edge is still 5-planar (see Fig. 5.8e). In the case of 6-planar graphs we cannot provide such an edge-exact bound, since the corresponding calculation was to extensive.

Now we turn our attention to complete bipartite graphs $K_{a,b}$ with $a \leq b$. The first general observation (not only for k-planar graphs) is that the graph $K_{a,b}$ is even planar for $a \leq 2$, which implies that graphs with this property belong trivially to all beyond-planar graph classes.

As already stated at the beginning of this chapter, the graph $K_{a,b}$ is 1-planar if and only if $a \leq 2$, or $a = 3$ and $b \leq 6$, or $a = b = 4$ [53]. Further, Angelini et al. proved that $K_{3,b}$ is k-planar if and only if $b \leq 4k + 2$ [13]. Due to these facts we can focus on the case where $a \geq 4$.

By a recent result, complete bipartite 2-planar graphs have at most $3.5n - 7$ edges [14]. Consequently neither of the graphs $K_{4,15}$ nor $K_{5,8}$ are 2-planar. However, with our implementation we were able to conclude that even $K_{4,7}$ and $K_{5,5}$ are not 2-planar, while in Fig. 5.9a we provide a 2-planar drawing for $K_{4,6}$.

The following characterization depicts a summary of these results.

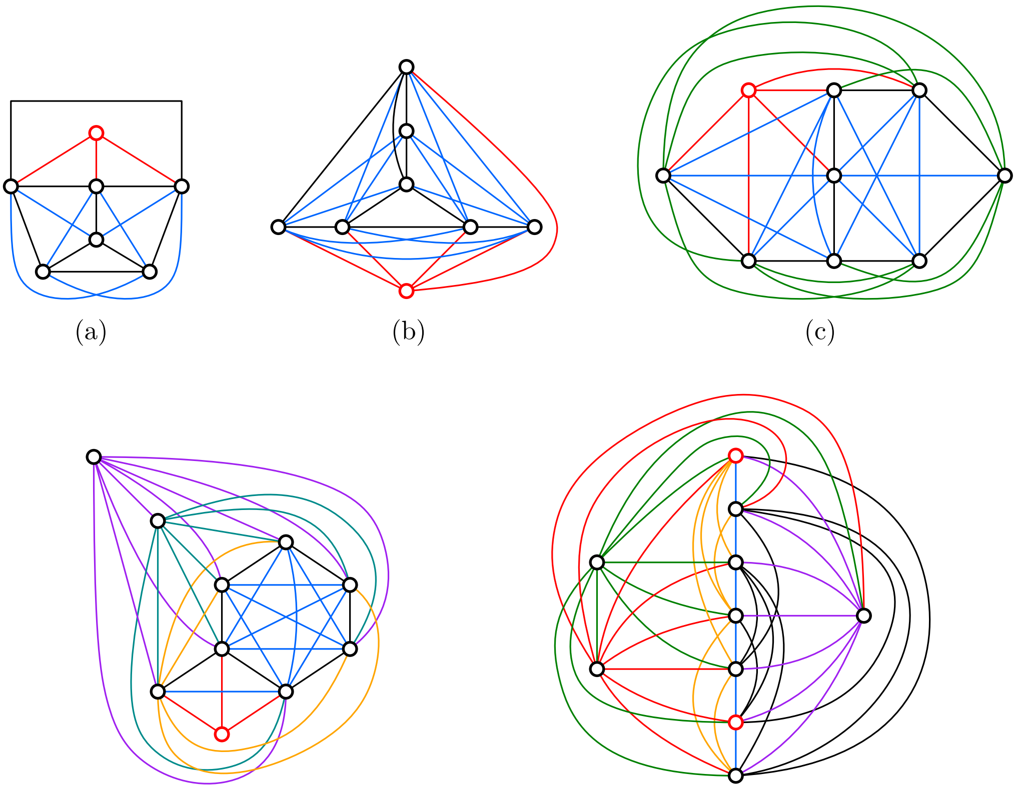

Fig. 5.8: Drawings for edge-exact bounds in the case of (a) the 1-planar graphs: K_6 plus a vertex (red) with 3 edges; (b) the 2-planar graphs: K_7 plus a vertex with 5 edges; (c) the 3-planar graphs: K_8 plus a vertex with 5 edges; (d) the 4-planar graphs: K_9 plus a vertex with 3 edges; (e) the 5-planar graphs: K_{10} minus one edge (the edge between the red vertices is missing).

Characterization 5.4. *The complete bipartite graph $K_{a,b}$ (with $a \leq b$) is 2-planar if and only if*

(i) $a \leq 2$, *or*

(ii) $a = 3$ *and* $b \leq 10$, *or*

(iii) $a = 4$ *and* $b \leq 6$.

The upper bound of $5.5n - 11$ edges [106] for general 3-planar graphs implies that $K_{6,b}$, with $b \geq 45$, is not 3-planar, while the result by Angelini et al. [13] even implies that graphs $K_{a,15}$ with $a \geq 3$ do not belong to this class. However, with our approach we could improve this upper bound significantly by reporting the graphs $K_{4,10}$, $K_{5,7}$, and $K_{6,6}$ as not 3-planar, while, in contrast, the graphs $K_{4,9}$ and $K_{5,6}$ belong to the class of 3-planar graphs (see Figs. 5.9b and 5.9c for certificate drawings). We want to note here that recently there was proven an edge density of $4n - 8$ edges tailored for 3-planar bipartite graphs [112], implying that neither $K_{5,13}$ nor $K_{6,9}$ are 3-planar.

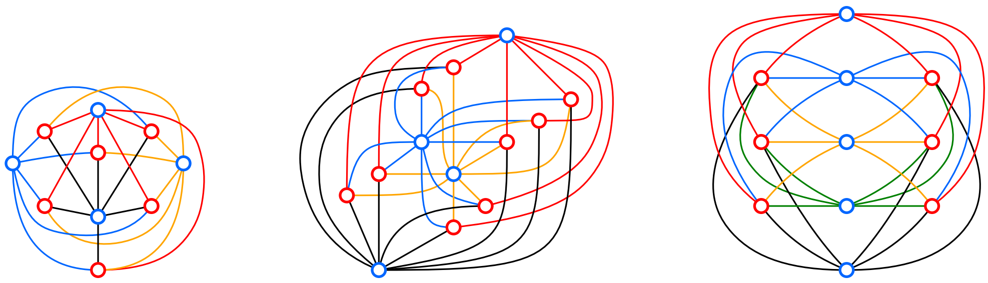

(a) (b) (c)

Fig. 5.9: (a) A drawing of $K_{4,6}$ that is both, 2-planar and fan-crossing free. (b) A 3-planar drawing of $K_{4,9}$. (c) A 3-planar drawing of $K_{5,6}$.

Even compared to this new result, our findings present much better upper bounds for the class of 3-planar graphs.

Our results are summarized in the following characterization.

Characterization 5.5. *The complete bipartite graph $K_{a,b}$ (with $a \leq b$) is 3-planar if and only if*

(i) $a \leq 2$, *or*

(ii) $a = 3$ *and* $b \leq 14$, *or*

(iii) $a = 4$ *and* $b \leq 9$, *or*

(iv) $a = 5$ *and* $b \leq 6$.

For the 4-planar bipartite complete graphs, there is an upper bound of $5.741n$ edges [112], implying an upper bound of $K_{5,134}$. However, this bound is by far worse than the one obtained from the fact that $K_{3,19}$ is not 4-planar [13], namely the graphs $K_{a,19}$ are not 4-planar for $a \geq 3$.

In the case of this graph class, we were not able to provide better upper bounds, since the search space turned out to be drastically larger compared to the previous cases and therefore our generation technique could not terminate. Again we want to refer to Sec. 5.8 and especially to Table 5.3, where one can find clear evidence about this increase of the search space.

In order to obtain at least some certificate drawings for the lower bound, we slightly refined our generation technique. We explain this refinement in Sec. 5.7.2. With this addition to our implementation we were able to report the graphs $K_{4,11}$, $K_{5,8}$, and $K_{6,6}$ as 4-planar (see Fig. 5.10).

The following observation summarizes our results regarding the 4-planar graphs.

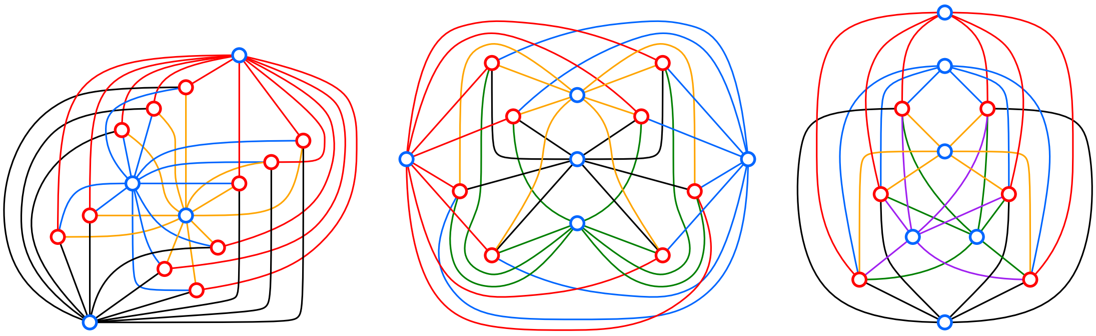

(a) (b) (c)

Fig. 5.10: Illustration of 4-planar drawings for (a) $K_{4,11}$, (b) $K_{5,8}$ and (c) $K_{6,6}$.

Observation 5.6. *The complete bipartite graph $K_{a,b}$ (with $a \leq b$) is 4-planar if*

(i) $a \leq 2$, *or*

(ii) $a = 3$ *and* $b \leq 18$, *or*

(iii) $a = 4$ *and* $b \leq 11$, *or*

(iv) $a = 5$ *and* $b \leq 8$, *or*

(v) $a = 6$ *and* $b = 6$.

Further, $K_{a,b}$ is not 4-planar if $a \geq 3$ and $b \geq 19$.

Finally, for the 5-planar graphs we did not even try to find a characterization, since such graphs are a super-class of the 4-planar graphs and we explained already the problems with the latter class. So the upper bound stems again from Angelini et al. [13], namely the complete bipartite graph $K_{a,23}$ is not 5-planar for all $a \geq 3$. However, we were able to provide at least a certificate drawing for $K_{6,7}$ in Fig. 5.11, again by using our refined generation technique.

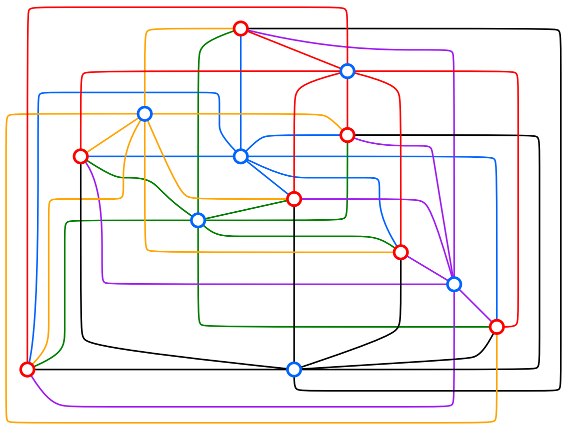

Fig. 5.11: A 5-planar drawing for $K_{6,7}$.

The following observation summarizes our findings. Note that, since $K_{4,11}$ and $K_{5,8}$ are both 4-planar, they are also 5-planar.

Observation 5.7. *The complete bipartite graph $K_{a,b}$ (with $a \leq b$) is 5-planar if*

(i) $a \leq 2$, *or*

(ii) $a = 3$ *and* $b \leq 22$, *or*

(iii) $a = 4$ *and* $b \leq 11$, *or*

(iv) $a = 5$ *and* $b \leq 8$, *or*

(v) $a = 6$ *and* $b \leq 7$.

Further, $K_{a,b}$ is not 5-planar if $a \geq 3$ and $b \geq 23$.

5.7.2 A DFS-like approach to obtain certificate drawings

As mentioned above, for certain graph classes $\mathcal{C}$ it is not always possible to calculate all simple non-isomorphic complete or complete bipartite $\mathcal{C}$-drawings. We have already seen that the complete bipartite 4-planar graphs are such an example. Later on we will see more examples where we cannot calculate all drawings needed for a characterization (at least not in appropriate time). Nonetheless, by a modification of our technique we can at least obtain partial results. In particular, in order to calculate a simple $\mathcal{C}$-drawing for $K_{a,b}$, we try to compute a few sample drawings of $K_{a,b-1}$ or $K_{a-1,b}$, instead of computing *all* possible non-isomorphic simple $\mathcal{C}$-drawings for them. The hope is to find a corresponding certificate drawing for $K_{a,b}$ only based on these few samples.

We call this the *DFS-like approach*, since we aim at going "deep", that is, insert as many vertices as fast as possible into a base drawing. Figure 5.12 shows a sketch of this approach and also the original one, which we denote by *BFS-like approach*.

The advantage of the DFS-like approach is indeed that one may obtain drawings with many vertices fast. On the other hand, since not all the drawings for a graph $K_{a,b}$ are calculated, it is not possible to benefit from the isomorphic test in such a large scale as in the BFS-like approach. As a consequence, the latter should be applied to show that a certain graph is not $\mathcal{C}$-drawable, and in contrast, the DFS-like approach should be used when the BFS-like approach does not terminate within reasonable time, aiming to find at least positive certificate drawings for some graphs.

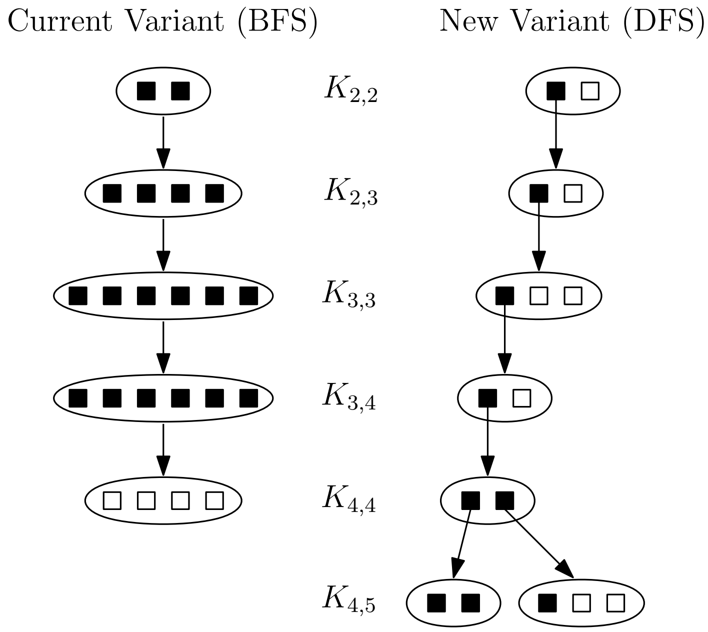

Fig. 5.12: A sketch of the BFS-like (left) and the DFS-like (right) approach. Each square represents a drawing. Filled squares indicate that the next vertex has already been inserted into the corresponding drawing, while this step was not yet executed for empty ones. Note that in the BFS-like approach, the next vertex is inserted into *every* drawing of a certain graph $K_{a,b}$, while in the DFS-like approach the next vertex is inserted in only *one* drawing of a certain graph $K_{a,b}$.

5.7.3 The classes of fan-crossing and fan-planar graphs

Recall that it is not allowed for an edge to be crossed by two independent edges in a fan-crossing drawing, and it is additionally not allowed for an edge to be crossed by two adjacent edges from different directions in a fan-planar drawing. We remark that both graph classes have the same edge density of $5n - 10$ edges [43, 93][14], but despite this, the class of fan-planar graphs is a proper subclass of the class of fan-crossing graphs [43]. In this section we will see that these two graph classes are also "equivalent" regarding the largest complete and complete bipartite graphs belonging to them.

Again we consider first the complete graphs. The density bound mentioned above implies that the graph K_9 is neither fan-crossing nor fan-planar. Since Fig. 7 in [39] shows that K_7 is fan-planar (and thus fan-crossing), the only open case is the graph K_8. With our implementation we could solve this case in the negative: K_8 is not fan-crossing and therefore also not fan-planar. We summarize these results in the following characterization.

[14]Kaufmann and Ueckerdt [93] observed that the bound for the edge density is tight for both classes.

Characterization 5.8. *The complete graph K_n is fan-crossing and fan-planar if and only if $n \leq 7$.*

Like for k-planar graphs, we could even determine an edge-exact bound for both graph classes. Namely, the graph obtained from K_8 by removing one edge is fan-planar (refer to Fig. 5.13) and thus also fan-crossing.[15]

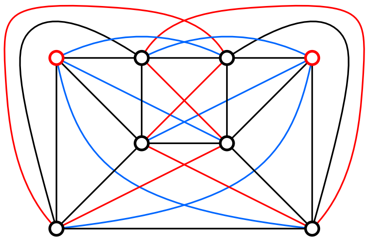

Fig. 5.13: A fan-planar drawing of the graph obtained from K_8 by removing one edge (the edge connecting the two red-colored vertices is missing).

Next we consider complete bipartite graphs $K_{a,b}$ with $a \leq b$. Kaufmann and Ueckerdt [93] observed that for $a \leq 4$ the graph $K_{a,b}$ is fan-planar for any value of b (and consequently also fan-crossing). Using the upper bound of $4n - 12$ edges [14] for bipartite fan-planar graphs, we can conclude that $K_{5,9}$ is not fan-planar. (As far as we know, there exists no density bound for fan-crossing graphs that is specially tailored for bipartite graphs.) With our implementation we were able to concluded that even the graph $K_{5,5}$ is not fan-crossing, and thus not fan-planar. We summarize these results in the following characterization.

Characterization 5.9. *The complete bipartite graph $K_{a,b}$ (with $a \leq b$) is fan-crossing and fan-planar if and only if $a \leq 4$.*

5.7.4 The class of fan-crossing free graphs

First we recall that in each fan-crossing free drawing, no edge is allowed to be crossed by a fan (i. e. two or more adjacent edges). An immediate consequence of this definition and the one for 1-planar graphs is that each 1-planar drawing is fan-crossing free. To obtain a characterization for complete fan-crossing free graphs we combine two known results: The graph K_6 is fan-crossing free, since it is 1-planar; second, the edge density of $4n - 8$ edges for a fan-crossing free graph [50] implies that K_7 is not fan-crossing free. Thus we have the following characterization.

[15] Brandenburg [45] claimed that the graph obtained from K_8 by removing one edge is not fan-crossing, but without giving the details of the proof of this claim. Our result shows that this claim does not hold.

Characterization 5.10 (Cheong et al. [50], Czap et al. [53])**.** *The complete graph K_n is fan-crossing free if and only if $n \leq 6$.*

Moreover, with our implementation we could report that K_6 has a unique (up to isomorphism) fan-crossing free drawing (see Sec. 5.8), and further determine an edge-exact bound of K_6 plus one additional vertex with 3 edges (see Fig. 5.8a).

We already proved in Sec. 4.4.2 the following characterization for complete bipartite fan-crossing free graphs.[16]

Characterization 5.11. *The complete bipartite graph $K_{a,b}$ (with $a \leq b$) is fan-crossing free if and only if*

(i) $a \leq 2$*, or*

(ii) $a \leq 4$ *and* $b \leq 6$*.*

5.7.5 The class of gap-planar graphs

Recall that a drawing is gap-planar if there is a mapping from the crossings to the edges, such that each edge gets at most one crossings assigned to it. Regarding complete gap-planar graphs, Bae et al. [30] already provided a characterization.

Characterization 5.12 (Bae et al. [30])**.** *The complete graph K_n is gap-planar if and only if $n \leq 8$.*

Again we could refine the characterization by determining the edge-exact bound. Namely, the graph K_8 is still gap-planar when it is extended by a vertex together with four edges incident to it (refer to Fig. 5.14), while there is no gap-planar drawing when adding a vertex and five edges to K_8.

Also for complete bipartite gap-planar graphs Bae et al. [30] were able to provide some partial results: They showed that the graphs $K_{3,12}$, $K_{4,8}$, and $K_{5,6}$ are gap-planar, while neither $K_{3,15}$, nor $K_{4,11}$, nor $K_{5,7}$ belong to this class. Note that the latter results were obtained by using the technique mentioned in Sec. 5.1.3, which compares the crossing number of these graphs with the maximum number of crossings allowed in gap-planar drawings.[17]

Bachmaier et al. [29] refined this technique and showed that even the graphs $K_{3,14}$, $K_{4,10}$, and $K_{6,6}$ are not gap-planar. It remains to answer the question if the two

[16] We stress that the scale of the case analysis in the proof is dramatically long. However, we obtained the same result using our implementation in less than a second!

[17] Bae et al. [30] observed that a k-gap-planar graph allows at most $k|E|$ crossings.

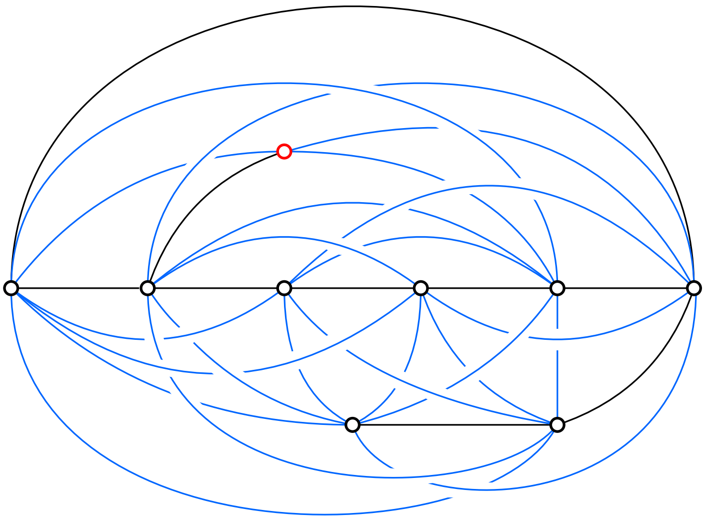

Fig. 5.14: A gap-planar drawing of the graph obtained from K_8 by inserting a vertex (in red) and four edges incident to it. The edge to which a crossing is mapped to is drawn with a gap.

graphs $K_{3,13}$ and $K_{4,9}$ are gap-planar or not. We were able to answer this question for $K_{4,9}$, which is in fact not gap-planar, while our implementation could not give a result for $K_{3,13}$ until now. The difficulty in solving this question is the large number of non-isomorphic gap-planar drawings, which becomes already evident while considering $K_{3,7}$ (at the time of writing, our implementation has been running for three months and already reported more than one million such drawings; however, it was not even close to finish the creation of drawings for $K_{3,7}$).

The results are summarized in the following observation.

Observation 5.13. *The complete bipartite graph $K_{a,b}$ (with $a \leq b$) is gap-planar if*

(i) $a \leq 2$, *or*

(ii) $a = 3$ *and* $b \leq 12$, *or*

(iii) $a = 4$ *and* $b \leq 8$, *or*

(iv) $a = 5$ *and* $b \leq 6$.

Further, $K_{a,b}$ is not gap-planar if

(i) $a = 3$ *and* $b \geq 14$, *or*

(ii) $a = 4$ *and* $b \geq 9$, *or*

(iii) $a = 5$ *and* $b \geq 7$, *or*

(iv) $a \geq 6$ *and* $b \geq 6$.

5.7.6 The class of quasi-planar graphs

Finally we consider the class of quasi-planar graphs, where three pairwise crossing edges are forbidden. Here we obtain a characterization for the complete graphs by combining two known results. On one side, the graph K_{11} is not quasi-planar, since every simple quasi-planar graph has at most $6.5n-20$ edges [4]. On the other hand, Brandenburg [42] observed that K_{10} is quasi-planar.[18] These two observations are summarized in the following characterization.

Characterization 5.14 (Ackerman et al. [4], Brandenburg [42]). *The complete graph K_n is quasi-planar if and only if $n \leq 10$.*

Again we determined the edge-exact bound also for quasi-planar graphs. Namely, the graph K_{10} still belongs to the quasi-planar graphs after adding another vertex v together with six edges incident to it (refer to Fig. 5.15), while K_{10} cannot be enriched by v and seven edges incident to v, such that the resulting graph is still quasi-planar.

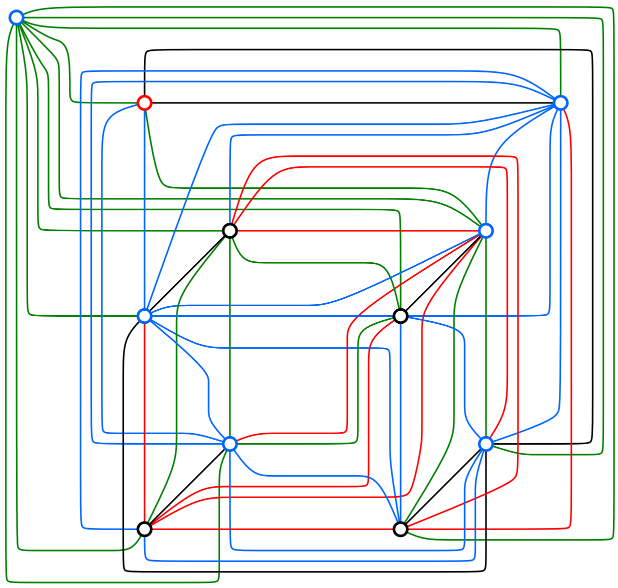

Fig. 5.15: A quasi-planar drawing of the graph obtained from K_{10} by inserting a vertex (red) together with six edges incident to it (between the red vertex and the blue vertices).

We consider now a complete bipartite graph $K_{a,b}$ with $a \leq b$. Since $K_{a,b}$ is fan-planar for $a \leq 4$ and every value of b [93], and the fan-planar graphs are a subclass of the quasi-planar graphs, these graphs are quasi-planar as well. Further, the fact

[18] Since it is in general not easy to observe that a specific drawing is quasi-planar, we describe in Sec. 5.7.7 how to achieve this systematically.

that a quasi-planar graph with n vertices has at most $6.5n-20$ edges [4] only implies that $K_{7,52}$ is not quasi-planar, while for $a \in \{5, 6\}$ no bound on b is known.

With our implementation we were not able to improve the upper bounds for quasi-planar graph, due to a similar problem as the one described for complete bipartite 4-planar graphs. For more details we refer to Sec. 5.8. However, our DFS-like approach provided at least some positive certificate drawings for $K_{5,18}$ (Fig. 5.16a), $K_{6,10}$ (Fig. 5.16b), and $K_{7,7}$ (Fig. 5.16c).

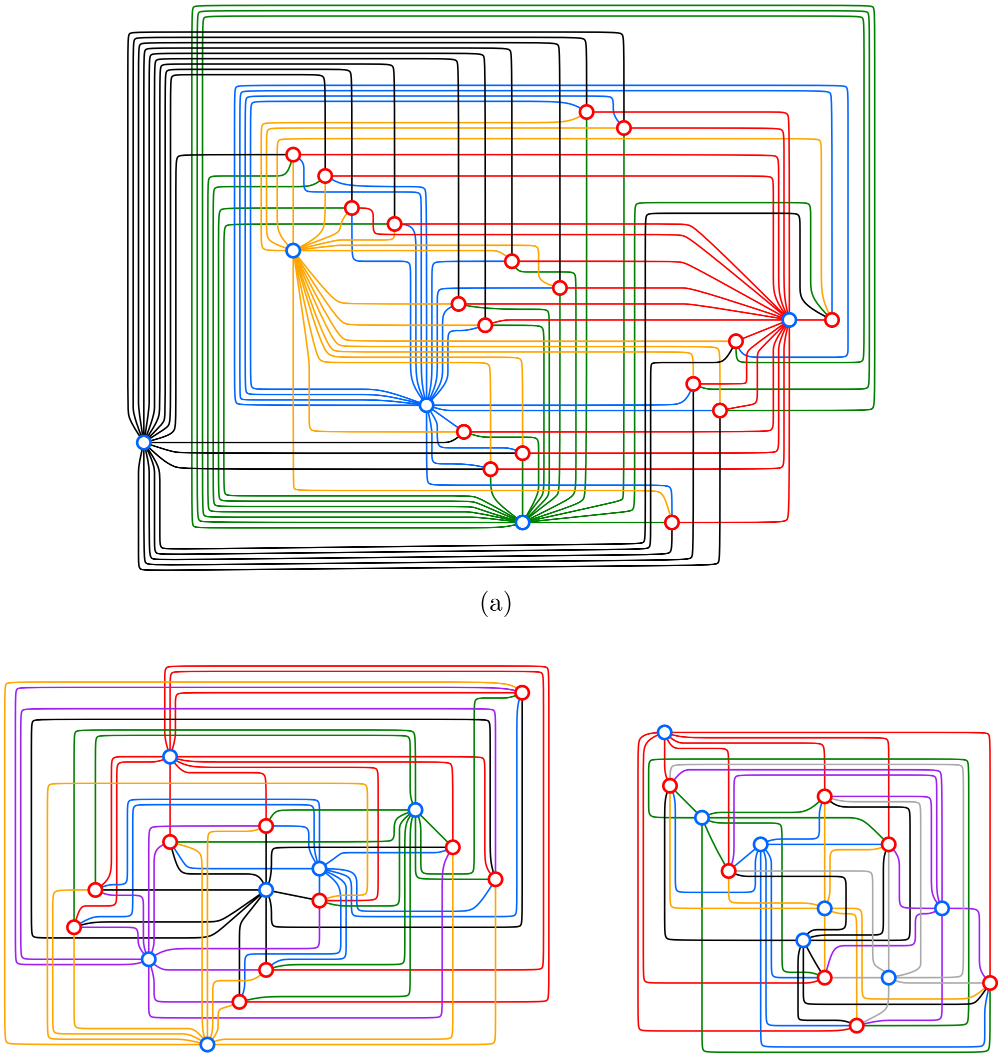

(a) (b) (c)

Fig. 5.16: Quasi-planar drawings of (a) $K_{5,18}$, (b) $K_{6,10}$, and (c) $K_{7,7}$.

The results for complete bipartite quasi-planar graphs from above are summarized in the following observation.

Observation 5.15. *The complete bipartite graph $K_{a,b}$ (with $a \leq b$) is quasi-planar for the following values of a and b:*

(i) $a \leq 4$, *or*

(ii) $a = 5$ *and* $b \leq 18$, *or*

(iii) $a = 6$ *and* $b \leq 10$, *or*

(iv) $a = 7$ *and* $b \leq 7$.

Further, $K_{a,b}$ is not quasi-planar if $a \geq 7$ and $b \geq 52$.

5.7.7 How to decide if a drawing is quasi-planar

In the previous section we provided several quasi-planar drawings, without showing that they are indeed quasi-planar. Instead of doing this for each of these drawings, we explain here a method how to decide if a drawing has the quasi-planar property and apply it exemplary to the drawing of $K_{7,7}$ depicted in Fig. 5.16c.

The key of this method is to consider an edge e and determine if e belongs to a triple of mutually crossing edges. If this is not the case we delete e from the drawing and continue with another edge in the reduced drawing.

There are several cases for an edge e:

(1) If e is crossing free, then it is surely not part of three mutually crossing edges.

(2) If e is crossed by a single edge, then it also cannot belong to such a triple.

(3) If e is crossed by edges $e_1, \ldots, e_k$, where $k \geq 2$, and none of the edges $e_1, \ldots, e_k$ cross each other, then e does not belong to a set of three mutually crossing edges. Otherwise it does and the drawing is not quasi-planar.

To test case (3) it is useful to color all edges which cross e in the same color; then edges of the same color must not cross. In order to accelerate this process, we can even use this coloring technique to test several non-crossing edges at the same time. To this end, first color the edges that should be tested in one color, say red. The red edges should be chosen such that they do not cross each other. Further, color all edges that cross at least one of the red edges in another color, say blue. If the blue edges do also not cross each other, then none of the red edges is part of three mutually crossing edges and all of them can be removed from the drawing.

As already mentioned, we show an example for this procedure in Fig. 5.17.

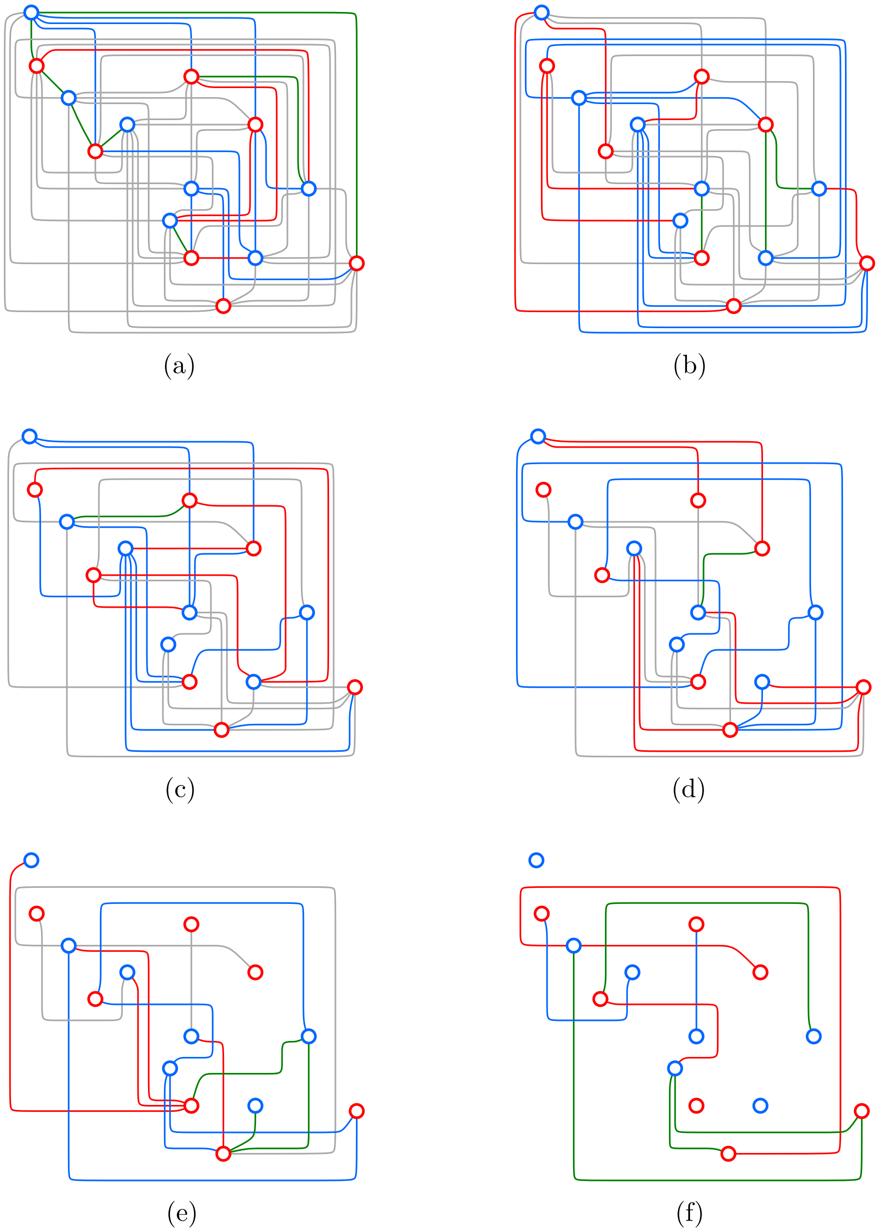

(a) (b) (c) (d) (e) (f)

Fig. 5.17: The figures show step-by-step how the quasi-planarity for the drawing of $K_{7,7}$, given in Fig. 5.16c, can be decided. Green edges are crossed by at most one edge, so they are not part of three mutually crossing edges and can be deleted immediately. Red edges are tested in the current step; every edge that is crossed by a red edge is colored blue. Note that neither a red edge crosses another red edge, nor a blue edge crosses another blue edge.

5.8 Statistics

In this section we present some statistics from the computations we made in order to check whether certain complete and complete bipartite graphs belong to a specific graph class. Our algorithm was implemented in Java and executed on a Windows machine with 2 cores at 2.9 GHz, 8 GB RAM and an SSD for fast access to the hard disc.

5.8.1 General statistics

Recall that our algorithm works with two main steps (see Sec. 5.5): All possible $\mathcal{C}$-drawings are constructed for a certain complete or complete bipartite graph $G = (V, E)$ by adding a vertex $v \in V$ to each of the non-isomorphic drawings of the subgraph $G[V \setminus \{v\}]$; then the obtained drawings are compared for isomorphism and out of isomorphic drawings only one drawing is saved. In Tables 5.3 and 5.4 we report the number of drawings generated in this process in the column "Gen" (generated), while the number of the non-isomorphic drawings can be found in the column "N-I" (non-isomorphic). In the column "time" one can find the total time (in seconds) our implementation needed for generating the drawings and filtering them for isomorphism. The bottommost row of each section in the table corresponds to a negative instance, i. e. our implementation reported that there were no simple $\mathcal{C}$-drawings and thus, the corresponding graph does not belong the the considered graph class. There are two exceptions, namely the classes of complete bipartite 4-planar and quasi-planar graphs, since, in both cases, we were not able to calculate all non-isomorphic drawings of $K_{4,5}$ in appropriate time.

In the following we give a typical example for an intermediate step in our computations. While we tried to calculate all 3-planar drawings for the bipartite graph $K_{6,6}$ (which resulted in a negative answer), our implementation created all non-isomorphic drawings of $K_{4,5}$. The number of such drawings was 7,653. Into each of these drawings, a new vertex was inserted in all possible ways, aiming to calculate all non-isomorphic drawings of $K_{5,5}$ (see gray colored entry of Table 5.3). Thereby a total number of 20,043 drawings were generated (column "Gen"), and further, after testing for isomorphism, there remained 1,899 drawings (column "N-I"). The time it took to calculate these 20,043 drawings and reduce them to 1,899 non-isomorphic drawings was 199.908 seconds (column "Time"). The two steps of generating all drawings and testing them for isomorphism were repeated, first for $K_{5,6}$ (which resulted in 2,516 generated and 438 non-isomorphic drawings), and then for $K_{6,6}$ (where no drawing was found).

Table 5.3: A summary of the required time (in sec.), the number of generated drawings (Gen.), and the number of non-isomorphic drawings (N-I.) for different complete and complete bipartite graphs in case of k-planar graphs ($1 \leq k \leq 5$).

	complete				complete bipartite			
Class	Graph	Gen	N-I	Time	Graph	Gen	N-I	Time
1-planar	K_4	8	2	0.043	$K_{2,3}$	34	3	0.061
	K_5	13	1	0.043	$K_{3,3}$	14	2	0.049
	K_6	4	1	0.020	$K_{3,4}$	16	3	0.065
	K_7	0	0	0.006	$K_{4,4}$	5	2	0.044
					$K_{4,5}$	0	0	0.010
	total:	25	4	0.112	total:	69	10	0.229
2-planar	K_4	8	2	0.028	$K_{2,3}$	76	6	0.090
	K_5	89	4	0.105	$K_{3,3}$	243	19	0.254
	K_6	56	6	0.233	$K_{3,4}$	526	71	1.458
	K_7	38	2	0.119	$K_{4,4}$	310	38	1.152
	K_8	0	0	0.029	$K_{4,5}$	318	37	1.826
					$K_{5,5}$	0	0	0.357
	total:	191	14	0.514	total:	1473	171	5.137
3-planar	K_4	8	2	0.042	$K_{2,3}$	76	6	0.234
	K_5	109	5	0.195	$K_{3,3}$	678	69	1.802
	K_6	548	39	0.953	$K_{3,4}$	7141	1188	16.969
	K_7	648	39	3.459	$K_{4,4}$	24058	2704	97.801
	K_8	20	3	1.153	$K_{4,5}$	44822	7653	310.194
	K_9	0	0	0.065	$K_{5,5}$	20043	1899	199.908
					$K_{5,6}$	2516	438	47.396
					$K_{6,6}$	0	0	4.822
	total:	1333	88	5.867	total:	99334	13957	679.126
4-planar	K_4	8	2	0.040	$K_{2,3}$	76	6	0.108
	K_5	109	5	0.222	$K_{3,3}$	968	102	2.146
	K_6	1374	95	4.080	$K_{3,4}$	32454	6194	163.000
	K_7	14728	1266	79.842	$K_{4,4}$	681196	81817	34096.183
	K_8	7922	833	84.725	$K_{4,5}$	?	?	?
	K_9	353	35	33.672				
	K_{10}	0	0	1.175				
	total:	24494	2236	203.756	total:	?	?	?
5-planar	K_4	8	2	0.059				
	K_5	109	5	0.259				
	K_6	1752	119	4.716				
	K_7	83710	8318	1396.781				
	K_8	1190765	138750	262419.413				
	K_9	285847	29939	32299.196				
	K_{10}	0	0	2783.813				
	total:	1562191	177133	298904.237				

Table 5.4: A summary of the required time (in sec.), the number of generated drawings (Gen.), and the number of non-isomorphic drawings (N-I.) for different complete and complete bipartite graphs. Here the remaining graph classes considered in this chapter are depicted.

	complete				complete bipartite			
Class	Graph	Gen	N-I	Time	Graph	Gen	N-I	Time
fan-crossing	K_4	8	2	0.034	$K_{2,3}$	76	6	0.110
	K_5	89	5	0.133	$K_{3,3}$	127	9	0.292
	K_6	147	39	0.226	$K_{3,4}$	295	43	0.757
	K_7	75	39	0.405	$K_{4,4}$	255	29	0.972
	K_8	0	0	0.196	$K_{4,5}$	324	48	1.624
					$K_{5,5}$	0	0	0.637
	total:	319	22	0.994	total:	1077	135	4.392
fan-crossing free	K_4	8	2	0.049	$K_{2,3}$	34	3	0.057
	K_5	13	1	0.054	$K_{3,3}$	38	5	0.092
	K_6	4	1	0.038	$K_{3,4}$	28	5	0.098
	K_7	0	0	0.009	$K_{4,4}$	19	4	0.106
					$K_{4,5}$	16	2	0.075
					$K_{5,5}$	0	0	0.012
	total:	25	4	0.150	total:	135	19	0.440
gap-planar	K_4	14	2	0.135	$K_{2,3}$	169	14	0.256
	K_5	243	10	0.366	$K_{3,3}$	1425	266	4.359
	K_6	739	237	4.726	$K_{3,4}$	16898	7466	170.396
	K_7	1124	665	13.943	$K_{3,5}$	148527	56843	12032.226
	K_8	1	1	16.347	$K_{4,5}$	199778	148367	28457.751
	K_9	0	0	0.019	$K_{4,6}$	408476	246318	132622.664
					$K_{4,7}$	173271	101428	32958.628
					$K_{4,8}$	5981	4015	2708.278
					$K_{4,9}$	0	0	99.583
	total:	2121	915	35.536	total:	954525	564717	209054.141
quasi-planar	K_4	8	2	0.082	$K_{2,3}$	76	6	0.187
	K_5	109	5	0.193	$K_{3,3}$	604	53	0.859
	K_6	936	63	1.820	$K_{3,4}$	11902	2248	34.073
	K_7	16505	1607	69.943	$K_{4,4}$	386241	46711	11328.401
	K_8	173199	20980	4044.264	$K_{4,5}$	?	?	?
	K_9	209248	23011	35163.772				
	K_{10}	81	9	7593.865				
	K_{11}	0	0	5.225				
	total:	400086	45677	46879.164	total:	?	?	?

The numbers depicted in the tables also give evidence for the limitations of our algorithm. As already mentioned, we were not able to derive characterizations for complete bipartite 4-planar and quasi-planar graphs, since our implementation got stuck on the generation of the drawings for $K_{4,5}$. When looking at the corresponding entries in Table 5.3 (4-planar) and Table 5.4 (quasi-planar), the reason for this becomes clear: The calculation of all 81,817 non-isomorphic 4-planar drawings for $K_{4,4}$ already took a large amount of time, namely more than 34,000 seconds (which is more than 9 hours). Also for the quasi-planar graphs there exist 47,711 non-isomorphic drawings of $K_{4,4}$, which were calculated in 11,328 seconds.

We conclude our discussion of Tables 5.3 and 5.4 by making some additional observations.

First, it is eye-catching that the number of both, the generated and the non-isomorphic drawings, are significantly smaller for the complete graphs compared the corresponding numbers for the complete bipartite graphs. This large difference can be explained by the fact that the complete graphs are very symmetric and denser than the complete bipartite graphs. We also refer to the discussion in Sec. 5.8.2.

Moreover, regarding the k-planar graphs, we observe a behavior which we expected for the numbers of generated and non-isomorphic drawings: As k grows, these numbers also grow in both, the complete and the complete bipartite setting. This growth becomes significantly larger from 3-planar to 4-planar graphs, up to the point that it is highly time consuming to calculate all complete bipartite drawings for the class of 4-planar graphs, as already mentioned above.

Another observation concerns the fan-crossing and fan-crossing free graphs, which are in a sense complementary to each other. Here we can observe significant differences in the number of drawings. In particular, the number of non-isomorphic fan-crossing free drawings are always single digits, while this is not the case for non-isomorphic fan-crossing drawings.

Finally we observe that, if all non-isomorphic drawings of the maximal realizable graph of a certain graph class have been computed, it is not very time-consuming to conclude that a graph does not belong to this class; refer to the bottommost row of every section in Tables 5.3 and 5.4, where mostly a few seconds were reported for executing this task. More generally, the numbers of non-isomorphic drawings grow until they reach a peak, and then they decrease again. These peaks seems to appear more “to the end” (i. e. belong to a graph where only a very small number of additional vertices can be added, such that the graph still belongs to the considered graph class), rather than at the beginning.

Table 5.5: A comparison between the two most "extremal" orders while showing that $K_{5,5}$ is not 2-planar and $K_{6,6}$ is not 3-planar, respectively. Listed are the required time (in sec.), the number of generated drawings (Gen.), and the number of non-isomorphic drawings (N-I.).

	non-alternating order				alternating order			
Class	Graph	Gen.	N-I	Time	Graph	Gen.	N-I	Time
2-planar	$K_{2,3}$	76	6	0.150	$K_{2,3}$	76	6	0.090
	$K_{2,4}$	131	20	0.275	$K_{3,3}$	243	19	0.254
	$K_{2,5}$	415	52	0.471	$K_{3,4}$	526	71	1.458
	$K_{3,5}$	625	91	3.619	$K_{4,4}$	310	38	1.152
	$K_{4,5}$	141	37	2.875	$K_{4,5}$	318	37	1.826
	$K_{5,5}$	0	0	0.540	$K_{5,5}$	0	0	0.357
	total:	1388	206	7.930	total:	1473	171	5.137
3-planar	$K_{2,3}$	76	6	0.101	$K_{2,3}$	76	6	0.234
	$K_{2,4}$	236	40	0.488	$K_{3,3}$	678	69	1.802
	$K_{2,5}$	1450	221	2.973	$K_{3,4}$	7141	1188	16.969
	$K_{2,6}$	7281	1093	11.162	$K_{4,4}$	24058	2704	97.801
	$K_{3,6}$	53396	12334	583.402	$K_{4,5}$	44822	7653	310.194
	$K_{4,6}$	27047	6413	341.739	$K_{5,5}$	20043	1899	199.908
	$K_{5,6}$	2242	438	59.433	$K_{5,6}$	2516	438	47.396
	$K_{6,6}$	0	0	5.327	$K_{6,6}$	0	0	4.822
	total:	91728	20545	1,004.625	total:	99334	13957	679.126

5.8.2 Comparing different insertion orders for complete bipartite graphs

For the statistics shown in Tables 5.3 and 5.4, we inserted vertices into drawings of complete bipartite graphs in an alternating order[19]; that is, for the vertices in the independent parts U and W, after we inserted a vertex from U, we inserted one from W and vice versa. First, this seems a random choice, but in fact it turned out to be a good one.

In Table 5.5, we compare the alternating order we used in our implementation to calculate all drawings of $K_{a,b}$ with the following one (which is in a sense complementary to the alternating order): We first compute all drawings for the graphs $K_{2,2}, K_{2,3}, \ldots, K_{2,b}$, and continue with $K_{3,b}, K_{4,b}, \ldots, K_{a,b}$.

One huge disadvantage of the second order is that we do not know which graph $K_{a,b}$ is "the first" one that does not belong to $\mathcal{C}$ (since this is exactly the question

[19]Note that for the general complete graphs there is no such choice.

we want to answer). So the second order cannot be used without prior knowledge, while the alternating order allows it to find such an "upper bound" graph, more precisely one with the property that a and b differ at most by one.

The other disadvantage we are aware of is the slower running time when using the second order. Also the total number of non-isomorphic drawings is higher for this order (at least for the considered classes), as well as the number of generated drawings in the peak. However, the total number of generated graphs is smaller in comparison with the corresponding number for the alternating inserting order (refer to the columns "total" in Table 5.5). We cannot explain why, despite this lower number, the running time is slower for the non-alternating order. Our guess is that one reason for this effect is the larger number of non-isomorphic drawings and also the larger number of generated drawings in the peaks (which are the graphs $K_{3,5}$ in the non-alternating order and $K_{3,4}$ in the alternating order for 2-planar graphs, and $K_{3,6}$ and $K_{4,5}$ in the non-alternating and alternating order, respectively, in case of 3-planar graphs).

On the other hand, we believe that the smaller number for the non-alternating order is due to an effect that only appears while considering graphs of the form $K_{b,b}$. During the isomorphic test for drawings of a graph $K_{b,b}$, $b \geq 3$, we rightly discard isomorphic drawings that map all vertices of one independent part of $K_{b,b}$ to the other one (for an example see Fig. 5.18). However, in the next step, that is the insertion of one vertex into all these non-isomorphic drawings in order to generate the drawings for $K_{b,b+1}$, one then has to be careful: For a drawing Γ, the new vertex $w_{b+1} \in W$ must be connected to each vertex $u_1, \dots, u_b$. But, since we discarded isomorphic drawings, this new vertex must also be regarded as belonging to set U and connected to $w_1, \dots, w_b$, otherwise we would miss some configurations. This issue can be solved by creating a copy of Γ with switched labels for the two independent parts of $K_{b,b}$.

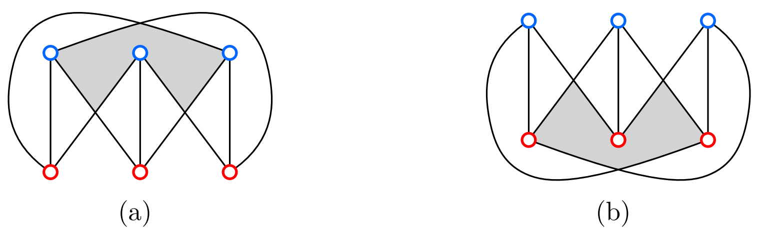

Fig. 5.18: The drawings of $K_{3,3}$ in (a) and (b) are isomorphic, but a (new) vertex in the gray area of (a) can be connected to the blue vertices by crossing-free edges, while this is not possible in (b).

Note that this special treatment of graphs $K_{b,b}$ is only needed when aiming at calculating all drawings for graphs $K_{a,b}$, where $a < b$. Otherwise, that is, if our goal is to compute all non-isomorphic $\mathcal{C}$-drawings for $K_{b,b}$, where $b \geq 3$, (or showing that no such drawing exists), then it is not necessary. Although we miss some configurations for the drawings of $K_{b',b'+1}$ $(3 \leq b' < b)$ in this case, we in fact do *not* miss any configuration for $K_{b'+1,b'+1}$ because this graph is symmetric regarding its two independent parts. For an example, consider Fig. 5.18, where vertices from U are blue (this set belongs to the first index of $K_{a,b}$) and vertices from W are red. Inserting vertex $w_{b'+1}$ into the gray area of the left drawing in all possible ways, and then inserting the vertex $u_{b'+1}$ into all these drawings (again in all possible ways), is equivalent to inserting vertex $w_{b'+1}$ into the right drawing in all possible ways, and then inserting the vertex $u_{b'+1}$ into the gray area of all these drawings.

Finally, also observe the following regarding the different orders: The graph $K_{2,b}$ is planar for every b. So one can expected to find "many" $\mathcal{C}$-drawings for those graphs (and for graphs $K_{a,b}$, where $a \ll b$), while there should be less and less such drawings when "diverging" from $K_{2,b}$, where diverging means to get closer to a graph of the form $K_{b,b}$. This could also explain why it is beneficial to use the alternating order while calculating all non-isomorphic drawings.

5.8.3 The effect of the isomorphic test

One of the two main steps of our algorithm is the elimination of isomorphic drawings. Table 5.6 shows that this test brings indeed a huge benefit. Thereby we consider the computations for complete and complete bipartite graphs in case of the 1- and 2-planar graphs. By comparing the number of generated drawings and the running time while using the isomorphism test and while not using it, we already observe a significant difference in these measures for both graph classes. For example, to test whether K_7 is 1-planar, our implementation created 25 drawings in total and needed 0.112 seconds (including the time for performing all isomorphism tests and eliminations), while disabling the isomorphic test yields a total number of 158 drawings in 1.434 seconds. Even more evident is this difference when showing that $K_{5,5}$ is not 2-planar. Here our implementation created 1333 drawings in total in approximately 5 seconds, compared to 1,423,684 drawings created in about 22,159 seconds without isomorphic test.

Table 5.6: A comparison of the number of drawings reported by our algorithm with the elimination of isomorphic drawings (col. "Gen.") and without it (col. "All") for the classes of 1- and 2-planar graphs; the corresponding execution times (in sec.) to compute these drawings are reported next to them.

	complete					complete bipartite				
Class	Graph	Gen.	Time	All	Time	Graph	Gen.	Time	All	Time
1-planar	K_4	8	0.043	8	0.043	$K_{2,3}$	34	0.061	34	0.061
	K_5	13	0.043	30	0.206	$K_{3,3}$	14	0.049	84	0.539
	K_6	4	0.020	120	0.737	$K_{3,4}$	16	0.065	960	5.642
	K_7	0	0.006	0	0.448	$K_{4,4}$	5	0.044	1584	10.871
						$K_{4,5}$	0	0.010	0	7.198
	total:	25	0.112	158	1.434	total:	69	0.229	2662	24.311
2-planar	K_4	8	0.028	8	0.028	$K_{2,3}$	76	0.090	76	0.090
	K_5	89	0.105	294	2.661	$K_{3,3}$	243	0.254	2352	10.571
	K_6	56	0.233	2664	3.292	$K_{3,4}$	526	1.458	52248	244.964
	K_7	38	0.119	8400	55.323	$K_{4,4}$	310	1.152	168624	1128.457
	K_8	0	0.029	0	51.321	$K_{4,5}$	318	1.826	1200384	8135.843
						$K_{5,5}$	0	0.357	0	12639.293
	total:	191	0.514	11366	112.625	total:	1333	5.137	1423684	22159.218

5.9 Conclusions and Open Problems

We presented an efficient algorithm to generate all non-isomorphic drawings for complete and complete bipartite graphs for topological graph classes. This algorithm consists of two main steps, which are executed alternately: the insertion of a new vertex and the test for isomorphism. In Sec. 5.8 we stated clearly the importance of this isomorphism test.

As a proof of concept, we implemented our algorithm and applied it to several important graph classes, in order to deduce characterizations for them. Further, if this was not possible due to running time issues, we gave at least certificate drawings for several classes.

Note that these results also have some theoretical implications regarding problems stated in other works. Namely, Char. 5.9 implies that the graph $K_{5,5}$ is not fan-crossing, which answers the conjecture of Angelini et al. [14] that this graph is not fan-planar in the positive. Further the fact that the graph $K_{5,5}$ is gap-planar (Obs. 5.13), but not fan-planar (Char. 5.9), shows that there are gap-planar graphs which are not fan-planar. On the other hand, the graph $K_{4,9}$ is fan-planar but not gap-planar. Both observations combined imply that the classes of fan-planar graphs and gap-planar graphs are not comparable. This answers a related question in [30] about the relationship between 1-gap-planar and fan-planar graphs.

One main open problem is the question if our approach (or our implementation) can be accelerated such that it provides characterizations for more graph classes, e. g. for complete and complete bipartite k-planar graphs where $k \geq 6$ and $k \geq 4$, respectively. A promising idea in this direction would be to use multi-threading[20] in an intelligent way.

Another question is, if our algorithm can be extended to other types of graphs, apart from complete and complete bipartite ones, e. g. to multipartite graphs, k-trees or k-degenerate graphs (for small values of k). In fact it is possible to apply our approach on multipartite graphs. However, we expect the running time to be to slow, even for tripartite graphs, so we didn't tailor our implementation for this setting. Also the issue discussed in Sec. 5.8.2 about bipartite graphs of the form $K_{a,b}$, where $a = b$, has to be considered for tripartite graphs $K_{a,b,c}$ (where $a \leq b \leq c$). This problem becomes even more complex, since one needs to treat each of the three cases $a \neq b$ and $b = c$, $a = b$ and $b \neq c$, and $a = b = c$ differently. Moreover, for graphs that are not as symmetric as complete and complete bipartite graphs, there are more non-isomorphic drawings. This increases the search space and therefore the running time of our algorithm.

Finally, we observe that there exists a characterization for general k in case of bipartite graphs $K_{3,b}$ [13]. So we ask whether it is possible to obtain corresponding characterizations for complete graphs or complete bipartite graphs $K_{a,b}$, where $a > 3$, by means of combinatorial proofs.[21] In this direction, our result might help by giving ideas how such characterizations could look like (refer to Fig. 5.19). Specifically we want to state the questions, if the following graphs are k-planar for every $k \geq 3$: The bipartite graphs $K_{4,3k}$, $K_{5,2k}$ and $K_{6,k+2}$.

[20]Up to the time of writing we could not provide an idea that helps accelerating by more than a small factor; the main issue is that with multi-threading it becomes difficult to execute the isomorphic test

[21]The known general edge density [3] of at most $3.81n\sqrt{k}n$ edges implies that complete graphs K_n, where $n > 7.62\sqrt{k} - 1$ are not k-planar. This indicates that the growth of n with respect to k is less than linear. The same is true for complete bipartite graphs $K_{n/2,n/2}$, since the edge density of at most $3.01\sqrt{k}n$ edges for bipartite graphs [14] imply that such graphs are not k-planar when $n > 12.04\sqrt{k}$.

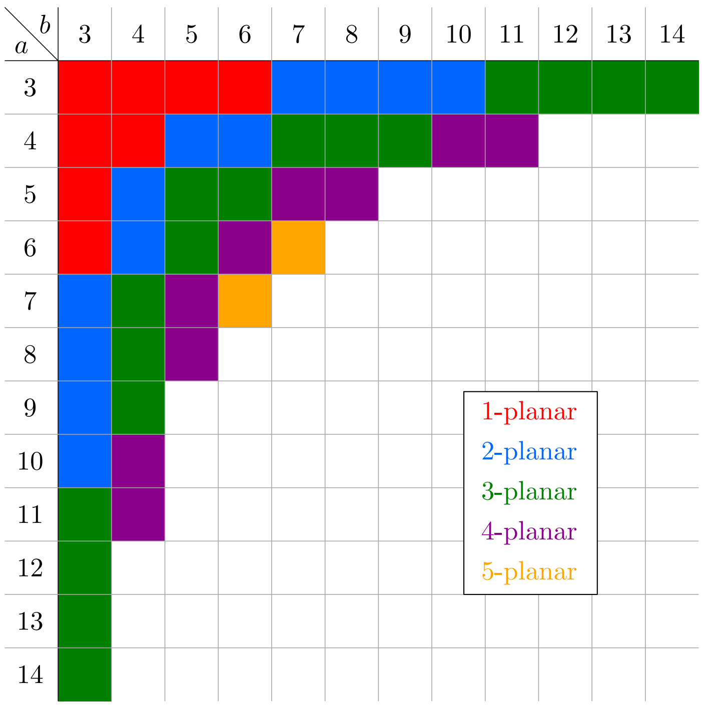

Fig. 5.19: Illustration of the k-planar graphs $K_{a,b}$ (here we don't assume $a < b$) for small values of k.

Chapter 6

A Meta Crossing Lemma and Edge Densities

In Chapter 5 we learned that the crossing number may be used to decide which complete and complete bipartite graphs do not belong to a certain graph class. Beyond that, it is also an important measure for the readability of a graph drawing [116] and has many applications in combinatorial geometry [105, 107, 133] and VLSI (Very large-scale integration) design [35, 101, 102].

In this direction, the Crossing Lemma for general graphs G with n vertices and m edges, where $m \geq 4n$, states that the number of crossings $cr(G)$ in every drawing of G is lower bounded by $c\frac{m^3}{n^2}$, where c is a (known) constant. This relation was first conjectured by Erdős and Guy [67] and proved by Leighton [102] and Ajtai et al. [7] independently. The first value that was derived for c was $\frac{1}{64}$. It was improved successively and is currently at $\frac{1}{29}$ [3].

Chazelle, Sharir and Welzl provided a simple probabilistic proof for the Crossing Lemma [6, Chapter 35], which is commonly adapted when deriving better lower bounds in the Crossing Lemma, see e. g. [3, 108]. Moreover, the proof of Chazelle, Sharir and Welzl was adapted recently for bipartite k-planar graphs [14]. Since Chapter 7 contains a corresponding Crossing Lemma for 2-layer k-planar drawings, we generalize the proof by Chazelle, Sharir and Welzl and also show some applications in this chapter.[1]

[1] The Meta Crossing Lemma (Sec. 6.2), as well as the general edge density bound for k-planar graphs (Thm. 6.3), together with results from Chapter 7 are part of our paper "2-Layer k-Planar graphs: Density, Crossing Lemma, Relationships, and Pathwidth" [19].

6.1 Preliminaries

As usually we denote a graph by $G = (V, E)$, and the number of its vertices and edges by $n = |V|$ and $m = |E|$, respectively. Let $\mathcal{R}$ be some restriction on a graph, e. g. $\mathcal{R}$ can be "no restriction", "bipartite", or "drawable on 2 layers". Further, to simplify notation, we sometimes use the term "0-planar" instead of "planar".

In the following we assume that upper bounds $m \leq \alpha_i n - \beta_i$ for the number of edges in $\mathcal{R}$-restricted i-planar graphs are given, where $i = 0, \ldots, \hat{k}-1$ for some appropriate $\hat{k} > 0$, and $\alpha_i, \beta_i \in \mathbb{R}$ are non-negative. Note that, since the class of i-planar graphs is a subclass of the class of $(i+1)$-planar graphs, the family $(\alpha_i n - \beta_i)_{i \geq 0}$ is non-decreasing in i. Let $\alpha := \sum_{i=0}^{\hat{k}-1} \alpha_i$ and $\beta := \sum_{i=0}^{\hat{k}-1} \beta_i$. Note that α_i and β_i, and hence α and β depend on the restriction $\mathcal{R}$.

6.2 The Crossing Lemma

Our goal is to formulate the Crossing Lemma in terms of the variables α, β and $\hat{k}$. Thereby we follow the proof of Chazelle, Sharir and Welzl [6].

Lemma 6.1. *Let G be a simple $\mathcal{R}$-restricted graph with $n \geq 4$ vertices and m edges. Then the following inequality holds for the crossing number $cr(G)$:*

$$cr(G) \geq \hat{k}m - \alpha n + \beta.$$

Proof. Assume that $m > \alpha_0 n - \beta_0$. Then, in every drawing of G, there exists at least $m - (\alpha_0 n - \beta_0)$ edges of G which are crossed at least once. If $m > \alpha_1 n - \beta_1$, there exists at least $m - (\alpha_1 n - \beta_1)$ edges in G that are crossed at least twice. Iteratively we obtain that, if $m > \alpha_{i-1} n - \beta_{i-1}$, there exists at least $m - (\alpha_i n - \beta_i)$ edges in G that have at least i crossings. This implies

$$cr(G) \geq \sum_{i=0}^{\hat{k}-1} [m - (\alpha_i n - \beta_i)] = \hat{k}m - \alpha n + \beta.$$

On the other hand, if there exists a $j \in \{0, \ldots, \hat{k}-1\}$ such that $m > \alpha_i n - \beta_i$ for all $0 \le i \le j-1$ and $m \le \alpha_i n - \beta_i$ for all $i \ge j$, we obtain

$$\begin{aligned} cr(G) &\ge \sum_{i=0}^{j-1} [m - (\alpha_i n - \beta_i)] \\ &\ge \sum_{i=0}^{j-1} [m - (\alpha_i n - \beta_i)] + \sum_{i=j}^{\hat{k}-1} \underbrace{[m - (\alpha_i n - \beta_i)]}_{\le 0} \\ &= \sum_{i=0}^{\hat{k}-1} [m - (\alpha_i n - \beta_i)] \\ &= \hat{k}m - \alpha n + \beta. \end{aligned}$$

The statement follows. □

With the help of the previous auxiliary lemma we are able to prove the following theorem, which generalizes the Crossing Lemma.

Theorem 6.2 (Meta Crossing Lemma)**.** *Let G be a simple $\mathcal{R}$-restricted graph with $n \ge 4$ vertices and $m \ge \frac{3\alpha}{2\hat{k}} n$ edges. Then the following inequality holds for the crossing number $cr(G)$:*

$$cr(G) \ge \frac{4\hat{k}^3}{27\alpha^2} \frac{m^3}{n^2}. \tag{6.1}$$

Proof. Consider a drawing Γ of G with $cr(G)$ crossings and let $p = \frac{3\alpha n}{2\hat{k}m} \le 1$. With probability p choose every vertex of G independently. Let G_p be the subgraph of G induced by the randomly chosen vertices and Γ_p the subdrawing of Γ representing G_p. Consider random variables n_p, m_p and c_p, which denote the number of vertices, edges and crossings in Γ_p. Then the expectations are $\mathbf{E}[n_p] = np$, $\mathbf{E}[m_p] = p^2 m$ (both end points of an edge must be chosen) and $\mathbf{E}[c_p] = p^4 cr(G)$ (all four end points of the two edges involved in the crossing must be chosen).

By Lemma 6.1 the inequality $c_p \ge \hat{k}m_p - \alpha n_p + \beta$ holds. Taking expectations on this relationship, we have:

$$p^4 cr(G) \ge \hat{k}p^2 m - \alpha p n \implies cr(G) \ge \frac{\hat{k}m}{p^2} - \frac{\alpha n}{p^3}.$$

We obtain Inequality (6.1) by plugging $p = \frac{3\alpha n}{2\hat{k}m}$ into the inequality above.[2] □

[2]The value for p is obtained by maximizing $\frac{\hat{k}m}{p^2} - \frac{\alpha n}{p^3}$.

6.3 Upper Bounds on the Number of Edges

The Crossing Lemma is used to derive upper bounds for the maximal number of edges in $\mathcal{R}$-restricted k-planar graphs (see e. g. [3, 14]). In this direction, our generalized version of the Crossing Lemma implies the following theorem.

Theorem 6.3. *Let G be a simple $\mathcal{R}$-restricted k-planar graph with $n \geq 4$ vertices for some $k \geq 0$. Then*

$$m \leq \left(\max\left\{1, \sqrt{\frac{3k}{2\hat{k}}}\right\}\right) \cdot \frac{3\alpha}{2\hat{k}} n.$$

Proof. If $m \leq \frac{3\alpha}{2\hat{k}}n$, the statement follows immediately. Otherwise, we obtain from Thm. 6.2 and from the fact that a k-planar graph has at most $\frac{1}{2}mk$ crossings[3]:

$$\frac{4\hat{k}^3}{27\alpha^2}\frac{m^3}{n^2} \leq cr(G) \leq \frac{1}{2}mk.$$

This implies:

$$m \leq \frac{3\alpha}{2\hat{k}}\sqrt{\frac{3k}{2\hat{k}}}n$$

which completes the proof. □

Using the Meta Crossing Lemma, we can also give a generalized version for the edge density in k-gap-planar graphs (for the original formulation see [30]).

Theorem 6.4. *Let G be a simple $\mathcal{R}$-restricted k-gap-planar graph with $n \geq 4$ vertices for some $k \geq 1$. Then*

$$m \leq \left(\max\left\{1, \sqrt{\frac{3k}{\hat{k}}}\right\}\right) \cdot \frac{3\alpha}{2\hat{k}} n.$$

Proof. If $m \leq \frac{3\alpha}{2\hat{k}}n$, the statement follows immediately. Otherwise, we obtain from Thm. 6.2 and from the fact that $cr(G) \leq km$ in k-gap-planar graphs [30]:

$$\frac{4\hat{k}^3}{27\alpha^2}\frac{m^3}{n^2} \leq cr(G) \leq km.$$

[3]Note that every edge in G can be crossed at most k times; since each crossing involves two edges, G cannot have more than $\frac{1}{2}mk$ crossings.

This implies:

$$m \leq \frac{3\alpha}{2\hat{k}}\sqrt{\frac{3k}{\hat{k}}} \cdot n.$$

The statement follows. □

6.4 Edge Density of Outer-k-Planar Graphs

As already mentioned, Crossing Lemmas were formulated for general graphs (most recently by Ackerman [3]) and for bipartite graphs [14]. However, we are not aware of such a formulation regarding outer-k-planar graphs, in which all vertices are placed on the outer face and each edge is crossed at most k times. So we provide one here, using our Meta Crossing Lemma.

First note that each outerplanar graph has at most $2n-3$ edges. Auer et al. [28] showed that the edge density of an outer-1-planar graph is $2.5n-4$. Thus, we have $\hat{k} = 2$, $\alpha_0 = 2$, $\alpha_1 = 2.5$ and $\alpha = 4.5$. We derive a Crossing Lemma for outer-k-planar graphs by plugging these values for $\hat{k}$ and α into Thm. 6.2.

Corollary 6.5. *Let G be a simple outer-k-planar graph with $n \geq 4$ vertices and $m \geq \frac{27}{8}$. Then*

$$cr(G) \geq \frac{2^7 m^3}{3^5 n^2} = \frac{128 m^3}{243 n^2} \geq 0.526 \cdot \frac{m^3}{n^2}.$$

The associated upper bound on the maximal number of edges in outer-k-gap planar graphs, derived from Thm. 6.3, is the following.

Corollary 6.6. *Let G be a simple outer-k-planar graph with $n \geq 4$ vertices for some $k \geq 2$. Then*

$$m \leq \max\left\{\frac{27}{8}, \frac{27\sqrt{3}}{16}\sqrt{k}\right\} n = \frac{27\sqrt{3}}{16}\sqrt{k}n =\leq 2.923\sqrt{k}n.$$

6.5 The Class of k-Gap-Planar Graphs

Bae et al. [30] provided already an edge density of $\max(5.58\sqrt{k}, 17.17) \cdot n$ edges for general k-gap-planar graphs. Very recently, Angelini et al. [14] derived a Crossing Lemma and an edge density of $3.005\sqrt{k}n$ for bipartite k-planar graphs. Their results imply $\hat{k} = 3$ and $\alpha = 8.5$; consequently we are able to formulate the following corollary due to Thm. 6.4.

Corollary 6.7. *Let G be a simple bipartite k-gap-planar graph with $n \geq 4$ for some $k \geq 1$. Then*

$$m \leq \left(\max\left\{1, \sqrt{\frac{3k}{3}}\right\}\right) \cdot \frac{3 \cdot 8.5}{2 \cdot 3} n = \left(\max\left\{1, \sqrt{k}\right\}\right) \cdot 4.25n = 4.25\sqrt{k}n.$$

For bipartite 1-gap-planar graphs (denoted just by "gap-planar graphs") whose crossing graph has special properties, we are able to provide an upper bound for the maximum number of edges that is even better than $4.25n$. Recall from Chapter 2 that the crossing graph of a gap-planar graph is a pseudo forest [30], that is a set of pseudo trees; thereby a pseudo tree is "almost" a tree, except that it is allowed to have *one* cycle in a pseudo tree, while a tree cannot have cycles at all.

We start by considering a lower bound for the maximal number of edges in bipartite gap-planar graphs.

Theorem 6.8. *There are infinitely many embeddings with $4n - 16$ edges that are gap-planar and bipartite.*

Proof. Consider the drawing Γ in Fig. 6.1. Clearly a drawing with the same pattern as in Γ can be constructed for every $n \geq 16$ where $n = |V|$ is a multiple of 4. We count the number of edges for such a drawing. There are 8 vertices of degree 5 (refer to the vertices of the innermost and outermost ring), and 8 vertices of degree 7 (refer to the vertices of the second-innermost and second-outermost ring). All other vertices have degree 8. Thus, the number of edges is

$$\tfrac{1}{2}(8 \cdot 5 + 8 \cdot 7 + (n - 16) \cdot 8) = 4n - 16. \qquad \square$$

As mentioned before, we consider gap-planar graphs with certain properties and show an upper bound on the number of edges for them. Thereby this bound is "almost" tight, since it differs only by a constant number of edges from the lower bound stated in Thm. 6.8.

In the following we assume that $G = (V, E)$ is a simple connected bipartite gap-planar graph with $n = |V|$ and $m = |E|$, and $V = U \dot\cup W$ are the two independent parts of G. Let Γ be a simple gap-planar drawing of G and $X = (E, E_X)$ the crossing graph of Γ. Since X is a pseudo forest [30], its connected components $X_1, \ldots, X_t$, $t \geq 1$, are pseudo trees.

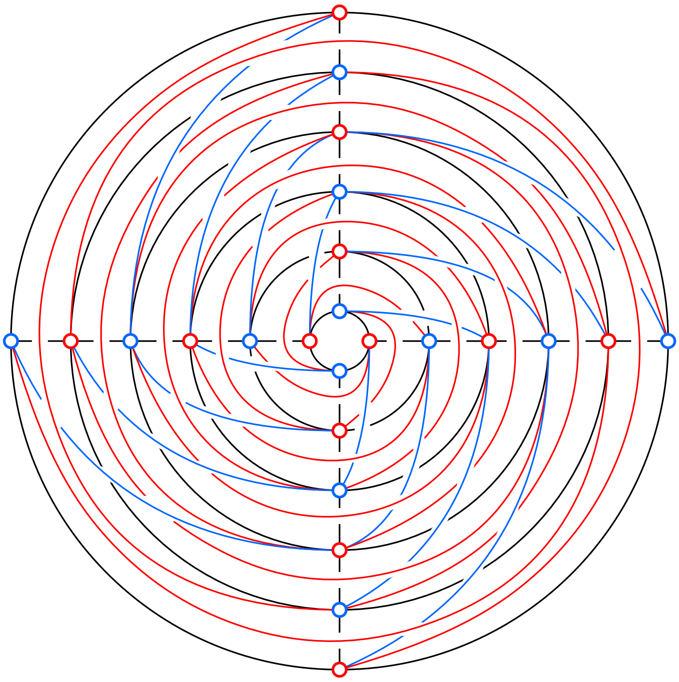

Fig. 6.1: A drawing of a bipartite gap-planar graph with $4n - 16$ edges. The edge, to which a crossing is assigned to, has a gap. Every time a red or blue edge crosses a black edge, the gap is assigned to the black edge. Every blue edge crosses two red edges. The inner crossing is assigned to the red edge and the outer crossing to the blue edge.

Lemma 6.9. *Let $I \subseteq E$ be an independent set in X. If I contains at least $\frac{m}{2}$ elements, then Γ has at most $4n - 8$ edges.*

Proof. We observe that, by definition of the crossing graph, two vertices $e_1, e_2 \in E$ of X are connected by an edge in X if and only if they cross each other in Γ. Since I is an independent set in X, no two edges in I cross pairwise in Γ. Thus, the subdrawing Γ_p of Γ, which consists of the vertices V and the edges I, is planar. As a consequence of the Euler Theorem (see e. g. [121, Chapter 12]), the bipartite planar drawing Γ_p has at most $2n - 4$ edges. Since $|I| \geq \frac{m}{2}$, we conclude

$$m \leq 2|I| \leq 4n - 8. \qquad \square$$

Lemma 6.9 provides a tool for finding conditions such that Γ has an edge density of $4n - 8$. Namely, it is sufficient to find an independent set of size at least $\frac{m}{2}$ in the crossing graph of Γ. The following lemma proves a result in this direction.

Lemma 6.10. *Let $X = X_1$, i. e. the crossing graph X of Γ consists of only one component, and let $I \subseteq E$ be a maximal independent set in X. Then the following hold:*

(i) If $|E|$ is even or X contains no cycle of odd length, then I has at least $\frac{m}{2}$ elements;

(ii) if $|E|$ is odd and X contains a cycle of odd length, then I has at least $\frac{m-1}{2}$ elements.

Since the two conditions cover all cases, we have $I \geq \frac{m-1}{2}$ for a component X in every case.

Proof. We color the vertices of X in red and blue, such that red vertices form an independent set. Let the set of red vertices be $R \subseteq E$, and the set of blue vertices be $B \subseteq E$. The red vertices are independent if the endpoints of every edge in E_X are not both red. Our goal is to construct such a set R that complies with Statements i and ii, (except that R might not be maximal), which implies the existence of a corresponding maximal independent set I.

First consider the configuration, where X has no cycle, that is, X is a tree. Choose one vertex as root of the tree X, and then color the vertices red (including the root), if their distance to the root is even, and otherwise blue. Then both sets R and B are independent and one of them has at least $\frac{|E|}{2} = \frac{m}{2}$ elements. Without loss of generality we can assume that the larger set is R (otherwise switch the sets). So, if X has no cycles, the statement is true.

In the next step we assume that X has a cycle c. In this case we remove one edge $e \in E_X$ from c and obtain a tree $T = (E, E_X \setminus \{e\})$. We determine the sets R and B for T as described above.

If the length of c is even, then the endpoints of e have different colors, since their distance in T is odd. Thus, set R is also an independent set in X and has at least $\frac{m}{2}$ elements. Note that we have shown now that the statement of the lemma is true if X contains no cycle of odd length.

Finally we assume that the length of c is odd. Then both endpoints of e have the same color. If their color is blue, the set R has the required property. So let us assume that they are both red. We consider several cases. To this end let $e = (u, v)$ for vertices $u, v \in E$.

(1) $|R| \geq |B| + 2$: We change the color of u from red to blue, and set $R' := R \setminus \{u\}$ and $B' := B \cup \{u\}$. Then we have $|R'| = |R| - 1 \geq |B| + 1 = |B'|$, that is, R'

contains at least $\frac{m}{2}$ elements and is still an independent set. Note that in this case the number of elements in $E = R \dot{\cup} B$ might be even or odd.

(2) $|R| = |B|$: We exchange R and B. Then the endpoints of e are both blue and we can reinsert e such that R is still an independent set. Here the number of elements in R is $\frac{m}{2}$. Note that $|E|$ is even, since $m = |E| = |R| + |B| = 2|R|$.

(3) $|R| = |B| + 1$: Like in the first case we set $R' := R \setminus \{u\}$ and $B' := B \cup \{u\}$. Then we have $|R'| = |R| - 1 = |B| + 1 - 1 = |B'| - 1$ and further $m = |R'| + |B'| = |R'| + |R'| + 1 = 2|R'| + 1$, which implies $|R'| = \frac{m-1}{2}$. Since we selected a certain coloring at the beginning, another such choice might yield a larger independent set, that is $|I| \geq \frac{m-1}{2}$. Note that $|E|$ is odd, since $|E| = |R| + |B| = 2|B| + 1$.

This completes the proof of the lemma. □

By means of the previous lemmas we formulate conditions for a bipartite gap-planar drawing to have at most $4n - 8$ edges.

Theorem 6.11. *Let $G = (V, E)$ be a simple connected bipartite gap-planar graph with $n = |V|$ and $m = |E|$. Further let Γ be a simple gap-planar drawing of G, $X = (E, E_X)$ the crossing graph of Γ, and $X_1, \ldots, X_t$ (where $t \geq 1$) the connected components of X. Then Γ has at most $4n - 8$ edges if at least one of the following conditions holds:*

(i) X has no cycles at all;

(ii) X has only cycles of even length;

(iii) the number of crossing-free edges in Γ is at least as large as the number of components in X which have both, a cycle of odd length and also an odd number of vertices.

In general, the graph G has at most $\min(4n - 8 + t, 4.25n)$ *edges.*

Proof. For $j = 1, \ldots, t$ let E_j be the vertices of component X_j, and let I_j be a maximal independent set in X_j. Note that $E = E_1 \dot{\cup} E_2 \dot{\cup} \cdots \dot{\cup} E_t$. Further assume without loss of generality that, for some $s \in \{0, \ldots, t\}$, each of the components $X_1, \ldots, X_s$ has both, a cycle of odd length and an odd number of vertices. By Lemma 6.10 each independent set I_j has at least $\frac{|E_j|}{2}$ elements for $j = s + 1, \ldots, t$.

Let Γ' be the drawing obtained from Γ when removing edges $e_1, \ldots, e_s$, where e_j belongs to the odd cycle of X_j for every $j = 1, \ldots, s$. For $j = 1, \ldots, s$ let X'_j be the corresponding component without e_j and vertex set $E'_j := E_j \setminus \{e_j\}$. Note that $|E'_j| > 0$, since X_j contains an odd cycle. Let I'_j, $j = 1, \ldots, s$ be a maximal independent set in X'_j. By Lemma 6.10 each independent set I'_j has at least $\frac{|E'_j|}{2}$ elements for $j = 1, \dots, s$.

Since X_i and X_j are disjoint for $1 \leq i < j \leq t$, and therefore also X'_i and X'_j for $1 \leq i < j \leq s$, as well as X'_i and X_j for $1 \leq i \leq s$ and $s+1 \leq j \leq t$, the set $I' := I'_1 \cup \cdots \cup I'_s \cup I_{s+1} \cup \cdots \cup I_t$ is independent in $X' := X'_1 \cup \cdots \cup X'_s \cup X_{s+1} \cup \cdots \cup X_t$. If $E' := E \setminus \{e_1, \dots, e_s\}$ are the edges of Γ', we have

$$
\begin{aligned}
|I'| &= |I'_1| + \cdots + |I'_s| + |I_{s+1}| + \cdots + |I_t| \\
&\geq \tfrac{|E'_1|}{2} + \cdots + \tfrac{|E'_s|}{2} + \tfrac{|E_{s+1}|}{2} + \cdots + \tfrac{|E_t|}{2} \\
&= \tfrac{|E'|}{2}.
\end{aligned}
$$

Thus, Lemma 6.9 implies that Γ' has at most $4n - 8$ edges. It follows that Γ has at most $|E'| + s = 4n - 8 + s$ edges.

If X has no cycles at all or only cycles of even length, we have $s = 0$ and therefore at most $4n - 8$ edges in Γ. On the other hand, if $s = t$ the drawing Γ has at most $4n - 8 + t$ edges. Together with the result from Cor. 6.7, this yields an upper bound of $\min(4n - 8 + t, 4.25n)$ edges.

Finally consider the case when $1 < s < t$ and there are at least s crossing free edges in Γ. Each such edge is represented by a component consisting of a single vertex in the crossing graph X. For each $j = 1, \dots, s$, we uniquely map a crossing free edge with X_j. Let $e^\star$ and $X^\star$ be such a mapped pair. We merge $e^\star \in E = V(X)$ and $X^\star$ to a single component in X by adding an edge to E_X which connects $e^\star$ with an arbitrary vertex in $X^\star$. Then the number of vertices in the new component is even, which corresponds to Statement i in Lemma 6.10. In a similar manner as above we obtain that Γ has at most $4n - 8$ edges. □

If each optimal bipartite gap-planar drawing Γ, that fulfills neither of the conditions in Thm. 6.11, could be transformed into another bipartite gap-planar drawing Γ', such that the number of edges in Γ and Γ' are equal and such that Γ' fulfills one of the conditions in Thm. 6.11, then the density bound of $4n - 8$ could be extended to general bipartite gap-planar graphs. We are not sure if this is possible; however, we conjecture that the upper bound on the number of edges in bipartite gap-planar graphs is $4n - 8$.

We finish our study of gap-planar graphs by determining the edge density for such graphs in the outerplanar setting, that is, when all the vertices are placed on the outer face.

Theorem 6.12. *Every outer-1-gap-planar graph has at most $3n - 5$ edges.*

Proof. Let $G = (V, E)$ be an outer-1-gap-planar graph with a maximum number of edges, and let $m = |E|$ and $n = |V|$. Further let Γ be an outer-1-gap-planar drawing of G, and let $V = \{v_1, \ldots, v_n\}$ be the vertices on the outer face in counter-clockwise order.

We can assume without loss of generality that the edges (v_i, v_{i+1}), $i = 1, \ldots, n$ (where $n + 1$ is identified with 1) are bounding the outer face of Γ (otherwise one may first delete these edges and draw them as described). We call edges, that are not on the outer face, *interior edges* of Γ (refer to the blue edges in Fig. 6.2). The number of interior edges is $m - n$.

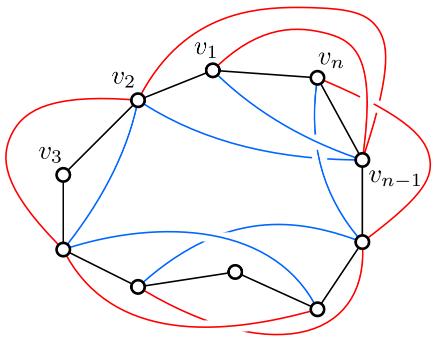

Fig. 6.2: Illustration for the proof of Thm. 6.12. The black edges are the edges on the outer face of Γ, while blue edges are interior edges. The red edges are copies of the interior edges.

Now consider the drawing $\Gamma^\star$ that is obtained from Γ by copying the interior edges of Γ into the outerface of Γ (refer to the red edges in Fig. 6.2). Clearly the drawing $\Gamma^\star$ is 1-gap-planar and even though it has multiple edges, there are no homotopic edges. By Bae at all [30], a 1-gap-planar drawing with such properties has at most $5n - 10$ edges. Since $\Gamma^\star$ has $n + 2 \cdot (m - n) = 2m - n$ edges, we conclude $2m - n \leq 5n - 10$, and subsequently $m \leq 3n - 5$. □

Figure 6.3 shows that the lower bound of $3n-5$ is almost tight, except for one edge. The figure gives rise to a lower bound construction for outer-gap-planar graphs.

Theorem 6.13. *For every $n \geq 4$, where n is even, there exists an outer-gap-planar drawing with $3n - 6$ edges.*

Proof. We construct an outer-gap-planar drawing Γ with n vertices and $m = 3n - 6$ edges. The vertices $v = v_1, v_2, v_3, \ldots, v_n$ of Γ are placed on a circle in clockwise or counter-clockwise order (refer also to Fig. 6.3). The edges of Γ are the following:

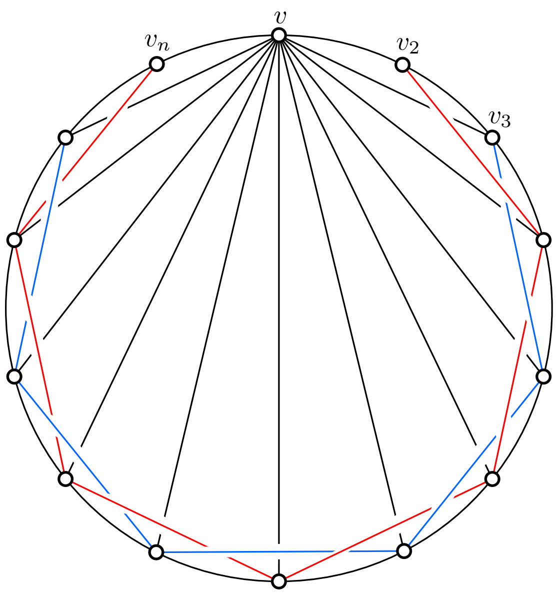

Fig. 6.3: A drawing of an outer-1-gap-planar graph with $3n-6$ edges: On the outer face are n edges; there is an interior edge from vertex v to every other vertex, except to v itself and its two neighbors, yielding $n-3$ edges; each interior black edge is crossed by another (blue or red) interior edge, which gives $n-3$ additional edges.

– For every $i = 1, \ldots, n$ (where v_{n+1} is identified with v_1) there is an edge (v_i, v_{i+1});

– for every $i = 3, \ldots, n-1$ there is an edge (v, v_i);

– and for every $i = 2, \ldots, n-2$ there is an edge (v_i, v_{i+2}).

All these edges are drawn as straight lines (in Fig. 6.3 edges (v_i, v_{i+1}) are drawn slightly curved for aesthetic reasons).

For $i = 2, \ldots, n-2$, the edge (v_i, v_{i+2}) crosses (v, v_{i+1}); this crossing is assigned to (v, v_{i+1}). Further, for $i = 2, \ldots, n-3$, the edge (v_i, v_{i+2}) crosses (v_{i+1}, v_{i+3}); this crossing is assigned to (v_i, v_{i+2}). As no edge has more than one crossing assigned to it, the drawing is indeed gap-planar.

The counting of the edges is as follows: On the outer face are n edges (black edges on the circle in Fig. 6.3), the number of interior edges incident to v (black edges) is $n-3$, and also the number of edges (v_i, v_{i+2}), where $i = 2, \ldots, n-2$ (red and blue edges), is $n-3$. Thus the total number of edges sums up to $3n-6$. □

6.6 Conclusions and Open Problems

We generalized the Crossing Lemma to a Meta Theorem and used it to prove Meta Theorems also for the maximal number of edges in k-planar and in k-gap-planar graphs. Further, we applied these Meta Theorems to outer-k-planar graphs and bipartite k-gap-planar drawings. For $k = 1$, the latter have an edge density of $4.25n$ by Thm. 6.11. We were able to improve this bound to $4n - 8$ under certain assumptions on the drawing. Finally, we showed an upper bound of $3n - 5$ edges for outer-1-gap-planar graphs.

Since the upper bound for bipartite 1-gap-planar graphs is only applicable for drawings with certain properties, we ask if this bound can be extended to general bipartite 1-gap-planar graphs. Moreover, the lower bound construction for such graphs gives $4n - 16$ edges, leaving a gap of 8 edges. Is it possible to close this gap by either constructing a lower bound example with more edges, or by improving the upper bound? We state a similar question for the outer-1-gap planar graphs: Our lower bound construction has $3n - 6$ edges, while we proved an upper bound of $3n - 5$ edges for these graphs; is it possible to close this gap?

Regarding the Meta Theorems, we have seen that applications for them can be found in the classes of k-planar and k-gap-planar graphs. Do these Theorems give rise to more Meta Theorems, maybe also in other graph classes? Finally, we state the question if there are more graph types – beside the general graphs, the bipartite graphs, the outer-planar graphs, and the 2-layer graphs – where an application of these Meta Theorems might be interesting.

Chapter 7

Drawing Graphs on Two Layers

The hierarchical drawing of graphs is of importance in various fields, e. g. in the visualization of software architecture [31, 124], social networks [84], or in profiling [92]. One main approach in this direction is to place all vertices on parallel (horizontal) lines, so-called *layers*. There exist different settings regarding the vertex placement on these layers: Mostly it is not allowed to place adjacent vertices on the same layer, in order to increase the readability of the drawing. Apart from this, another requirement may be that adjacent vertices are positioned on consecutive layers (refer e. g. to Biedl et al. [36]). Restrictions can also be imposed on the edges. Namely, a common assumption is that each edge is drawn as a straight line (see e. g. [38, 56]) or as a sequence of straight lines, using bends (see e. g. [131]).

The concept of drawing graphs on parallel layers was originally introduced by Sugiyama [131], together with a corresponding drawing algorithm. An important part of this so-called Sugiyama framework is the visualization of a graph using only two layers. Other than illustrating the structure of bipartite graphs clearly, this is one of the main motivations to study the problem of placing vertices of a graph on two parallel horizontal layers.

Since edge crossings disturb the readability of a drawing, but cannot always be avoided, many papers focus on the minimization of crossings in 2-layer drawings, see e. g. [65, 91, 136]. Other works study specifically a particular graph class beyond planarity. For example, characterizations for graphs admitting a 2-layer drawing, as well as testing and drawing algorithms for such graphs, were provided for RAC-graphs by Di Giacomo et al. [56], and for fan-planar graphs by Binucci et al. [38] (for examples of different types of 2-layer graphs refer to Fig. 7.1).

An important parameter for 2-layer graphs is the maximal number of edges that a certain graph class admits. In this direction, known edge density bounds tailored for the 2-layer setting are $n - 1$ edges for planar graphs [77], $\frac{3}{2}n - 2$ edges for 1-planar graphs [57] and RAC graphs [56], $2n - 4$ edges for fan-planar graphs [39],

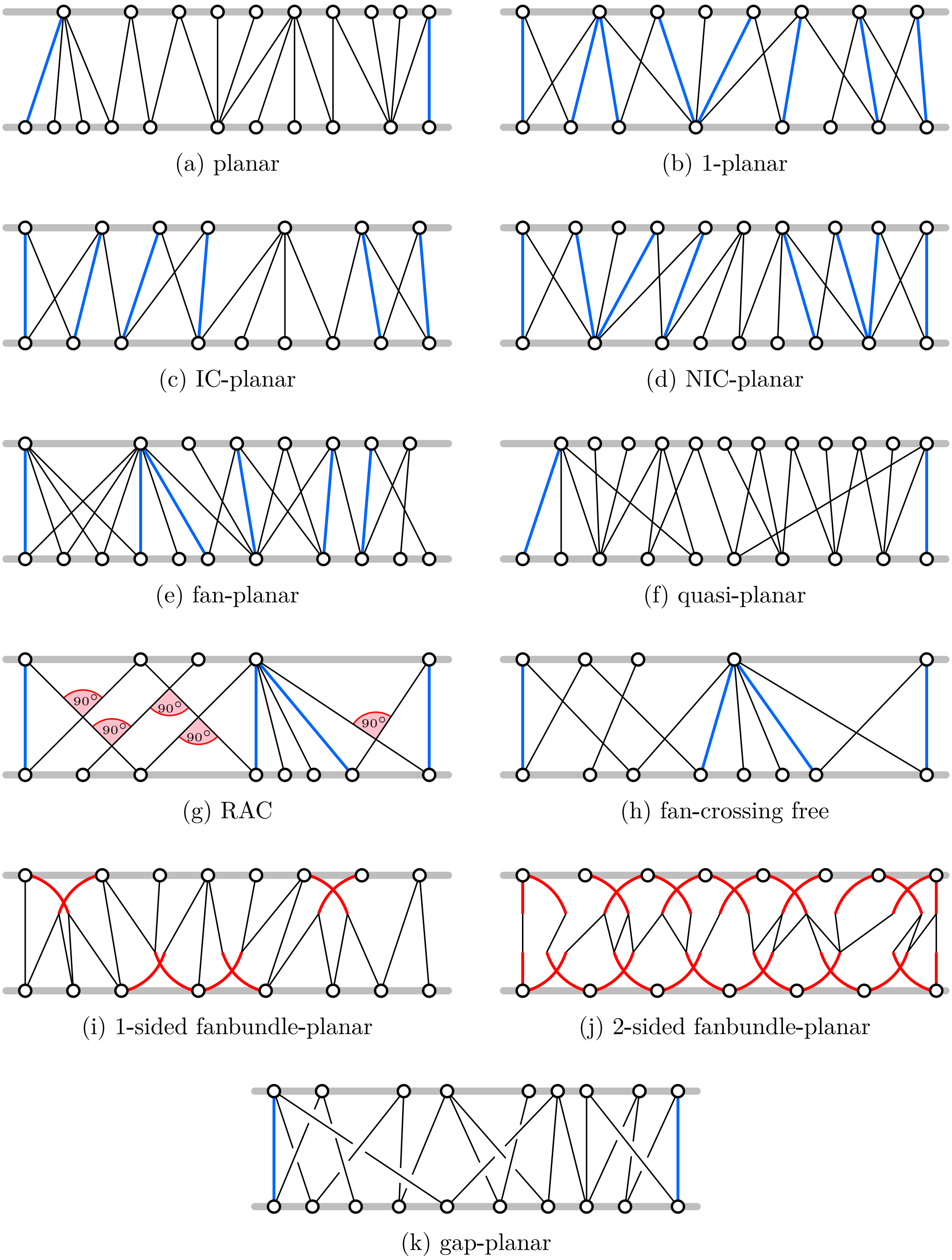

(a) planar
(b) 1-planar
(c) IC-planar
(d) NIC-planar
(e) fan-planar
(f) quasi-planar
(g) RAC
(h) fan-crossing free
(i) 1-sided fanbundle-planar
(j) 2-sided fanbundle-planar
(k) gap-planar

Fig. 7.1: Examples for 2-layer drawings of different graph classes.

$\frac{5n-7}{3}$ edges for 1-sided fanbundle-planar (1-sided fbp) graphs [13], and $3n-7$ edges for 2-sided fanbundle-planar (2-sided fbp) graphs [13]. All these bounds are tight with the exception of 2-sided fanbundle-planar graphs, since there only exists a lower bound construction with $2n-4$ edges [13].

Further, Di Giacomo et al. [56] showed that a connected graph is 2-layer RAC, if and only if it has a 2-layer drawing without fan-crossings. Note that the latter is exactly the definition for connected 2-layer fan-crossing free graphs; thus, the classes of 2-layer RAC and 2-layer fan-crossing free graphs coincide[1], which yields the following observation.

Observation 7.1. *Every 2-layer fan-crossing free graph has at most* $1.5n-2$ *edges. This bound is tight.*

Note also that the class of fan-planar graphs is a subclass of the class of fan-crossing graphs. Their definitions differ in only one point: In contrast to fan-planar graphs, different edges of a fan may cross an edge from different directions in fan-crossing graphs. However, such a crossing configuration is not possible in 2-layer graphs, since each edge e divides a 2-layer drawing in a "left" and a "right" side, and every edge incident to a vertex on the left (right) side of e crosses e from the left (right). As a consequence, the class of fan-crossing graphs and the class of fan-planar graphs are the same in the 2-layer setting, yielding a tight upper bound of $2n-4$ edges for fan-crossing graphs as well:

Observation 7.2. *Every 2-layer fan-crossing graph has at most* $1.5n-2$ *edges, which is a tight bound.*

In this chapter we study the edge densities of several 2-layer graph classes.[2] An overview of our findings and the state of the art can be found in Table 7.1. We stress that one of our results is a tight bound for 2-sided fanbundle-planar graphs, which closes the gap between the upper bound and the lower bound constructions in [13]. Further, we were able to provide characterizations for optimal 2-layer 2- and 4-planar graphs, each of which is a consequence of the proof for the corresponding edge density. In the last part of this chapter, relations between different classes of 2-layer graphs are discussed.

[1] If a 2-layer graph is not connected, the connected components can be drawn independently. So this statement is in fact true without the connectivity assumption.

[2] The results for the 2-layer k-planar edge densities and the inclusion relationship between 2-layer k-planar and 2-layer k-quasi-planar graphs of this chapter are part of our paper "2-Layer k-Planar graphs: Density, Crossing Lemma, Relationships, and Pathwidth" [19], together with the Meta Crossing Lemma (Sec. 6.2), and the general edge density bound for k-planar graphs (Thm. 6.3).

Table 7.1: Lower and upper bounds on the maximal number of edges in 2-layer drawings for several graph classes. The general bound for k-planar graphs is valid for $k \geq 6$. For quasi-planar graphs, the upper bound holds for $k \geq 3$ and $n \geq 3$, while the lower bound holds for $k \geq 3$ and sufficiently large n. For k-gap-planar drawings the general bound is valid for $k \geq 2$.

Class	Lower Bound	Reference	Upper Bound	Reference
planar	$n-1$	[77]	$n-1$	[77]
1-planar	$\frac{3}{2}n-2$	[57]	$\frac{3}{2}n-2$	[57]
2-planar	$\frac{5}{3}n-\frac{7}{3}$	Thm. 7.15	$\frac{5}{3}n-\frac{7}{3}$	Thm. 7.15
3-planar	$2n-4$	Thm. 7.17	$2n-4$	Thm. 7.19
4-planar	$2n-3$	Thm. 7.20	$2n-3$	Thm. 7.23
5-planar	$\frac{9}{4}n-\frac{9}{2}$	Thm. 7.25	$\frac{9}{4}n-\frac{9}{2}$	Thm. 7.31
6-planar	$\frac{5}{2}n-6$	Thm. 7.32	$3.19n$	Cor. 7.34
k-planar	$\frac{\lfloor\sqrt{k}\rfloor+2}{2}n-\mathcal{O}(\sqrt{k})$	Thm. 7.36	$\frac{125}{96}\sqrt{k}n$	Cor. 7.34
IC-planar	$\frac{5}{4}n-1$	Thm. 7.7	$\frac{5}{4}n-1$	Thm. 7.9
NIC-planar	$\frac{4}{3}n-\frac{4}{3}$	Thm. 7.7	$\frac{4}{3}n-\frac{4}{3}$	Thm. 7.10
k-quasi-planar	$(k-1)n-(k-1)^2$	Thm. 7.6	$(k-1)(n-3)+2$	Thm. 7.4
fan-planar	$2n-4$	[39]	$2n-4$	[39]
fan-crossing	$2n-4$	Obs. 7.2	$2n-4$	Obs. 7.2
fan-cr. free	$\frac{3}{2}n-2$	Obs. 7.1	$\frac{3}{2}n-2$	Obs. 7.1
gap-planar	$2n-4$	Thm. 7.37	$2n-4$	Thm. 7.41
k-gap-planar	$2n-4$	Thm. 7.37	$\frac{125}{48\sqrt{2}}\sqrt{k}n$	Cor. 7.35
1-sided 1-fbp	$\frac{5}{3}n-\frac{7}{3}$	[13]	$\frac{5}{3}n-\frac{7}{3}$	[13]
2d-layer 2-sided 1-fbp	$2n-4$	[13]	$2n-4$	Thm. 7.42
2-sided 1-fbp	$\frac{17}{8}n-\frac{13}{4}$	Thm. 7.44	$\frac{17}{8}n-\frac{13}{4}$	Thm. 7.47
RAC	$\frac{3}{2}n-2$	[56]	$\frac{3}{2}n-2$	[56]

7.1 Preliminaries

We consider the following beyond-planarity graph classes:[3]

- the class of k-planar graphs $\mathcal{P}_k$, where $k \geq 1$ (see e. g. Figs. 7.1a and 7.1b);
- the class of k-quasi-planar graphs $\mathcal{Q}_k$, where $k \geq 3$ (see e. g. Fig. 7.1f); if $k = 3$, we also use the notation "quasi-planar" and $\mathcal{Q}$ instead of "3-quasi-planar" and $\mathcal{Q}_3$;
- the class of k-gap-planar graphs $\mathcal{G}_k$, where $k \geq 1$ (see e. g. Fig. 7.1k); if $k = 1$, we also use the notation "gap-planar" and $\mathcal{G}$ instead of "1-gap-planar" and $\mathcal{G}_1$;
- the class of fan-planar graphs $\mathcal{F}$ (see e. g. Fig. 7.1e);
- the class of fan-crossing free graphs $\mathcal{X}$; (see e. g. Fig. 7.1h)
- the class of 1-sided fbp graphs $\mathcal{B}_1$ (see e. g. Fig. 7.1i);
- the class of 2-sided fbp graphs $\mathcal{B}_2$ (see e. g. Fig. 7.1i);
- the class of independent crossing (IC) graphs $\mathcal{P}_{IC}$ (see e. g. Fig. 7.1c);
- and the class of nearly independent crossing (NIC) graphs $\mathcal{P}_{NIC}$ (see e. g. Fig. 7.1d).

For a graph class $\mathcal{C}$, we denote the corresponding 2-layer graph class by $\mathcal{C}^=$. Note that by Di Giacomo et al. [56] (see above) the class of 2-layer RAC graphs and the class $\mathcal{X}^=$ of 2-layer fan-crossing free graphs coincide, so we only consider the class $\mathcal{X}^=$ in the following. Further note that for 2-sided fbp graphs we introduce two corresponding 2-layer graph classes, denoted by $\mathcal{B}_2^=$ and $\mathcal{B}_{2d}^=$. We explain later the difference between them (refer to Sec. 7.6).

Let $G = (V, E)$ be a connected graph belonging to the 2-layer graph class $\mathcal{C}^=$, that is $G \in \mathcal{C}^=$, and let Γ be a corresponding drawing. We say that G is a $\mathcal{C}^=$-graph, and Γ is $\mathcal{C}^=$-drawable. In an abuse of notation, we denote the latter also by $\Gamma \in \mathcal{C}^=$. Except for the class of 2-sided fbp graphs, we require that Γ is simple and that the edges are straight lines.[4] We specify the requirements for 2-sided fbp graphs later (see Sec. 7.6).

Let $V = U \dot\cup W$ be the disjoint union of the two independent sets U and W; further we define $a := |U| \geq 1$, $b := |W| \geq 1$, $n := |V|$ and $m := |E|$. We assume that the vertex orders of Γ along the top and bottom layers (from left to right) are given by

[3]Definitions for the classes can be found in Chapter 2, and also later in this chapter, when the density of the corresponding 2-layer graph class is studied.

[4]It is not difficult to see that the simplicity and the existence of a 2-layer $\mathcal{C}^=$-drawing (that has not necessarily straight edges) implies that there is a simple 2-layer $\mathcal{C}^=$-drawing, where all edges are straight. However, some 2-layer graph classes may require straight line edges by definition, e. g. the 2-layer RAC graphs.

$u_1, \ldots, u_a$ and $w_1, \ldots, w_b$, respectively. The order of the vertices along one of the layers is denoted by "$\prec$", that is $u_i \prec u_j$ for two vertices u_i and u_j of the top layer if and only if $i < j$, and $u_i \preccurlyeq u_j$ if and only if $i \leq j$; the order for the bottom layer is defined in a similar way. We also use the indexes i and j to describe the order of u_i and u_j.

For $1 \leq \ell \leq r \leq a$ and $1 \leq \ell' \leq r' \leq b$, we call the subdrawing $\Gamma[U' \cup W']$, where $U' = \{u_\ell, \ldots, u_r\}$ and $W' = \{w_{\ell'}, \ldots, w_{r'}\}$, a *snippet* Γ' of Γ and denote it solely by its extremal indexes, that is, by $\Gamma' = [\ell, r \mid \ell', r']$. A snipped $[\ell, r \mid \ell', r']$ is called a *brick* if the following two properties hold (see Fig. 7.2 for an illustration):

(i) The edges $(u_\ell, w_{\ell'})$ and $(u_r, w_{r'})$ are planar in Γ, and $(u_\ell, w_{\ell'}) \neq (u_r, w_{r'})$;

(ii) if $(u_i, w_{i'}) \in E$ for some $\ell \leq i \leq r$ and $\ell' \leq i' \leq r'$, then $(u_i, w_{i'})$ is planar (in Γ) if and only if ($i = \ell$ and $i' = \ell'$) or ($i = r$ and $i' = r'$).

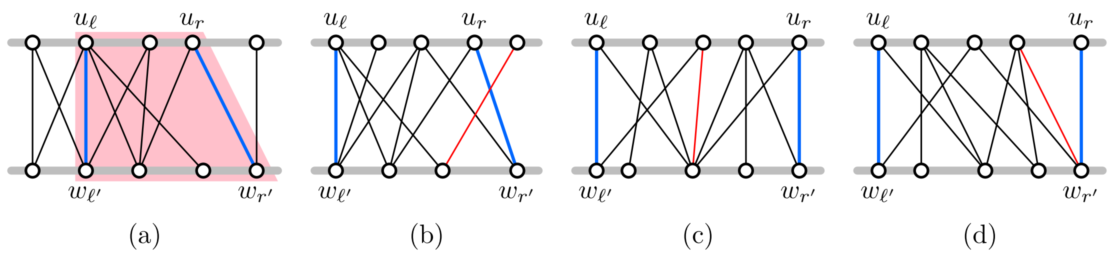

Fig. 7.2: (a) The brick $[\ell, r \mid \ell', r']$ is highlighted in red. (b) The snippet $[\ell, r \mid \ell', r']$ is no brick, since Property i is violated. In (c) and (d) the snippet $[\ell, r \mid \ell', r']$ is no brick, since Property ii is violated.

We call Γ *maximal* if no edge can be added to it without violating the properties of class $\mathcal{C}^=$. The drawing Γ (and graph G) is *optimal*, if it has the maximal possible number of edges regarding class $\mathcal{C}^=$. Note that every optimal drawing is maximal, but not vice versa. Also observe that every maximal drawing (and therefore every optimal drawing) Γ contains both planar edges (u_1, w_1) and (u_a, w_b) and hence at least one brick.

Similar to the chapters before, we usually use "embedding" and "drawing" as synonyms. For 2-layer drawings, we use the term "weakly isomorphic" as defined in Sec. 5.3, that is, two drawings are weakly isomorphic if their edges appear in the same order around each vertex. Note that for two drawings to be isomorphic, also the order in which an edge is crossed by other edges must be the same in both drawings. However, we do not need to consider this order for 2-layer graphs, since the regions bounded by three or more mutually crossing edges will be empty (in contrast to the drawings in Sec. 5.3, where we used these regions to place vertices; refer also to Fig. 7.3). For this reason, we denote weakly isomorphic drawings – in an abuse of notation – just as isomorphic drawings.

Fig. 7.3: Two 2-layer drawings that are weakly isomorphic, but not isomorphic. Note that in the red areas the order of the edges differ, when walking along the border clockwise. However, these areas will always be empty by the definition of 2-layer drawings.

7.2 Density of 2-Layer Quasi-Planar Graphs

We start by considering quasi-planar graphs. Recall that, for $k \leq 3$, in a k-quasi-planar drawing the existence of k mutually crossing edges is forbidden. For the class of 2-layer 3-quasi-planar graphs $\mathcal{Q}^=$, a lower bound construction can easily be obtained.

Theorem 7.3. *For infinitely many n there is a $\mathcal{Q}^=$-graph on n vertices with $2n-4$ edges.*

Proof. We describe a family of graphs with $n = a + b = 2a$ vertices, where each layer has $a = b$ vertices; for an illustration refer to Fig. 7.4. A graph of our family has the edges:

- (u_i, w_i) for $1 \leq i \leq a$;
- (u_i, w_{i+1}) for $1 \leq i \leq a-1$;
- (u_i, w_{i-1}) for $2 \leq i \leq a$;
- and (u_i, w_{i+2}) for $1 \leq i \leq a-2$.

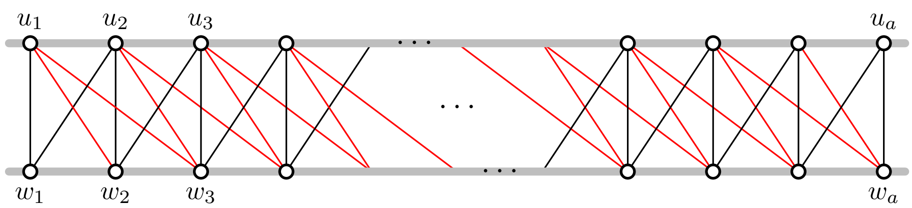

Fig. 7.4: A family of quasi-planar graphs with $n = 2a$ vertices and $2n-4$ edges. The two colors depict two sets of crossing free edges. The number of black edges is $n-1$, and the number of red edges is $n-3$.

Then each vertex has degree 4, except the following ones: the four vertices u_1, u_{a-1}, w_2 and w_a have degree three, and the two vertices u_a and w_1 have degree two. Therefore the sum of all vertex degrees is $4n-8$, yielding $2n-4$ edges. □

We show that $2n-4$ is also an upper bound for the number of edges in 2-layer quasi-planar graphs, that is, the upper bound of $2n-4$ edges for the class $\mathcal{Q}^{=}$ is tight. In fact, we even prove a more general statement.

Theorem 7.4. *Let $k \geq 3$. Every 2-layer k-quasi-planar graph on $n \geq 3$ vertices has at most $(k-1)(n-3)+2$ edges.*

Observe that a $\mathcal{Q}_k^{=}$-graph on $n=2$ vertices has at most 1 edge; so the bound does not hold for $n=2$.

In order to prove Thm. 7.4, we follow the argumentation of Bartosz Walczak, who addressed this problem in his invited talk[5] at *The 27th International Symposium on Graph Drawing and Network Visualization* [137] (as far as we know, there exist no corresponding publication). However, we were able to improve the upper bound of $(k-1)(n-1)$ which he stated in his talk to $(k-1)(n-3)+2$.

We start by recalling the so-called permutation graphs, which play a major role in our proof. Let $\pi = (\pi_1, \ldots, \pi_N)$ be a permutation of the set $\{1, \ldots, N\}$ for some $N \geq 1$. Consider the drawing Γ_π, whose edges are line segments L_i, $1 \leq i \leq N$, with endpoints $(i, 1)$ and $(\pi_i, 0)$, and whose vertices are these endpoints (see also Fig. 7.5). Then the *permutation graph* $G_\pi = (V_\pi, E_\pi)$ is the crossing graph of Γ_π, that is $V_\pi = \{L_1, \ldots, L_N\}$ and for $i \neq j$, edge $(L_i, L_j) \in E_\pi$ if and only if L_i and L_j cross in Γ_π.

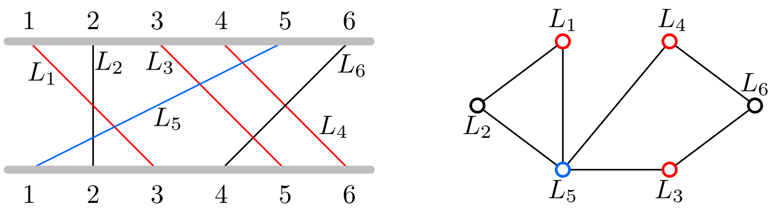

Fig. 7.5: Left: A drawing Γ_π, where the permutation is given by $\pi = (3, 2, 5, 6, 1, 4)$. Right: The corresponding permutation graph.

Permutation graphs were first introduced in [70, 113]. Even et al. [70] showed that such graphs are perfect, i. e. the size $\omega = \omega(G_\pi)$ of the maximal clique in G_π (referred to as *clique number*; see also Chapter 2) equals the chromatic number $\chi = \chi(G_\pi)$. Recall that the *(vertex) chromatic number* χ is defined as follows: Let $t \geq 1$ be a positive integer. A *(vertex) coloring* of G_π (or some other graph) is a mapping $\mathbf{c} : V_\pi \longrightarrow \{c_1, \ldots, c_t\}$, such that no two adjacent vertices are mapped to the same color c_i. The chromatic number χ is the minimal number of colors needed over all possible colorings; in the following we denoted a coloring that needs only χ colors a

[5]Slides to his talk are currently available at `https://kam.mff.cuni.cz/gd2019/program.html`.

minimal (vertex) coloring. Analogously, an *edge coloring* of Γ_π (or some arbitrary drawing) is a mapping $\mathbf{c} : E_\pi \longrightarrow \{c_1, \ldots, c_t\}$, such that edges which cross each other are mapped to different colors; the *edge chromatic number* χ_e is the minimal possible value for the number of colors t.

By definition of the crossing graph, a vertex coloring of G_π corresponds to an edge coloring of Γ_π (refer to the colors in Fig. 7.5). On the other hand, a clique of size k in G_π corresponds to a set of k mutually crossing edges in Γ_π, which establishes a relation to k-quasi-planar graphs. We use this relation as one ingredient in our proof of Thm. 7.4. Another ingredient is the following observation by Even et al. [70].

Observation 7.5 (Even)**.** *The crossing graph of every 2-layer drawing* Γ *is a permutation graph.*

Fig. 7.6: (a) A 2-layer drawing Γ. (b) The "trimming" Γ' of Γ. Note that the crossing graphs of Γ and Γ' are identical.

To see that this observation is correct, "subdivide" each vertex of Γ, such that each subdivided part of the original vertex has just one edge incident to it (see Fig. 7.6 for an illustration). The drawing obtained in this way corresponds to the drawing Γ_π described in the definition of permutation graphs, and has the same crossing graph as Γ. Evan referred to this subdividing operation as "trimming" [70].

Now we are prepared to prove the upper bound on the number of edges for $\mathcal{Q}_k^=$.

Proof of Thm. 7.4. Let $G = (V, E)$ be a 2-layer k-quasi-planar graph with $n \geq 3$ edges and m vertices, and let Γ be a corresponding $\mathcal{Q}_k^=$-drawing of G. Without loss of generality we can assume that the planar edges (u_1, w_1) and (u_a, w_b) are part of Γ (otherwise, augmenting Γ by them yields a drawing with even more edges); refer to the dashed blue edges in Fig. 7.7. Since $n \geq 3$, these edges are different, that is $(u_1, w_1) \neq (u_a, w_b)$.

Let $\chi = \chi(\Gamma)$ be the edge chromatic number of Γ. Consider a minimal edge coloring $\mathbf{c} : E \longrightarrow \{c_1, \ldots, c_\chi\}$ of Γ. For $1 \leq i \leq \chi$ we denote the set of edges mapped to color c_i by $C_i := \mathbf{c}^{-1}(c_i)$. The subdrawing $\Gamma[C_i]$, consisting of the vertices of Γ and the edges C_i, is planar (recall that edges with the same color do not cross each other in an edge coloring); refer to the differently colored edges in Fig. 7.7. Like above,

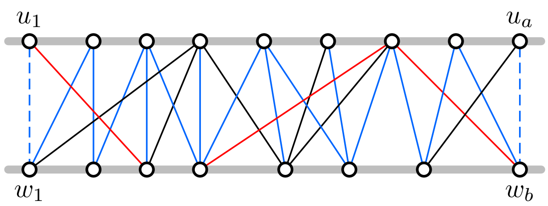

Fig. 7.7: Illustration for the proof of Thm. 7.4.

we argue that, if the planar edges $e_1 := (u_1, w_1)$ and $e_2 := (u_a, w_b)$ do not belong to $\Gamma[C_i]$, one may add these edges to $\Gamma[C_i]$ without violating the planarity, that is, $\Gamma[C_i \cup \{e_1, e_2\}]$ is still a planar drawing. Since planar 2-layer graphs have at most $n-1$ edges, and since $e_1, e_2 \in \Gamma[C_i \cup \{e_1, e_2\}]$ for each $1 \le i \le \chi$, we obtain

$$m = m_1 + \cdots + m_\chi - 2(\chi - 1) \le \chi(n-1) - 2(\chi-1) = \chi(n-3) + 2,$$

where m_i is the number of edges in $\Gamma[C_i \cup \{e_1, e_2\}]$.

Let X be the crossing graph of Γ. As each edge coloring of Γ corresponds to a vertex coloring in X, the vertex chromatic number of X equals χ. Moreover, due to k-quasi-planarity, drawing Γ does not contain k mutually crossing edges. So the size of the largest clique in X is at most $k-1$, yielding $\omega \le k-1$ for the clique number ω of X. By Obs. 7.5, the graph X is a permutation graph, which implies $\chi = \omega$ [70], and consequently

$$m \le \chi(n-3) + 2 = \omega(n-3) + 2 \le (k-1)(n-3) + 2.$$

The statement follows. □

As already mentioned, the bound of $(k-1)(n-3)+2$ edges is tight for $k = 3$. However, we believe that this is not the case for $k > 3$, due to the following reason. If, in the previous proof, we assume that edges e_1 and e_2 belong to C_1, then C_1 has at most $n-1$ edges, while C_i has at most $n-3$ edges for $i = 2, \ldots, \chi$. But it seems that the upper bound of $n-3$ edges is an overestimation for most of the sets $C_2, \ldots, C_\chi$, since again there are edges in $\Gamma' := \Gamma[E \setminus \{e_1, e_2\}]$ that play the same role as e_1 and e_2 in Γ. In fact, we believe that it is possible to show that there is a coloring, such that $|C_i| \le n - 1 - 2(i-1)$ for $i = 1, \ldots, \chi$, which would yield an upper bound of $(k-1)n - (k-1)^2$ edges in k-quasi-planar graphs for sufficiently large n. We support this conjecture by a corresponding lower bound construction for 2-layer k-quasi-planar graphs.

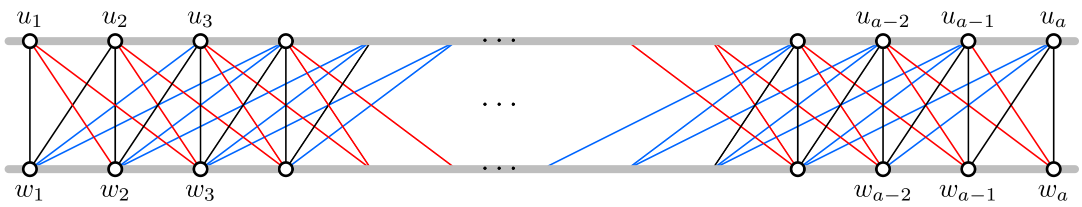

Fig. 7.8: A family of 4-quasi-planar graphs with $n = 2a$ vertices and $3n - 9$ edges.

Theorem 7.6. *Let $k \geq 3$. For infinitely many n there is a 2-layer k-quasi-planar graph on n vertices with $(k-1)n - (k-1)^2$ edges.*

Proof. According to Thm. 7.3, there exists such a family for $k = 3$. Note that, in a drawing Γ_3 constructed as in Thm. 7.6, there are two disjoint paths: one path $p_1 := (u_1, w_1, u_2, w_2, \ldots, u_{a-1}, w_{a-1}, u_a, w_a)$ of length $n-1$ (black edges in Figs. 7.4 and 7.8), and a second path $p_2 := (w_2, u_1, w_3, u_2, w_4, u_3, \ldots, w_{a-1}, u_{a-2}, w_a, u_{a-1})$ of length $n-3$ (red edges in Figs. 7.4 and 7.8). Each path p_1 and p_2 has the property that no two edges of the same path cross each other; so there are no three mutually crossing edges in Γ_3 for $k = 3$.

For $k = 4$, we create a drawing Γ_4 from Γ_3 by augmenting it with another path p_3. Thereby we ensure that p_3 has the same property as p_1 and p_2, namely, no two edges of p_3 cross each other, which implies that Γ_4 does not contain four mutually crossing edges. Let $p_3 := (u_3, w_1, u_4, w_2, u_5, w_3, \ldots, u_{a-1}, w_{a-3}, u_a, w_{a-2})$ (blue edges in Fig. 7.8). Path p_3 has $n-5$ edges, since u_1, u_2, w_{a-1} and w_a do not belong to p_3. Thus, Γ_4 has exactly $3n - 9 = (k-1)n - (k-1)^2$ edges.

It is possible to iteratively create k-quasi-planar drawings Γ_k for $k \geq 5$ by adding another path p_{k-1} of length $n - 2k + 3$ to Γ_{k-1}. More precisely, we add the path $p_{k-1} := (u_{k-1}, w_1, u_k, w_2, u_{k+1}, w_3, \ldots, u_{a-1}, w_{a-k}, u_a, w_{a-k+1}))$ if k is odd, and the path $p_{k-1} := (w_{k-1}, u_1, w_k, u_2, w_{k+1}, u_3, \ldots, w_{a-1}, u_{a-k}, w_a, u_{a-k+1})$ if k is even. By construction, all edges of the paths $p_1, \ldots, p_{k-1}$ are distinct. The number of edges in Γ_k sums up to

$$\begin{aligned}\sum_{i=2}^{k}(n - 2i + 3) &= (k-1)(n+3) - 2\left(\frac{k(k+1)}{2} - 1\right) \\ &= (k-1)(n+3) - k(k+1) + 2 \\ &= (k-1)n + 3(k-1) - k(k-1) - 2k + 2 \\ &= (k-1)n - (k-1)^2,\end{aligned}$$

which completes the proof. □

We conclude this section by mentioning that most of the density proofs in this chapter differentiate between the case, where the drawing is quasi-planar and therefore has at most $2n-4$ edges (or respectively $2n-3$ for $n=2$), and the case where there exists a triple of mutually crossing edges in the drawing.

7.3 Density of 2-Layer IC-Planar and NIC-Planar Graphs

We study the maximal number of edges in the class $\mathcal{P}^{=}_{IC}$ of 2-layer IC-planar graphs, and the class $\mathcal{P}^{=}_{NIC}$ of NIC-planar graphs. Recall from Chapter 2 the definition of these graphs: If each of $\{(u_1,w_1),(u_2,w_2)\}$ and $\{(u_3,w_3),(u_4,w_4)\}$ is a pair of crossing edges, then the set $\{u_1,u_2,w_1,w_2\} \cap \{u_3,u_4,w_3,w_4\}$

- must be empty in IC-planar drawings (where "IC" stands for "independent crossing"),
- is not allowed to contain more than one element in NIC-planar drawings (where "NIC" stands for "nearly independent crossing").

By definition, IC-planar graphs are a subclass of NIC-planar graphs, while NIC-planar graphs represent a subclass of 1-planar graphs. This implies that, in the 2-layer setting, the number of edges in both graph classes is at most $\frac{3}{2}n-2$. In this section we establish tight upper bounds that are even smaller than $\frac{3}{2}n-2$ for both graph classes. Thereby we start by considering lower bound constructions.

Theorem 7.7. *For infinitely many n, there is a $\mathcal{P}^{=}_{IC}$-graph on n vertices with $\frac{5}{4}n-1$ edges, and a $\mathcal{P}^{=}_{NIC}$-graph with $\frac{4}{3}n-\frac{4}{3}$ edges.*

Proof. First we describe a family of IC-planar graphs with $n=a+b=2a$ vertices, where each layer has $a=b$ vertices and a is even; for an illustration refer to Fig. 7.9a. Our graph contains the edges

- (u_i,w_i) for $1 \le i \le a$,
- (u_i,w_{i-1}) for $2 \le i \le a$, and
- (u_i,w_{i+1}) for all odd i where $1 \le i \le a-1$.

Then the number of edges is $m = a+(a-1)+\frac{1}{2}a = \frac{5}{2}a-1 = \frac{5}{4}n-1$.

Now we describe a family of NIC-planar graphs with $\frac{4}{3}n-\frac{4}{3}$ edges. The family consists of $t>0$ consecutive drawings of $K_{2,2}$, such that each two consecutive drawings are joined at one vertex; see Fig. 7.9b. Depending on t, the number of vertices is $n=1+3t$, and the number of edges is $m=4t=\frac{4}{3}(n-1)=\frac{4}{3}n-\frac{4}{3}$. □

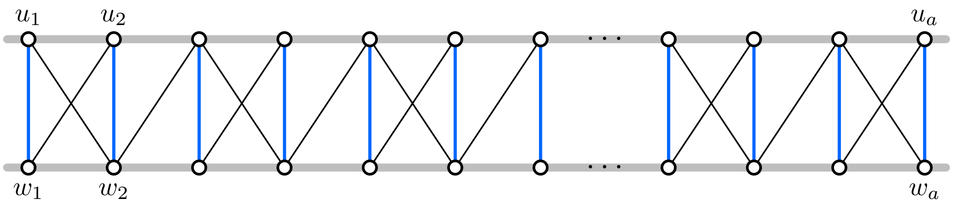

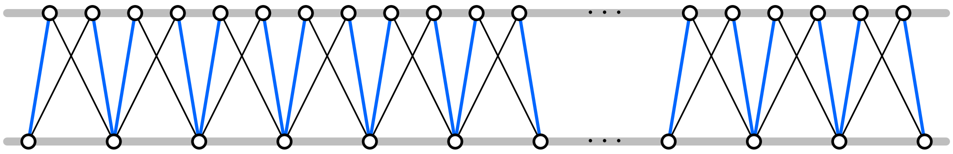

Fig. 7.9: (a) A family of IC-planar graphs with n vertices and $\frac{5}{4}n - 1$ edges. (b) A family of NIC-planar graphs with n vertices and $\frac{4}{3}n - \frac{4}{3}$ edges.

In the following we prove that $\frac{5}{4}n - 1$ and $\frac{4}{3}n - \frac{4}{3}$ are upper bounds for 2-layer IC-planar and NIC-planar graphs, respectively. We start with an auxiliary lemma.

Lemma 7.8. *Let G be a graph that has a vertex v with degree 1. If the induced subgraph $G' := G[V \setminus \{v\}]$ has at most $(1 + \varepsilon)n' - c$ edges, where $n' = n - 1$ is the number of vertices in G', and $\varepsilon \geq 0$ and $c \geq 0$ are some constants, then G has at most $(1 + \varepsilon)n - c$ edges.*

Proof. Let G and G' be as described in the lemma, m the number of edges in G, and m' the number of edges in G'. Since $\deg(v) = 1$, we have $m = m' + 1$ and hence

$$\begin{aligned} m = m' + 1 &\leq (1 + \varepsilon)n' - c + 1 = (1 + \varepsilon)(n - 1) - c + 1 \\ &= (1 + \varepsilon)n - c - \varepsilon \leq (1 + \varepsilon)n - c. \end{aligned}$$

The statement follows. □

Lemma 7.8 shows that it suffices to consider graphs without degree-1 vertices, when proving upper bounds of the form $(1 + \varepsilon)n - c$. We use this fact in the next two theorems.

Theorem 7.9. *A 2-layer IC-planar graph has at most $\frac{5}{4}n - 1$ edges.*

Proof. Let Γ be a $\mathcal{P}^{=}_{IC}$-drawing with n vertices and m edges. We prove the statement by induction on the number of vertices. For the base of the induction, assume that Γ has $n \leq 3$ vertices. Then Γ is planar and has $n - 1 \leq \frac{5}{4}n - 1$ edges.

For the induction step assume that Γ has $n > 3$ vertices and every graph with less than n vertices has at most $\frac{5}{4}n - 1$ edges. Again, if Γ is planar the statement follows immediately. On the other hand, if Γ has a vertex of degree 1, the induction hypothesis and Lemma 7.8 imply $m \leq \frac{5}{4}n - 1$.

Suppose now that Γ is not planar and contains no vertex of degree 1. Then there exists a pair $(u_h, w_{i'})$, $(u_i, w_{h'})$ of crossing edges in Γ for some $1 \leq h < i \leq a$ and $1 \leq h' < i' \leq b$. If $i > h+1$, then there is a vertex between u_h and u_i on the top layer which has degree 0 – a contradiction to the connectivity of Γ. So we have $i = h+1$ and for similar reasons $i' = h'+1$.

Consider the case, where drawing Γ contains edges $(u_h, w_{x'})$ and $(u_h, w_{y'})$ for $1 \leq x' < y' < h'$ (see red edges in Fig. 7.10a). Then the vertex $w_{y'}$ has degree 1, since otherwise IC-planarity would be violated. But this contradicts our assumption that there is no degree-1 vertex in Γ. Thus u_h is incident to at most one edge $(u_h, w_{x'})$, where $1 \leq x' < h'$, and – if this edge exists – we have $x' = h-1$, since Γ is connected. Similarly, each of the vertices u_{h+1}, $w_{h'}$, and $w_{h'+1}$ has at most one neighbor outside the set $\{u_h, u_{h+1}, w_{h'}, w_{h'+1}\}$, and if they have one neighbor it is the vertex $w_{h'+2}$ for u_{h+1}, the vertex u_{h-1} for $w_{h'}$, and the vertex u_{h+2} for $w_{h'+1}$.

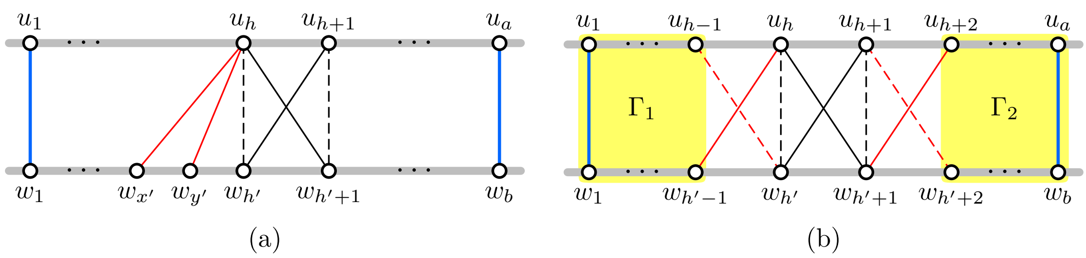

Fig. 7.10: Illustration for the proof of Thm. 7.9.

Next observe that at most one of the two edges $(u_h, w_{h'-1})$ and $(u_{h-1}, w_{h'})$ is in Γ, otherwise IC-planarity would be violated; the same holds for $(u_{h+1}, w_{h'+2})$ and $(u_{h+2}, w_{h'+1})$ (see red edges in Fig. 7.10b).

For $h > 1$, $h' > 1$, $h+1 < a$ and $h'+1 < b$ we define the two snippets $\Gamma_1 := [1, h-1 \mid 1, h'-1]$ and $\Gamma_2 := [h+2, a \mid h'+2, b]$. Let n_i and m_i be the number of vertices and edges of Γ_i, where $i = 1, 2$. Then Γ_1 and Γ_2 clearly have less pairs of crossing edges than Γ, so $m_i \leq \frac{5}{4}n_i - 1$. Moreover, we have $n = n_1 + n_2 + 4$ and $m \leq m_1 + m_2 + 6$, yielding

$$m \leq \left(\tfrac{5}{4}n_1 - 1\right) + \left(\tfrac{5}{4}n_2 - 1\right) + 6 = \tfrac{5}{4}(n_1 + n_2) + 4 = \tfrac{5}{4}(n-4) + 4 = \tfrac{5}{4}n - 1.$$

On the other hand, if $h = h' = 1$, $h+1 = a$ and $h'+1 = b$, the drawing Γ consists of 4 vertices and thus at most 4 edges, implying $m \leq \frac{5}{4}n - 1$.

Consider the case where $h = 1$, and $h+1 < a$ or $h'+1 < b$. If $h' > 1$, vertex w_1 has degree 1, because the edge $(u_h, w_{h'+1}) = (u_1, w_{h'+1})$ is already crossed once, and therefore every vertex $w \prec w_{h'}$ can only be adjacent to u_1. As a consequence we have $h' = 1$ as well. Similar arguments show that a vertex of degree 1 exists if $h+1 = a$ or $h'+1 = b$; thus we can assume that $h+1 < a$ and $h'+1 < b$. This implies the existence of exactly one of the edges $(u_{h+1}, w_{h'+2}) = (u_2, w_3)$ or $(u_{h+2}, w_{h'+1}) = (u_3, w_2)$, so the snippets $\Gamma_1' := [1, 2 \mid 1, 2]$ and $\Gamma_2' := [3, a \mid 3, b]$ are connected by exactly one edge. Because Γ_1' has 4 vertices and at most 4 edges, while Γ_2' has $n' = n - 4$ vertices and at most $m' \leq \frac{5}{4}n' - 1$ edges by induction, we obtain

$$m \leq m' + 4 + 1 \leq \left(\tfrac{5}{4}n' - 1\right) + 5 = \tfrac{5}{4}(n-4) - 1 + 5 = \tfrac{5}{4}n - 1.$$

Since the cases $h' = 1$, $h+1 = a$ and $h'+1 = b$ are symmetric to the considered case, the statement follows. □

We conclude this section by showing a corresponding upper bound for NIC-planar graphs. The proof uses similar arguments as the one for IC-planar graphs.

Theorem 7.10. *A 2-layer NIC-planar graph has at most $\frac{4}{3}n - \frac{4}{3}$ edges.*

Proof. Let Γ be a $\mathcal{P}^{=}_{NIC}$-drawing with n vertices and m edges. We prove the statement by induction on the number of vertices. For the base of the induction, assume that Γ has $n \leq 3$ vertices. Then Γ is planar and has $m \leq n-1 \leq \frac{4}{3}n - \frac{4}{3}$ edges.

For the induction step assume that Γ has $n > 3$ vertices and every graph with less than n vertices has at most $\frac{4}{3}n - \frac{4}{3}$ edges. If Γ is planar the statement follows immediately, and if Γ has a vertex of degree 1, the induction hypothesis and Lemma 7.8 imply $m \leq \frac{4}{3}n - \frac{4}{3}$.

Suppose now that Γ is not planar and contains no vertex of degree 1. Then there exists a pair $(u_h, w_{i'})$, $(u_i, w_{h'})$ of crossing edges in Γ for some $1 \leq h < i \leq a$ and $1 \leq h' < i' \leq b$. Similar to the proof of Thm. 7.9, we have $i = h+1$ and $i' = h'+1$.

For $1 \leq x < h$ and $1 \leq x' < h'$, at most one of the edges $(u_x, w_{h'})$ and $(u_h, w_{x'})$ is in Γ, otherwise NIC-planarity would be violated. Similarly, for $h+1 < y \leq a$ and $h'+1 < y' \leq b$, at most one of the edges $(u_y, w_{h'+1})$ and $(u_{h+1}, w_{y'})$ is in Γ (see red edges in Fig. 7.11). We assume without loss of generality that $(u_x, w_{h'})$ and $(u_y, w_{h'+1})$ does not belong to Γ.

Define the snippets $\Gamma_1 := [1, h \mid 1, h'-1]$ and $\Gamma_2 := [h+1, a \mid h'+2, b]$ (where Γ_1 consists only of u_h when $h' = 1$, and Γ_2 consists only of u_a when $h'+1 = b$). For $i = 1, 2$ let n_i and m_i be the number of vertices and edges of Γ_i. Then Γ_1 and Γ_2 have less vertices than Γ, so we obtain inductively $m_i \leq \frac{4}{3}n_i - \frac{4}{3}$.

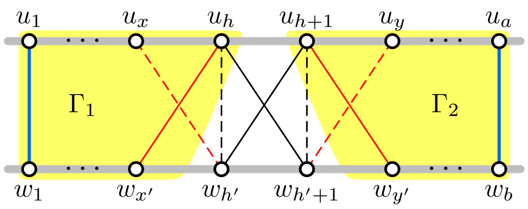

Fig. 7.11: Illustration of the proof for Thm. 7.10.

The number of vertices is given by $n = n_1 + n_2 + 2$. Since Γ contains at most four edges more than $m_1 + m_2$ (the edges $(u_h, w_{h'})$, $(u_h, w_{h'+1})$, $(u_{h+1}, w_{h'})$, and $(u_{h+1}, w_{h'+1})$), and since there are no edges between Γ_1 and Γ_2, we obtain $m \leq m_1 + m_2 + 4$. This yields

$$m \leq \left(\tfrac{4}{3}n_1 - \tfrac{4}{3}\right) + \left(\tfrac{4}{3}n_2 - \tfrac{4}{3}\right) + 4 = \tfrac{4}{3}(n_1 + n_2) + \tfrac{4}{3} = \tfrac{4}{3}(n-2) + \tfrac{4}{3} = \tfrac{4}{3}n - \tfrac{4}{3}. \quad \square$$

Combining the results of this section, that is Thms. 7.7, 7.9 and 7.10, we obtain that $\frac{5}{4}n - 1$ is a tight upper bound for the number of edges in 2-layer IC-planar graphs, while $\frac{4}{3}n - \frac{4}{3}$ is the corresponding tight upper bound for the number of edges in 2-layer NIC-planar graphs.

7.4 Density of 2-Layer k-Planar Graphs

In this section we study k-planar graphs on 2-layers, in particular their edge density. For $k \in \{2, \ldots, 5\}$ we give tight bounds on the maximum number of edges in such graphs. Additionally, we provide a lower bound for the number of edges in optimal 2-layer 6-planar graphs.

7.4.1 2-planar graphs

First we consider the class of 2-layer 2-planar graphs $\mathcal{P}_2^{=}$. To this end, let Γ be a $\mathcal{P}_2^{=}$-drawing. We start by giving a lower bound construction for the class $\mathcal{P}_2^{=}$.

Theorem 7.11. *For infinitely many n there is a $\mathcal{P}_2^{=}$-graph on n vertices with $\frac{5}{3}n - \frac{7}{3}$ edges.*

Proof. Consider the family of graphs defined in Fig. 7.12, which consist of $t > 0$ bricks, such that each of them represents a graph $K_{2,3}$ and consecutive bricks share a planar edge. Then the number of vertices is $n = 2 + 3t$, while the number of edges is

$$m = 1 + 5t = 1 + \tfrac{5}{3}(n-2) = \tfrac{5}{3}n - \tfrac{7}{3}. \quad \square$$

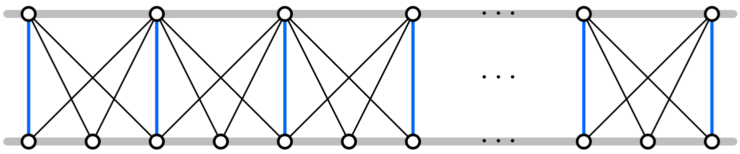

Fig. 7.12: A family of 2-layer 2-planar graphs with $n = 2a$ vertices and $\frac{5}{3}n - \frac{7}{3}$ edges.

We aim at proving that $\frac{5}{3}n - \frac{7}{3}$ is also the upper bound for the number of edges in 2-layer 2-planar graphs. In this direction, we start with an auxiliary lemma.

Lemma 7.12. *Let* $\mathbf{B} = [\ell, r \mid \ell', r']$ *be a brick in a* $\mathcal{P}_2^=$*-drawing* Γ. *Then one of the following properties holds:*

(i) The brick $\mathbf{B}$ *contains only two vertices on the top layer, or only two vertices on the bottom layer, i. e.* $r = \ell + 1$ *or* $r' = \ell' + 1$.

(ii) There exists a vertex in $\mathbf{B}$ *with degree one.*

(iii) There exists a non-planar edge e *in* $\mathbf{B}$ *such that removing* e *and adding one of the edges* $(u_\ell, w_{\ell'+1})$, $(u_{\ell+1}, w_{\ell'})$, *or* $(u_{\ell+1}, w_{\ell'+1})$ *(in a crossing free way), yields a* $\mathcal{P}_2^=$*-drawing* Γ', *where* $[\ell, r \mid \ell', r']$ *is subdivided into two bricks; one of the bricks is* $[\ell, \ell+1 \mid \ell', \ell']$, $[\ell, \ell \mid \ell', \ell'+1]$, *or* $[\ell, \ell+1 \mid \ell', \ell'+1]$.

(iv) The edge $(u_{\ell+2}, w_{\ell'+1})$ *or the edge* $(u_{\ell+1}, w_{\ell'+2})$ *can be added crossing-free to* Γ*; this subdivides* $\mathbf{B}$ *into two smaller bricks, one of which is a* $K_{2,3}$ *brick.*

Proof. If $r = \ell + 1$ or $r' = \ell' + 1$ the statement follows immediately. On the other hand, if $r = \ell$ (or $r' = \ell'$), then $\mathbf{B}$ is a star and we have $r' = \ell' + 1$ by the properties of a brick. Hence we assume $r > \ell + 1$ and $r' > \ell' + 1$. We consider three cases.

First assume that neither $(u_\ell, w_{\ell'+1})$ nor $(u_{\ell+1}, w_{\ell'})$ belongs to E (see dashed red edges in Fig. 7.13a). If u_ℓ is incident to only one single edge $e = (u_\ell, w_{i'})$ for $\ell' + 1 < i' \leq r'$ (see green edge in Fig. 7.13a), we obtain a drawing Γ' by removing e from Γ and adding the edge $(u_{\ell+1}, w_{\ell'})$, which is then planar; i. e. $[\ell, r \mid \ell', r']$ is subdivided into the two bricks $[\ell, \ell+1 \mid \ell', \ell']$ and $[\ell+1, r \mid \ell', r']$. A symmetric argument holds if $w_{\ell'}$ is incident to only one edge $(u_i, w_{\ell'})$ for $\ell + 1 < i \leq r$. On the other hand, if both, u_ℓ and $w_{\ell'}$, are incident to two such edges, that is, if there are edges $(u_\ell, w_{i'})$ and $(u_\ell, w_{j'})$ for $\ell' + 1 < i' < j' \leq r'$, and $(u_i, w_{\ell'})$ and $(u_j, w_{\ell'})$ for $\ell + 1 < i < j \leq r$ (see Fig. 7.13b), we observe that $u_{\ell+1}$ and $w_{\ell'+1}$ are both inside regions bounded by two edges that are crossed twice. Hence $u_{\ell+1}$ and $w_{\ell'+1}$ are isolated (degree-0) vertices, contradicting the connectivity of G.

Secondly, consider the case where exactly one of the edges $(u_\ell, w_{\ell'+1})$ and $(u_{\ell+1}, w_{\ell'})$ belongs to E, say $(u_\ell, w_{\ell'+1}) \in E$ (see solid and dashed red edges in Fig. 7.13c). If u_ℓ is not incident to any edge $(u_\ell, w_{i'})$ for $\ell' + 1 < i' \leq r'$, we obtain Γ' by removing

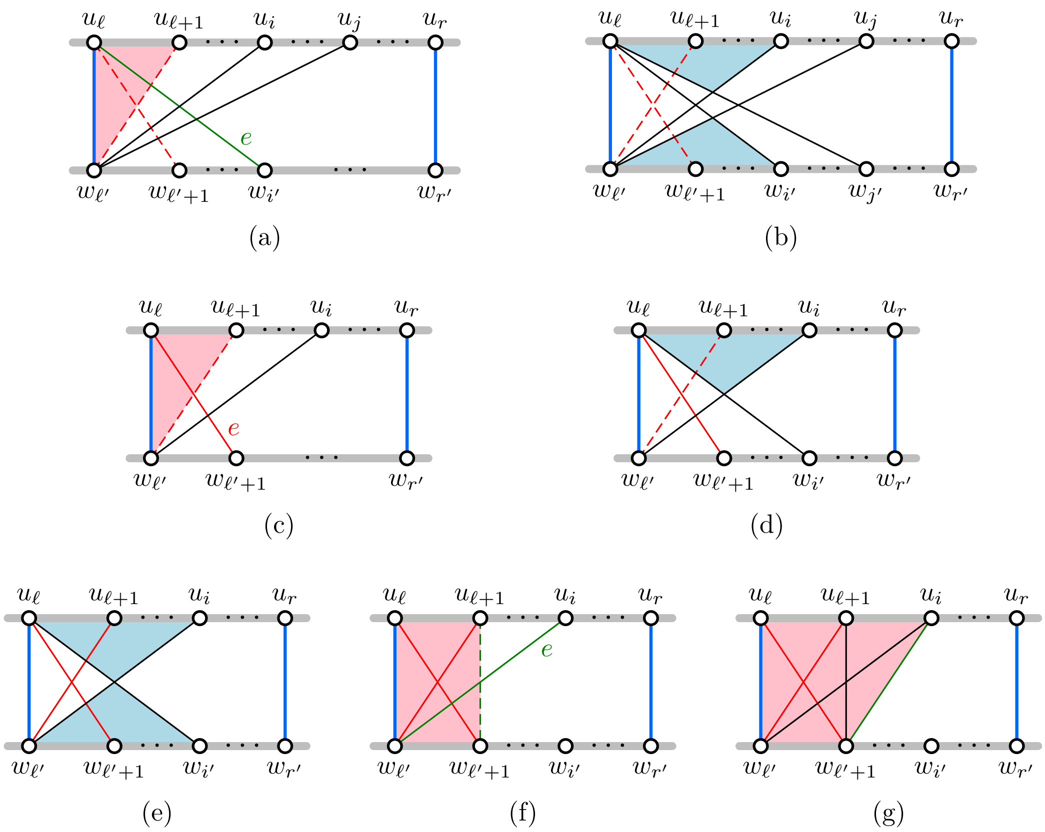

Fig. 7.13: Illustrations for the proof of Lemma 7.12. (a) First case: u_ℓ is incident to only one edge $(u_\ell, w_{i'})$, $\ell' < i' \leq r'$. (b) First case: the vertices u_ℓ and $w_{\ell'}$ are isolated. (c) Second case: u_ℓ is not incident to an edge $(u_\ell, w_{i'})$, $\ell'+1 < i' \leq r'$. (d) Second case: exactly one of $(u_{\ell+1}, w_{\ell'})$ and $(u_\ell, w_{\ell'+1})$ is in E. (e) Third case: both edges $(u_\ell, w_{i'})$ and $(u_i, w_{\ell'})$ are in E. (f) and (g) Third case: edge $(u_i, w_{\ell'})$ is in E and $(u_\ell, w_{i'})$ not.

$e = (u_\ell, w_{\ell'+1})$ and adding the – then planar – edge $(u_{\ell+1}, w_{\ell'})$; this yields a brick $[\ell, \ell+1 \mid \ell']$. Otherwise an edge $(u_\ell, w_{i'})$ is part of Γ, where $\ell'+1 < i' \leq r'$ (see Fig. 7.13d). By the properties of a brick, edge $(u_\ell, w_{\ell'+1})$ is not planar, which implies that there is also an edge $(u_i, w_{\ell'})$ in E, where $\ell+1 < i \leq r$. Since this edge is crossing both, $(u_\ell, w_{\ell'+1})$ and $(u_\ell, w_{i'})$, the vertex $u_{\ell+1}$ cannot have any edges incident to it without violating 2-planarity and is therefore isolated – again a contradiction.

Finally we assume that both edges $(u_\ell, w_{\ell'+1})$ and $(u_{\ell+1}, w_{\ell'})$ are in E (see solid red edges in Fig. 7.13e). Then, due to 2-planarity, vertex u_ℓ can be incident to at most one more edge $(u_\ell, w_{i'})$ with $\ell'+1 < i' \leq r'$. Also $w_{\ell'}$ can be incident to at most one more edge $(u_i, w_{\ell'})$ with $\ell+1 < i \leq r$.

– Suppose that both edges $(u_\ell, w_{i'})$ and $(u_i, w_{\ell'})$ are in E. In this case the vertices $u_{\ell+1}$ and $w_{\ell'+1}$ are located inside regions that are bounded by two edges with two crossings (refer to the blue areas in Fig. 7.13e). Thus, each of these vertices is incident to only one edge, namely to $(u_{\ell+1}, w_{\ell'})$ and $(u_\ell, w_{\ell'+1})$, respectively, implying that $u_{\ell+1}$ and $w_{\ell'+1}$ are degree-1 vertices.

– Now suppose that only one of the edges $(u_\ell, w_{i'})$ and $(u_i, w_{\ell'})$ in in E, say $(u_i, w_{\ell'})$ (green edge in Fig. 7.13f). If $(u_{\ell+1}, w_{\ell'+1})$ does not belong to E, we replace $e = (u_i, w_{\ell'})$ by it and obtain a smaller brick $[\ell, \ell+1 \mid \ell', \ell'+1]$ (see red area in Fig. 7.13f).

  On the other hand, if $(u_{\ell+1}, w_{\ell'+1})$ already belongs to E, the edge $(u_i, w_{\ell'})$ is crossed twice. Hence, Γ contains no edge $(u_{\ell+1}, w_{j'})$, where $j' > \ell' + 1$, and – since G is connected – we have $i = \ell + 2$. As a consequence it is possible to add the planar edge $(u_i, w_{\ell'+1})$ to Γ (by the assumption $r > \ell + 1$, $r' > \ell' + 1$, and the properties of $\mathbf{B} = [\ell, r \mid \ell', r']$ it is not yet in Γ). This yields a smaller brick $[\ell, \ell+2 \mid \ell', \ell'+1]$ corresponding to a graph $K_{2,3}$ (see Fig. 7.13g). □

Note that Properties iii and iv of Lemma 7.12 imply that Γ' has the same vertices as Γ and also the same number of edges. However, the drawing Γ' has more planar edges and might not be maximal – even if Γ is maximal.

By the fact that there is a unique[6] 2-layer drawing (up to isomorphism) of $K_{3,3}$ and of $K_{2,4}$ (see Fig. 7.14a and Fig. 7.14b), we observe the following.

Observation 7.13. *The bipartite graphs $K_{3,3}$ and $K_{2,4}$ are not 2-layer 2-planar.*

(a) (b)

Fig. 7.14: (a) Unique 2-layer drawing of $K_{3,3}$. (b) Unique 2-layer drawing of $K_{2,4}$. In both drawings the red edges have more than 2 crossing, which violates 2-planarity.

The following lemma, together with Lemma 7.12, are main ingredients for proving an upper bound for the number of edges in 2-layer 2-planar graphs, and for a characterization of corresponding optimal graphs.

Lemma 7.14. *Let Γ be an optimal 2-layer 2-planar drawing and $\mathbf{B} = [\ell, \ell+1 \mid \ell', r']$ a brick. Then either $r' \leq \ell' + 2$, or there is a vertex $w_{i'}$ with $\ell' < i' < r'$ of degree at most one.*

[6] Whenever we speak of “unique” 2-layer drawings, we assume implicitly that edges are represented as a single Jordan curve, i. e. there are no bundles and no gaps allowed; otherwise the drawings might not be unique.

Proof. If $r' \leq \ell' + 2$ the lemma follows directly from the fact that $K_{2,3}$ is 2-layer 2-planar.

Otherwise there are at least four vertices $w_{\ell'}, \dots, w_{r'}$ on the bottom layer. By the definition of a brick, the edges $(u_\ell, w_{\ell'})$ and $(u_{\ell+1}, w_{r'})$ must be in E and drawn crossing free (blue edges in Fig. 7.15). So each vertex $w_{\ell'+1}, \dots, w_{r'-1}$ is only adjacent to u_ℓ or $u_{\ell+1}$. Further note that both edges $(u_\ell, w_{r'})$ and $(u_{\ell+1}, w_{\ell'})$ must be in E (solid black edges in Fig. 7.15), otherwise the – then planar – edges $(u_{\ell+1}, w_{r'-1})$ or $(u_\ell, w_{\ell+1})$ are part of Γ by optimality, contradicting the definition of a brick. Since Γ cannot contain a $K_{2,4}$-subdrawing (refer to Obs. 7.13), at least one of the vertices $w_{\ell'+1}$ or $w_{r'-1}$ has a degree smaller than two. □

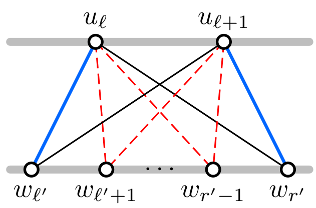

Fig. 7.15: Illustration for the proof of Lemma 7.14.

In the next theorem we prove an upper bound for the maximal number of edges in a 2-layer 2-planar graph.

Theorem 7.15. *Any 2-layer 2-planar graph on $n \geq 2$ vertices has at most $\frac{5}{3}n - \frac{7}{3}$ edges.*

Proof. Let G be an optimal 2-layer 2-planar graph and Γ a corresponding drawing. By optimality, the edges (u_1, w_1) and (u_a, w_b) are part of Γ.

First consider the case were G is a star, that is $G = K_{1,b}$. Then G is 2-layer planar and has exactly $m = n - 1$ edges, yielding $m = n - 1 < \frac{5}{3}n - \frac{7}{3}$ for $n > 2$ and $m = \frac{5}{3}n - \frac{7}{3}$ for $n = 2$. In the following we assume that G is not a star.

We use induction on the number of vertices. For $n \in \{2, 3\}$ graph G is a star. For $n = 4$ consider the graph $K_{2,2}$, which provides an upper bound on the number of edges of $m \leq 4 < \frac{5}{3}n - \frac{7}{3}$. Similarly, for $n = 5$ the graph $K_{2,3}$ provides the upper bound $m \leq 6 \leq \frac{5}{3}n - \frac{7}{3}$.

Assume now that Γ is a 2-layer 2-planar drawing with $n > 5$ vertices.

Suppose that Γ contains a planar edge $(u_i, w_{i'})$, where $(i, i') \notin \{(1, 1), (a, b)\}$. Let $\Gamma_1 := [1, i \mid 1, i']$ and $\Gamma_2 := [i, a \mid i', b]$; further, for $i = 1, 2$, let n_i and m_i be the number of vertices and edges of Γ_i. Then we have $n = n_1 + n_2 - 2$ and, since $(u_i, w_{i'})$

is shared by Γ_1 and Γ_2, $m = m_1 + m_2 - 1$. By induction we obtain

$$m \leq \tfrac{5}{3}n_1 - \tfrac{7}{3} + \tfrac{5}{3}n_2 - \tfrac{7}{3} - 1 = \tfrac{5}{3}(n+2) - \tfrac{7}{3} - \tfrac{10}{3} = \tfrac{5}{3}n - \tfrac{7}{3}.$$

On the other hand, if Γ contains no planar edge $(u_i, w_{i'})$ except (u_1, w_1) and (u_a, w_b), then Γ is a maximal brick. If Γ has a degree-1 vertex v, consider the subdrawing $\Gamma[V \setminus \{v\}]$ with $n^\star = n - 1$ vertices and $m^\star = m - 1$ edges. Inductively we obtain

$$m = m^\star + 1 \leq \tfrac{5}{3}n^\star - \tfrac{7}{3} + 1 = \tfrac{5}{3}n - \tfrac{5}{3} - \tfrac{7}{3} + 1 < \tfrac{5}{3}n - \tfrac{7}{3}.$$

Assume now that Γ has no degree-1 vertex. Then Lemma 7.14 and the assumption $n > 5$ implies $a > 2$ and $b > 2$. Thus, Properties i and ii of Lemma 7.12 do not hold; observe that, by optimality of Γ, Property iv does not hold as well. Consequently, by Property iii, there is a drawing Γ' with n vertices and m edges, consisting of two bricks $\mathbf{B}_1$, $\mathbf{B}_2$; moreover, one of the bricks, say $\mathbf{B}_1$, is $[1,2 \mid 1,1]$, $[1,1 \mid 1,2]$, or $[1,2 \mid 1,2]$ (here the indexes correspond to drawing Γ'). For $i = 1, 2$, let n'_i and m'_i be the number of vertices and edges of $\mathbf{B}_i$ If $\mathbf{B}_1 = [1,2 \mid 1,1]$, or $\mathbf{B}_1 = [1,1 \mid 1,2]$, vertex u_1 or w_1, respectively has degree 1; we already showed that the upper bound holds in this case. Otherwise $\mathbf{B}_1 = [1,2 \mid 1,2]$, $n'_1 = 4$, $m'_1 = 4$, and $n'_2 = n - 2$. By induction we obtain

$$m \leq m'_1 + m'_2 - 1 \leq 4 + \tfrac{5}{3}n'_2 - \tfrac{7}{3} - 1 = 3 + \tfrac{5}{3}(n-2) - \tfrac{7}{3} = \tfrac{5}{3}n - \tfrac{7}{3} - \tfrac{1}{3} < \tfrac{5}{3}n - \tfrac{7}{3}. \qquad \square$$

A close inspection of the proof for Thm. 7.15 yields a characterization for optimal 2-layer 2-planar graphs.

Theorem 7.16. *For $n > 2$ a 2-layer 2-planar graph is optimal if and only if it is a sequence of copies of $K_{2,3}$, such that consecutive $K_{2,3}$-graphs are merged at one planar edge.*

Proof. Clearly a sequence of $K_{2,3}$ bricks is optimal; refer also to Thm. 7.11.

Assume now that G is an optimal 2-layer 2-planar graph and Γ is a corresponding drawing of G. Then Γ is maximal. The optimality of Γ implies the optimality of each brick of Γ. So it suffices to consider a brick Γ. The proof of Thm. 7.15 shows the following:

– Brick Γ is no star (hence $a > 1$ and $b > 1$);

– it has no degree-1 vertices;

– it must contain two vertices on the top layer, or two vertices on the bottom layer (otherwise there is a drawing with the same number of vertices and edges containing a $K_{2,2}$ brick, which yields less edges than $\frac{5}{3}n - \frac{7}{3}$).

This implies that Γ represents a graph $K_{2,b}$ for some $b \geq 2$. The proof of Thm. 7.15 excludes the case $b = 2$, and Lemma 7.14 excludes $b > 3$. The statement follows. □

We conclude our study of 2-layer 2-planar graphs by pointing out that not every maximal $\mathcal{P}_2^{=}$-drawing is optimal; Fig. 7.16 shows a counterexample, i.e., a $\mathcal{P}_2^{=}$-drawing which is maximal and consists of only one brick that is not a $K_{2,3}$-drawing, and is hence not optimal. Note that it has $n + 1$ edges.

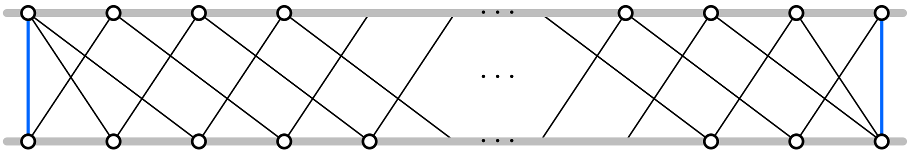

Fig. 7.16: A maximal $\mathcal{P}_2^{=}$-drawing that is not optimal.

7.4.2 3-planar graphs

In this section we give a tight bound for 2-layer 3-planar graphs. We start with a lower bound construction.

Theorem 7.17. *For infinitely many n there is a $\mathcal{P}_3^{=}$-graph on n vertices with $2n-4$ edges.*

Proof. The quasi-planar family of graphs defined in Thm. 7.3, which has $2n - 4$ edges, is also 2-layer 3-planar; refer also to Fig. 7.17. □

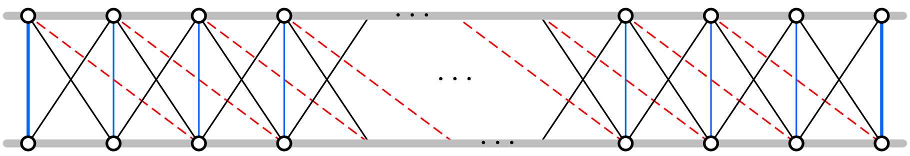

Fig. 7.17: A family of 3-planar graphs with $n = 2a$ vertices and $2n - 4$ edges.

The following lemma is a key ingredient to prove a corresponding upper bound for 2-layer 3-planar graphs.

Lemma 7.18. *For* $1 \le h < i < j \le a$ *and* $1 \le h' < i' < j' \le b$*, let* $(u_h, w_{j'})$*,* $(u_i, w_{i'})$ *and* $(u_j, w_{h'})$ *be a triple of pairwise crossing edges in a 2-layer 3-planar drawing* Γ*. Then the number of edges adjacent to* $(u_i, w_{i'})$ *is at most* 2*.*

Proof. Consider the triple of edges defined in the lemma; for an illustration see Fig. 7.18. If u_i has an edge to a vertex $w \ne w_{i'}$, then the edge (u_i, w) intersects $(u_h, w_{j'})$ or $(u_j, w_{h'})$ (see dashed red edge in Fig. 7.18). The same is true if $w_{i'}$ is connected to a vertex $u \ne u_i$. Since the triple of crossing edges yields two crossings for each of $(u_h, w_{j'})$ and $(u_j, w_{h'})$, the edge $(u_i, w_{i'})$ can be adjacent to at most two edges. □

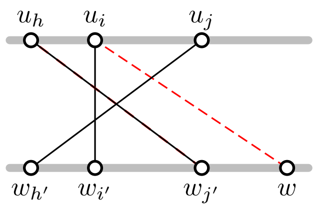

Fig. 7.18: A triple of pairwise intersecting edges in a 2-layer 3-planar drawing.

Now we provide the mentioned upper bound on the maximal number of edges in 2-layer 3-planar graphs.

Theorem 7.19. *Any 2-layer* 3*-planar graph* G *on* $n \ge 3$ *vertices has at most* $2n-4$ *edges. Moreover, optimal 2-layer* 3*-planar graphs are also 2-layer quasi-planar.*

Proof. Consider a $\mathcal{P}_3^{=}$-drawing Γ of G. We show the statement with induction on the number of triples of pairwise crossing edges. If there is no such triple, Γ is quasi-planar and hence has at most $2n-4$ edges for $n \ge 3$ by Thm. 7.4.

Assume now that $(u_h, w_{j'})$, $(u_i, w_{i'})$ and $(u_j, w_{h'})$ is a triple of pairwise crossing edges in Γ for some $1 \le h < i < j \le a$ and $1 \le h' < i' < j' \le b$. Lemma 7.18 implies that $(u_i, w_{i'})$ is adjacent to at most two edges. Let Γ' be the drawing obtained from Γ by removing u_i and $w_{i'}$. Then Γ' has $n' = n-2$ vertices and $m' \ge m-3$ edges. By induction we obtain $m' \le 2n'-4$, and consequently

$$m \le m' + 3 \le (2n'-4) + 3 = 2(n-2) - 1 = 2n-4-1 < 2n-4.$$

In particular, a $\mathcal{P}_3^{=}$-drawing with three mutually crossing edges is not optimal. □

7.4.3 4-planar graphs

We follow the approach from Sec. 7.4.2 and start with a lower bound on the number of edges for 2-layer 4-planar graphs.

Theorem 7.20. *For infinitely many n there exists a $\mathcal{P}_4^{=}$-graph on n vertices with $2n-3$ edges.*

Proof. We describe a family of drawings with $n = 2a$ vertices, where each layer has $a = b$ vertices; for an illustration refer to Fig. 7.19. Each drawing Γ consists of a sequence $\mathbf{B}_1, \ldots, \mathbf{B}_t$ of $K_{3,3}$-bricks such that $\mathbf{B}_i$ and $\mathbf{B}_{i+1}$ share a planar edge for $1 \le i \le t-1$.

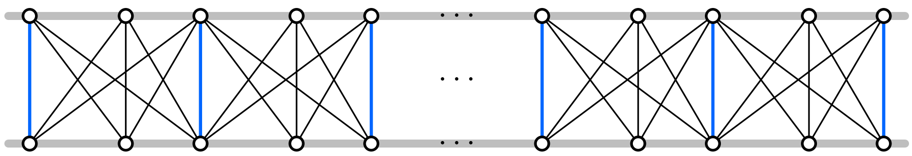

Fig. 7.19: A family of $\mathcal{P}_4^{=}$-graphs with $n = 2a$ vertices and $2n-3$ edges.

Since $K_{3,3}$ has a total of 9 edges and since consecutive bricks share one edge, drawing Γ, which consists of t such bricks, has $m = 8t+1$ edges. Further, as a brick has 6 vertices, Γ has $n = 4t+2$ vertices. It follows that $t = \frac{1}{4}(n-2)$ and therefore $m = 8 \cdot \frac{1}{4}(n-2) + 1 = 2n-3$. □

In the following we show that $2n-3$ is also an upper bound for the number of edges in 2-layer 4-planar graphs. We begin with two auxiliary lemmas.

Lemma 7.21. *Let Γ be a 2-layer 4-planar drawing with the following properties:*

(i) There is a triple of pairwise crossing edges $(u_h, w_{j'})$, $(u_i, w_{i'})$ and $(u_j, w_{h'})$ in Γ for some $1 \le h < i < j \le a$ and $1 \le h' < i' < j' \le b$;

(ii) there is a vertex $u_x \in U$ such that $h < x < j$ and $x \neq i$, or a vertex $w_{x'} \in W$ such that $h' < x' < j'$ and $x' \neq i'$.

Let Γ' be the subdrawing of Γ obtained by deleting u_i, $w_{i'}$, u_x, $w_{x'}$ (if present in Γ), and their incident edges. If Γ' has at most $2n'-3$ edges, where n' is the number of vertices in Γ', then Γ has at most $2n-3$ edges.

Proof. Let Γ and Γ' be as described in the lemma.

We assume that there is a vertex u_x in Γ such that $h < x < j$ and $x \neq i$ (see Fig. 7.20 for an illustration of Γ). Each of the edges $(u_h, w_{j'})$ and $(u_j, w_{h'})$ has two

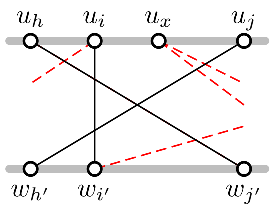

Fig. 7.20: The configuration when there exists a vertex $u_x \neq u_i$ between u_h and u_j in Γ.

crossings from the triple of pairwise crossing edges, so each of them can only be intersected by two more edges. Hence, there are at most five edges incident to the vertices u_i, u_x and $w_{i'}$ in Γ (including the edge $(u_i, w_{i'})$; see e. g. the dashed red edges in Fig. 7.20). So for the number of edges m' in Γ' the inequality $m' \geq m - 5$ holds, and we have also $n' = n - 3$. This implies

$$m \leq m' + 5 \leq 2n' - 3 + 5 = 2(n-3) - 3 + 5 = 2n - 3 - 1 < 2n - 3.$$

The case where only $w_{x'}$ is in Γ is symmetric, and the case where both vertices u_x and $w_{x'}$ are in Γ yields $m \leq 2n-3-3 < 2n-3$. The statement of the lemma follows.[7] □

In order to prove an upper bound for 2-layer 4-planar graphs, we know from Lemma 7.21 that it is sufficient to consider only drawings where in each triple of pairwise crossing edges $(u_h, w_{j'})$, $(u_i, w_{i'})$ and $(u_j, w_{h'})$ the vertices u_h, u_i and u_j are consecutive, as well as the vertices $w_{h'}$, $w_{i'}$ and $w_{j'}$. So we assume in the following that all 2-layer 4-planar drawings have this property, and call it the *triple-crossing property*. It is essential for proving the following lemma.

Lemma 7.22. *Let Γ be a 2-layer 4-planar drawing with the triple-crossing property, such that edges $(u_h, w_{h'+2})$, $(u_{h+1}, w_{h'+1})$ and $(u_{h+2}, w_{h'})$ form a triple of mutually crossing edges for some $1 \leq h \leq a$ and $1 \leq h' \leq b$. Further let Γ_1 be the snippet $[1, h \mid 1, h']$, and Γ_2 the snippet $[h+2, a \mid h'+2, b]$. Then the only edges of Γ not belonging to Γ_1 or Γ_2 are $(u_h, w_{h'+2})$, $(u_{h+2}, w_{h'})$, and all edges incident to the vertices u_{h+1} or $w_{h'+1}$.*

Proof. Assume to the contrary that Γ_1 and Γ_2 are not only connected by $(u_h, w_{h'+2})$, $(u_{h+2}, w_{h'})$, or edges incident to u_{h+1} or $w_{h'+1}$. Then there is an edge $(u_x, w_{x'}) \neq (u_h, w_{h'+2})$ such that $1 \leq x \leq h$ and $h' + 2 \leq x' \leq b$. This edge intersects $(u_{h+1}, w_{h'+1})$, and at least one of the edges $(u_h, w_{h'+2})$ or $(u_{h+2}, w_{h'})$, say $(u_{h+2}, w_{h'})$. Thus, $(u_x, w_{x'})$, $(u_{h+2}, w_{h'})$ and $(u_i, w_{i'})$ form a triple of pairwise crossing edges with

[7] Note that the proof of Lemma 7.21 shows even more: Every 2-layer 4-planar drawing with three mutually crossing edges that also fulfills Property ii, cannot be optimal regarding the edge density.

$u_x \prec u_h \prec u_{h+1} \prec u_{h+2}$ (for an illustration see Fig. 7.21); this is a contradiction to the triple-crossing property. □

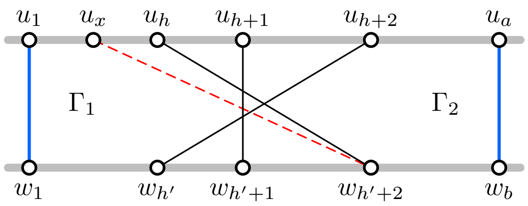

Fig. 7.21: The situation with a vertex u_x between u_1 and u_h, and an edge $(u_x, w_{h'+2})$; note that $w_{x'} = w_{h'+2}$ in this figure.

Now we have the means to prove the tight upper bound on the number of edges for 2-layer 4-planar graphs.

Theorem 7.23. *Any 2-layer 4-planar graph on n vertices has at most $2n-3$ edges.*

Proof. Let Γ be a $\mathcal{P}_4^{=}$-drawing on n vertices. As already mentioned, we can assume without loss of generality that Γ has the triple-crossing property.

We prove the statement by induction on the number of triples of pairwise crossing edges. If Γ has no such triple, then it is quasi-planar and has therefore at most $2n-4$ edges if $n \geq 3$, and at most $1 = 2n-3$ edges for $n = 2$.

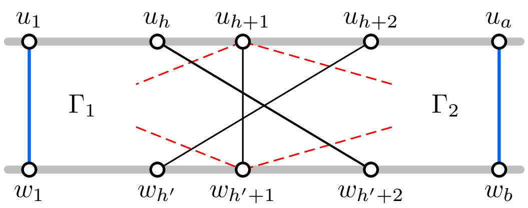

Fig. 7.22: A triple of pairwise crossing edges "separates" a $\mathcal{P}_4^{=}$-drawing.

For the induction step, we assume that Γ has a triple of pairwise crossing edges $(u_h, w_{h'+2})$, $(u_{h+1}, w_{h'+1})$ and $(u_{h+2}, w_{h'})$ for some $1 \leq h \leq a$ and $1 \leq h' \leq b$. Further let $\Gamma_1 = [1, h \mid 1, h']$ and $\Gamma_2 = [h+2, a \mid h'+2, b]$ be snippets of Γ. Then both subdrawings of Γ are only connected by $(u_h, w_{h'+2})$, $(u_{h+2}, w_{h'})$ and possibly edges incident to u_{h+1} or $w_{h'+1}$, as stated in Lemma 7.22 (see also Fig. 7.22). By 4-planarity, we deduce that u_{h+1} and $w_{h'+1}$ together are incident to at most 5 edges, including the edge $(u_{h+1}, w_{h'+1})$.

For $i = 1, 2$ let n_i and m_i denote the number of vertices and edges, respectively, in Γ_i. Clearly, each of these snippets have less triples of pairwise crossing edges than Γ, so we obtain $m_i \leq 2n_i - 3$ by induction. Further we observe that $n = n_1 + n_2 + 2$

and $m \leq m_1 + m_2 + 7$. We conclude that Γ has at most

$$m \leq (2n_1 - 3) + (2n_2 - 3) + 7 = 2(n_1 + n_2) + 1 = 2(n - 2) + 1 = 2n - 3$$

edges. □

Reading the proof of Thm. 7.23 carefully, we observe that Γ is optimal, if and only if the subdrawings Γ_1 and Γ_2 are optimal (that is $m_1 = 2n_1 - 3$ and $m_2 = 2n_2 - 3$), and if there are exactly four edges adjacent to $(u_{h+1}, w_{h'+1})$ (that is $m = m_1+m_2+7$). We use this observation to conclude our study of 2-layer 4-planar graphs by showing a characterization for optimal $\mathcal{P}_4^=$-graphs.

Theorem 7.24. *A graph is an optimal $\mathcal{P}_4^=$-graph if and only if*

(a) it has $n = 2$ vertices $u \in U$ and $w \in W$, and an edge (u, w), or

(b) it has $n \geq 3$ vertices and consist of a series $G_1, \ldots, G_t$ of subgraphs $K_{3,3}$, such that

- *G_i and G_{i+1} (where $1 \leq i < t$) share exactly one edge (u, w), and*
- *the edge shared between G_i and G_{i-1} (where $1 < i < t$) is not incident to one of the vertices u or w.*

Proof. Clearly each graph consisting of a series of $K_{3,3}$ is optimal, refer to Thms. 7.20 and 7.23.

Assume now that Γ is a drawing of an optimal 2-layer 4-planar graph. Then Γ has $2n - 3$ edges. Like in the proof of Thm. 7.23, we use induction on the number of triples of pairwise crossing edges. If Γ has no such triple, then it is quasi-planar and can only be optimal if $a = b = 1$ and if it has an edge (u_1, w_1), otherwise the number of edges is less than $2n - 3$.

For the induction step we assume that Γ has a triple of pairwise crossing edges $(u_h, w_{h'+2})$, $(u_{h+1}, w_{h'+1})$ and $(u_{h+2}, w_{h'})$ for some $1 \leq h \leq a$ and $1 \leq h' \leq b$ (the vertices of the triple are consecutive by the proof of Lemma 7.21; the triple of crossing edges is colored green in Fig. 7.23).

Consider the snippets $\Gamma_1 = [1, h \mid 1, h']$ and $\Gamma_2 = [h + 2, a \mid h' + 2, b]$. For $i = 1, 2$ let n_i and m_i be the number of vertices edges in Γ_i. Since Γ is optimal we have $m_i = 2n_i - 3$ (see the note before this theorem). Therefore Γ_1 and Γ_2 are also optimal. Thus, by induction each drawing Γ_1 and Γ_2 consists of a series of graphs $K_{3,3}$ (or of a single edge if $h = h' = 1$, or if $h + 2 = a$ and $h' + 2 = b$).

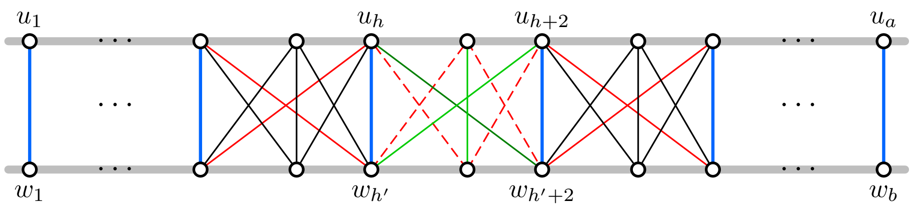

Fig. 7.23: Illustration of the proof for Thm. 7.24.

Observe that either $h = h' = 1$, or both edges $(u_{h-2}, w_{h'})$ and $(u_h, w_{h'-2})$ of Γ_1 are crossed already four times (see solid red edges in Fig. 7.23). So, if there is an edge from u_{h+1} or $w_{h'+1}$ to a vertex in Γ_1, it must be to $w_{h'}$ or to u_h, respectively. Similarly, if there is an edge from u_{h+1} or $w_{h'+1}$ to a vertex in Γ_2, it must be incident to $w_{h'+2}$ or to u_{h+2}, respectively. The optimality of Γ implies that there are exactly four edges adjacent to $(u_{h+1}, w_{h'+1})$, yielding the four edges $(u_h, w_{h'+1})$, $(u_{h+2}, w_{h'+1})$, $(u_{h+1}, w_{h'})$, and $(u_{h+1}, w_{h'+2})$. The statement follows. □

7.4.4 5-planar graphs

Again we start by providing a lower bound on the maximal number of edges.

Theorem 7.25. *For infinitely many n there exists a 2-layer 5-planar graph on n vertices with $\frac{9}{4}n - \frac{9}{2}$ edges.*

Proof. Consider the lower bound construction Γ from Thm. 7.20 for 2-layer 4-planar graphs, consisting of a sequence of $K_{3,3}$-bricks $\mathbf{B}_1, \dots, \mathbf{B}_t$ such that consecutive bricks share a planar edge. Recall that Γ has $n = 4t + 2$ vertices and $m = 8t + 1 = 2n - 3$ edges. We augment Γ to a 5-planar drawing Γ' by adding a path p of length $t - 1$. More precisely, for i odd, where $1 \leq i \leq t - 1$, we add an edge between the middle vertex on the top layer of $\mathbf{B}_i$ and the middle vertex on the bottom layer of $\mathbf{B}_{i+1}$; for i even, where $1 \leq i \leq t - 1$, we add an edge between the middle vertex on the bottom layer of $\mathbf{B}_i$ and the middle vertex on the top layer of $\mathbf{B}_{i+1}$ (refer to the dashed red edges in Fig. 7.24). Then Γ' still has $n = 4t+2$ vertices, but the number of edges is now $m = 8t + 1 + (t - 1) = 9t$, yielding $m = \frac{9}{4}n - \frac{9}{2}$ edges for Γ'. The drawing Γ' is 5-planar: By construction, no two different edges of p cross the same edge of Γ, hence the original edges of Γ have at most one additional crossing in Γ' (which is a crossing with an edge of p); also by construction, every edge of p has exactly 5 crossings. The statement follows. □

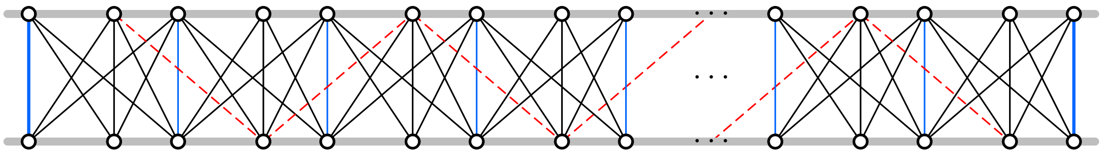

Fig. 7.24: A family of 5-planar graphs with $n = 2a$ vertices and $\frac{9}{4}n - \frac{9}{2}$ edges.

In order to establish $\frac{9}{4}n - \frac{9}{2}$ as a tight upper bound for the number of edges in $\mathcal{P}_5^=$ (as we will see later with the exception of $n = 2, 8$), we first prove a few auxiliary lemmas.

Lemma 7.26. *Let $\Gamma \in \mathcal{P}_5^=$ be a 2-layer 5-planar drawing with the following properties:*

(i) There is a triple of pairwise crossing edges $(u_h, w_{j'})$, $(u_i, w_{i'})$ and $(u_j, w_{h'})$ in Γ for some $1 \leq h < i < j \leq a$ and $1 \leq h' < i' < j' \leq b$;

(ii) there are two vertices $u_x, u_y \in U \setminus \{u_i\}$ such that $h < x < y < j$, or two vertices $w_{x'}, w_{y'} \in W \setminus \{w_{i'}\}$ such that $h' < x' < y' < j'$, or a vertex $u_x \in U \setminus \{u_i\}$ and a vertex $w_{x'} \in W \setminus \{w_{i'}\}$ such that $h < x < j$ and $h' < x' < j'$.

Let Γ' be the subdrawing of Γ obtained by deleting u_i, $w_{i'}$, u_x, u_y, $w_{x'}$, $w_{y'}$ (if present in Γ), and their incident edges. If Γ' has at most $\frac{9}{4}n' - \frac{9}{2}$ edges, where n' is the number of vertices in Γ', then Γ has at most $\frac{9}{4}n - \frac{9}{2}$ edges.

Moreover, if Γ' has $n' = 8$ vertices and 14 edges, then Γ also has not more than $\frac{9}{4}n - \frac{9}{2}$ edges (Note that $14 > \frac{9}{4}n' - \frac{9}{2}$ for $n' = 8$).

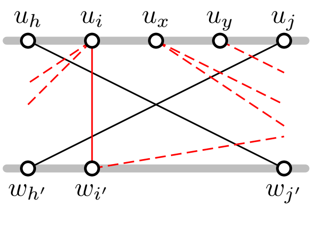

Fig. 7.25: The configuration when there exist distinct vertices $u_x \neq u_i$ and u_y between u_h and u_j in Γ.

Proof. Let Γ and Γ' be as described in the lemma. (see Fig. 7.25 for an illustration).

We assume that there are vertices u_x and u_y in Γ such that $h < x < y < j$ and $x, y \neq i$. Each of the edges $(u_h, w_{j'})$ and $(u_j, w_{h'})$ has two crossings from the triple of pairwise crossing edges, so each of them can only be intersected by three more edges. Hence, there are at most seven edges incident to the vertices u_i, u_x, $u_{x'}$ and $w_{i'}$ in Γ, including the edge $(u_i, w_{i'})$ (see e. g. the red edges in Fig. 7.25). So for the number of edges m' in Γ' the inequality $m' \geq m-7$ holds, and we have $n' = n-4$. This implies

$$m \leq m' + 7 \leq \tfrac{9}{4}n' - \tfrac{9}{2} + 7 = \tfrac{9}{4}(n-4) - \tfrac{9}{2} + 7 = \tfrac{9}{4}n - \tfrac{9}{2} - 2 < \tfrac{9}{4}n - \tfrac{9}{2}.$$

The case where both vertices $w_{x'}$ and $w_{y'}$ are in Γ is symmetric, while the cases where there are at least the vertices u_x and $w_{x'}$ are in Γ also yields $m < \frac{9}{4}n - \frac{9}{2}$.

Finally, for $n' = 8$ and $m' \leq 14$ we have

$$m \leq m' + 7 \leq 21 < 22.5 = \tfrac{9}{4}(n'+4) - \tfrac{9}{2} < \tfrac{9}{4}n - \tfrac{9}{2}.$$

The statement of the lemma follows. □

So, when proving an upper bound for 2-layer 5-planar graphs, we can assume that for each triple of pairwise crossing edges $(u_h, w_{j'})$, $(u_i, w_{i'})$ and $(u_j, w_{h'})$, there is either at most one vertex $u_x \neq u_i$ such that $u_h \prec u_x \prec u_j$ and only $w_{i'}$ between $w_{h'}$ and $w_{j'}$, or at most one vertex $w_{x'} \neq w_{i'}$ such that $w_{h'} \prec w_{x'} \prec w_{j'}$ and only u_i between u_h and u_j. We call this property *triple*$^+$*-crossing property.*

Lemma 7.27. *Let $\Gamma \in \mathcal{P}_5^=$ have the triple$^+$-crossing property and let $(u_h, w_{j'})$, $(u_i, w_{i'})$ and $(u_j, w_{h'})$ form a triple of mutually crossing edges in Γ for some $1 \leq h < i < j \leq a$ and $1 \leq h' < i' < j' \leq b$. Further let $\Gamma_1 = [1, h \mid 1, h']$, and $\Gamma_2 = [j, a \mid j', b]$. Then Γ_1 and Γ_2 are only connected by*

- *edges $(u_h, w_{j'})$ and $(u_j, w_{h'})$ (black in Fig. 7.26),*
- *possibly edges incident to u_i or $w_{i'}$ (dashed red in Fig. 7.26),*
- *possibly edges either incident to a vertex u_x, where $h < x < j$ and $x \neq i$ (dashed orange in Fig. 7.26), or incident to a vertex $w_{x'}$, where $h' < x' < j'$ and $x' \neq i'$,*
- *possibly edges $(u_y, w_{y'})$, where $y \in \{h, j\}$ or $y' \in \{h', j'\}$ (dashed purple in Fig. 7.26).*

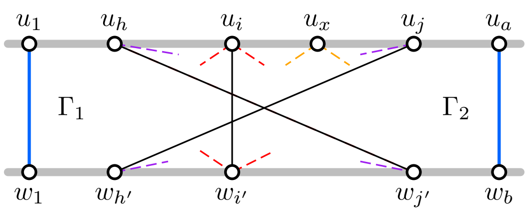

Fig. 7.26: Illustration of Lemma 7.27.

Proof. Assume to the contrary that there is an edge $(u_y, w_{y'})$ such that $1 \le y < h$ and $j < y' \le b$. This edge intersects all three edges $(u_h, w_{j'})$, $(u_i, w_{i'})$ and $(u_j, w_{h'})$. But then $(u_y, w_{y'})$, $(u_i, w_{i'})$ and $(u_j, w_{h'})$ form a triple of pairwise crossing edges and u_h is between u_y and u_j, while $w_{j'}$ is between $w_{h'}$ and $w_{y'}$ – a contradiction to the triple$^+$-crossing property (for an illustration see Fig. 7.27). □

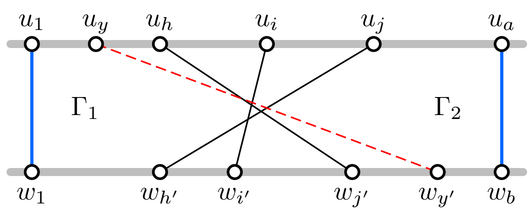

Fig. 7.27: The situation with a vertex u_y between u_1 and u_h, a vertex $w_{y'}$ between $w_{j'}$ and w_b, and an edge between them.

The following observation is a consequence of 5-planarity.

Observation 7.28. *Let Γ_1 and Γ_2 be defined as in Lemma 7.27, m_1 the number of edges in Γ_1, and m_2 the number of edges in Γ_2. If m is the number of edges in Γ, then the difference between m and $m_1 + m_2$ is at most $m - (m_1 + m_2) \le 9$.*

This observation is used in the proof of the next lemma, that gives already upper bounds on the number of edges for small values of n and will serve later, in the proof of Thm. 7.31, as base of the induction.

Lemma 7.29. *The maximal number of edges for 2-layer 5-planar graphs on $n \le 9$ vertices are as follows (where (n, m) means that for n vertices the upper bound is m): $(0, 0)$, $(1, 0)$, $(2, 1)$, $(3, 2)$, $(4, 4)$, $(5, 6)$, $(6, 9)$, $(7, 11)$, $(8, 14)$ and $(9, 15)$.*

Proof. Clearly there exist no edges at all in graphs with $n \in \{0, 1\}$.

Consider the graph $K_{x,n-x}$, for some $1 \le x < n$, which has n vertices and $f(x) := x(n - x)$ edges. An easy calculation shows that $f(x)$ has a global maximum in $x = \frac{1}{2}n$. So, for even n, the graph $K_{\frac{1}{2}n,\frac{1}{2}n}$ is the bipartite graph with the maximal number of edges, while the same holds for $K_{\frac{1}{2}(n-1),\frac{1}{2}(n+1)}$ and odd n. We use this fact for our argumentation.

- For $n = 2$, the graph $K_{1,1}$ has 1 edge.
- For $n = 3$, the graph $K_{1,2}$ has 2 edges.
- For $n = 4$, the graph $K_{2,2}$ has 4 edges.
- For $n = 5$, the graph $K_{2,3}$ has 6 edges.

– For $n = 6$, the graph $K_{3,3}$ has 9 edges.

Note that all these graphs are 2-layer 5-planar, as Fig. 7.28 shows.

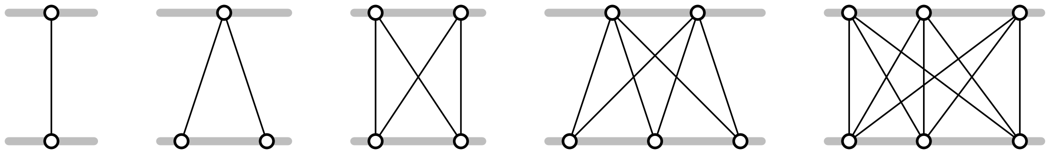

(a) (b) (c) (d) (e)

Fig. 7.28: Unique 2-layer drawings (up to isomorphism) of (a) graph $K_{1,1}$; (b) graph $K_{1,2}$; (c) graph $K_{2,2}$; (d) graph $K_{2,3}$; (e) graph $K_{3,3}$. All these drawings are 5-planar.

For $n = 7$, the graph $K_{3,4}$ has 12 edges. However, this graph is not 2-layer 5-planar, see Fig. 7.29. But removing one edge from the (up to isomorphism) unique 2-layer drawing of $K_{3,4}$ yields a $\mathcal{P}_5^=$-drawing with 11 edges. This (and the fact that $K_{2,5}$ has only 10 edges) implies that any $\mathcal{P}_5^=$-graph with 7 vertices has at most 11 edges.

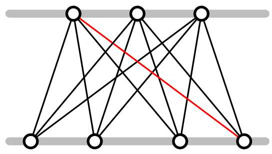

Fig. 7.29: Unique 2-layer drawing (up to isomorphism) of $K_{3,4}$. Removing the red edge yields an optimal 5-planar drawing with 11 edges.

Next consider a 2-layer drawing Γ with $n = 8$ vertices. Note that, since $K_{4,4}$ is not 5-planar, it is not sufficient to consider only $a = b = 4$. If Γ is quasi-planar, it has at most $2n - 4 = 13$ edges. Otherwise there is a triple $(u_h, w_{j'})$, $(u_i, w_{i'})$, $(u_j, w_{h'})$ of mutually crossing edges in Γ, where $1 \le h < i < j \le a$ and $1 \le h' < i' < j' \le b$. This implies $(a, b) \in \{(3, 5), (4, 4)\}$. By Lemma 7.26 we can assume that one of the following configurations holds for a 2-layer 5-planar drawing Γ:

(1) There exists exactly one vertex $u_x \ne u_i$ with $h < x < j$, and the vertices $w_{h'}$, $w_{i'}$ and $w_{j'}$ are consecutive, i. e. $i' = h' + 1$ and $j' = h' + 2$;

(2) there exists exactly one vertex $w_{x'} \ne w_{i'}$ with $h' < x' < j'$, and the vertices u_h, u_i and u_j are consecutive, i. e. $i = h + 1$ and $j = h + 2$;

(3) the vertices u_h, u_i and u_j are consecutive on the top layer, and the vertices $w_{h'}$, $w_{i'}$ and $w_{j'}$ are consecutive on the bottom layer, i. e. $i = h + 1$, $j = h + 2$, $i' = h' + 1$, and $j' = h' + 2$.

If Γ is a drawing with $a = 3$ and $b = 5$, then its number of edges is at most $M := \max(1 + 9 + 3, 2 + 9 + 2, 1 + 9 + 2) = 13$. Instead of explaining these numbers with a tedious case analysis, we refer to Fig. 7.30, where the red area represents the

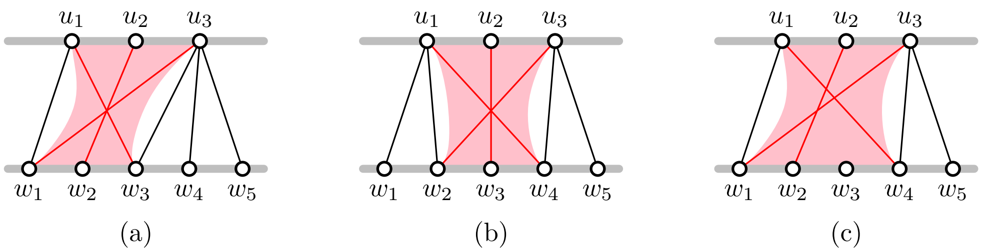

Fig. 7.30: Different configurations for three mutually crossing edges in a drawing with $(a, b) = (3, 5)$. Except for the triple of mutually crossing edges, the edges belonging to $\Gamma \setminus (\Gamma_1 \cup \Gamma_2)$ are not drawn. (a) The subdrawing $\Gamma_1 = [1, 1 \mid 1, 1]$ has at most 1 edge, while $\Gamma_2 = [3, 3 \mid 3, 5]$ has at most 3 edges, yielding an upper bound of $1 + 9 + 3 = 13$ edges. (b) This configuration has at most $2 + 9 + 2 = 13$ edges. (c) This configuration has at most $1 + 9 + 2 = 12$ edges.

difference between Γ and the union of $\Gamma_1 := [1, h \mid 1, h']$ and $\Gamma_2 := [j, 3 \mid j', 5]$ for different values of h, h', j and j'.

The counting in the different sums of the maximum M is as follows: The first summand is the maximal number of edges in Γ_1 (left of the red area in the figures), while the last summand is the maximal number of edges in Γ_2 (right of the red area). The middle summand is an upper bound on the additional number of edges of Γ compared to the union of Γ_1 and Γ_2. According to Obs. 7.28 this upper bound is 9. When we consider the different cases to calculate the maximal number of edges, we refrain from showing isomorphic settings.

We also take into account the three configurations deduced from Lemma 7.26. Observe that Configs. 1 and 2, i. e. the configurations where the snippet $[h, j \mid h', j']$ contains more than 6 vertices, do never yield the maximum in our calculation: The red area contributes at most 9 edges to Γ, no matter how many vertices are in this area, but more vertices in the red area imply less vertices in Γ_1 or Γ_2, and hence less edges in Γ_1 and Γ_2 (refer to Fig. 7.30c). So it suffices to consider Config. 3.

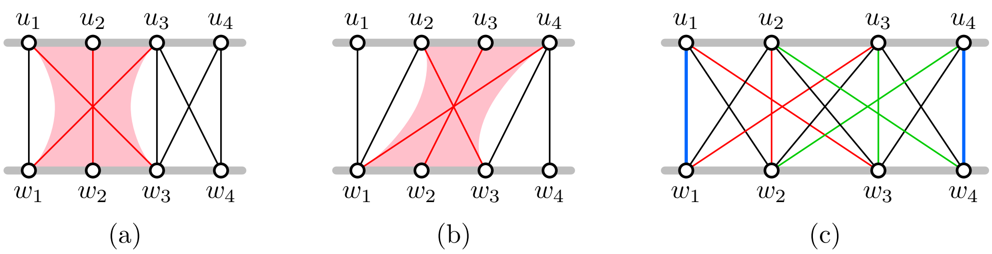

Fig. 7.31: Different configurations for three mutually crossing edges in a drawing with $(a, b) = (4, 4)$. (a) The subdrawing $\Gamma_1 = [1, 1 \mid 1, 1]$ has at most 1 edge, and $\Gamma_2 = [3, 4 \mid 3, 4]$ has at most 4 edges, yielding an upper bound of $1 + 9 + 4 = 14$ edges. (b) This configuration has at most $2 + 9 + 2 = 13$ edges. (c) A 2-layer 5-planar drawing with $(a, b) = (4, 4)$ that has exactly 14 edges, which is the unique optimal such drawing for 8 vertices.

If Γ is a $\mathcal{P}_5^{=}$-drawing with $a = 4$ and $b = 4$, similar considerations as above imply an upper bound of $\max(1+9+4, 2+9+2) = 14$ edges (refer to Fig. 7.31). Figure 7.31c shows a corresponding drawing with 14 edges, hence this bound is tight.

Finally we study drawings Γ with $n = 9$ vertices. If Γ is quasi-planar, it has at most $2n - 4 = 14$ edges. Otherwise there is a triple $(u_h, w_{j'})$, $(u_i, w_{i'})$, $(u_j, w_{h'})$ of mutually crossing edges in Γ, where $1 \leq h < i < j \leq a$ and $1 \leq h' < i' < j' \leq b$. This implies $(a, b) \in \{(3, 6), (4, 5)\}$. Similar as for $n = 8$, we obtain an upper bound of $\max(1 + 9 + 4, 2 + 9 + 3) = 14$ edges for $(a, b) = (3, 6)$, and an upper bound of $\max(1+9+6, 2+9+4, 3+9+2) = 16$ edges for $(a, b) = (4, 5)$ (refer to Fig. 7.32). Note that only the configuration from Fig. 7.32c (or one symmetric to it) is responsible that the maximum for $(a, b) = (4, 5)$ is 16. For this reason we study the drawing Γ in Fig. 7.32c in detail.

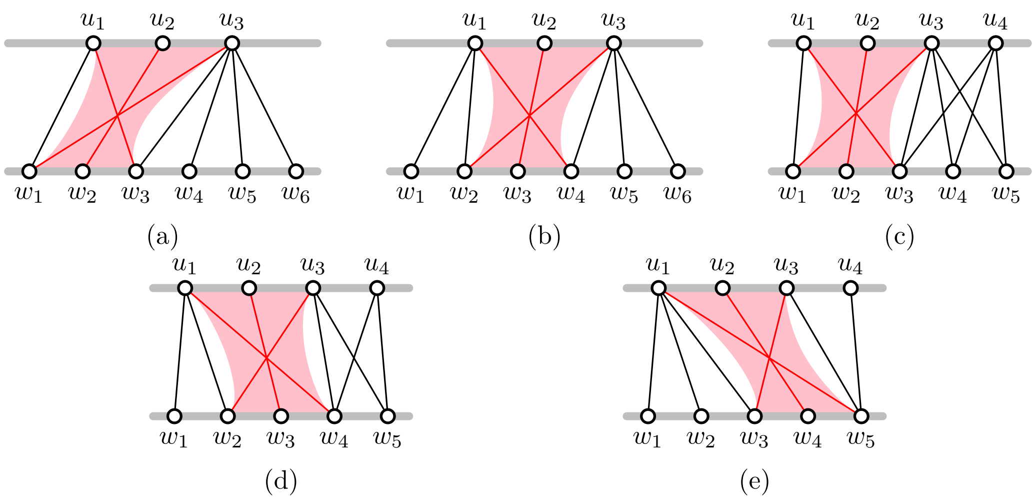

Fig. 7.32: Different configurations for three mutually crossing edges in a drawing with $(a, b) = (3, 6)$ in (a) and (b), and with $(a, b) = (4, 5)$ in (c)–(e). (a) The subdrawing $\Gamma_1 = [1, 1 \mid 1, 1]$ has at most 1 edge and $\Gamma_2 = [3, 3 \mid 3, 6]$ has at most 4 edges, yielding an upper bound of $1 + 9 + 4 = 14$ edges. (b) This configuration has at most $2 + 9 + 3 = 14$ edges. (c) This configuration has at most $1 + 9 + 6 = 16$ edges. (d) This configuration has at most $2 + 9 + 4 = 15$ edges. (e) This configuration has at most $3 + 9 + 2 = 14$ edges.

First observe that, if the snippet $[3, 4 \mid 3, 5]$ in Γ is not a complete bipartite graph, then Γ has at most 15 edges. Thus we assume in the following that it is a complete bipartite graph. Further note that there can be neither an edge (u_1, w_5), nor an edge (u_1, w_4), nor an edge (u_4, w_1), as otherwise the (smaller) upper bound of another configuration applies (e. g., in the presence of edge (u_1, w_4), the triple (u_1, w_4), (u_2, w_2) and (u_3, w_1) of mutually crossing edges yields an upper bound of $1 + 9 + 4 = 14$ edges). So each vertex u_1 and w_1 can only be incident to one more edge, namely (u_1, w_2) and (u_2, w_1), respectively.

It is also not possible that Γ contains both edges (u_2, w_4) and (u_4, w_2), since this would give rise to another triple of crossing edges, namely (u_2, w_4), (u_3, w_3), and (u_4, w_2), with at most $4 + 9 + 2 = 15$ edges. Similarly Γ cannot contain both edges (u_2, w_5) and (u_4, w_2).

Assume first that edge (u_4, w_2) is in Γ (solid green edge in Fig. 7.33a). Then the only other edges Γ can possibly have are (u_1, w_2), (u_2, w_1), (u_2, w_3), and (u_3, w_2) (dashed green edges in Fig. 7.33a), so that in this case Γ has at most 15 edges.

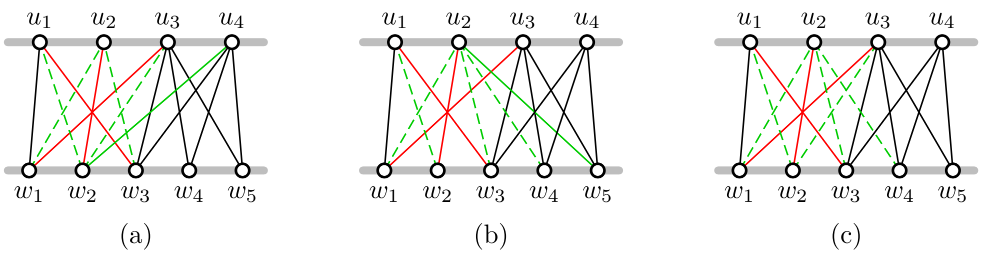

Fig. 7.33: Different configurations for three mutually crossing edges in the drawing with $(a, b) = (4, 5)$ that has potentially 16 edges. (a) Edge (u_4, w_2) is in Γ. (b) Edge (u_4, w_2) is not in Γ and (u_2, w_5) belongs to it. (c) Edges (u_4, w_2) and (u_2, w_5) are not in Γ.

Now we assume that the edge (u_4, w_2) is not part of Γ. If (u_2, w_5) is in Γ (solid green edge in Fig. 7.33b), none of the edges (u_3, w_3) and (u_4, w_3) belongs to Γ, since otherwise 5-planarity is violated by (u_2, w_5). So Γ potentially contains the edges (u_1, w_2), (u_2, w_1), (u_2, w_3), and (u_3, w_2) (dashed green edges in Fig. 7.33b), and again Γ has at most 15 edges (in fact, the upper bound is even 14, since (u_3, w_1) is not allowed to have 6 crossings).

Last, consider the case where (u_2, w_5) also does not belong to Γ. Here Γ potentially contains only the five additional edges (u_1, w_2), (u_2, w_1), (u_2, w_3), (u_3, w_2), and (u_3, w_2) (dashed green edges in Fig. 7.33c), yielding at most 15 edges for Γ.

Since, in none of the cases, we obtain a valid drawing with more than 15 edges, the upper bound on the number of edges for 2-layer 5-planar graphs with $n = 9$ vertices is $m = 15$. □

Inspecting the proof for $n = 8$ closely, we observe that only a configuration like the one depicted in Fig. 7.31a leads to $m = 14$ edges. Since the snippets $\Gamma_1 = [1, 1 \mid 1, 1]$ and $\Gamma_2 = [3, 4 \mid 3, 4]$ in this drawing can have at most $m_1 \leq 1$ and $m_2 \leq 4$ edges, respectively, and since the difference $m - (m_1 + m_2)$ in the number of edges between Γ and the union of Γ_1 and Γ_2 is at most 9, the value of 14 edges can only be achieved if $m_1 = 1$, $m_2 = 4$ and $m - (m_1 + m_2) = 9$. So both edges (u_1, w_3) and (u_3, w_1) must necessarily have 5 crossings, which implies that all the edges (u_1, w_2), (u_2, w_1), (u_2, w_3), (u_2, w_4), (u_3, w_2), and (u_4, w_5) are present in Γ. As a consequence, the drawing from Fig. 7.31c is the only drawing for an optimal 2-layer 5-planar graph (up to isomorphism) with 8 vertices.

Observation 7.30. *There is only one drawing (up to isomorphism) for an optimal 2-layer 5-planar graph on $n = 8$ vertices, namely the drawing from Fig. 7.31c.*

At this point, we are finally prepared to prove an upper bound for $\mathcal{P}_5^=$-graphs.

Theorem 7.31. *Any 2-layer 5-planar graph on $n \geq 3$ vertices has at most $\frac{9}{4}n - \frac{9}{2}$ edges, except for $n = 8$, where the upper bound is $14 > 13.5 = \frac{9}{4}n - \frac{9}{2}$.*

Proof. Let Γ be a 2-layer 5-planar drawing with n vertices and m edges. According to Lemma 7.26, we can assume that Γ has the triple$^+$-crossing property. If Γ has no triple of mutually crossing edges, it is quasi-planar and has therefore at most $2n - 4$ edges, which is smaller than $\frac{9}{4}n - \frac{9}{2}$ for $n \geq 3$. Thus, we can assume that Γ has a triple of pairwise crossing edges $(u_h, w_{j'})$, $(u_i, w_{i'})$ and $(u_j, w_{h'})$ for some $1 \leq h < i < j \leq a$ and $1 \leq h' < i' < j' \leq b$. We prove the statement by induction on the number of vertices.

For $3 \leq n \leq 9$ the claim holds by Lemma 7.29, and for $n = 2$ the number of edges is at most 1. In the following we assume that $n \geq 10$ and the lemma is true for all 2-layer 5-planar drawings with less than n vertices..

Let Γ_1 and Γ_2 be the snippets $[1, h \mid 1, h']$ and $[j, a \mid j', b]$, respectively, and for $i = 1, 2$, let n_i and m_i the number of vertices and edges for Γ_i. By Obs. 7.28, we conclude that $m - (m_1 + m_2) \leq 9$, that is, Γ_1 and Γ_2 are connected by at most 8 edges (excluding $(u_i, w_{i'})$). Further, we observe that $n = n_1 + n_2 + 2$ or $n = n_1 + n_2 + 3$ by the triple$^+$-crossing property, so $n_1 + n_2 \leq n - 2$, and $m \leq m_1 + m_2 + 9$. Since each of Γ_1 and Γ_2 have less vertices than Γ, we can apply induction on them. We consider several configurations, aiming at covering all cases.

General Configuration. Suppose first that there exists a triple of pairwise crossing edges, such that $n_1, n_2 \notin \{2, 8\}$. Then we inductively have $m_1 \leq \frac{9}{4}n_1 - \frac{9}{2}$ and $m_2 \leq \frac{9}{4}n_2 - \frac{9}{2}$, yielding

$$\begin{aligned} m &\leq m_1 + m_2 + 9 \leq \left(\tfrac{9}{4}n_1 - \tfrac{9}{2}\right) + \left(\tfrac{9}{4}n_2 - \tfrac{9}{2}\right) + 9 \\ &= \tfrac{9}{4}(n_1 + n_2) \leq \tfrac{9}{4}(n - 2) = \tfrac{9}{4}n - \tfrac{9}{2}. \end{aligned}$$

In the following we consider the case where (without loss of generality) $n_1 \in \{2, 8\}$.

Three-Vertex Configuration. We assume that $n = n_1 + n_2 + 3$. Note that we cannot have $(n_1, n_2) = (2, 2)$, because n is at least 10. If $n_1 = 2$ and $n_2 \neq 8$, we obtain

$$\begin{aligned} m &\leq m_1 + m_2 + 9 \leq m_2 + 10 \leq \tfrac{9}{4}n_2 - \tfrac{9}{2} + 10 \\ &= \tfrac{9}{4}(n-5) - \tfrac{9}{2} + 10 = \tfrac{9}{4}n - \tfrac{9}{2} - \tfrac{5}{4} < \tfrac{9}{4}n - \tfrac{9}{2}. \end{aligned}$$

If $n_1 = 8$ and $n_2 \notin \{2, 8\}$, we obtain

$$\begin{aligned} m &\leq m_1 + m_2 + 9 \leq m_2 + 23 \leq \tfrac{9}{4}n_2 - \tfrac{9}{2} + 23 \\ &= \tfrac{9}{4}(n-11) - \tfrac{9}{2} + 23 = \tfrac{9}{4}n - \tfrac{9}{2} - \tfrac{7}{4} < \tfrac{9}{4}n - \tfrac{9}{2}. \end{aligned}$$

If $n_1 = 2$ and $n_2 = 8$, we have

$$m \leq m_1 + m_2 + 9 \leq 1 + 14 + 9 = 24 \leq \tfrac{99}{4} = \tfrac{9}{4} \cdot 13 - \tfrac{9}{2} = \tfrac{9}{4}n - \tfrac{9}{2},$$

and if $n_1 = 8$ and $n_2 = 8$, we have

$$m \leq m_1 + m_2 + 9 \leq 14 + 14 + 9 = 37 \leq \tfrac{153}{4} = \tfrac{9}{4} \cdot 19 - \tfrac{9}{2} = \tfrac{9}{4}n - \tfrac{9}{2}.$$

Since all other cases are symmetric, the statement is true when $n = n_1 + n_2 + 3$. Thus, it remains to consider the cases where $n = n_1 + n_2 + 2$, that is $i = h + 1$, $j = h + 2$, $i' = h' + 1$, and $j' = h' + 2$.

Left-2 General-Right Configuration. If $n_1 = 2$ and $n_2 \notin \{2, 8\}$, we have $m_2 \leq \frac{9}{4}n_2 - \frac{9}{2}$, $n_2 = n - 4$, and $m_2 \leq 1$, yielding an upper bound of

$$m \leq m_1 + m_2 + 9 \leq \left(\tfrac{9}{4}n_2 - \tfrac{9}{2}\right) + 1 + 9 \leq \tfrac{9}{4}(n-4) - \tfrac{9}{2} + 10 = \tfrac{9}{4}n - \tfrac{9}{2} + 1$$

edges. However, this upper bound can only be achieved if $m_1 = 1$, $m_2 = \frac{9}{4}n_2 - \frac{9}{2}$, and $m - (m_1 + m_2) = 9$. We show that this is not the case in a valid 2-layer 5-planar drawing.

First observe that, for $n_1 = 2$, we have $h = h' = 1$. Moreover, we can assume that there is neither an edge $(u_1, w_{x'})$ for some $x' > 3$ (for an illustration see Fig. 7.34a), nor an edge (u_x, w_1) for some $x > 3$, since otherwise we would have the *Three-Vertex Configuration* for the triple $(u_1, w_{x'})$, (u_2, w_2), (u_3, w_1), or to the triple (u_1, w_3), (u_2, w_2), (u_x, w_1). Thus, there exist at most 5 edges which are incident to u_1 or w_1, including (u_1, w_1). If this number is smaller than 5, we apply induction on the snippet $[2, a \mid 2, b]$ and obtain

$$m \leq 4 + \tfrac{9}{4}(n-2) - \tfrac{9}{2} < \tfrac{9}{4}n - \tfrac{9}{2},$$

for $n > 10$, or

$$m \leq 4 + 14 = 18 = \tfrac{9}{4}n - \tfrac{9}{2}$$

for $n = 10$ (that is, the snippet $[2, a \mid 2, b]$ has 8 vertices and 14 edges). Otherwise Γ contains the edges (u_1, w_1), (u_1, w_2) and (u_2, w_1) (see red edges in Fig. 7.34b).

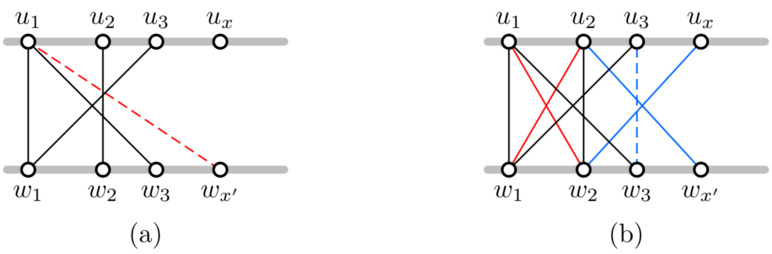

Fig. 7.34: Illustrations for the proof of Thm. 7.31, where $n_1 = 2$ and $n_2 \notin \{2, 8\}$. (a) An edge $(u_1, w_{x'})$ for some $x' > 3$ gives rise to another triple of pairwise crossing edges. (b) Vertices u_1 and w_1 are incident to five edges; there are edges $(u_2, w_{x'})$ and (u_x, w_2) in Γ.

Because of 5-planarity and $m - (m_1 + m_2) = 9$, each vertex u_2 and w_2 is incident to exactly two more edges. Thus, there is an edge $(u_2, w_{x'})$ for some $x' > 3$, and an edge (u_x, w_2) for some $x > 3$ (refer to the solid blue edges in Fig. 7.34b). We identify two cases regarding edge (u_3, w_3).

- This edge does not belong to Γ. Then we can enrich Γ_2 with this edge, apply induction on the new drawing, and obtain $m_2 + 1 \leq \frac{9}{4}n_2 - \frac{9}{2}$, which yields an upper bound of

$$m \leq m_1 + m_2 + 9 \leq 1 + \tfrac{9}{4}n_2 - \tfrac{9}{2} - 1 + 9 = \tfrac{9}{4}(n - 4) - \tfrac{9}{2} + 9 = \tfrac{9}{4} - \tfrac{9}{2}$$

  edges for Γ.

- Otherwise (u_3, w_3) belongs to Γ (refer to the dashed blue edge in Fig. 7.34b), and $(u_2, w_{x'})$, (u_3, w_3) and (u_x, w_2) form a triple of mutually crossing edges. We can assume that $x = x' = 4$, since otherwise we find the *Three-Vertex Configuration* in Γ.

  Consider the snippets $\Gamma'_1 = [1, 2 \mid 1, 2]$ and $\Gamma'_2 = [4, a \mid 4, b]$ with $n'_1 = 4$ and n'_2 vertices. Since $n \geq 10$, we do not have $n'_2 = 2$, and since we already considered the *General Configuration* (and $n'_1 \notin \{2, 8\}$), we can assume that Γ'_2 has exactly 8 vertices. Then Γ'_1 has $m'_1 = 4$ edges, Γ'_2 has at most $m'_2 \leq 14$ edges, while $m - (m'_1 + m'_2) \leq 9$. This results in

$$m \leq m'_1 + m'_2 + 9 \leq 4 + 14 + 9 = 27 = \tfrac{9}{4}n - \tfrac{9}{2}$$

  for $n = n'_1 + n'_2 + 2 = 14$ vertices.

We conclude that the statement holds for $n_1 = 2$ and $n_2 \notin \{2, 8\}$.

Left-8 General-Right Configuration. If $n_1 = 8$ and $n_2 \notin \{2, 8\}$, we have $m_1 \leq 14$, $m_2 \leq \frac{9}{4}n_2 - \frac{9}{2}$, $m - (m_1 + m_2) \leq 9$, and $n = n_2 + 10$. The triple of crossing edges is in this case (u_4, w_6), (u_5, w_5) and (u_6, w_4). If $m_1 \leq 13$ we immediately obtain

$$\begin{aligned} m &\leq m_1 + m_2 + 9 \leq 13 + \tfrac{9}{4}n_2 - \tfrac{9}{2} + 9 \\ &= 22 + \tfrac{9}{4}(n - 10) - \tfrac{9}{2} = \tfrac{9}{4}n - \tfrac{9}{2} - \tfrac{1}{2} < \tfrac{9}{4}n - \tfrac{9}{2}. \end{aligned}$$

Otherwise $m_1 = 14$, that is, Γ_1 is the unique drawing depicted in Fig. 7.31c. In this case we consider the triple (u_1, w_3), (u_2, w_2), (u_3, w_1) of pairwise crossing edges (red edges in Fig. 7.35), the snippets $\Gamma'_1 = [1, 1 \mid 1, 1]$ (left yellow part in Fig. 7.35) and $\Gamma'_2 = [3, a \mid 3, b]$ (right yellow part in Fig. 7.35). Since Γ'_1 has 2 vertices and Γ'_2 has at least 9 vertices (as a consequence of the assumption $n_2 \notin \{2, 8\}$), the statement follows by applying the *Left-2 General-Right Configuration* to Γ'_1 and Γ'_2.

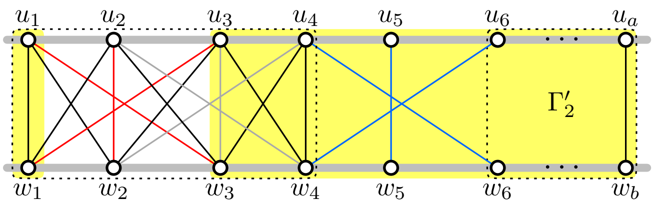

Fig. 7.35: Illustration for the *Left-8 General-Right Configuration*. The snippets Γ_1 and Γ_2 are indicated by the dotted rectangles, and the snippets Γ'_1 and Γ'_2 by the yellow area.

Left-2 Right-8 Configuration. If $n_1 = 2$ and $n_2 = 8$, we have $m_1 \leq 1$, $m_2 \leq 14$ and $n = n_1 + n_2 + 2 = 12$. First assume that Γ_2 contains no triple of mutually crossing edges. Then Γ_2 is quasi-planar and has at most $2n_2 - 4 = 12$ edges, yielding

$$m \leq m_1 + m_2 + 9 \leq 1 + 12 + 9 = 22 < 22.5 = \tfrac{9}{4}n - \tfrac{9}{2}.$$

Otherwise $m_2 \in \{13, 14\}$, and Γ_2 contains a triple of crossing edges (see e. g. green edges in Fig. 7.36). Then this triple must be (u_{a-2}, w_b), (u_{a-1}, w_{b-1}), (u_a, w_{b-2}), otherwise we are in the *General Configuration* or the *Three-Vertex Configuration*. Note that, since this second triple belongs entirely to Γ_2, the edges (u_1, w_3), (u_2, w_2), (u_3, w_1), (u_{a-2}, w_b), (u_{a-1}, w_{b-1}), and (u_a, w_{b-2}) are all different.

Consider the drawing Γ' obtained from Γ by deleting (u_2, w_2) and (u_{a-1}, w_{b-1}). If Γ' contains at most 20 edges, then Γ contains at most $22 < \frac{9}{4}n - \frac{9}{2}$ edges. On the other hand, if Γ' contains at least $21 > 2n - 4$ edges (recall that $n = 12$), it is not quasi-planar, and therefore contains a triple $(u_x, w_{x'+2})$, $(u_{x+1}, w_{x'+1})$, $(u_{x+2}, w_{x'})$ of

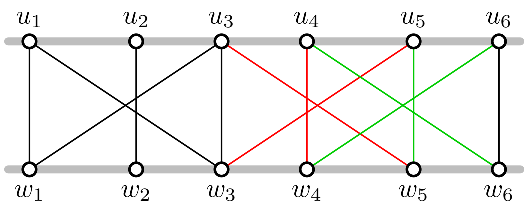

Fig. 7.36: Illustration for the *Left-2 Right-8 Configuration*.

pairwise crossing edges (the vertices can be assumed to be consecutive because of the *Three-Vertex Configuration*), where $1 \leq x \leq a-2$, $1 \leq x' \leq b-2$ (see e. g. red edges in Fig. 7.36). By construction of Γ', this triple also belongs to Γ, and we have $x \neq 1$ or $x' \neq 1$, and $x+2 \neq a$ or $x'+2 \neq a$. So the number of vertices of each snippet $[1, x \mid 1, x']$ and $[x+2, a \mid x'+2, b]$ is different from 2 and 8, and we can apply the *General Configuration* on them.[8] The statement follows for the case $n_1 = 2$ and $n_2 = 8$.

Left-8 Right-8 Configuration. In the final configuration we have $n_1 = 8$ and $n_2 = 8$, thus $m_1 \leq 14$, $m_2 \leq 14$, and $n = n_1 + n_2 + 2 = 18$. If $m_1 = m_2 = 14$, Γ_1 and Γ_2 are both copies of the unique optimal drawing for 8 vertices depicted in Fig. 7.31c (see Fig. 7.37 for an illustration). Since the four edges (u_2, w_4), (u_4, w_2), (u_6, w_8), and (u_8, w_6) are fully crossed, we have $m - (m_1 + m_2) \leq 7$, yielding an upper bound of

$$m \leq m_1 + m_2 + 7 = 14 + 14 + 7 = 35 < 36 = \tfrac{9}{4}n - \tfrac{9}{2}$$

edges.

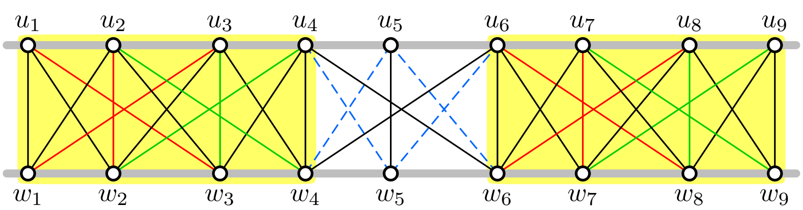

Fig. 7.37: Illustration for the *Left-8 Right-8 Configuration*, where $m_1 = m_2 = 14$. The copies of the unique optimal drawings with 8 vertices are highlighted in yellow.

On the other hand, if $m_1 \leq 13$, or $m_2 \leq 13$, we obtain

$$m \leq m_1 + m_2 + 9 \leq 13 + 14 + 9 = 36 = \tfrac{9}{4}n - \tfrac{9}{2}.$$

This completes the proof of Thm. 7.31. □

[8]Note that the General Configuration implies that Γ has at most $m \leq \frac{9}{4}n - \frac{9}{2} = 22.5$ edges; it follows that a subdrawing Γ' with 2 edges less than Γ has in fact not more than 20 edges.

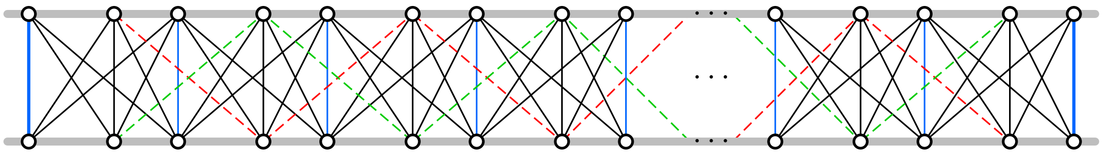

Fig. 7.38: A family of 6-planar graphs with $n = 2a$ vertices and $\frac{5}{2}n - 6$ edges.

7.4.5 6-planar graphs

We were not able to derive an upper bound on the number of edges for the class of 2-layer 6-planar graphs; however, we can provide at least a lower bound.

Theorem 7.32. *For infinitely many n, there exists a $\mathcal{P}_6^=$-graph with $\frac{5}{2}n - 6$ edges.*

Proof. We augment the lower bound construction for $\mathcal{P}_5^=$-graphs (see Thm. 7.25) by a path of length $t-1$ (symmetric to the path added in Thm. 7.25), where t is the number of $K_{3,3}$ subgraphs; for an illustration refer to the dashed green edges in Fig. 7.38. The graph we obtain still has $n = 4t + 2$ vertices; the number of edges is $m = 8t + 1 + 2(t-1) = 10t - 1$. An easy calculation shows $m = \frac{5}{2}n - 6$. $\square$

We conjecture that, for n large enough, $\frac{5}{2}n - 6$ is also an upper bound for the number of edges in 2-layer 6-planar graphs.

7.4.6 k-planar graphs for $k \geq 6$

Recall the Meta Crossing Lemma (see Thm. 6.2) of Chapter 6: If, for $i = 0, \ldots, \hat{k}-1$ and some $\hat{k} > 0$, edge densities for $\mathcal{R}$-restricted i-planar graphs are given by $\alpha_i n - \beta_i$, and $\alpha := \sum_{i=0}^{\hat{k}-1} \alpha_i$, then the number of crossings in every drawing of an $\mathcal{R}$-restricted graph G is lower bounded by

$$cr(G) \geq \frac{4\hat{k}^3}{27\alpha^2} \frac{m^3}{n^2}$$

for $m \geq \frac{3\alpha}{2\hat{k}} n$ and $n \geq 4$. Further, every $\mathcal{R}$-restricted k-planar graph has at most

$$m \leq \left(\max \left\{ 1, \sqrt{\frac{3k}{2\hat{k}}} \right\} \right) \cdot \frac{3\alpha}{2\hat{k}} n$$

edges (see Thm. 6.3), while $\mathcal{R}$-restricted k-gap-planar graphs have at most

$$m \leq \left(\max \left\{ 1, \sqrt{\frac{3k}{\hat{k}}} \right\} \right) \cdot \frac{3\alpha}{2\hat{k}} n$$

edges (see Thm. 6.4).

We apply Thms. 6.2 and 6.3 to $\mathcal{P}_{\hat{k}}^{=}$-graphs for $\hat{k} = 6$ and the following values α_i:

- $\alpha_0 = 1$, corresponding to the edge density $m \leq n-1$ for the class $\mathcal{P}_0^{=}$ (refer to [77]);
- $\alpha_1 = \frac{3}{2}$, corresponding to the edge density $m \leq \frac{3}{2}n - 2$ for $\mathcal{P}_1^{=}$ (refer to [57]);
- $\alpha_2 = \frac{5}{3}$, corresponding to the edge density $m \leq \frac{5}{3}n - \frac{7}{3}$ for $\mathcal{P}_2^{=}$ (refer to Thm. 7.15);
- $\alpha_3 = 2$, corresponding to the edge density $m \leq 2n-4$ for $\mathcal{P}_3^{=}$ (refer to Thm. 7.19);
- $\alpha_4 = 2$, corresponding to the edge density $m \leq 2n-3$ for $\mathcal{P}_4^{=}$ (refer to Thm. 7.23);
- $\alpha_5 = \frac{9}{4}$, corresponding to the edge density $m \leq \frac{9}{4}n - \frac{9}{2}$ for $\mathcal{P}_5^{=}$ when $n \geq 9$ (refer to Thm. 7.31).

This yields a value of $\alpha = \frac{125}{12}$ and thus the following Crossing Lemma for 2-layer graphs.

Corollary 7.33. *Let G be a simple 2-layer graph with $n \geq 9$ vertices and $m \geq \frac{125}{48}n$ edges. Then, the following inequality holds for the crossing number $cr(G)$:*

$$cr(G) \geq \frac{4.608}{15.625}\frac{m^3}{n^2} \approx 0.295\frac{m^3}{n^2}.$$

By plugging the numbers into Thm. 6.3, we obtain the following corollary.

Corollary 7.34. *Let G be a simple 2-layer k-planar graph on $n \geq 9$ vertices with m edges. For $k \geq 6$ we have*

$$m \leq \max\left\{\frac{125}{48}, \frac{125}{96}\sqrt{k}\right\} \cdot n = \frac{125}{96}\sqrt{k}n.$$

And by plugging the numbers into Thm. 6.4, we obtain a corresponding corollary for 2-layer gap-planar graphs.

Corollary 7.35. *Let G be a simple 2-layer k-gap-planar graph with $n \geq 9$ vertices and m edges. Then*

$$m \leq \max\left\{1, \frac{\sqrt{k}}{\sqrt{2}}\right\} \frac{125}{48} \cdot n.$$

Especially we have $m \leq \frac{125}{48}n$ for $k = 1$, and $m \leq \frac{125\sqrt{k}}{48 \cdot \sqrt{2}} \cdot n$ for $k \geq 2$.

We remark that $m \leq 3.19n$ for 2-layer 6-planar graphs by Cor. 7.34, which leaves only a gap of $0.69n$ regarding the lower bound established in Thm. 7.32. In the following theorem, we additionally show that the multiplicative constant $\frac{125}{96}\sqrt{k}$ in Cor. 7.34 is within a factor of 1.85 of the optimal achievable upper bound for large k.

Theorem 7.36. *For any k and infinitely many n, there exists a 2-layer k-planar graph on n vertices with $\left\lfloor \sqrt{k/2} \right\rfloor n - \mathcal{O}(k)$ edges.*

Proof. We construct a drawing Γ with the properties demanded in the theorem. Let the number n of vertices in Γ be even; further, let both layers have the same number of vertices, that is $a = b = \frac{n}{2}$, and let $c := \left\lfloor \sqrt{k/2} \right\rfloor$. For $i = 1, \ldots, a-1$ and $c(i) := \min(c, a-i)$, the vertex u_i has edges to $w_{i+1}, w_{i+2}, \ldots, w_{i+c(i)}$, and w_i has edges to $u_{i+1}, u_{i+2}, \ldots, u_{i+c(i)}$. Suppose that the edges are oriented from left to right. Since we aim at calculating an upper bound for the number of crossings a single edge can have, we assume $c(i) = c$ for all $1 \le i \le a$. We count the number of crossings for an edge $e := (u_x, w_{x'})$, where $1 \le x \le a-1$ and $x < x' \le x + c$.

– For $x' - c < j < x$, all edges $(u_j, w_{j'})$, where $x' < j' \le j + c$, cross e; see Fig. 7.39a. This contributes the following number of crossings for e:

$$\begin{aligned} 1 + 2 + \cdots + (x + c - 1 - x') &= \tfrac{1}{2}(x + c - 1 - x')(x + c - x') \\ &= \tfrac{1}{2}(c - (x' - x))^2 - \tfrac{1}{2}(x - x') + \tfrac{1}{2}c. \end{aligned}$$

– For $x < j < x' - 1$, all edges $(u_j, w_{j'})$, where $j < j' < x'$, cross e; see Fig. 7.39b. Hence, e is crossed by

$$\begin{aligned} 1 + 2 + \cdots + (x' - 1 - (x + 1)) &= \tfrac{1}{2}(x' - x)(x' - x + 1) \\ &= \tfrac{1}{2}(x' - x)^2 + \tfrac{1}{2}(x' - x) \end{aligned}$$

such edges.

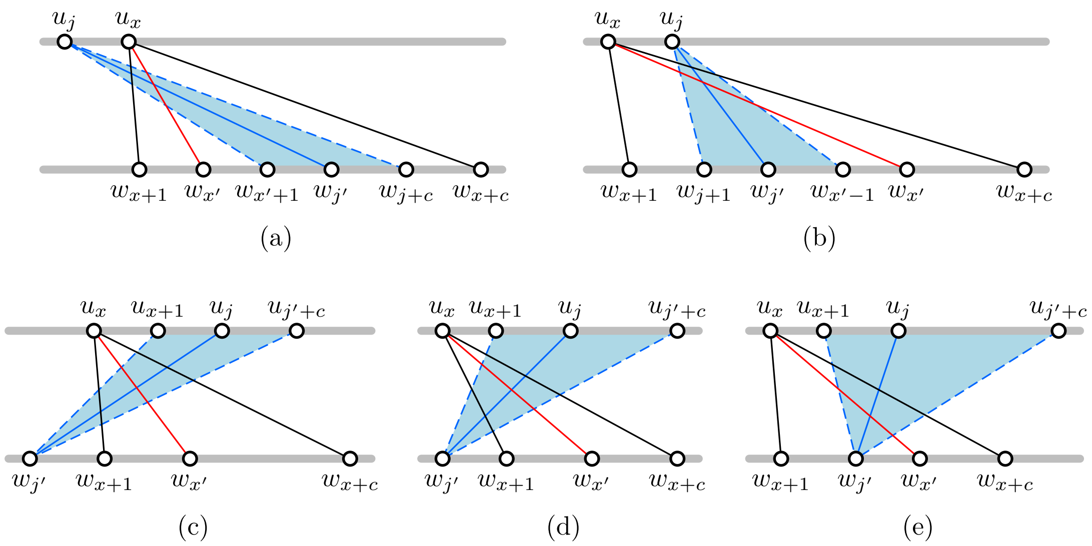

Fig. 7.39: Illustration for the proof of Thm. 7.36. (a) The case $x' - c < j < x$. (b) The case $x < j < x' - 1$. (c) The case $x - c < j' < x$. (d) and(e) The case $x \le j' < x'$.

– For $x - c < j' < x$, all edges $(u_j, w_{j'})$, where $x < j \leq j' + c$, cross e; see Fig. 7.39c. We obtain

$$1 + 2 + \cdots + (c - 1) = \tfrac{1}{2}(c-1)c = \tfrac{1}{2}c^2 - \tfrac{1}{2}c$$

crossings on e from this case.

– For $x \leq j' < x'$, all edges $(u_j, w_{j'})$, where $j' < j \leq j' + c$, cross e; see Figs. 7.39d and 7.39e. Here the contribution to the number of crossings of e is $c(x' - x)$.

The numbers of crossings on e in the different cases sum up to

$$\tfrac{1}{2}(c - (x' - x))^2 + \tfrac{1}{2}(x' - x)^2 + \tfrac{1}{2}c^2 + c(x' - x) = c^2 + (x' - x)^2 \leq 2c^2.$$

Further we have

$$2c^2 = 2\left(\left\lfloor \sqrt{k/2} \right\rfloor\right)^2 \leq 2\left(\sqrt{k/2}\right)^2 = k.$$

It remains to count the edges. Recall that they are oriented from left to right. By construction, the out-degree for every vertex is $c = \left\lfloor \sqrt{k/2} \right\rfloor$, except for such vertices u_i and v_i, where $a - c < i \leq a$. These vertices have out-degree $a - i$. This yields $cn - 2 \cdot (1 + 2 + \cdots + c) = cn - c(c+1) = cn - c^2 - c$ edges for Γ. Hence, the number of edges is $\left\lfloor \sqrt{k/2} \right\rfloor n - \mathcal{O}(k)$. □

As already mentioned, the multiplicative constant $\frac{125}{96}\sqrt{k}$ in Cor. 7.34 is within a factor of

$$\frac{\frac{125\sqrt{k}}{96}}{\left\lfloor \frac{\sqrt{k}}{\sqrt{2}} \right\rfloor} \leq \frac{\frac{125\sqrt{k}}{96}}{\frac{\sqrt{k}}{\sqrt{2}} - 1} = \frac{125}{96} \cdot \frac{1}{\frac{1}{\sqrt{2}} - \frac{1}{\sqrt{k}}} \xrightarrow[k \to \infty]{} \frac{125}{96} \cdot \sqrt{2} \leq \frac{250}{96} < 1.85$$

of the optimal achievable upperbound, when k is large enough.

7.5 Edge Density of Gap-Planar Graphs

Recall that in gap-planar graphs, a crossing is represented by a gap in one of the two corresponding edges, such that each edge has not more than one gap. We start by giving a lower bound for the number of edges in optimal 2-layer gap-planar graphs.

Theorem 7.37. *For infinitely many n, there exists a 2-layer gap-planar graph on n vertices with $2n - 4$ edges.*

Proof. We observe that the 2-layer quasi-planar family of graphs with $2n - 4$ edges presented in Thm. 7.3 is also gap-planar. For a corresponding 2-layer gap-planar drawing refer to Fig. 7.40. □

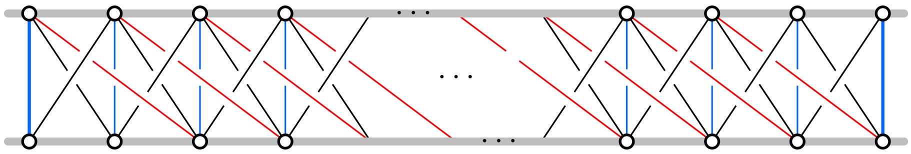

Fig. 7.40: The family of 3-planar graphs presented in Fig. 7.17 is also gap-planar.

By Cor. 7.35, gap-planar graphs on 2-layers have at most $\frac{125}{48}n \approx 2.604n$ edges. In the following we even show an upper bound of $2n - 4$ edges for such graphs, which provides – together with Thm. 7.37 – a tight bound. In order to achieve this, we introduce the following three lemmas.

Lemma 7.38. *Let Γ be a 2-layer gap-planar drawing with a triple of pairwise crossing edges $(u_h, w_{j'})$, $(u_i, w_{i'})$ and $(u_j, w_{h'})$ for some $1 \leq h < i < j \leq a$ and $1 \leq h' < i' < j' \leq b$. Then there is no edge $(u_x, w_{x'})$ in Γ, where*

- *index $x < i$ and $x' > i'$, or*
- *index $x > i$ and $x' < i'$, or*
- *index $x = i$, $h' < x' < j'$ and $x' \neq i'$, or*
- *index $x' = i$, $h < x < j$ and $x \neq i$.*

Proof. Recall that the crossing graph $X = (E, E_X)$ of Γ is a pseudo forest [30], that is, each connected component of X has at most one cycle. The triple $(u_h, w_{j'})$, $(u_i, w_{i'})$ and $(u_j, w_{h'})$ of mutually crossing edges already yields a cycle of length 3 in X (see black vertices in Fig. 7.41b, which correspond to the black edges in Fig. 7.41a). Thus, no other edge in Γ may cross two of the edges of this triple. If an edge $(u_x, w_{x'})$ exists in Γ with one of the properties described in the statement of the lemma, then it would cross two edges of the triple (see e. g. the dashed red edge in Fig. 7.41a and the corresponding red vertex and dashed red edges in Fig. 7.41b). The statement follows. □

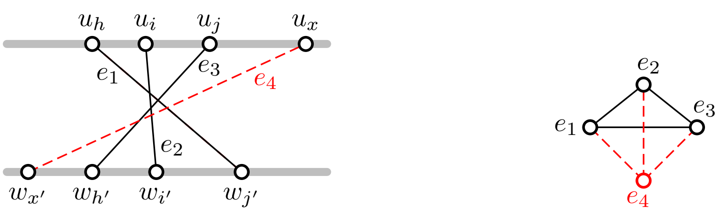

(a) (b)

Fig. 7.41: Illustration for the proof of Lemma 7.38. (a) The triple $(u_h, w_{j'})$, $(u_i, w_{i'})$ and $(u_j, w_{h'})$ of pairwise crossing edges is shown in black, an edge $(u_x, w_{x'})$ for $x < i$ and $x' > i'$ in red. (b) The corresponding crossing graph for Fig. 7.41a.

Lemma 7.38 shows that the edge $(u_i, w_{i'})$ represents a kind of a barrier: Except $(u_h, w_{j'})$ and $(u_j, w_{h'})$, there is no edge between the snippet $[1, i-1 \mid 1, i'-1]$ (the "left" side of $(u_i, w_{i'})$) and the snippet $[i+1, a \mid i'+1, b]$ (the "right" side of $(u_i, w_{i'})$). The next lemma defines another forbidden configuration, given a triple of mutually crossing edges.

Lemma 7.39. *Let Γ be a connected 2-layer gap-planar drawing with a triple of pairwise crossing edges $(u_h, w_{j'})$, $(u_i, w_{i'})$ and $(u_j, w_{h'})$ for some $1 \le h < i < j \le a$ and $1 \le h' < i' < j' \le b$. Consider two edges $(u_x, w_{y'})$ and $(u_y, w_{x'})$.*

(i) For $1 \le x < h$, $h < y \le i$, $1 \le x' < h'$, and $h' < y' \le i'$ (that is $u_x \prec u_h$, $w_{h'} \prec w_{y'} \preccurlyeq w_{i'}$, $u_h \prec u_y \preccurlyeq u_i$ and $w_{x'} \prec w_{h'}$), only one of the edges $(u_x, w_{y'})$ and $(u_y, w_{x'})$ can be in Γ.

(ii) For $i \le x < j$, $j < y \le a$, $i' \le x' < j'$, and $j' < y' \le b$, (that is $u_i \preccurlyeq u_x \prec u_j$, $w_{j'} \prec w_{y'}$, $u_j \prec u_y$ and $w_{i'} \preccurlyeq w_{x'} \prec w_{j'}$) only one of the edges $(u_x, w_{y'})$ and $(u_y, w_{x'})$ can be in Γ.

Proof. Let $X = (E, E_X)$ be the crossing graph of Γ. Then $e_1 := (u_h, w_{j'})$, $e_2 := (u_i, w_{i'})$ and $e_3 := (u_j, w_{h'})$ form a cycle in X. Since the two statements of the lemma are symmetric, it suffices to consider only one of them, say the first one.

Assume to the contrary that two edges $e_4 := (u_x, w_{y'})$ and $e_5 := (u_y, w_{x'})$ are in Γ, where $1 \le x < h$, $h < y \le i$, $1 \le x' < h'$, and $h' < y' \le i'$ (for an illustration see Fig. 7.42). But then e_4 crosses e_3 and e_5, while e_5 crosses additionally e_1, which yields a second cycle in X – a contradiction to the gap-planarity of Γ. □

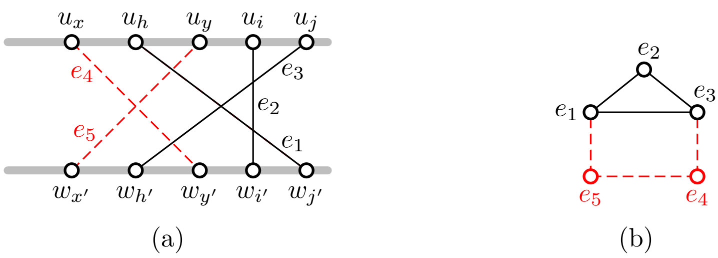

Fig. 7.42: Illustration for the proof of Lemma 7.39. (a) The triple $(u_h, w_{j'})$, $(u_i, w_{i'})$ and $(u_j, w_{h'})$ of pairwise crossing edges is shown in black, edges $(u_x, w_{y'})$ and $(u_y, w_{x'})$ in red. (b) The corresponding crossing graph for Fig. 7.42a.

Lemma 7.39 especially implies that, if Γ is connected and has a triple $(u_h, w_{j'})$, $(u_i, w_{i'})$, $(u_j, w_{h'})$ of pairwise crossing edges, not both edges $(u_i, w_{x'})$ and $(u_x, w_{i'})$ (where $x < h$ and $x' < h'$) can be part of Γ.

In the third lemma we define a forbidden configuration for three edges.

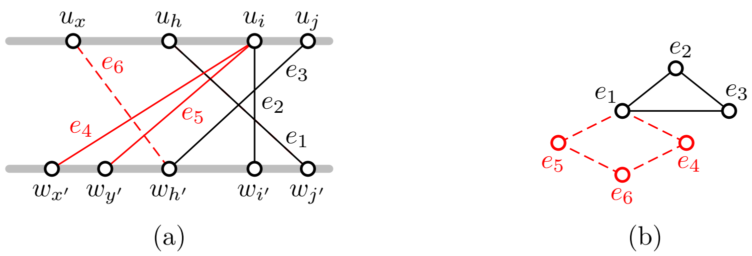

Fig. 7.43: Illustration for the proof of Lemma 7.40. (a) The triple $(u_h, w_{j'})$, $(u_i, w_{i'})$ and $(u_j, w_{h'})$ of pairwise crossing edges is shown in black, edges $(u_i, w_{x'})$ and $(u_i, w_{y'})$ in solid red and $(u_x, w_{h'})$ in dashed red. (b) The corresponding crossing graph for Fig. 7.43a.

Lemma 7.40. *Let Γ be a connected 2-layer gap-planar drawing with a triple $(u_h, w_{j'})$, $(u_i, w_{i'})$ and $(u_j, w_{h'})$ of pairwise crossing edges for some $1 \leq h < i < j \leq a$ and $1 \leq h' < i' < j' \leq b$.*

(i) If there are two edges $(u_i, w_{x'})$ and $(u_i, w_{y'})$ in Γ for $1 \leq x' < y' < h'$, then Γ does not contain an edge $(u_x, w_{h'})$ for $1 \leq x < i$.

(ii) If there are two edges $(u_i, w_{x'})$ and $(u_i, w_{y'})$ in Γ for $j' < x' < y' \leq b$, then Γ does not contain an edge $(u_x, w_{j'})$ for $i \leq x \leq a$.

(iii) If there are two edges $(u_x, w_{i'})$ and $(u_y, w_{i'})$ in Γ for $1 \leq x < y < h$, then Γ does not contain an edge $(u_h, w_{x'})$ for $1 \leq x' < i'$.

(iv) If there are two edges $(u_x, w_{i'})$ and $(u_y, w_{i'})$ in Γ for $j < x < y \leq a$, then Γ does not contain an edge $(u_j, w_{x'})$ for $i' \leq x' \leq b$.

Proof. Let $X = (E, E_X)$ be the crossing graph of Γ. Then $e_1 := (u_h, w_{j'})$, $e_2 := (u_i, w_{i'})$ and $e_3 := (u_j, w_{h'})$ form a cycle in X. Since the four statements of the lemma are symmetric, it suffices to consider only one of them, say the first one. So let $e_4 := (u_i, w_{x'})$ and $e_5 := (u_i, w_{y'})$ for $1 \leq x' < y' < h'$ be in Γ (see solid red edges in Fig. 7.43a).

Assume to the contrary that Γ also contains an edge $e_6 := (u_x, w_{h'})$ for some $1 \leq x < i$ (dashed red edge in Fig. 7.43a). But then e_6 crosses (at least) e_4 and e_5, while e_4 and e_5 both cross e_1, yielding a second cycle $(e_1, e_4, e_6, e_5, e_1)$ in X – a contradiction to the gap-planarity of Γ. □

Using the three previous lemmas, we have the means to prove the mentioned upper bound for the class of 2-layer gap-planar graphs $\mathcal{G}^=$.

Theorem 7.41. *Every 2-layer gap-planar graph on $n \geq 3$ vertices has at most $2n-4$ edges.*

Proof. Let Γ be a $\mathcal{G}^{=}$-drawing with $n \geq 3$ vertices and m edges. Note that every drawing with 2 vertices has at most $1 = 2n - 3$ edges. If Γ is quasi-planar, it clearly has at most $2n - 4$ edges. So we can assume in the following that there is a triple of pairwise crossing edges $(u_h, w_{j'})$, $(u_i, w_{i'})$, $(u_j, w_{h'})$ in Γ, where $1 \leq h < i < j \leq a$ and $1 \leq h' < i' < j' \leq b$.

We show the theorem by induction on the number of vertices. For the base of the induction, observe that Γ is quasi-planar if $n < 6$, and therefore has at most $2n - 4$ edges.

Now assume that the statement holds for all drawings with less than n vertices. If Γ contains a vertex u of degree at most 2, we consider the drawing Γ' obtained from Γ by deleting u and edges incident to u. Then Γ' has $n' = n - 1$ vertices and at most $m' \leq 2n' - 4 = 2n - 6$ edges by induction. Thus, $m \leq 2n - 6 + 2 = 2n - 4$ and the statement follows. In the following we assume that each vertex has at least degree 3.

Since u_i and $w_{i'}$ have degree at least 3, there are edges $(u_i, w_{x'})$, $(u_i, w_{y'})$, $(u_x, w_{i'})$ and $(u_y, w_{i'})$ in Γ for some $1 \leq x < y \leq a$, $x, y \neq i$, and $1 \leq x' < y' \leq b$, $x', y' \neq i'$. Observe the following:

- By Lemma 7.38 we have: $x \leq h$ or $x \geq j$, $y \leq h$ or $y \geq j$, $x' \leq h'$ or $x' \geq j'$, and $y' \leq h'$ or $y' \geq j'$.
- By Lemma 7.39 we further conclude that either $x, y \leq h$ and $x', y' \geq j'$, or $x, y \geq j$ and $x', y' \leq h'$. Without loss of generality we assume the latter (see Fig. 7.44a).
- Since also u_j and $w_{h'}$ have at least degree 3, Lemmas 7.38 and 7.40 imply that $x = j$ and $y' = h'$ (see Fig. 7.44b).
- We have already seen that for all neighbors w of u_i the condition $w \preccurlyeq w_{h'}$ holds. We have also seen that u_i cannot have two neighbors that lie left of $w_{h'}$, since it would block the third edge incident to $w_{h'}$. As a consequence, u_i has degree 3. Similarly, $w_{i'}$ has degree 3.

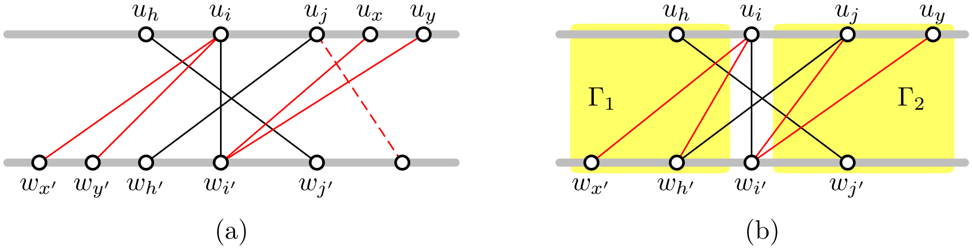

Fig. 7.44: Illustration for the proof of Thm. 7.41. (a) The edges $(u_i, w_{x'})$, $(u_i, w_{y'})$, $(u_x, w_{i'})$ and $(u_y, w_{i'})$ in solid red. The dashed red edge represents a forbidden configuration by Lemma 7.40. (b) The subdrawings Γ_1 and Γ_2 are highlighted in yellow.

Consider the subdrawings $\Gamma_1 := [1, i-1 \mid 1, i'-1]$ with $n_1 < n$ vertices, and $\Gamma_2 := [i+1, a \mid i'+1, b]$ with $n_2 < n$ vertices (illustrated in Fig. 7.44b). Since Γ_1 contains the distinct vertices u_h, $w_{x'}$, and $w_{h'}$, we have $n_1 \geq 3$; similarly $n_2 \geq 3$ holds, because u_j, u_y and $w_{j'}$ are three different vertices in Γ_2. Thus, we can apply induction on Γ_1 and Γ_2, and obtain an upper bound of $m_1 \leq 2n_1 - 4$ edges for Γ_1, and a corresponding upper bound of $m_2 \leq 2n_2 - 4$ edges for Γ_2.

By Lemma 7.38 the only edges of Γ that do not belong to Γ_1 or Γ_2 are the seven edges $(u_h, w_{j'})$, $(u_i, w_{x'})$, $(u_i, w_{h'})$, $(u_i, w_{i'})$, $(u_j, w_{h'})$, $(u_j, w_{i'})$, and $(u_y, w_{i'})$. So we have $m \leq m_1 + m_2 + 7$, which yields (together with $n = n_1 + n_2 + 2$)

$$
\begin{aligned}
m &\leq (2n_1 - 4) + (2n_2 - 4) + 7 = 2(n_1 + n_2) - 1 \\
&= 2(n-2) - 1 = 2n - 5 < 2n - 4.
\end{aligned}
$$

This completes the proof. □

7.6 Edge Density of 2-Layer 2-Sided Fanbundle-Planar Graphs

Recall that in 2-sided fanbundle-planar (short: fbp) graphs, it is allowed to bundle edges that are incident to the same vertex. Thereby each edge (u, w) has three parts: Two end parts, that belong to a bundle B_u of u and a bundle B_w of w, respectively, and a middle part. While each bundle is allowed to have at most one crossing, the middle part of each edge must be drawn planar.

We use the notation introduced by Angelini et al. [13]: If B_u is a fanbundle incident to vertex u, then u is called the *origin* of B_u, while B_u is called *anchored* at u. The endpoint of B_u that is different from u is called *terminal* of B_u.

As mentioned at the beginning of this chapter, for 2-layer 2-sided fbp graphs different requirements are needed, compared to the other graph classes in this chapter. Since each edge consists of three parts, and some edges may belong to the same bundle and therefore share the same end part, we would restrict the drawing extremely by forcing the whole edge with all three parts to be straight-line. Instead, we only require that

(a) the middle part of each edge is straight;

(b) the end parts, that is the bundles, are straight (allowing bends between the bundle parts and the non-bundle part of an edge);

(c) all parts of an edge are drawn between the top and the bottom layer.

In the following we often draw bundles slightly curved for aesthetic reasons. In fact, it is easy to see that drawing bundles straight or slightly curved makes no difference in the sense that exchanging a straight-line bundle by such a curved bundle produces an isomorphic drawing, and vice versa (as long as the curved bundle does not introduce new crossings).

Note that 2-sided fanbundle-planar drawings are "almost simple", that is, no two bundles incident to the same vertex cross each other. However, two edges may cross twice and edges incident to the same vertex can also cross.

Angelini et al. [13] provided an upper bound of $3n - 7$ edges for the class of 2-layer 2-sided fbp graphs. However, this bound is not tight, since their lower bound construction has only $2n - 4$ edges (we have redrawn it in Fig. 7.45). Observe also that the bundles in this construction only cross if they are anchored at vertices belonging to the same layer. We call the class, where all bundles have this property *2d-layer 2-sided fbp* and denote it by $\mathcal{B}_{2d}^{=}$. (The "d" stands for "double", since beside the vertices, also the terminals of the bundles can be placed on a layer, such that terminals of bundles whose origin is a top-layer vertex are on one layer, and terminals of bundles anchored at bottom-layer vertices are on another extra layer.) Clearly 2d-layer 2-sided fbp graphs are a subclass of 2-layer 2-sided fbp graphs (denoted by $\mathcal{B}_{2}^{=}$). However, in the following we will see that both classes are different, so the first one is a proper subclass of the second one.[9] We start by giving an upper bound for 2d-layer 2-sided fbp graphs.

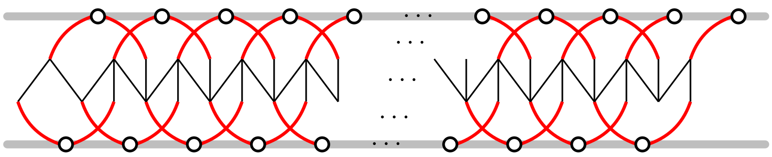

Fig. 7.45: The lower bound construction for 2-layer 2-sided fbp graphs of Angelini et al. [13]. In fact, this is a even a lower bound construction for 2d-layer 2-sided fbp graphs.

Theorem 7.42. *Every 2d-layer 2-sided fanbundle-planar graph on $n \geq 3$ vertices has at most $2n - 4$ edges.*

Proof. Let Γ be a connected $\mathcal{B}_{2d}^{=}$-graph on $n \geq 3$ vertices with m edges. First observe that, if two bundles B_h and B_j anchored at non-consecutive top-layer vertices u_h and u_j cross (that is, $j \geq h + 2$), then all vertices between u_h and u_j have degree

[9]We note that this is not true for 1-sided fbp graphs: The corresponding 2d-layer 1-sided fbp graph class coincides with the one of 2-layer 1-sided fbp graphs; refer to the results for 2-layer 1-sided fbp graphs in [13] (and their proofs).

0 (for an illustration see Fig. 7.46a); a contradiction to our assumption. A similar observation holds for bundles anchored at two bottom-layer vertices.

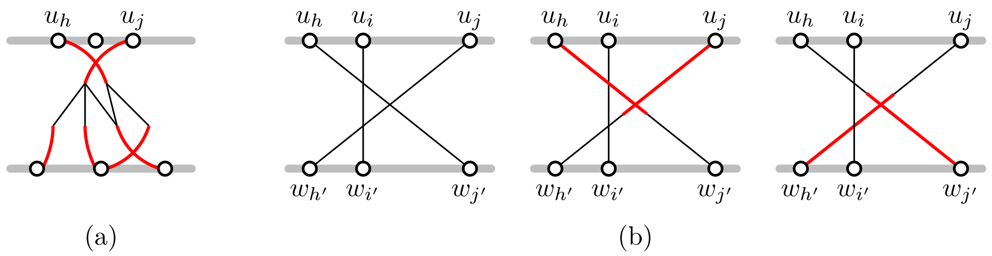

Fig. 7.46: Illustration for the proof of Thm. 7.42. (a) Two crossing bundles with origins that are not consecutive. (b) Left: A triple $(u_h, w_{j'})$, $(u_i, w_{i'})$ and $(u_j, w_{h'})$ of pairwise crossing edges. Middle and Right: The two options for the bundle crossing, indicated by the thick red lines.

Suppose now that there are three mutually crossing edges $(u_h, w_{j'})$, $(u_i, w_{i'})$, $(u_j, w_{h'})$ in Γ. To allow the crossing of $(u_h, w_{j'})$ and $(u_j, w_{h'})$, we have two options: Either a bundle B_h anchored at u_h crosses a bundle B_j anchored at u_j, or a bundle $B_{h'}$ anchored at $w_{h'}$ crosses a bundle $B_{j'}$ anchored at $w_{j'}$ (see Fig. 7.46b). In the former case, the vertex u_i is isolated, while in the latter case the vertex $w_{i'}$ is isolated. This yields that Γ cannot contain any triple of pairwise crossing edges. Thus, Γ is quasi-planar and has therefore at most $2n - 4$ edges. □

Note that Thm. 7.42 shows even more: The class of 2d-layer 2-sided fbp graphs is a subclass of the 2-layer quasi-planar graphs.

Observation 7.43. *We have* $\mathcal{B}_{2d}^{=} \subseteq \mathcal{Q}^{=}$.

The next theorem, which gives a lower bound for 2-layer 2-sided fbp graphs, shows that this class is indeed a proper superclass of 2d-layer 2-sided fbp graphs.

Theorem 7.44. *For infinitely many n, there exists a 2-layer 2-sided fanbundle-planar drawing on n vertices with $\frac{17}{8}n - \frac{13}{4}$ edges.*

Proof. Consider the $\mathcal{B}_2^{=}$-drawing Γ from Fig. 7.47. It consists of t identical bricks (delimited by the blue edges). Each brick consists of 10 vertices, such that five vertices are on the top layer, and five vertices are on the bottom layer. We only give the 18 edges of the first brick (which is sufficient, since all bricks are identical). These are (u_1, w_1), (u_1, w_2), (u_1, w_3), (u_2, w_1), (u_2, w_2), (u_2, w_3), (u_3, w_1), (u_3, w_2), (u_3, w_3), (u_3, w_4), (u_3, w_5), (u_4, w_2), (u_4, w_3), (u_4, w_4), (u_4, w_5), (u_5, w_3), (u_5, w_4), and (u_5, w_5). Then Γ has $n = 2 + 8t$ vertices and $m = 1 + 17t = \frac{17}{8}n - \frac{13}{4}$ edges. □

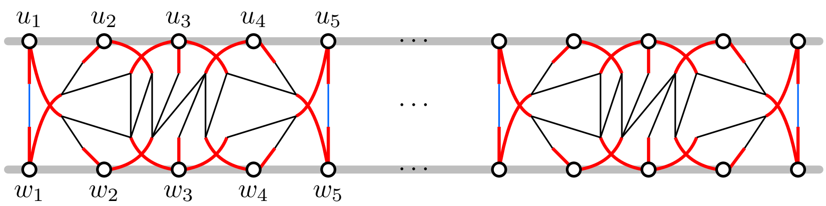

Fig. 7.47: The lower bound construction for 2-layer 2-sided fbp graphs with $\frac{17}{8}n - \frac{13}{4}$ edges. The bricks are delimited by blue edges.

We conclude this section by showing that the maximal number of edges in 2-layer 2-sided fbp graphs is $\frac{17}{8}n - \frac{13}{4}$, as well. To this end we first prove the following lemma.

Lemma 7.45. *Let* $\Gamma \in \mathcal{B}_2^=$ *and* $n \geq 3$ *be the number of vertices in* Γ*. If* Γ *contains a triple* $(u_h, w_{j'})$, $(u_i, w_{i'})$, $(u_j, w_{h'})$ *such that* $1 \leq h < i < j \leq a$ *and* $1 \leq h' < i' < j' \leq b$ *then*

– *two bundles anchored at* u_h *and* $w_{h'}$ *cross each other, or*

– *two bundles anchored at* u_j *and* $w_{j'}$ *cross each other.*

On the other hand, if no such triple exists in Γ*, the number of edges is at most* $2n-4$.

Proof. Assume that Γ contains a triple $(u_h, w_{j'})$, $(u_i, w_{i'})$, $(u_j, w_{h'})$ such that $1 \leq h < i < j \leq a$ and $1 \leq h' < i' < j' \leq b$. The crossing of $(u_h, w_{j'})$ and $(u_j, w_{h'})$ must be covered by bundles. Since, in a valid drawing, it is not possible that bundles anchored at u_h and u_j cross each other, or bundles anchored at $w_{h'}$ and $w_{j'}$ cross each other (refer also to the proof of Thm. 7.42), there must be bundles anchored at u_h and $w_{h'}$ that cross, or bundles anchored at u_j and $w_{j'}$ that cross.

If Γ contains no triple $(u_h, w_{j'})$, $(u_i, w_{i'})$, $(u_j, w_{h'})$ such that $1 \leq h < i < j \leq a$ and $1 \leq h' < i' < j' \leq b$, then the drawing Γ_q with the same vertex order along the two layers and straight-line edges is quasi-planar. Since Γ_q and Γ have the same number of vertices and edges, and the edge density of quasi-planar graphs is $2n-4$ (refer to Thm. 7.4), we obtain $m \leq 2n-4$ for Γ. □

In the following we call a bundle crossing between bundles anchored at vertices of different layers a *UW-bundle crossing.*

The next lemma is useful for proving the edge density of $\mathcal{B}_2^=$, as well as in the characterization of complete $\mathcal{B}_2^=$-graphs.

Lemma 7.46. *The graph* $K_{3,4}$ *is not in* $\mathcal{B}_2^=$*.*

Proof. For a contradiction let Γ be a drawing of $K_{3,4}$ such that $\Gamma \in \mathcal{B}_2^{=}$. First observe that a UW-bundle crossing of two bundles anchored at u_i and $w_{i'}$, where $(i, i') \notin \{(1,1),(3,4)\}$, isolates at least one vertex in Γ (see e. g. Fig. 7.48a). Hence such a crossing cannot be part of Γ.

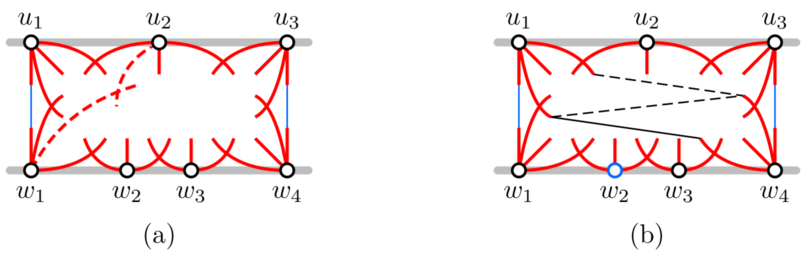

Fig. 7.48: (a) The dashed bundle crossing isolates u_1. (b) The edge (u_1, w_4) isolates vertex u_2.

On the other hand, even if crossing bundles anchored at u_1 and w_1, or at u_3 and w_4 are allowed, the edge (u_1, w_4) isolates vertex u_2 (refer to Fig. 7.48b) – no matter how this edge is drawn. □

The following theorem uses induction to show the mentioned upper bound on the number of edges for 2-layer 2-sided fanbundle-planar graphs.

Theorem 7.47. *Every $\mathcal{B}_2^{=}$-graph on $n \geq 2$ vertices has at most $\frac{17}{8}n - \frac{13}{4}$ edges.*

Proof. Let Γ be a $\mathcal{B}_2^{=}$-drawing on $n \geq 2$ vertices with m edges. We prove the statement by induction on the number of vertices.

For $n = 2$, the drawing Γ has at most $1 = \frac{17}{8}n - \frac{13}{4}$ edges; for $3 \leq n \leq 5$, drawing Γ is quasi-planar and has at most $2n - 4 \leq \frac{17}{8}n - \frac{13}{4}$ edges; and for $n = 6$, the number of edges in $K_{3,3}$ provides an upper bound of $9 < 9.5 = \frac{17}{8}n - \frac{13}{4}$ edges for Γ. Assume now that Γ has $n > 6$ vertices and the statement is true for all drawings with less than n vertices.

If Γ contains a degree-0 or a degree-1 vertex v, the drawing $\Gamma \setminus \{v\}$ has $n - 1$ vertices and by induction $m \leq \frac{17}{8}(n-1) - \frac{13}{4} + 1 < \frac{17}{8}n - \frac{13}{4}$ edges. Further, if $\Gamma \in \mathcal{B}_{2d}^{=}$ then it has at most $2n - 4 \leq \frac{17}{8}n - \frac{13}{4}$ edges.

In the following we assume that Γ is connected, has no degree-1 vertices, and that Γ contains a UW-bundle crossing, that is, a pair of crossing bundles B_h and $B_{h'}$, anchored at vertices u_h and $w_{h'}$, respectively.

First suppose that $h > 1$ or $h' > 1$, and $h < a$ or $h' < b$ (see e. g. Fig. 7.49). Then B_h and $B_{h'}$ represent a barrier in Γ, since these bundles are already crossed once: There cannot be an edge $(u_x, w_{x'})$, where $x < h$ and $x' > h'$ (refer to the gray edge in Fig. 7.49), or where $x > h$ and $x' < h'$.

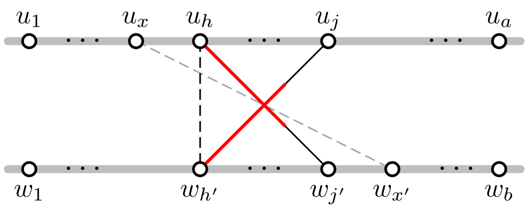

Fig. 7.49: Illustration for the proof of Thm. 7.47. The red segments represent a *UW*-bundle crossing; the dashed gray edge cannot be part of Γ.

We can assume that the edge $(u_h, w_{h'})$ is part of Γ, as otherwise we can add it in a planar way and obtain a drawing with more edges (see dashed black edge in Fig. 7.49).

Let $\Gamma_1 := [1, h \mid 1, h']$ and $\Gamma_2 := [h, a \mid h', b]$ be snippets of Γ. Further let n_i and m_i, where $i = 1, 2$, be the number of vertices and edges of Γ_i. The assumption $h > 1$ or $h' > 1$, and $h < a$ or $h' < b$ implies $n_i < n$, thus $m_i \leq \frac{17}{8}n_i - \frac{13}{4}$ by induction. For the number of vertices we have $n = n_1 + n_2 - 2$, since Γ_1 and Γ_2 share the vertices u_h and $u_{h'}$. Because the edge $(u_h, w_{h'})$ belongs to both, Γ_1 and Γ_2, the equation $m = m_1 + m_2 - 1$ holds for the number of edges. This yields

$$\begin{aligned} m &\leq \left(\tfrac{17}{8}n_1 - \tfrac{13}{4}\right) + \left(\tfrac{17}{8}n_2 - \tfrac{13}{4}\right) - 1 \\ &= \tfrac{17}{8}(n_1 + n_2) - \tfrac{13}{4} - \tfrac{17}{4} \\ &= \tfrac{17}{8}(n + 2) - \tfrac{13}{4} - \tfrac{17}{4} \\ &= \tfrac{17}{8}n + \tfrac{17}{4} - \tfrac{13}{4} - \tfrac{17}{4} \\ &= \tfrac{17}{8}n - \tfrac{13}{4}. \end{aligned}$$

Now suppose that $(h, h') = (1, 1)$ or $(h, h') = (a, b)$ holds for every choice of B_h and $B_{h'}$, that is, there are at most two *UW*-bundle crossings in Γ.

If Γ contains no triple $(u_h, w_{j'})$, $(u_i, w_{i'})$, $(u_j, w_{h'})$ for some $1 \leq h < i < j \leq a$ and $1 \leq h' < i' < j' \leq b$, then we obtain $m \leq 2n - 4$ by quasi-planarity and the statement follows.

On the other hand, if such a triple exists, then bundles anchored at u_h and $w_{h'}$ cross each other, or bundles anchored at u_j and $w_{j'}$ cross each other by Lemma 7.45. Assume without loss of generality the former. Then we have $h = h' = 1$; refer to Fig. 7.50a for an illustration. Further $a, b \geq 3$ and, since $n > 6$, at least one of a and b is larger than 3, say $b \geq 4$.

The crossings between $(u_i, w_{i'})$ and (u_j, w_1), and between $(u_i, w_{i'})$ and $(u_1, w_{j'})$ require bundle crossings of bundles anchored at u_i and u_j, and of bundles anchored

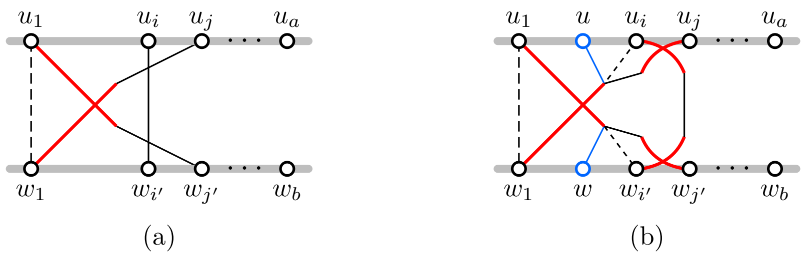

Fig. 7.50: (a) A UW-bundle crossing of bundles anchored at the leftmost vertices. (b) Bundle crossings between bundles anchored at u_i and u_j, and between bundles anchored at $w_{i'}$ and $w_{j'}$.

at $w_{i'}$ and $w_{j'}$, respectively (illustrated in Fig. 7.50b). Note that these two bundle crossings are even needed if the second UW-bundle crossing is present.

Vertex u_1 can only be adjacent to $w_1, w_{i'}, w_{j'}$ and possible degree-1 vertices between w_1 and $w_{i'}$ (colored blue in Fig. 7.50b). By assumption, Γ has no degree-1 vertex, so u_1 has at most 3 neighbors. Similarly, w_1 has at most 3 neighbors, and one of them is possibly u_1. Thus, there are at most 5 edges incident to $\{u_1, w_1\}$. Connectivity implies $u_i = u_2$, $u_j = u_3$, $w_{i'} = w_2$ and $w_{j'} = w_3$;

Let n' and m' be the number of vertices and edges of $\Gamma' := [2, a \mid 2, b]$. Then $n' = n - 2$ and $m' \geq m + 5$. If Γ' does not contain a triple of mutually crossing edges, we have $m' \leq 2n' - 4$ by quasi-planarity and consequently

$$m \leq m' + 5 \leq 2(n-2) - 4 + 5 = 2n - 3 \leq \tfrac{17}{8}n - \tfrac{13}{4}.$$

Otherwise, using the same arguments as above again for the drawing Γ', there is a triple (u_{a-2}, w_b), (u_{a-1}, w_{b-1}) and (u_a, w_{b-2}) of mutually crossing edges in Γ', a UW-bundle crossing between bundles anchored at u_a and w_b, and at most 5 edges are incident to $\{u_a, w_b\}$.

Let $n^\star$ and $m^\star$ be the vertices and edges of $\Gamma^\star := [2, a-1 \mid 2, b-1]$. Then $n^\star = n-4$ and $m^\star \geq m + 10$. Since Γ contains at most two UW-bundle crossings, $\Gamma^\star$ cannot contain a triple of mutually crossing edges by Lemma 7.45, hence

$$m \leq m^\star + 10 \leq 2n^\star - 4 + 10 = 2(n-4) + 6 = 2n - 2 \leq \tfrac{17}{8}n - \tfrac{13}{4}$$

for $n \geq 10$. It remains to study the cases $n \in \{7, 8, 9\}$.

The case $\mathbf{n = 7}$. Since $a \geq 3$ and $b \geq 4$, we have $(a, b) = (3, 4)$. We have already seen in Lemma 7.46 that $K_{3,4}$ is not $\mathcal{B}_2^=$-drawable, which implies that Γ has at most 11 edges. So $m \leq \frac{17}{8}n - \frac{13}{4}$ is satisfied.

The case n = 8. Since $\frac{17}{8}n - \frac{13}{4} = 13.75$, we have to show that Γ has at most 13 edges. Since $a \geq 3$ and $b \geq 4$, it suffices to consider $(a, b) \in \{(3, 5), (4, 4)\}$.

First assume that Γ represents a subgraph of $K_{3,5}$. By Lemma 7.46 there are values $1 \leq x \leq 3$ and $1 \leq x' \leq 5$, such that $(u_x, w_{x'})$ does not belong to Γ. Applying Lemma 7.46 to $\Gamma[V \setminus \{w_{x'}\}]$, which represents a subgraph of $K_{3,4}$, implies that there are values $1 \leq y \leq 3$ and $1 \leq y' \leq 5$, $y' \neq x'$, such that $(u_y, w_{y'})$ is not in Γ. We obtain that Γ has at most $3 \cdot 5 - 2 = 13$ edges.

Next assume that Γ represents a subgraph of $K_{4,4}$. By the arguments above, Γ contains the edges (u_1, w_3), (u_2, w_2), (u_3, w_1), (u_2, w_4), (u_3, w_3), and (u_4, w_2), and these edges must be routed like the black edges in Fig. 7.51a (refer also to Fig. 7.50b). Possible other edges are (u_1, w_1), (u_1, w_2), (u_2, w_1), (u_4, w_4), (u_4, w_3), (u_3, w_4), (u_2, w_3), and (u_3, w_2) (refer to the blue edges in Fig. 7.51a), which yields 14 edges in total. However, not both edges (u_2, w_3) and (u_3, w_2) can be in Γ, thus we have $m \leq 13$.

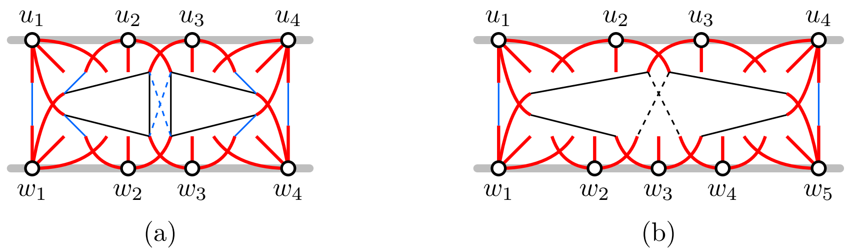

Fig. 7.51: (a) The case $n = 8$. Not both dashed blue edges can be in Γ. (b) The case $n = 9$. Not both dashed black edges can be in Γ.

The case n = 9. Since $\frac{17}{8}n - \frac{13}{4} = 15.875$, we have to show that Γ has at most 15 edges. Since $a \geq 3$ and $b \geq 4$, it suffices to consider $(a, b) \in \{(3, 6), (4, 5)\}$.

First assume that Γ represents a subgraph of $K_{3,6}$. Note that $K_{3,6}$ has 18 edges. Similar as in the case $n = 9$ (for $(a, b) = (3, 5)$) we obtain that Γ has at most $3 \cdot 6 - 3 = 15$ edges.

Next assume that Γ represents a subgraph of $K_{4,5}$. By the arguments above, Γ contains the edges (u_1, w_3), (u_2, w_2), (u_3, w_1), (u_2, w_5), (u_3, w_4), and (u_4, w_3), and these edges must be routed like the solid and dashed black edges in Fig. 7.51b. This is a contradiction to the properties of class $\mathcal{B}_2^{=}$, since the planar parts of (u_2, w_2) and (u_3, w_4) cross each other (refer to the dashed black edges in Fig. 7.51b). The statement follows. □

7.7 Characterizations of Complete Bipartite 2-Layer Graphs

In Chapter 5 we already provided several characterizations for complete bipartite graphs. However, many drawings that are valid $\mathcal{C}$-drawings for a bipartite graph class $\mathcal{C}$ become invalid when imposing the restriction on them that the vertices must be placed on two parallel layers. In contrast to drawings without this restriction, where large case analyses are most common when proving characterizations, it is much easier to derive such characterizations for the 2-layer setting. This stems from the fact that drawings of complete bipartite graphs on 2-layers are unique (up to isomorphism) for many graph classes. Also the density bounds for the number of edges[10] are a very helpful tool in showing that certain graphs do not belong to some 2-layer graph class. Our first lemma makes use of this tool.

Lemma 7.48. *The following negative results for complete bipartite graphs hold.*

(i) A graph class with edge density $\frac{3}{2}n - 2$ does not allow a drawing of $K_{2,3}$.

(ii) A graph class with edge density $\frac{5}{3}n - \frac{7}{3}$ does neither allow a drawing of $K_{2,4}$, nor a drawing of $K_{3,3}$.

(iii) A graph class with edge density $2n - 4$ does not allow a drawing of $K_{3,3}$.

(iv) A graph class with edge density $2n - 3$ or edge density $\frac{9}{4}n - \frac{9}{2}$ does not allow a drawing of $K_{3,4}$.

Proof. All claims follow by density arguments: The graph $K_{2,3}$ has $n = 5$ vertices and 6 edges, while the density of $\frac{3}{2}n - 2$ only allows 5 edges; the graph $K_{2,4}$ has $n = 6$ vertices and $8 > 7 = \frac{5}{3}n - \frac{7}{3}$ edges; the graph $K_{3,3}$ has $n = 6$ vertices and 9 edges, which exceeds $2n - 4 = 8$ and $\frac{5}{3}n - \frac{7}{3} = 7$; the graph $K_{3,4}$ has 7 vertices and 12 edges, which exceeds $2n - 3 = 11$ and $\frac{9}{4}n - \frac{9}{2} = 11.25$. □

We observe that the graph $K_{2,2}$ belongs to a certain graph class $\mathcal{C}^=$ if it is "more than planar", that is, if $\mathcal{C}^=$ allows at least one pair of crossing edges. Further, the graph $K_{1,b}$ is planar for every $b \geq 1$ and therefore belongs to every graph class beyond planarity. These two observations already provide partial characterizations for several 2-layer graph classes.

Recall that 2-layer 1-planar and 2-layer fan-crossing free graphs both have an edge density of $\frac{3}{2} - 2$, which yields, together with Lemma 7.48, the following theorem.

[10]Refer to Table 7.1 for the edge densities.

Theorem 7.49. *Let $\mathcal{C}^= \in \{\mathcal{P}_1^=, \mathcal{P}_{IC}^=, \mathcal{P}_{NIC}^=, \mathcal{X}^=\}$. Then, for $a \leq b$, the graph $K_{a,b}$ is $\mathcal{C}^=$-drawable, if and only if $a = 1$ or $a = b = 2$.*

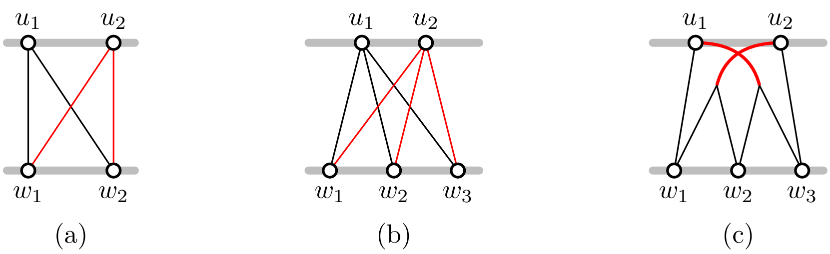

Fig. 7.52: (a) A 2-layer drawing of $K_{2,2}$. (b) A 2-layer drawing of $K_{2,3}$. (c) A 2-layer 1-sided fanbundle-planar drawing of $K_{2,3}$.

Proof. Since each of the classes in the theorem allows for one crossing, the graph $K_{2,2}$ belongs to them (refer also to Fig. 7.52a, which shows the unique $\mathcal{C}^=$-drawing of $K_{2,2}$). On the other hand, $K_{2,3}$ is not in $\mathcal{C}^=$ by Lemma 7.48, and by the fact that the classes of IC-planar and NIC-planar graphs are subclasses of the 1-planar graphs. □

Recall that for both, 2-layer 2-planar and 2-layer 1-sided fbp graphs, the edge density is $\frac{5}{3}n - \frac{7}{3}$. Moreover, it is not difficult to verify that $K_{2,3}$ belongs to a certain graph class. Thus, we can state the following theorem.

Theorem 7.50. *Let $\mathcal{C}^= \in \{\mathcal{P}_2^=, \mathcal{B}_1^=\}$. Then, for $a \leq b$, the graph $K_{a,b}$ is $\mathcal{C}^=$-drawable, if and only if $a = 1$ or $a = 2$ and $b \leq 3$.*

Proof. For both classes, the graph $K_{2,3}$ is drawable on two layers; refer to Figs. 7.52b and 7.52c. Further there exist no $\mathcal{C}^=$-drawings of $K_{2,4}$ or of $K_{3,3}$ by Lemma 7.48. The statement follows. □

In fact, in the 2-layer setting we are able to characterize complete bipartite k-planar graphs for every k.

Theorem 7.51. *For $a \leq b$, we have $K_{a,b} \in \mathcal{P}_k^=$ if and only if $k \geq (a-1)(b-1)$.*

Proof. Consider a 2-layer drawing Γ of $K_{a,b}$ (recall that such a drawing is unique up to isomorphism). Let $u_1, \ldots, u_a$ be the vertices on the top layer (in this order), and $w_1, \ldots, w_b$ the vertices on the bottom layer (in this order); see e. g. Fig. 7.53, which shows the case $a = 2$. The edge (u_1, w_b) (and also edge (u_a, w_1)) receives the most crossings, since it is crossed by all edges (u_i, w_j), where $2 \leq i \leq a$ and $1 \leq j \leq b-1$. This implies that Γ is 2-layer k-planar if and only if edge (u_1, w_b) has at most k crossings. The statement follows by the observation that (u_1, w_b) has $(a-1)(b-1)$ crossings. □

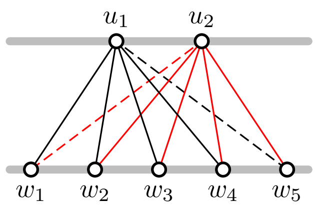

Fig. 7.53: The unique 2-layer drawing of $K_{2,5}$. It is 3-planar, but not 2-planar, since the dashed edges are crossed three times.

We apply Thm. 7.51 exemplary to the class of 2-layer 3-planar graphs.

Corollary 7.52. *For $a \leq b$ the graph $K_{a,b}$ is 2-layer 3-planar if and only if $a = 1$, or $a = 2$ and $b \leq 4$.*

Since Thm. 7.51 is used several times in Sec. 7.8 for $a = 2$, we formulate this case separately.

Corollary 7.53. *The graph $K_{2,b}$ belongs to $\mathcal{P}_k^=$ if and only if $b \leq k+1$. In particular, the graph $K_{2,k+2}$ is 2-layer $(k+1)$-planar but not 2-layer k-planar.*

Binucci et al. [39] gave $K_{2,n-2}$ as an example for an optimal 2-layer fan-planar graph. Since it is also quasi-planar (it consists of two fans, where each fan can be drawn planar), we obtain the following characterization.

Corollary 7.54. *For $a \leq b$ the graph $K_{a,b}$ is 2-layer fan-planar and 2-layer quasi-planar, if and only if $a \leq 2$.*

Proof. The edge density bounds of $2n - 4$ for 2-layer fan-planar and 2-layer quasi-planar graphs imply that $K_{3,3}$ does not belong to these classes (refer to Lemma 7.48). Together with Binucci's observation [39] the statement follows. □

The key to observe quasi-planarity for $K_{2,n-2}$ is the partitioning of a drawing in two planar parts. We generalize this concept to k-quasi-planar graphs, where $k \geq 3$.

Lemma 7.55. *Let Γ be a drawing of a graph with vertex set V and edge set E, and let $E_1, \ldots, E_{k-1}$ be a partition of E. Further, for $1 \leq i \leq k-1$, let Γ_i be the subdrawing consisting of V and E_i. If Γ_i is planar for every $1 \leq i \leq k-1$, then Γ is k-quasi-planar.*

Proof. For a contradiction suppose that Γ_i is planar for every $1 \leq i \leq k$ but Γ is not k-quasi-planar. Then there is a set $E' \subseteq E$ with size k whose edges cross each other pairwise. By the pigeonhole principle two edges $e_1, e_2 \in E'$ belong to the same subdrawing Γ_j for some $j \in \{1, \ldots, k-1\}$. Since e_1 and e_2 cross each other, this is a contradiction to the planarity of Γ_j. □

A consequence of Lemma 7.55 is that, for each $k \geq 3$ and each $b \geq 1$, the graph $K_{k-1,b}$ is 2-layer k-quasi-planar (the unique drawing of this graph consists of $k-1$ fans, see Fig. 7.54a). On the other hand, the graph $K_{k,k}$ is not k-quasi-planar, since the edges $(u_1, w_k), (u_2, w_{k-1}), (u_3, w_{k-2}), \ldots, (u_k, w_1)$ are a set of k pairwise crossing edges in its (unique) drawing (refer to Fig. 7.54b). Thus we obtain the following theorem.

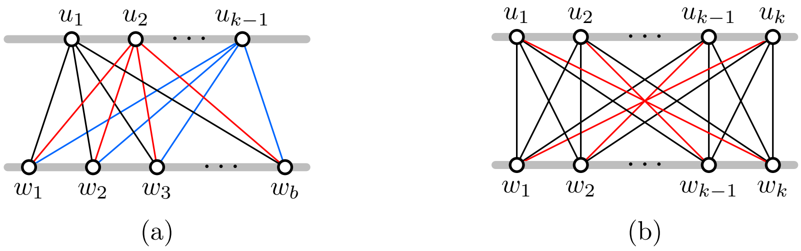

Fig. 7.54: (a) A 2-layer k-quasi-planar drawing of $K_{k-1,b}$; the different colors show a partitioning into $k-1$ planar subdrawings, each of them is a fan. (b) The unique 2-layer drawing of $K_{k,k}$. The red edges form a set of k pairwise crossing edges.

Theorem 7.56. *For $a \leq b$ the graph $K_{a,b}$ is 2-layer k-quasi-planar if and only if $a \leq k-1$.*

We are also able to characterize 2-layer gap-planar graphs, by means of the crossing graph and the fact that such graphs have at most $2n-4$ edges.

Theorem 7.57. *For $a \leq b$ the graph $K_{a,b}$ is 2-layer gap-planar if and only if $a = 1$ or $a = 2$ and $b \leq 4$.*

Proof. The drawing of $K_{2,4}$ in Fig. 7.55a is 2-layer gap-planar. Graph $K_{2,5}$ is not gap-planar, since the crossing graph of the unique drawing (i. e. unique when not considering gaps) of this graph is not a pseudo-forest (refer to Fig. 7.55b). By Lemma 7.48, graph $K_{3,3}$ is not gap-planar, which concludes the proof. □

For 2d-layer 2-sided fanbundle-planar graphs there exists already a characterization (see [126, Theorem 8.4]). The 2d-layer 2-sided fbp drawing for $K_{2,6}$ can also be found in Fig. 7.56a.

Theorem 7.58 ([126])**.** *For $a \leq b$, the graph $K_{a,b}$ is 2d-layer 2-sided fanbundle-planar if and only if $a = 1$ or $a = 2$ and $b \leq 6$.*

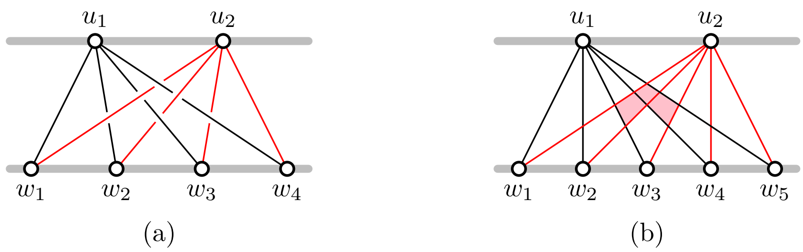

Fig. 7.55: (a) A 2-layer gap-planar drawing of $K_{2,4}$. (b) The unique straight-line 2-layer drawing of $K_{2,5}$. The red area indicates cycles in the crossing graph.

Recall that, in 2-layer 2-sided fbp graphs we additionally allow that bundles anchored at vertices of different layers may cross. Although this definition is only slightly different than the one of 2d-layer 2-sided fbp graphs, we could observe that 2-layer 2-sided fbp graphs have a higher edge density. The next theorem shows that the latter graph class also allows drawings for complete bipartite graphs with a larger number of vertices.

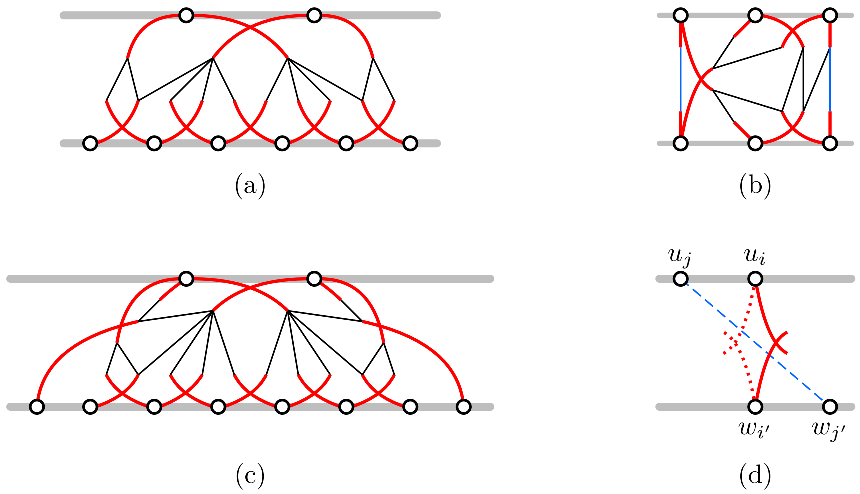

Fig. 7.56: (a) A 2d-layer 2-sided 1-fbp drawing of $K_{2,6}$. (b) A 2-layer 2-sided 1-fbp drawing of $K_{3,3}$. (c) A 2-layer 2-sided 1-fbp drawing of $K_{2,8}$. (d) Illustration of the barrier property for two crossing bundles anchored at different layers.

Theorem 7.59. *For $a \le b$ the graph $K_{a,b}$ is 2-layer 2-sided fanbundle-planar if and only if $a = 1$, or $a = 2$ and $b \le 8$, or $a = b = 3$.*

Proof. By Lemma 7.46, the graph $K_{3,4}$ does not belong to $\mathcal{B}_2^{=}$, while Figs. 7.56b and 7.56c depict $\mathcal{B}_2^{=}$-drawings of $K_{2,8}$ and $K_{3,3}$, respectively.

It remains to show that $K_{2,9}$ is not 2-layer 2-sided fbp. For a contradiction assume that there is such a drawing Γ of $K_{2,9}$. Suppose that in Γ two bundles B and B' cross, where B is anchored at u_i for $i \in \{1, 2\}$, and B' is anchored at $w_{i'}$ for some $1 \le i' \le 9$. Note that, since B and B' are already crossed and may not be crossed by another bundle, they represent a "barrier" in Γ in the following sense: There cannot be an edge $(u_j, w_{j'})$, such that $j < i$ and $j' > i'$, or such that $j > i$ and $j' < i'$ (refer to the dashed blue edge in Fig. 7.56d). Thus, if $(i, i') \notin \{(1,1), (2,9)\}$, it is not possible to draw all edges.

As a consequence we can assume that, if there are crossing bundles anchored at vertices of different layers, then they are anchored at u_1 and w_1, or at u_2 and w_9. Consider the subdrawing $\Gamma' = [1, 2 \mid 2, 8]$ of Γ. It is a 2-layer 2-sided fbp drawing of $K_{2,7}$ with the property that only bundles anchored at vertices of the same layer cross; hence, it is a 2d-layer 2-sided fbp drawing of $K_{2,7}$ – a contradiction to Thm. 7.58. It follows that $K_{2,9}$ cannot belong to the class of 2-layer 2-sided fbp graphs. $\square$

In Table 7.2 we give an overview of the characterizations of complete bipartite 2-layer graphs. On one side, the results in this section are of interest in itself and can help to decide whether certain graphs are $\mathcal{C}^{=}$-drawable. On the other side, they will help us to recognize how different 2-layer graph classes are related in Sec. 7.8.

Table 7.2: Characterizations for complete bipartite graphs $K_{a,b}$ (where $a \leq b$) in 2-layer drawings for several graph classes. Stated are values for b, given $a = 2$, $a = 3$, and $a \geq 4$. If no drawing exists for $b \geq a$, the corresponding entry is "–" (in words: minus). Question marks indicate that the characterization is still open.

Class	$a = 2$	$a = 3$	$a \geq 4$
1-planar	$b \leq 2$	–	–
2-planar	$b \leq 3$	–	–
3-planar	$b \leq 4$	–	–
4-planar	$b \leq 5$	$b \leq 3$	–
5-planar	$b \leq 6$	$b \leq 3$	–
k-planar	$b \leq 1 + k$	$b \leq 1 + \frac{k}{2}$	$b \leq 1 + \frac{k}{a-1}$
IC-planar	$b \leq 2$	–	–
NIC-planar	$b \leq 2$	–	–
3-quasi-planar	all b	–	–
4-quasi-planar	all b	all b	–
fan-planar	all b	–	–
fan-cr. free	$b \leq 2$	–	–
1-gap-planar	$b \leq 4$	–	–
k-gap-planar	$b \leq 2k + 2$?	?	?
1-sided 1-fbp	$b \leq 3$	–	–
2-sided 1-fbp	$b \leq 8$	$b \leq 3$	–
2d-layer 2-sided 1-fbp	$b \leq 6$	–	–

7.8 Relationships Between 2-Layer Beyond Planarity Graph Classes

In this section we study how the graph classes considered in this chapter are related. As already mentioned at the beginning of the chapter, in the 2-layer setting every RAC graph is fan-crossing free and vice versa [56]. For this reason, we only consider fan-crossing free graphs in the following.

An easy observation is that the class of planar graphs is a subclass of all other graph classes. Further, if there is a graph G that belongs to a certain graph class $\mathcal{C}_1$, but not to another class $\mathcal{C}_2$, it follows that $\mathcal{C}_1 \not\subset \mathcal{C}_2$. Using this argument, the characterizations from Sec. 7.7 (see also Table 7.2) yield that, if a certain complete bipartite graph $K_{a,b}$ (for some a and b) is in class $\mathcal{C}_1^=$, but not in $\mathcal{C}_2^=$, then $\mathcal{C}_1^= \not\subset \mathcal{C}_2^=$. The following corollary summarizes the implications of the results from Sec. 7.7.

Corollary 7.60. *By the characterizations of complete bipartite graphs the following holds (thereby the graph which causes the separation of the classes is in parenthesis).*

(a) *If* $\mathcal{C}^= \in \{\mathcal{P}_k^=, \mathcal{X}^=, \mathcal{G}^=, \mathcal{B}_1^=, \mathcal{B}_{2d}^=, \mathcal{B}_2^=\}$*, where* $k \geq 1$*, we have* $\mathcal{F}^= \not\subset \mathcal{C}^=$ *and* $\mathcal{Q}^= \not\subset \mathcal{C}^=$ *(graph* $K_{2,n}$*).*

(b) *If* $\mathcal{C}^= \in \{\mathcal{P}_k^=, \mathcal{B}_2^=\}$*, where* $k \geq 4$*, we have* $\mathcal{C}^= \not\subset \mathcal{F}^=$ *and* $\mathcal{C}^= \not\subset \mathcal{Q}^=$ *(graph* $K_{3,3}$*).*

(c) *For* $k \geq 2$ *we have* $\mathcal{P}_k^= \not\subset \mathcal{X}^=$ *(graph* $K_{2,3}$*).*

(d) *If* $\mathcal{C}^= \in \{\mathcal{P}_1^=, \mathcal{P}_2^=, \mathcal{X}^=, \mathcal{B}_1^=\}$*, we have* $\mathcal{G}^= \not\subset \mathcal{C}^=$ *(graph* $K_{2,4}$*).*

(e) *For* $k \geq 3$ *we have* $\mathcal{P}_k^= \not\subset \mathcal{B}_1^=$ *(graph* $K_{2,4}$*); also* $\mathcal{B}_1^= \not\subset \mathcal{P}_1^=$ *(graph* $K_{2,2}$*).*

(f) *For* $k \geq 6$ *we have* $\mathcal{P}_k^= \not\subset \mathcal{B}_2^=$ *(graph* $K_{3,4}$*), and for* $k \geq 4$ *we have* $\mathcal{P}_k^= \not\subset \mathcal{B}_{2d}^=$ *(graph* $K_{3,3}$*).*

(g) *If* $\mathcal{C}^= \in \{\mathcal{P}_k^=, \mathcal{X}^=, \mathcal{G}^=, \mathcal{B}_1^=, \mathcal{B}_{2d}^=\}$*, where* $k \leq 6$*, we have* $\mathcal{B}_2^= \not\subset \mathcal{C}^=$ *(graph* $K_{2,8}$*).*

(h) *If* $\mathcal{C}^= \in \{\mathcal{P}_k^=, \mathcal{X}^=, \mathcal{G}^=, \mathcal{B}_1^=\}$*, where* $k \leq 4$*, we have* $\mathcal{B}_{2d}^= \not\subset \mathcal{C}^=$ *(graph* $K_{2,6}$*).*

In this section we provide more results in this direction. We remark that corresponding results for general graphs (without the restriction of placing the vertices on two parallel lines) are known; for an overview refer to [61].

7.8.1 k-planar graphs

We start with the study of k-planar graphs and their relationship with themselves, that is with k'-planar graphs for $k' \geq k$. The result concerning these classes is not surprising: k-planar graphs are contained in the $(k+1)$-planar graphs.

Theorem 7.61. *In the 2-layer setting, the class of k-planar graphs is a proper subclass of the class of $(k+1)$-planar graphs for every $k \geq 1$.*

Proof. Clearly the k-planar graphs are a subclass of the $(k+1)$-planar graphs. By Cor. 7.53, the graph $K_{2,k+2}$ is $(k+1)$-planar, but not k-planar. The statement follows. □

7.8.2 k-quasi-planar graphs

Between k-quasi-planar and k'-quasi-planar graphs, where $k' \geq k$, the relationship is analogically to the one among k-planar graphs.

Theorem 7.62. *The relation $\mathcal{Q}_k^{=} \subsetneq \mathcal{Q}_{k+1}^{=}$ holds for every $k \geq 1$.*

Proof. By definition $\mathcal{Q}_k^{=} \subseteq \mathcal{Q}_{k+1}^{=}$ hold. Now consider the unique drawing Γ of $K_{k,k}$. It is $(k+1)$-quasi-planar, since its edges consist of k disjoint sets $V_i := \{(u_i, w_j) \mid 1 \leq j \leq k\}$, $i = 1, \ldots, k$, where each subdrawing $\Gamma[V_i]$ of Γ is planar; thus, only edges belonging to different sets V_i, V_j, $i \neq j$ may cross, which yields at most k mutually crossing edges. On the other hand, the k edges $(u_1, w_k), (u_2, w_{k-1}), (u_3, w_{k-2}), \ldots, (u_k, w_1)$ are mutually crossing in Γ, which shows that $K_{k,k}$ is not k-quasi-planar. □

For k-gap-planar and $(k+1)$-gap-planar graphs a corresponding theorem is true. However, we postpone it, since we first need to provide the tools to prove such a result.

7.8.3 k-planar and k-gap-planar graphs

We compare k-planar graphs and k'-gap-planar graphs for appropriate k'. For general graphs Bae et al. [30] showed that $(2k)$-planar graphs are a proper subclass of k-gap-planar graphs. However, while their construction to prove the "proper" part works for general graphs, it cannot be applied to the 2-layer model. Hence, we have to provide another construction for our case.

Lemma 7.63. *For every $k \geq 1$, the graph $K_{2,2k+2}$ is k-gap-planar.*

Proof. We start by considering the case $k = 1$ explicitly. Let Γ_1 be the unique drawing of $K_{2,4}$. We distribute the crossings of Γ_1 as follows:

– The crossing of (u_1, w_2) and (u_2, w_1) is assigned to (u_1, w_2);

– the crossing of (u_1, w_3) and (u_2, w_1) is assigned to (u_1, w_3);

– the crossing of (u_1, w_3) and (u_2, w_2) is assigned to (u_2, w_2);

– the crossing of (u_1, w_4) and (u_2, w_1) is assigned to (u_2, w_1);

– the crossing of (u_1, w_4) and (u_2, w_2) is assigned to (u_1, w_4);

– the crossing of (u_1, w_4) and (u_2, w_3) is assigned to (u_2, w_3).

Then no edge has more than one crossing assigned to it (as usually, we refer to it as a "gap"), hence Γ_1 is 1-gap-planar (for an illustration see Fig. 7.57a).

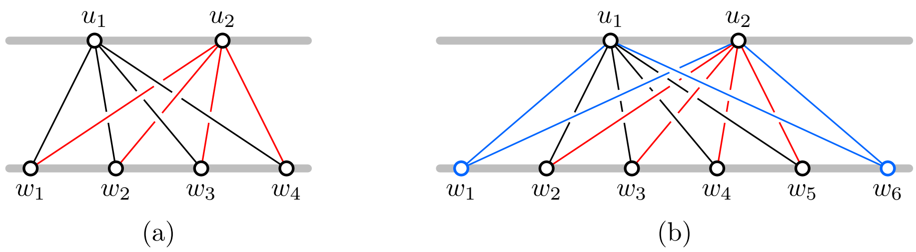

Fig. 7.57: Illustration for the proof of Lemma 7.63. (a) A 2-layer 1-gap-planar drawing of $K_{2,4}$. (b) A 2-layer 2-gap-planar drawing of $K_{2,6}$.

Next we construct a 2-layer 2-gap-planar drawing Γ_2 of $K_{2,6}$. In order to do this, we augment Γ_1 in several steps.

(1) First rename $w_1, \ldots, w_4$ to $w_2, \ldots, w_5$.

(2) In the next step, add a new vertex w_1 that is placed left of w_2, and a new vertex w_6 that is placed right of w_5 on the bottom layer (refer to the blue vertices in Fig. 7.57b). Also add the crossing-free edges (u_1, w_1) and (u_2, w_2).

(3) Now we add the edge (u_2, w_1) (colored blue in Fig. 7.57b) and assign each crossing of this edge to the other edge participating in the crossing; that is, each of (u_1, w_2), (u_1, w_3), (u_1, w_4) and (u_1, w_5) receives (another) gap. Since these edges had at most one gap before this operation (recall that they were part of the 1-gap-planar drawing Γ_1), they now have at most two gaps. Note that currently the new edge (u_2, w_1) has no gap at all. Further note that we did not touch any of the edges (u_2, w_2), (u_2, w_3), (u_2, w_4) and (u_2, w_5), which implies that each of them still has at most one gap.

(4) Finally we add edge (u_1, w_6), which has crossings with $(u_2, w_1), \dots, (u_2, w_5)$. Again we assign each crossing of (u_1, w_6) to the other edge participating in this crossing. By the same arguments as above, it follows that the number of crossings is not more than two for each such edge. Therefore the drawing Γ_2 of $K_{2,6}$, which we obtain in the end, is 2-gap-planar.

We stress that in the creation of Γ_2, each edge in Γ_1 received exactly one more gap; out of the four new edges (the blue edges in Fig. 7.57b), only the edge (u_2, w_1) received a gap, while the others are gap-free. Also, the construction does not depend on the number of vertices that are on the bottom layer in Γ_1, but only on the property that Γ_1 is a $\mathcal{G}_1^=$-drawing with 2 vertices on the top layer. As a consequence, by applying our construction algorithm to Γ_2 (adapted to the different number of vertices on the bottom layer), we obtain a drawing Γ_3 of $K_{2,8}$ that belongs to $\mathcal{G}_3^=$.

We conclude that, if we start with a $\mathcal{G}_k^=$-drawing Γ_k of $K_{2,2k+2}$, our construction algorithm creates a $\mathcal{G}_{k+1}^=$-drawing Γ_{k+1} of $K_{2,2(k+1)+2}$. The statement follows. □

With the construction of Lemma 7.63 we have the means to prove a theorem about the relationship between 2-layer k-gap-planar and 2-layer k-planar graphs, corresponding to the one Bae et al. showed for these graph classes in the general case [30].

Theorem 7.64. *The relation $\mathcal{P}_{2k}^= \subsetneq \mathcal{G}_k^=$ holds for every $k \geq 1$.*

Proof. By Bae et al. [30], general $2k$-planar graphs are a proper subclass of k-gap-planar graphs. Since they showed in fact a stronger result, namely that every $2k$-planar *drawing* is k-gap-planar, the relation $\mathcal{P}_{2k}^= \subseteq \mathcal{G}_k^=$ follows immediately. On the other hand, for $k \geq 1$, the graph $K_{2,2k+2}$ belongs to $\mathcal{G}_k^=$ by Lemma 7.63, but not to $\mathcal{P}_{2k}^=$ by Cor. 7.53. This proves that $\mathcal{P}_{2k}^=$ is a proper subclass of $\mathcal{G}_k^=$. □

Since, by Thm. 7.64, the 2-layer $(2k)$-planar graphs form a subclass of k-gap-planar graphs, the question arises, what the relation between 2-layer $(2k+1)$-planar and k-gap-planar graphs is. The next lemma answers this question partly.

Lemma 7.65. *For every $k \geq 1$ there is a 2-layer k-gap-planar graph that is not 2-layer $(2k+1)$-planar.*

Proof. According to Lemma 7.63, the graph $K_{2,2k+2}$ is 2-layer k-gap-planar. Further it has a unique 2-layer drawing (without taking the gaps into account). We create two copies $H_1 = (U_1 \dot\cup W_1, E_1)$ and $H_2 = (U_2 \dot\cup W_2, E_2)$ of this graph. Let $U_1 = \{u_1, u_2\}$, $W_1 = \{w_1, \dots, w_{2k+2}\}$, $U_2 = \{u_{k+4}, u_{k+5}\}$, and $W_2 = \{w_{3k+4}, \dots, w_{5k+5}\}$. We construct a graph $G = (U \dot\cup W, E)$ as follows (the case $k = 1$ is illustrated in Fig. 7.58):

$$\begin{aligned} U &:= U_1 \cup U_2 \cup \{u_3, \dots, u_{k+3}\}, \\ W &:= W_1 \cup W_2 \cup \{w_{2k+3}, \dots, w_{3k+3}\} \text{ and} \\ E &:= E_1 \cup E_2 \cup E_3 \cup \{(u_2, w_{2k+3}), (u_{k+4}, w_{2k+2})\}, \text{ where} \\ E_3 &:= \{(u_i, w_{2k+i}), (u_i, w_{2k+i+1}) \mid 3 \le i \le k+3\}. \end{aligned}$$

In order to create a k-gap-planar drawing Γ of G, we place a k-gap-planar drawing of H_1 to the left of a k-gap-planar drawing of H_2, such that u_2 and w_{2k+2} are the rightmost vertices of U_1 and W_1, and u_{k+4} and w_{3k+4} are the leftmost vertices of U_2 and W_2. Further, we place $u_3, \dots, u_{k+3}$ in this left-to-right order on the top layer of Γ between u_2 and u_{k+4}, and $w_{2k+3}, \dots, w_{3k+3}$ in this left-to-right order on the bottom layer of Γ between w_{2k+2} and w_{3k+4}. Then each of the edges in $E' := E_3 \cup \{(u_2, w_{2k+3})\}$ has exactly one crossing in Γ, namely a crossing with the edge $e := (u_{k+4}, w_{2k+2})$, and apart from crossings between edges of E_1 and between edges of E_2, these are all crossings in Γ. We assign the crossing of each edge $e' \in E'$ with e to e', which yields a 2-layer k-gap-planar drawing Γ.

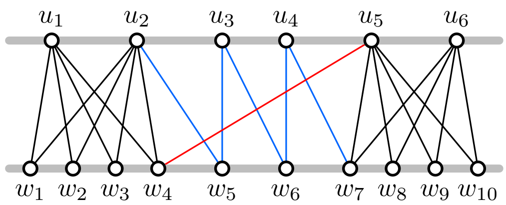

Fig. 7.58: Illustration for Lemma 7.65 in the case $k = 1$: A 2-layer 1-gap-planar drawing Γ of the graph G.

It remains to show that G is not in $\mathcal{P}^{=}_{2k+1}$. Assume to the contrary that there is a $\mathcal{P}^{=}_{2k+1}$-drawing Γ' of G. First note that the (up to isomorphism) unique drawing Γ_1 of H_1 in Γ has edges that are already fully crossed, and these edges do not allow for any vertex $v \in U \setminus (U_1 \cup W_1)$ to be placed "inside" Γ_1, that is, all vertices $v \in U \setminus (U_1 \cup W_1)$ must be placed either left of the leftmost vertex of Γ_1, or right of the rightmost vertex of Γ_1. Similarly, no vertex $v \in U \setminus (U_2 \cup W_2)$ can be placed "inside" Γ_2. We assume without loss of generality that Γ_1 is entirely to the left of Γ_2. Because of the edge (u_{k+4}, w_{2k+2}) (refer to the red edge in Fig. 7.58) and the path between u_2 and w_{3k+4} (refer to the blue path in Fig. 7.58), vertices u_2 and w_{2k+2} must be the rightmost vertices of Γ_1, and vertices u_{k+4} and w_{3k+4} must be the leftmost vertices of Γ_2. But then the edge (u_{k+4}, w_{2k+2}) receives a crossing from each of the $2k + 3$ edges in the set $E' = E_3 \cup \{(u_2, w_{2k+3})\}$ – a contradiction to $(2k + 1)$-planarity. $\square$

Lemma 7.65 shows that the class of 2-layer k-gap-planar graphs $\mathcal{G}_k^{=}$ is not included in $\mathcal{P}_{2k+1}^{=}$. However, we were not able to find a 2-layer $(2k+1)$-planar graph that is not 2-layer k-gap-planar. So the question if $\mathcal{P}_{2k+1}^{=} \subseteq \mathcal{G}_k^{=}$ remains open for general k. But at least for $k = 1$ we can answer this question in the negative.

Lemma 7.66. *There is a graph that is 2-layer 3-planar and 2-layer quasi-planar, but not 2-layer gap-planar.*

Proof. Consider the graph $G = (U \dot{\cup} W, E)$ defined by drawing Γ in Fig. 7.59. Note that Γ is 2-layer 3-planar and 2-layer quasi-planar. It remains to show that there exists no 2-layer gap-planar embedding of G.

For a contradiction assume that there exists a 2-layer gap-planar drawing Γ' of G. In our arguments we use the fact that the crossing graph $X(\Gamma')$ of Γ' is a pseudo forest [30], i. e. each connected component of $X(\Gamma')$ contains at most one cycle.

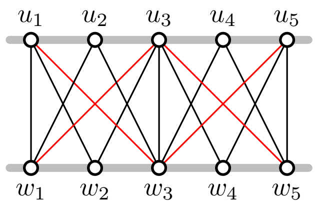

Fig. 7.59: A 2-layer drawing Γ of graph G, which is 3-planar and quasi-planar at the same time.

Both vertices u_3 and w_3 have degree 5. We differentiate between the "directions", in which the edges incident to them can point (thereby we neglect symmetric cases).

– Suppose u_1, u_2, u_4 and u_5 are placed right of u_3, while w_1, w_2, w_4 and w_5 are placed left of w_3 (refer to Fig. 7.60a).

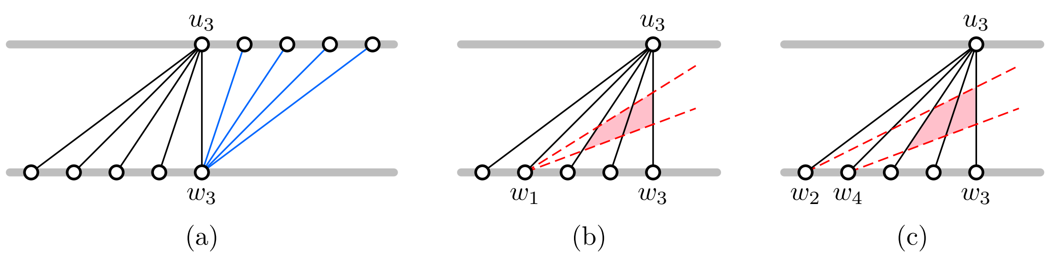

Fig. 7.60: Illustration for the proof of Lemma 7.66. (a) The case where the vertices u_1, u_2, u_4 and u_5 are right of u_3, while w_1, w_2, w_4 and w_5 are left of w_3. (b) The situation when w_1 or w_5 belongs to the two leftmost vertices. (c) The situation when w_2 and w_4 are the two leftmost vertices.

Assume that w_1 is one of the two leftmost vertices on the bottom layer of Γ' (see Fig. 7.60b). In this case the edges (u_1, w_1) and (u_2, w_1) cause two cycles in the crossing graph $X(\Gamma')$, no matter how the other vertices are placed (refer to the red area in Fig. 7.60b); a contradiction to gap-planarity. So w_1 cannot be one of the two leftmost vertices on the bottom layer. By the same argument, w_5 cannot be one of the two leftmost vertices on the bottom layer. Thus, w_2 and w_4 are the two leftmost vertices on the bottom layer. But then again, there are two edges, namely (u_1, w_2) and (u_5, w_4), that cause at least two cycles in the crossing graph $X(\Gamma')$ (refer to the red area in Fig. 7.60c), contradicting gap-planarity. We conclude that this configuration is not leading to a 2-layer gap-planar drawing of G.

– Suppose that exactly one of u_1, u_2, u_4 and u_5 is placed left of u_3, while three of them are right of u_3. Placing two or more of the vertices w_1, w_2, w_4, w_5 right of w_3 yields immediately two cycles in the crossing graph $X(\Gamma')$ (refer to Fig. 7.61a). Thus, there is exactly one such vertex placed to the right of w_3, while the others are placed left of w_3 (see Fig. 7.61b).

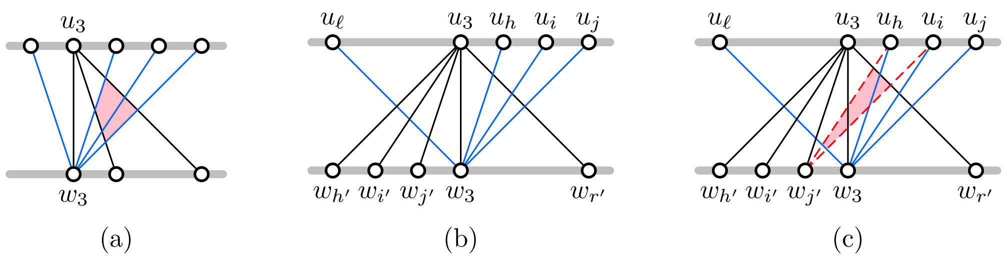

Fig. 7.61: Illustration for the proof of Lemma 7.66. (a) The case where three of the vertices u_1, u_2, u_4, u_5 are right of u_3, and two vertices of w_1, w_2, w_4, w_5 are right of w_3. (b) The situation when exactly one of the vertices u_1, u_2, u_4, u_5 is left of u_3, and exactly one of w_1, w_2, w_4, w_5 is right of w_3. (c) No two edges can cross (u_3, w_3).

Let the vertices be denoted as in Fig. 7.61b. We observe the following for a gap-planar drawing Γ':

($\sharp$) There is at most one edge (u, w) in Γ, where $u \in \{u_h, u_i, u_j\}$ and $w \in \{w_{h'}, w_{i'}, w_{j'}\}$.

The reason for this is the following: Each such edge crosses (u_ℓ, w_3), (u_3, w_3), and $(u_3, w_{r'})$; this yields at least two cycles in a single component of the crossing graph, contradicting the properties of gap-planar graphs (see also Fig. 7.61c).

Since there are edges (u_1, w_1) and (u_1, w_2) in G, as well as edges (u_5, w_4) and (u_5, w_5), not both vertices u_1 and u_5 can belong to $\{u_h, u_i, u_j\}$ by ($\sharp$). We assume without loss of generality that $u_\ell = u_1$. Then $\{u_h, u_i, u_j\} = \{u_2, u_4, u_5\}$. Again by ($\sharp$), the existence of (u_4, w_5) and (u_5, w_5) imply that $w_{r'} = w_5$. As a consequence, we have $\{w_{h'}, w_{i'}, u_{j'}\} = \{w_1, w_2, w_4\}$. But now the edges (u_2, w_1) and (u_5, w_4) violate ($\sharp$).

– Finally suppose that exactly two of the vertices u_1, u_2, u_4 and u_5 are placed left of u_3. Now placing three or more of the vertices w_1, w_2, w_4, w_5 right (or left) of w_3 yields immediately two cycles in the crossing graph $X(\Gamma')$ (refer also to Fig. 7.61a, which shows a symmetric case). Thus, there are also exactly two of w_1, w_2, w_4, w_5 placed to the right of w_3 (see Fig. 7.62a).

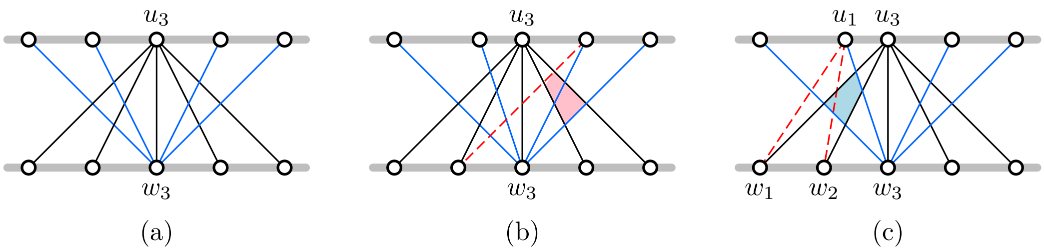

Fig. 7.62: Illustration for the proof of Lemma 7.66. (a) The case where exactly two of the vertices u_1, u_2, u_4, u_5 are right of u_3, and exactly two vertices of w_1, w_2, w_4, w_5 are right of w_3. (b) A crossing of (u_3, w_3) yields two cycles in the crossing graph. (c) The situation when u_1 is the second vertex on the top layer.

No edge in Γ' can cross (u_3, w_3), otherwise the crossing graph $X(\Gamma')$ is not a pseudo forest (refer to the red area in Fig. 7.62b). Without loss of generality we can assume that u_1 is right of u_3. Then the existence of edges (u_1, w_1) and (u_1, w_2) imply that w_1 and w_2 are left of w_3, and further, the existence of edge (u_2, w_1) yields that also u_2 is left of u_3.

If not both vertices u_1 and w_1 are the leftmost vertices on the top and bottom layer respectively, gap-planarity is violated (refer to the blue area in Fig. 7.62c). By symmetry we obtain that u_5 and w_5 are the rightmost vertices on the top and bottom layer, respectively. This yields exactly the drawing from Fig. 7.59, which is not gap-planar.

We conclude that the graph G is not gap-planar. □

By combining Lemma 7.65 and Lemma 7.66, we obtain the following theorem.

Theorem 7.67. *The classes $\mathcal{P}_3^=$ and $\mathcal{G}^=$ are incomparable.*

Another result regarding k-planar and k-gap-planar graphs is the following consequence of Cor. 7.53.

Corollary 7.68. *In the 2-layer setting, $(4k+1)$-planar graphs are not a subclass of k-gap-planar graphs.*

Proof. By Cor. 7.53 the graph $G := K_{2,4k+2}$ belongs to $\mathcal{P}^{=}_{4k+1}$. We show that G is not 2-layer k-gap-planar.

Let Γ be the unique drawing of $G = (U \,\dot{\cup}\, W, E)$, where $U = \{u_1, u_2\}$ are the vertices of the top layer and $W = \{w_1, \ldots, w_{4k+2}\}$ are the vertices on the bottom layer, in this order.

We count the crossings in Γ. Since edges incident to u_2 only cross edges incident to u_1, it suffices to count the crossings of edges incident to u_1. Edge (u_1, w_1) is crossing free; edge (u_1, w_2) has one crossing; edge (u_1, w_3) has two crossings; and in general, for $1 \leq i \leq 4k+2$, edge (u_1, w_i) has exactly $i-1$ crossings. So the number of crossings in G is $cr(G) = \frac{1}{2}(4k+1)(4k+2)$.

The number of crossings in k-gap-planar graphs is upper bounded by $k|E|$; refer to [30]. Here we have $k|E| = 2k(4k+2) < cr(G)$, which yields that G is not k-gap-planar. □

7.8.4 k-gap-planar graphs

We compare the classes of 2-layer k-gap-planar and 2-layer k'-gap-planar graphs, where $k' \geq k$.

Theorem 7.69. *For every $k \geq 1$ we have $\mathcal{G}^{=}_{k} \subsetneq \mathcal{G}^{=}_{k+1}$.*

Proof. By definition each k-gap-planar graph is $(k+1)$-gap-planar. It remains to show that there is a 2-layer $(k+1)$-gap planar graph that is not 2-layer k-gap-planar.

We know that $K_{2,2k+2}$ is 2-layer k-gap-planar (see Lemma 7.65), while $K_{2,4k+2}$ is not (refer to Cor. 7.68). As a consequence, there is an $x \in \{2k+2, \ldots, 4k+1\}$ such that $K_{2,x}$ is k-gap-planar, and $K_{2,x+1}$ is not. With a similar construction as in Lemma 7.65 it follows that $K_{2,x+1}$ (and even $K_{2,x+2}$) is $(k+1)$-gap-planar. □

7.8.5 k-planar and fan-planar graphs

Concerning general graphs, Binucci et al. [39] showed that for $k \geq 1$ there exist graphs which are fan-planar but not k-planar, and that for $k \geq 2$ there exists graphs which are k-planar but not fan-planar. However, their constructions are not tailored for the 2-layer setting and hence we can not apply them here.

Even so, from Cor. 7.60 we know already that 2-layer fan-planar graphs are not 2-layer k-planar for $k \geq 1$, while 2-layer k-planar graphs are not 2-layer fan-planar for $k \geq 4$. We improve the latter result by showing that even 2-layer 2-planar graphs are not necessarily 2-layer fan-planar.

Lemma 7.70. *There exist a graph that is both, 2-layer 2-planar and 2-layer quasi-planar, but not 2-layer fan-planar.*

Proof. Consider the bipartite graph $H = (U \dot{\cup} W, E)$, where $U = \{u_1, u_2, u_3, u_4\}$, $W = \{w_1, w_2, w_3, w_4\}$, and E consists of the edges (u_1, w_1), (u_1, w_2), (u_2, w_1), (u_2, w_3), (u_3, w_1), (u_3, w_4), (u_4, w_2), (u_4, w_3), and (u_4, w_4). Figure 7.63a shows a 2-layer drawing for H that is 2-planar and quasi-planar.

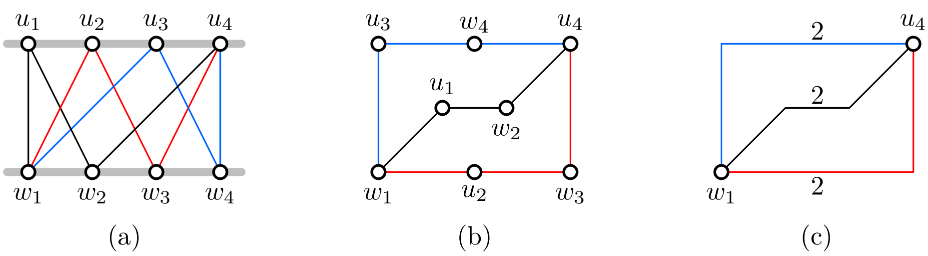

Fig. 7.63: Illustration for the proof of Lemma 7.70. (a) A 2-layer drawing of H that is 2-planar and quasi-planar. (b) A planar drawing of H; the three maximal degree-2 chains are colored differently. (c) A planar drawing of H' with the weights of the edges.

It remains to show that graph H is not 2-layer fan-planar. Note that H is biconnected. According to Binucci et al. [38], a biconnected graph G is 2-layer fan-planar if and only if it is a spanning subgraph of a snake.[11]

Binucci et al. [38] also gave another characterization for 2-layer fan-planar graphs. They consider chains $p = (v_0, v_1, \ldots, v_j, v_{j+1})$ of a graph G, such that every vertex $v_1, \ldots, v_j$ has degree 2, and p is a maximal path in G with this property. A weighted multi-graph G' is created from G, by contracting each such chain to an edge with weight j. Edges of G' that are also in G get a weight of 0. For our purpose, it is enough to consider one necessary condition of Binucci's characterization:

> *Let G be a bipartite biconnected graph that is not a simple cycle. If G is a spanning subgraph of a snake, then there exists an embedding of G' such that all edges of G' with weight at least 2 are on the external face.*

In Fig. 7.63c, one embedding of H' is shown. Clearly, in every one of the three embeddings (each face can be the outer face) of H', there is an edge of weight 2 that is not on the external face. Thus, H is not fan-planar. The statement follows. □

Now we are able to describe the relation between k-planar graphs and fan-planar graphs in the 2-layer setting completely.

[11] For the definition of a snake, see [38].

Theorem 7.71. *Consider 2-layer graphs. Then the following holds.*

(a) The 1-planar graphs are a proper subclass of the fan-planar graphs.

(b) For $k \geq 2$, the classes of k-planar and fan-planar graphs are incomparable.

Proof. Each 1-planar drawing is fan-planar by the definitions of 1-planar and fan-planar graphs. Further, 2-layer fan-planar graphs are not a subclass of the k-planar graphs, where $k \geq 1$ (refer to Cor. 7.60). Thus, the class of 1-planar graphs represents a proper subclass of the fan-planar graphs.

On the other hand, there is a 2-layer 2-planar graph that is not 2-layer fan-planar (refer to Lemma 7.70), yielding that, for $k \geq 2$, the class of 2-layer k-planar graphs cannot be contained in the class of 2-layer fan-planar graphs. □

Note that the relations stated in Thm. 7.71 are the same as the relations between $\mathcal{P}_k$ and $\mathcal{F}$ for general graphs (see [39]).

7.8.6 k-planar and fan-crossing free graphs

Here, like for the relation between fan-planar and k-planar graphs, we are as well able to give a complete description of the inclusion relationship between 2-layer fan-crossing free and 2-layer k-planar graphs. We start with the comparison of 1-planar and fan-crossing free graphs.

Lemma 7.72. *The relation $\mathcal{P}_1^= \subsetneq \mathcal{X}^=$ holds.*

Proof. By definition every 2-layer 1-planar drawing is a 2-layer fan-crossing free drawing, so we have $\mathcal{P}_1^= \subseteq \mathcal{X}^=$. It remains to show that there is a 2-layer fan-crossing free graph that is not 2-layer 1-planar.

First consider the bipartite graph H that corresponds to drawing Γ_H of Fig. 7.64a. Graph H is a subgraph of $K_{3,3}$, such that exactly four vertices of H have degree 2, and two vertices have degree 3.

We show that Γ_H is a unique 2-layer 1-planar drawing (up to isomorphism) of H. To this end, consider the unique drawing $\Gamma_{3,3}$ of $K_{3,3}$ in Fig. 7.64b. Suppose that, beside Γ_H, there is another 1-planar drawing Γ'_H of H. Because H is a subgraph of $K_{3,3}$, it follows that Γ'_H is a subdrawing of $\Gamma_{3,3}$. We denote the vertices of Γ'_H and $\Gamma_{3,3}$ as in Fig. 7.64b. The assumption $\Gamma'_H \neq \Gamma_H$ implies that at least one of the edges (u_1, w_3) or (u_3, w_1) is part of Γ'_H (see dashed red edges in Fig. 7.64b), say (u_1, w_3). But, since H has two edges less than $K_{3,3}$, and since (u_1, w_3) is crossed by the four edges (u_2, w_1), (u_2, w_2), (u_3, w_1) and (u_3, w_2) in $\Gamma_{3,3}$, the edge (u_1, w_3) is crossed by

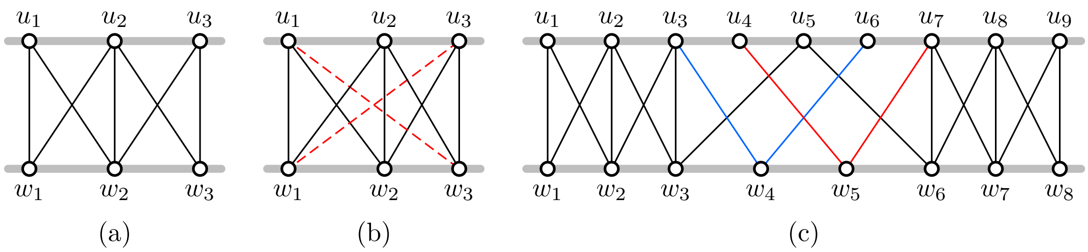

Fig. 7.64: (a) A 1-planar drawing Γ_H of a graph H. (b) The unique 2-layer drawing $\Gamma_{3,3}$ of $K_{3,3}$. Without the dashed red edges, it is a unique 2-layer 1-planar drawing of H. (c) A 2-layer drawing Γ that is fan-crossing free; the corresponding graph G is not 2-layer 1-planar.

at least two edges in Γ'_H – a contradiction to the 1-planarity of Γ'_H. So the drawing Γ_H is indeed a unique 2-layer 1-planar drawing of H.

We define a new graph G by the drawing Γ of Fig. 7.64a and denote the vertices of G accordingly. As Γ shows, this graph is 2-layer fan-crossing free. We prove that G has no 2-layer 1-planar embedding.

Note that the snippets $\mathbf{B}_1 := [1,3 \mid 1,3]$ and $\mathbf{B}_2 := [7,9 \mid 6,8]$ of Γ represent copies H_1 and H_2 of graph H, which has a unique drawing Γ_H. Thus, the vertices of each of the subgraphs H_1 and H_2 are fixed in every drawing of G.

Further observe that none of the vertices u_i of G, where $4 \leq i \leq 9$, can be placed between u_1 and u_3, since this would violate 1-planarity. Likewise, none of the vertices u_i of G, where $1 \leq i \leq 6$, can be placed between u_7 and u_9; none of the vertices $w_{i'}$ of G, where $4 \leq i' \leq 8$, can be placed between w_1 and w_3; none of the vertices $w_{i'}$ of G, where $1 \leq i' \leq 5$, can be placed between w_6 and w_8. So we can assume without loss of generality that drawing Γ_1 of H_1 is drawn left of drawing Γ_2 of H_2, and that the vertices u_4, u_5, u_6, w_4 and w_5 are placed between the unique drawings Γ_1 and Γ_2.

Note that by the arguments before also the drawing consisting of Γ_1, Γ_2, vertex u_5 and its incident edges (u_5, w_3) and (u_5, w_6) is unique (the black edges in Fig. 7.64c represent this drawing). For each of the paths (u_3, w_4, u_6) and (u_7, w_5, u_4) of G (blue and red paths in Fig. 7.64c) there exists two possible placements: While the placement of w_4 and w_5 must be between w_3 and w_6, the vertices u_4 and u_6 can be placed between u_3 and u_5, or between u_5 and u_7. However, since each of the edges (u_3, w_4), (u_4, w_5), (u_6, w_4) and (u_7, w_5) crosses either (u_5, w_3) or (u_5, w_6), four crossings are distributed among only two edges, which yields at least two crossings for one of (u_5, w_3) or (u_5, w_6). So G is not 1-planar. □

In the next step we study how the classes of 2-layer fan-crossing free (which coincide with 2-layer RAC graphs) and 2-layer k-planar graphs are related for $k \geq 2$. In order to do so, we use some terms and results from Giacomo et al. [56].

Let Γ be a 2-layer drawing. Then a path $p = (u_i, w_{j'}, u_j, w_{i'})$ is called a *butterfly blocker* if $i < j$ and $i' < j'$, or if $i > j$ and $i' < j'$; in other words, the edges $(u_i, w_{j'})$ and $(u_j, w_{i'})$ cross each other (see also Fig. 7.65a). In a butterfly blocker, we denote the edge $(u_j, w_{j'})$ as *wall* (refer to the red edge in Fig. 7.65a).

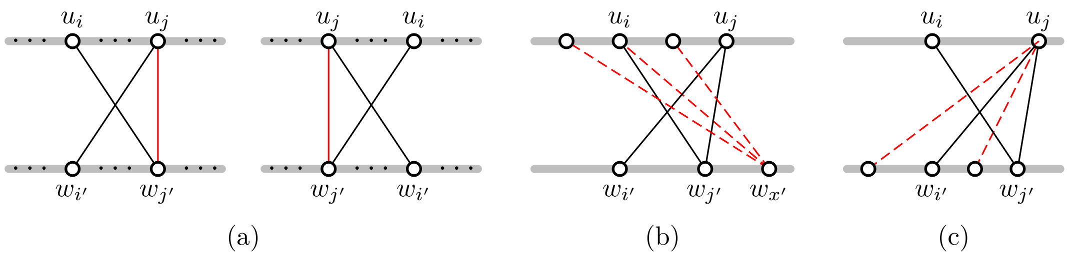

Fig. 7.65: (a) The two configurations for a butterfly blocker. The red edge is the wall. (b) and (c) A butterfly blocker "blocks" e. g. the dashed red edges.

As the name indicates, the butterfly blocker "blocks" edges in a fan-crossing free drawing. Namely, there cannot be an edge $(u_x, w_{x'})$ in Γ such that $x < j$ and $x' > j'$, or such that $x > j$ and $x' < j'$, without violating fan-crossing freeness (illustrated in Fig. 7.65b). Moreover, if $i < j$ and $i' < j'$, there can neither be an edge $(u_j, w_{x'})$ such that $x' < j'$ and $x' \neq i'$ (illustrated in Fig. 7.65c), nor an edge $(u_x, w_{j'})$ such that $x < j$ and $x \neq i$; if $i > j$ and $i' > j'$, there can neither be an edge $(u_j, w_{x'})$ such that $x' > j'$ and $x' \neq i'$, nor an edge $(u_x, w_{j'})$ such that $x > j$ and $x \neq i$. Again, such edges would not be compatible with the fan-crossing free property.

For some $t \geq 2$ a path $p = (v_1, \ldots, v_t)$ in a 2-layer drawing Γ is called *monotone*, if either $v_i \prec v_{i+2}$ for all $i = 1, \ldots, t-2$, or if $v_i \succ v_{i+2}$ for all $i = 1, \ldots, t-2$. For monotone paths, Giacomo et al. proved to following property:

Property 7 [56]: Let $v_1 \in U$, $z_1 \in W$ be two vertices belonging to different independent parts of G, and let $p_1 = (v_1, v_2, \ldots, v_t)$ and $p_2 = (z_1, z_2, \ldots, z_{t'})$ be two monotone paths in a 2-layer fan-crossing free drawing Γ. If (v_1, v_2) crosses (z_1, z_2) in Γ, then (v_{i-1}, v_i) crosses (z_{i-1}, z_i) in Γ for $2 \leq i \leq \min(t, t')$.

Using butterfly blockers, monotone paths, and Property 7, we are able to show the following lemma about the relationship between fan-crossing free and k-planar graphs.

Lemma 7.73. *For $k \geq 2$, the class of 2-layer fan-crossing free graphs is a proper subclass of the class of 2-layer k-planar graphs.*

Proof. Recall that we have $\mathcal{P}_k^= \not\subset \mathcal{X}^=$ for $k \geq 2$ (see Point c of Cor. 7.60); this proves the "proper".

Let Γ be a $\mathcal{X}^=$-drawing of a graph G. We can assume that Γ is connected, since otherwise the connected components can be drawn separately. In the following we show that no edge in Γ is crossed more than twice.

Assume to the contrary that there is an edge e that is crossed by (at least) three edges e_1, e_2, e_3. First observe that there are no three mutually crossing edges in a connected 2-layer fan-crossing free drawing Γ (refer to [56, Property 1]); thus the edges e_1, e_2 and e_3 are ordered, in the sense that (without loss of generality) e_2 lies completely right of e_2, while e_3 lies completely right of e_2; see also Fig. 7.66a. Let $e = (u_r, w_{\ell'})$, $e_1 = (u_h, w_{h'})$, $e_2 = (u_i, w_{i'})$, and $e_3 = (u_j, w_{j'})$. Then we have $h < i < j$ and $h' < i' < j'$. We assume without loss of generality that $j < r$ and $\ell' < h'$ (the case $r < h$ and $\ell' > j'$ is symmetric).

Since Γ is connected, there exists *shortest* paths p_s, $s = 1, 2, 3$, between e and e_s.[12] However, because Γ is fan-crossing free and due to the arguments before, none of the following edges can belong to such a path (see also the dashed gray edges in Fig. 7.66a as an example for two of these edges): $(u_h, w_{i'})$, $(u_h, w_{j'})$, $(u_i, w_{\ell'})$, $(u_i, w_{h'})$, $(u_i, w_{j'})$, $(u_j, w_{\ell'})$, $(u_j, w_{h'})$, $(u_j, w_{i'})$, $(u_r, w_{h'})$, and $(u_r, w_{i'})$.

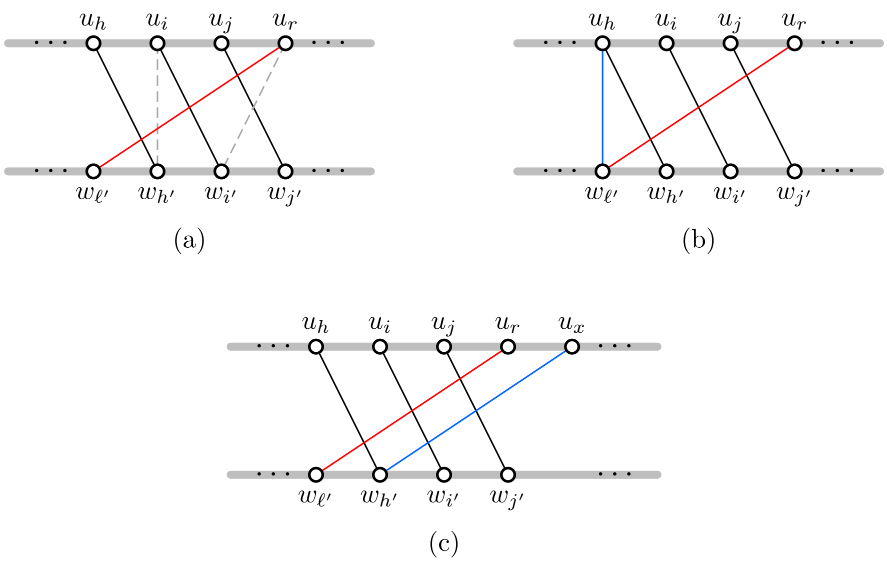

Fig. 7.66: Illustration for the proof of Lemma 7.73. (a) An edge (red) that violates 2-planarity. The dashed gray edges cannot be part of a fan-crossing free drawing. (b) The edge $(u_h, w_{\ell'})$ creates a butterfly blocker. (c) The vertex $w_{h'}$ has another edge incident to it.

[12]We define a shortest path p_s between e and e_s as a path consisting of edges e and e_s, together with a shortest path p'_s between end vertices of e and e_s with the following property: If $p' \neq p'_s$ is a shortest path between end vertices of e and e_s, then p' has at least the same length as p'_s.

Consider p_1, which is the path that contains e. We show that p_1 contains a butterfly blocker. If the edge $(u_h, w_{\ell'})$ is part of p_1 (see the blue edge in Fig. 7.66b), this edge already creates a butterfly blocker. Otherwise there is at least one more edge incident to one of $u_h, u_r, w_{\ell'}$, or $w_{h'}$. We consider the case where an edge $(u_x, w_{h'})$ exists, such that $x \notin \{h, i, j, r\}$ (refer to the blue edge in Fig. 7.66c; for the other cases similar arguments hold). Let $q_e = (v_1, v_2, \dots, v_t)$, where $v_1 = w_{\ell'}$, $v_2 = u_r$ and $t \geq 2$, be the maximal monotone subpath of p_1 starting in $w_{\ell'}$; further, for some $t' \geq 3$, let $q_1 = (z_1, \dots, z_{t'})$ be such that (i) $z_1 = u_h$, $z_2 = w_{h'}$, $z_3 = u_x$; (ii) q_1 is a monotone subpath of p_1; (iii) q_1 has no edge in common with q_e; and (iv) q_1 is maximal with this properties. Then, since (v_1, v_2) and (z_1, z_2) cross, Property 7 of [56] implies that (v_{s-1}, v_s) crosses (z_{s-1}, z_s) in Γ for $2 \leq s \leq \min(t, t')$. Now there might be two different situations:

(1) The vertices v_t and $z_{t'}$ are the same (illustrated in Fig. 7.67a). Here the subpath $(v_{t-2}, v_{t-1}, v_t, z_{t'-1})$ represents a butterfly blocker.

(2) The vertices v_t and $z_{t'}$ are not the same (illustrated in Fig. 7.67b). Assume that $t \leq t'$ and let $v_{t+1} \neq v_{t-1}$ be the vertex on path p_1 that is adjacent to v_t. Then v_{t+1} is left of v_{t-1} and also left of z_t, which implies that edge (v_t, v_{t+1}) crosses (z_{t-1}, z_t). But the latter edge is already crossed by (v_{t-1}, v_t), yielding a fan-crossing – a contradiction. Since the assumption $t \leq t'$ also leads to a contradiction, we conclude that v_t and $z_{t'}$ must coincide.

Next, consider the path p_2, which is the path that contains e and e_2. In the same way as for p_1, we obtain that also p_2 contains a butterfly blocker, which cannot have the same wall as p_1 (by the properties of a butterfly blocker and the assumption that Γ is fan-crossing free). Thus, the butterfly blocker of p_2 cannot be on the same side of e as the one for p_1, since otherwise either p_1 would block an edge of p_2, or vice versa (for an illustrated refer to Fig. 7.67c). Likewise p_3 contains a butterfly blocker in Γ, whose wall neither coincides with the one of p_1, nor with the one of p_2. But since it must be on one of the two sides of e, at least one edge of p_1, p_2 or p_3 is blocked by a butterfly blocker.

We conclude that there is no edge e in Γ that is crossed more than twice. □

The following theorem combines Lemmas 7.72 and 7.73 to provide a complete description of the inclusion relationship between 2-layer fan-crossing free and 2-layer k-planar graphs.

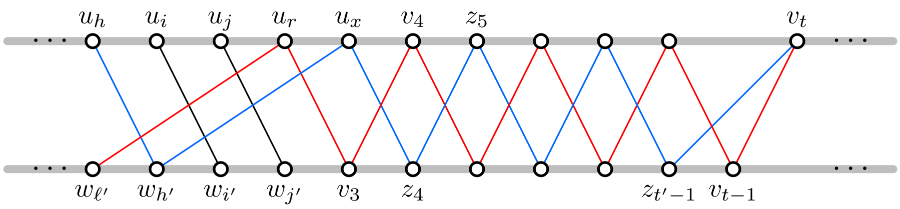

(a)

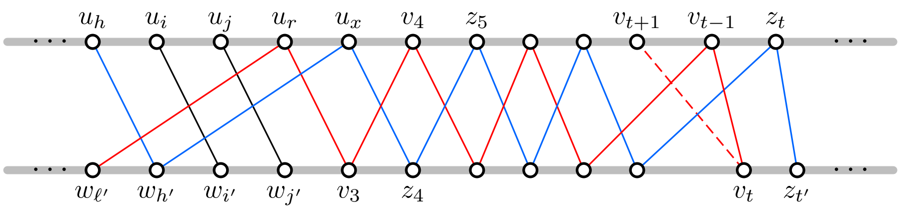

(b)

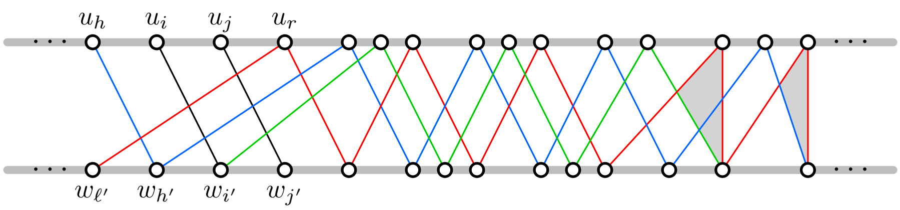

(c)

Fig. 7.67: Illustration for the proof of Lemma 7.73. The paths q_e and q_1 are colored in red and blue, respectively. (a) The case where v_t and $z_{t'}$ coincide. (b) The edge $(u_h, w_{\ell'})$ creates a butterfly blocker. (c) Both paths p_1 (red and blue edges) and p_2 (red and green edges) have a butterfly blocker on the same side of e (signified by the gray areas).

Theorem 7.74. *Consider 2-layer graphs. Then the following holds.*

(a) The 1-planar graphs are a proper subclass of the fan-crossing free graphs.

(b) For $k \geq 2$, the class of fan-crossing free graphs is a proper subclass of the one of k-planar graphs.

7.8.7 k-planar and k-quasi-planar graphs

Regarding general graphs, it is known that, for $k \geq 3$, every k-planar graph is $(k+1)$-quasi-planar [12, 86]. In the 2-layer setting an even stronger result holds.

Theorem 7.75. *Every 2-planar graph is 3-quasi-planar and, for $k \geq 3$, the relation $\mathcal{P}_k^= \subsetneq \mathcal{Q}_{k^\star}^=$ holds, where $k^\star := \lceil \frac{2}{3}k + 2 \rceil$.*

Proof. If $G \in \mathcal{P}_k^=$ is not connected, we can draw each connected component of G separately. So we assume in the following that G is connected.

First consider a 2-layer 2-planar graph G with a corresponding drawing Γ. Suppose that Γ contains 3-mutually crossing edges $(u_h, w_{j'})$, $(u_i, w_{i'})$ and $(u_j, w_{h'})$ for some $1 \leq h < i < j \leq a$ and $1 \leq h' < i' < j' \leq b$ (refer to Fig. 7.68a). Then $(u_h, w_{j'})$ and $(u_j, w_{h'})$ are already crossed twice and therefore the edge $(u_i, w_{i'})$ represents a connected component in Γ; a contradiction. Thus, every 2-layer 2-planar graph is 2-layer quasi-planar.

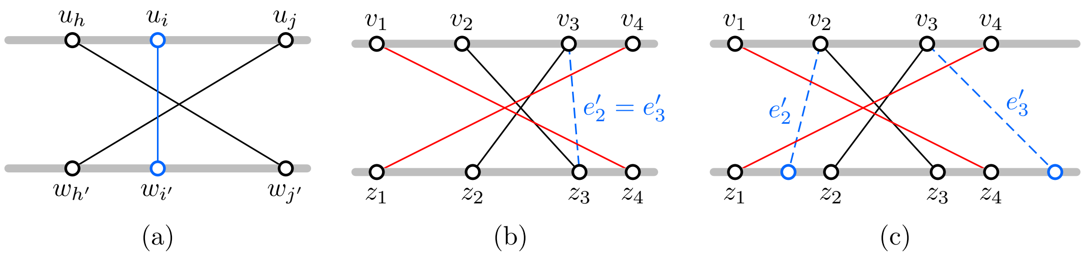

Fig. 7.68: Illustration for the proof of Thm. 7.75. (a) Three mutually crossing edges in a 2-planar graph. (b) and (c) Additional crossings in the presence of $k^\star = 4$ mutually intersecting edges.

Next we show the relationship $\mathcal{P}_k^= \subseteq \mathcal{Q}_{k^\star}^=$. To this end, let $k \geq 3$, and let Γ be a $\mathcal{P}_k^=$-drawing. Assume for a contradiction that Γ contains $k^\star$ mutually crossing edges $e_i := (v_i, z_{k^\star+1-i})$, where $1 \leq i \leq k^\star$, $v_1 \prec v_2 \prec \cdots \prec v_{k^\star}$, and $z_1 \prec z_2 \prec \cdots \prec z_{k^\star}$. Note that the $k^\star$ mutually crossing edges already imply $k^\star - 1$ crossings on each, $e_1 = (v_1, z_{k^\star})$ and $e_2 = (v_{k^\star}, z_1)$. Further note that, since Γ is connected, each edge e_i must be adjacent to at least one more edge $e'_i \notin \{e_1, \ldots, e_{k^\star}\}$. If $e'_i = e'_j$ for some $i \neq j$ and $i, j \notin \{1, k^\star\}$, then e'_i crosses both edges e_1 and $e_{k^\star}$ (see dashed blue edge in Fig. 7.68b); otherwise e'_i, where $1 < i < k^\star$, crosses at least one of e_1 or $e_{k^\star}$ (refer to the dashed blue edges in Fig. 7.68c). In total this gives rise to $k^\star - 2$ additional crossings on $\{e_1, e_{k^\star}\}$. Consequently, one of the edges e_1 or $e_k^\star$ receives at least

$$k^\star - 1 + \left\lceil \frac{k^\star - 2}{2} \right\rceil \geq k^\star - 1 + \frac{k^\star - 2}{2} = \frac{3}{2}k^\star - 2 \geq \frac{3}{2}\left(\frac{2}{3}k + 2\right) - 2 = k + 1$$

crossings; a contradiction to the k-planarity of Γ.

Finally observe that the graph $K_{2,k+2}$ is 2-layer quasi-planar for every $k \geq 1$, but not k-planar (refer to Cor. 7.53). This shows that $\mathcal{P}_k^= \neq \mathcal{Q}_{k^\star}^=$. □

By Cor. 7.60, the classes of 2-layer k-planar graphs $\mathcal{P}_k^=$ and the one of 2-layer quasi-planar graphs $\mathcal{Q}^= = \mathcal{Q}_3^=$ are incomparable for $k \geq 4$. On the other hand, Thm. 7.75 shows that $\mathcal{P}_2^= \subseteq \mathcal{Q}^=$ holds. We state the relations between $\mathcal{P}_k^=$ and $\mathcal{Q}^=$ in the following theorem.

Theorem 7.76. *Consider 2-layer graphs. Then the following holds.*

(a) For $k \leq 2$, the k-planar graphs are a proper subclass of the quasi-planar graphs.

(b) For $k \geq 4$, the classes of k-planar and quasi-planar graphs are incomparable.

(c) The quasi-planar graphs are not contained in the class of 3-planar graphs.

Proof. As already mentioned, by Cor. 7.60 the classes $\mathcal{P}_k^=$ and $\mathcal{Q}^=$ are incomparable for $k \geq 4$.

From Thm. 7.75 we conclude that the relation $\mathcal{P}_2^= \subseteq \mathcal{Q}^=$ holds. On the other hand, for every $k \geq 1$, the graph $K_{2,k+2}$ is 2-layer quasi-planar (for an illustration see Fig. 7.69), but not 2-layer k-planar (refer to Cor. 7.53). Thus, the class of 2-layer quasi-planar graphs is not a subclass of $\mathcal{P}_k^=$. The statement follows. □

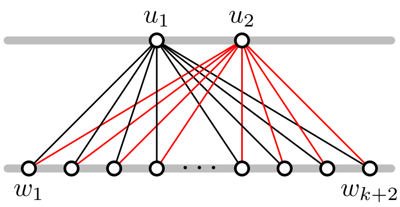

Fig. 7.69: The unique 2-layer drawing of $K_{2,k+2}$. It is quasi-planar (and fan-planar), but not k-planar.

We remark that we were not able to answer the question if every 2-layer 3-planar graph is 2-layer quasi-planar or not. However, Thm. 7.19 shows that every optimal 2-layer 3-planar graph is 2-layer quasi-planar; we conjecture that this is also true when neglecting the optimality. Note that a similar result is known in case of general graphs: Every optimal 3-planar graph is quasi-planar [33], while it is not known if the relation $\mathcal{P}_3 \subseteq \mathcal{Q}$ holds.

7.8.8 Fan-planar and quasi-planar graphs

It is known that a fan-planar drawing does not contain three mutually crossing edges [39]. Together with Lemma 7.70 we obtain that the class of 2-layer fan-planar graphs represents a proper subclass of the 2-layer quasi-planar graphs.

Theorem 7.77. *The inclusion relationship $\mathcal{F}^= \subsetneq \mathcal{Q}^=$ holds.*

7.8.9 Fan-planar and fan-crossing free graphs

Results of Binucci et al. [38] are that biconnected 2-layer RAC graphs form a proper subclass of the biconnected 2-layer fan-planar graphs, while there are 2-

layer RAC graphs which are not 2-layer fan-planar if neglecting the "biconnected". As a consequence of this and Cor. 7.60, the class of 2-layer fan-planar graphs is incomparable with the class of 2-layer fan-crossing free graphs (which coincides with the class of RAC graphs).

Theorem 7.78. *The classes $\mathcal{F}^=$ and $\mathcal{X}^=$ are incomparable.*

7.8.10 Fan-planar and k-gap-planar graphs

Regarding the relation of fan-planar graphs with k-gap-planar graphs, we observe the following: On one hand, for every $k \geq 1$, the graph $K_{2,4k+2}$ is 2-layer fan-planar but not 2-layer k-gap-planar (see Cor. 7.68).

On the other hand, the 2-layer 2-planar graphs are a subclass of 2-layer 1-gap-planar graphs; this yields, that, if the class of 2-layer 1-gap-planar graphs would be a subclass of the 2-layer fan-planar graphs, then every 2-layer 2-planar graph would also be 2-layer fan-planar, contradicting Lemma 7.70. Consequently the classes of 2-layer fan-planar and 2-layer k-gap-planar graphs are incomparable.

Theorem 7.79. *The classes of 2-layer fan-planar graphs and 2-layer k-gap-planar graphs are incomparable for every $k \geq 1$.*

7.8.11 Fanbundle-planar graphs

The relationships between the different classes of 2-layer fanbundle-planar graphs are clearly $\mathcal{B}_1^= \subsetneq \mathcal{B}_{2d}^= \subsetneq \mathcal{B}_2^=$ by definition; the "proper" follows from Cor. 7.60.

7.8.12 Fan-planar and fanbundle-planar graphs

For 2-layer 1-sided fbp graphs we have the chain $\mathcal{P}_1^= \subseteq \mathcal{B}_1^= \subseteq \mathcal{F}^=$ of inclusion relationships, which was already noticed by Angelini et al. [13] in case of general graphs. Using the statements of Cor. 7.60, namely the fact that $K_{2,4}$ is 2-layer fan-planar and not 2-layer 1-sided fbp, we conclude that the class of 2-layer 1-sided fbp graphs is a proper subclass of the 2-layer fan-planar graphs. The following theorem contains this relation as first statement.

Theorem 7.80.

(a) The relation $\mathcal{B}_1^= \subsetneq \mathcal{F}^=$ holds.

(b) The class $\mathcal{F}^=$ is incomparable with both, the class $\mathcal{B}_{2d}^=$ and the class $\mathcal{B}_2^=$.

Proof. We already explained why the first statement holds.

By Cor. 7.60 the class $\mathcal{B}_2^=$ is incomparable with $\mathcal{F}^=$. Also by Cor. 7.60, the class of 2-layer fan-planar graphs is not a subclass of 2d-layer 2-sided fbp graphs.

We conclude with the observation that the graph constructed in Lemma 7.70 is 2d-layer 2-sided fbp (see Fig. 7.70), but not 2-layer fan-planar; hence, 2d-layer 2-sided fbp graphs are not a subclass of 2-layer fan-planar graphs. □

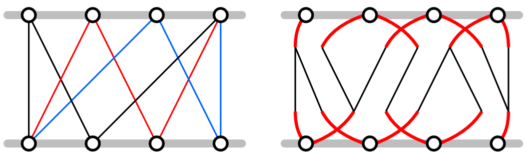

Fig. 7.70: The drawing from Lemma 7.70 (left), which is 2d-layer 2-sided fbp (right), but not fan-planar.

7.8.13 k-planar and fanbundle-planar graphs

As already mentioned in the previous section, for 2-layer 1-sided fbp graphs we have the inclusion relationship $\mathcal{P}_1^= \subseteq \mathcal{B}_1^=$; together with the results from Cor. 7.60, we conclude that the class of 2-layer 1-planar graphs is a proper subclass of the 2-layer 1-sided fbp graphs.

Since the 2-layer 1-sided fbp graphs are a subclass of the 2-layer fan-planar graphs, and since there is a 2-layer 2-planar graph that is not fan-planar (refer to Lemma 7.70), we conclude that, for $k \geq 2$, the class of 2-layer k-planar graphs cannot be a subclass of the 2-layer 1-sided fbp graphs. The following lemma provides a construction for a family of graphs which are 2-layer 1-sided fbp, but not 2-layer k-planar, yielding that the corresponding graph classes are incomparable.

Lemma 7.81. *For every $k \geq 2$, there exists a graph that is 2-layer 1-sided fbp, but not 2-layer k-planar.*

Proof. Let $G = (U \dot{\cup} W, E)$ be the graph consisting of vertices $u_1, u_2, u_3 \in U$, vertices $x, v_i, w_i, z_i \in W$, where $1 \leq i \leq 2k+1$, and the following edges:

– Edges (u_1, v_i), (u_2, w_i), and (u_3, z_i), where $1 \leq i \leq 2k+1$;

– and edges (u_i, x), where $1 \leq i \leq 3$.

Figure 7.71a shows a 2-layer 1-sided fbp drawing of this graph.

It remains to show that G is not 2-layer k-planar. Assume to the contrary that $G \in \mathcal{P}_k^=$ and Γ is a $\mathcal{P}_k^=$-drawing of G. For $i = 1, 2, 3$, let S_i be the subgraph induced

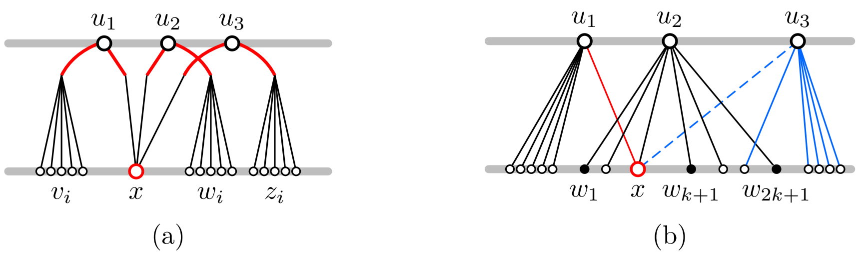

Fig. 7.71: (a) A 2-layer 1-sided fbp drawing of G (here we have $k = 2$). (b) In Γ, edge (u_1, x) requires vertex x (red) to be left of w_{k+1}, while edge (u_3, x) requires vertex x to be right of w_{k+1}.

by u_i and its neighbors in G. Then S_i is a star, and all stars S_i share one and only one vertex, namely x. By construction of G, the three vertices u_1, u_2, u_3 must be placed on one layer, say the top layer, while all other vertices must be placed on the bottom layer. By symmetry of S_1, S_2 and S_3, we suppose that $u_1 \prec u_2 \prec u_3$ in Γ.

In $\Gamma[S_1]$, each order of the vertices v_i along the bottom layer is equivalent; thus we assume that $v_1 \prec v_2 \prec \cdots \prec v_{2k+1}$. Similarly we can assume $w_1 \prec w_2 \prec \cdots \prec w_{2k+1}$, and $z_1 \prec z_2 \prec \cdots \prec z_{2k+1}$.

Since Γ is k-planar and $u_1 \prec u_2$, the edge (u_1, x) can cross at most k edges incident to u_2, namely the edges $(u_2, w_1), \ldots, (u_2, w_k)$. Thus, we have $x \prec w_{k+1}$ as a first condition (for an illustration see Fig. 7.71b). On the other hand, we have $u_2 \prec u_3$, which implies that (u_3, x) can cross at most the k edges $(u_2, w_{k+2}), \ldots, (u_2, w_{2k+1})$. As second condition, we obtain $w_{k+1} \prec x$; a contradiction to the first one. We conclude that G is not 2-layer k-planar. □

Theorem 7.82 summarizes our results for 1-sided fbp graphs.

Theorem 7.82. *In the 2-layer setting, the following holds.*

(a) The class of 2-layer 1-planar graphs is a proper subclass of the 1-sided fbp graphs.

(b) For $k \geq 2$, the classes of 2-layer k-planar and 2-layer 1-sided fbp graphs are incomparable.

For 2d-layer 2-sided fbp graphs we have the inclusion $\mathcal{P}_2^= \subseteq \mathcal{B}_{2d}^=$ (by definition of the two graph classes), which was also observed in [13] for general graphs. Together with Cor. 7.60 we conclude that $\mathcal{P}_2^= \subsetneq \mathcal{B}_2^=$. Note that, as $\mathcal{B}_1^= \subseteq \mathcal{B}_{2d}^= \subseteq \mathcal{B}_2^=$ holds, Lemma 7.81 also shows that $\mathcal{B}_{2d}^= \not\subset \mathcal{P}_k^=$ and $\mathcal{B}_2^= \not\subset \mathcal{P}_k$ for $k \geq 2$.

Since 2-layer 5-planar graphs have a tight edge density of $\frac{9}{4}n - \frac{9}{2}$, while 2-layer 2-sided fbp graphs only admit drawings with at most $\frac{17}{8}n - \frac{13}{4}$ edges, we have $\mathcal{P}_k^= \not\subset \mathcal{B}_2^=$ for $k \geq 5$. As a consequence, we obtain the following theorem.

Theorem 7.83. *For 2-layer 2-sided fanbundle-planar and k-planar graphs, the following holds.*

(a) We have $\mathcal{P}_2^{=} \subsetneq \mathcal{B}_2^{=}$.

(b) For $k \geq 5$*, the classes* $\mathcal{P}_k^{=}$ *and* $\mathcal{B}_2^{=}$ *are incomparable.*

(c) For $k = 3, 4$ *we have* $\mathcal{B}_2^{=} \not\subset \mathcal{P}_k^{=}$.

Note that it is still open if $\mathcal{P}_k^{=} \subset \mathcal{B}_2^{=}$ for $k \in \{3, 4\}$. However, we can give a complete characterization of the relationship between the classes $\mathcal{B}_{2d}^{=}$ and $\mathcal{P}_k^{=}$. In order to do so, we use the following lemma.[13]

Lemma 7.84 ([126])**.** *Let* Γ *be a connected 2d-layer 2-sided fbp drawing with vertices* $u_1, \ldots, u_a \in U$ *and* $w_1, \ldots, w_b \in W$*. If there is an edge* $(u_i, w_{i'})$ *in* Γ *for appropriate* i *and* i'*, then* Γ *cannot contain* $(u_j, w_{j'})$*, where* $j \leq i - 2$ *and* $j' \geq i' + 2$*, or where* $j \geq i + 2$ *and* $j \leq i' - 2$.

Proof. Let $(u_i, w_{i'})$ be in Γ. We assume that there is also an edge $(u_j, w_{j'})$ in Γ, where $j \leq i - 2$ and $j' \geq i' + 2$; the other cases are symmetric. Let B_i and $B_{i'}$ be the two bundle parts of $(u_i, w_{i'})$ in Γ, where B_i is anchored at u_i and $B_{i'}$ is anchored at $w_{i'}$. Further let B_j and $B_{j'}$ be the two bundle parts of $(u_j, w_{j'})$, where B_j is anchored at u_j and $B_{j'}$ is anchored at $w_{j'}$.

The two bundles B_i and B_j cannot cross each other, since this would isolate vertex u_{i-1}. Similarly, $B_{i'}$ cannot cross $B_{j'}$ without isolating $w_{i'+1}$. As a consequence, the terminal t_j of B_j is left of the terminal t_i of B_i, and the terminal $t_{j'}$ of $B_{j'}$ is right of the terminal $t_{i'}$ of $B_{i'}$ (refer to Fig. 7.72). Because the edge $(u_i, w_{i'})$ is planar between t_i and $t_{i'}$, and the edge $(u_j, w_{j'})$ is planar between t_j and $t_{j'}$, both edge parts cross each other in Γ – a contradiction to the definition of $\mathcal{B}_{2d}^{=}$. □

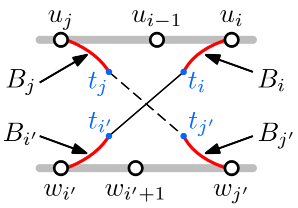

Fig. 7.72: Illustration for the proof of Lemma 7.84. The terminals $t_i, t_j, t_{i'}$ and $t_{j'}$ are blue. The supposedly planar edge parts $(t_i, t_{i'})$ and $(t_j, t_{j'})$ are solid black and dashed black, respectively.

Now we can compare the classes $\mathcal{P}_k^{=}$ and $\mathcal{B}_{2d}^{=}$. The only case that we have not proven yet is the one for $k = 3$, where the edge density for both classes is the same.

[13]This lemma corresponds to Lemma 8.7 in [126]. However, we reformulated it slightly and improved the structure of the proof.

Theorem 7.85. *For 2d-layer 2-sided fanbundle-planar and 2-layer k-planar graphs, the following holds.*

(a) We have $\mathcal{P}_2^{=} \subsetneq \mathcal{B}_{2d}^{=}$.

(b) For $k \geq 3$*, the classes* $\mathcal{P}_k^{=}$ *and* $\mathcal{B}_{2d}^{=}$ *are incomparable.*

Proof. The first statement follows directly from the definitions of $\mathcal{P}_2^{=}$ and $\mathcal{B}_{2d}^{=}$, and from their different tight edge densities.

Observe that $\mathcal{P}_k^{=} \not\subseteq \mathcal{B}_{2d}^{=}$ for $k \geq 4$, since $\mathcal{P}_4^{=}$ has a tight edge density of $2n-3$, while the edge density of $\mathcal{B}_{2d}^{=}$ is only $2n-4$. We have $\mathcal{B}_{2d}^{=} \not\subseteq \mathcal{P}_k^{=}$ for $k \geq 2$ by Lemma 7.81. This shows that the classes $\mathcal{P}_k^{=}$ and $\mathcal{B}_{2d}^{=}$ are incomparable for $k \geq 4$.

It remains to show that $\mathcal{P}_3^{=} \not\subseteq \mathcal{B}_{2d}^{=}$. In order to do so, consider the 2-layer drawing Γ of Fig. 7.73a, which is 3-planar. Let G be the graph defined by Γ. For a contradiction, we assume that $G \in \mathcal{B}_{2d}^{=}$. Let Γ' be a $\mathcal{B}_{2d}^{=}$-drawing of G.

Note that u_3 and w_3 both have degree 5. We observe that if in Γ' two or more vertices of u_1, u_2, u_4, u_5 are left (right) of u_3, and at the same time two or more of the vertices w_1, w_2, w_4, w_5 are left (right) of w_3, then Γ' cannot belong to $\mathcal{B}_{2d}^{=}$ by Lemma 7.84 (for an illustration see e. g. Fig. 7.73a).

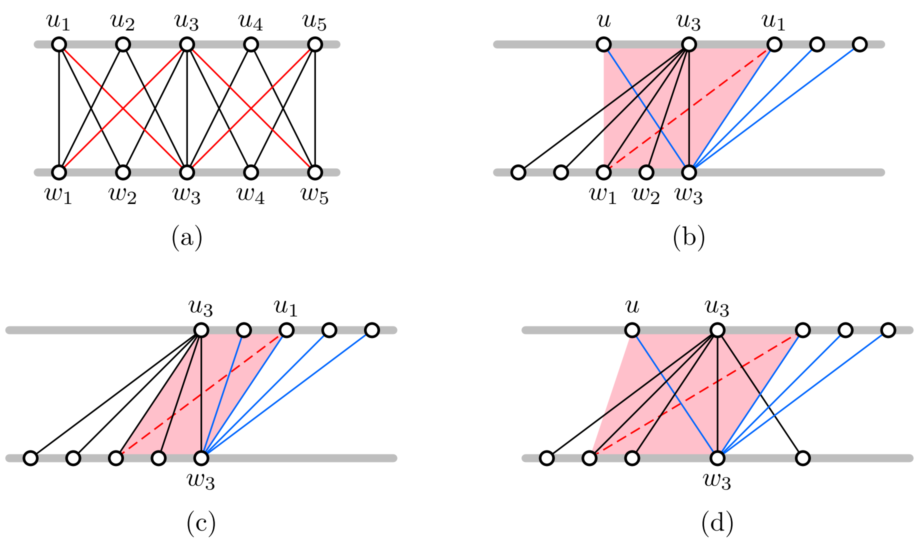

Fig. 7.73: (a) A 2-layer 3-planar drawing Γ. (b) The case where one vertex is left of u_3 and none is left of w_3. (c) The case where no vertex is left of u_3 and none is left of w_3. (d) The case where one vertex is left of u_3 and one is left of w_3. In (b)–(d) the regions which disagree with a $\mathcal{B}_{2d}^{=}$ drawing according to Lemma 7.84 are colored red.

Assume without loss of generality that there is at most one vertex left of u_3. Then there are at least three vertices right of u_3, implying that right of w_3 is not more than one vertex by Lemma 7.84. We analyze the different cases.

– One vertex u is left of u_3 and none is right of w_3 (refer to Fig. 7.73b): Then at least one of u_1 and u_5 is right of u_3, say u_1. If $w_1 \prec w_2$, we have $u \prec u_3 \prec u_1$ and $w_1 \prec w_2 \prec w_3$, which contradicts $\Gamma' \in \mathcal{B}_{2d}^{=}$ according to Lemma 7.84; otherwise we have $w_2 \prec w_1$, which also leads to a contradiction by Lemma 7.84.

– One vertex is right of w_3 and none is left of u_3: This is symmetric to the first case.

– No vertex is left of u_3 and none is right of w_3: In this case, both vertices u_1 and u_5 are right of u_3. Assume without loss of generality that $u_5 \prec u_1$. Like before, both cases $w_1 \prec w_2$ and $w_2 \prec w_1$ lead to a contradiction by Lemma 7.84 (refer to Fig. 7.73c).

– One vertex u is left of u_3 and one vertex w is right of w_3: The edges (u_1, w_2), (u_2, w_1), (u_4, w_5) and (u_5, w_4) are four independent edges in G. Thus, one of the two leftmost vertices on the bottom layer must necessarily be incident to an edge whose other endpoint is right of u_3 (refer to the dashed red edge in Fig. 7.73d). This yields again a contradiction by Lemma 7.84.

As no case leads to a valid $\mathcal{B}_{2d}^{=}$-drawing of G, we conclude that G does not belong to this class. The statement follows. □

7.8.14 Fan-crossing free graphs compared with gap-, quasi-, and fanbundle-planar graphs

The class of 2-layer fan-crossing free graphs is a proper subclass of the 2-layer 2-planar graphs (refer to Thm. 7.74), while the 2-layer 2-planar graphs represent a proper subclass of the following classes:

– 2-layer 1-gap-planar graphs (refer to Thm. 7.64),

– 2-layer 3-quasi-planar graphs (refer to Thm. 7.75),

– 2d-layer 2-sided fanbundle-planar graphs (refer to Thm. 7.85).

The next corollary is due to transitivity of the class inclusion relationship.

Corollary 7.86. *For 2-layer graphs we have the following inclusion relationships:*

(a) $\mathcal{X}^{=} \subsetneq \mathcal{G}_k^{=}$ *for all* $k \geq 1$;

(b) $\mathcal{X}^{=} \subsetneq \mathcal{Q}_k^{=}$ *for all* $k \geq 3$;

(c) $\mathcal{X}^{=} \subsetneq \mathcal{B}_{2d}^{=}$ *and consequently* $\mathcal{X}^{=} \subsetneq \mathcal{B}_2^{=}$.

Further, we have the following corollary regarding the relationship between fan-crossing free and 1-sided fbp graphs.

Corollary 7.87. *The classes $\mathcal{X}^=$ and $\mathcal{B}_1^=$ are incomparable.*

Proof. The 2-layer 1-sided fbp graphs are a subclass of the 2-layer fan-planar graphs (refer to Thm. 7.80), while there are 2-layer fan-crossing free graphs which do not belong to $\mathcal{F}^=$; hence $\mathcal{X}^= \not\subseteq \mathcal{B}_1^=$.

On the other hand, we have $\mathcal{X}^= \subseteq \mathcal{P}_2^=$ (refer to Thm. 7.74), and there exist 2-layer 1-sided fbp graphs which do not belong to $\mathcal{P}_2^=$ (see Lemma 7.81), and hence not to $\mathcal{X}^=$. We conclude that $\mathcal{B}_1^= \not\subseteq \mathcal{X}^=$. □

7.8.15 Quasi-planar and k-gap-planar graphs

Bae et al. [30] showed that every k-gap-planar drawing is $(2k + 2)$-quasi-planar. Together with the fact that the graph $K_{2,b}$ is quasi-planar for every $b \geq 2$, but $K_{2,4k+1}$ is not k-gap-planar by Cor. 7.68, we obtain the following theorem.

Theorem 7.88. *The relation $\mathcal{G}_k^= \subsetneq \mathcal{Q}_{2k+2}^=$ holds.*

By Thm. 7.88, 1-gap-planar graphs are a subclass of 4-quasiplanar graphs. The question arises if even $\mathcal{G}_1^= \subseteq \mathcal{Q}_3^=$ holds. We could answer this question neither in the positive, nor in the negative.

We conclude the comparison of the two graph classes by pointing out that the graph $K_{3,3}$ is a 2-layer 2-gap-planar graph (see Fig. 7.74) that is not 2-layer 3-quasiplanar. This is due to the edge density of $2n-4$ in $\mathcal{Q}_3^=$, which only allows 8 edges for graphs with $n = 6$ vertices. Hence we have $\mathcal{G}_2^= \not\subset \mathcal{Q}_3^=$

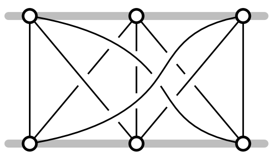

Fig. 7.74: Illustration for the proof of Thm. 7.88.

7.8.16 Quasi-planar and fanbundle-planar graphs

We start with the comparison of $\mathcal{Q}_3^=$ and $\mathcal{B}_1^=$. Since we have $\mathcal{B}_1^= \subsetneq \mathcal{F}^=$ (see Thm. 7.80) and $\mathcal{F}^= \subsetneq \mathcal{Q}_3^=$ (see Thm. 7.77), transitivity implies $\mathcal{B}_1^= \subsetneq \mathcal{Q}_k^=$ for all $k \geq 3$.

Corollary 7.89. *For 2-layer graphs the relationships $\mathcal{B}_1^= \subsetneq \mathcal{Q}_k^=$ holds for all $k \geq 3$.*

Note that Cor. 7.89 is also a consequence of the next theorem, as we have $\mathcal{B}_1^= \subseteq \mathcal{B}_{2d}^=$.

Theorem 7.90. *The relationships $\mathcal{B}_{2d}^= \subsetneq \mathcal{Q}_k^=$ holds for all $k \geq 3$. More precisely, every $\mathcal{B}_{2d}^=$-drawing is quasi-planar.*

Proof. Let Γ be a $\mathcal{B}_{2d}^=$-drawing. Assume to the contrary that Γ contains 3 mutually crossing edges $(u_h, w_{j'})$, $(u_i, w_{i'})$ and $(u_j, w_{h'})$ for some $1 \leq h < i < j \leq a$ and $1 \leq h' < i' < j' \leq b$. But this describes exactly the forbidden configuration for $\mathcal{B}_{2d}^=$-drawings stated in Lemma 7.84; a contradiction.

The inclusion relationship is proper, since $K_{2,b}$ is quasi-planar for every b, but $K_{2,7} \notin \mathcal{B}_{2d}^=$. The statement follows. □

It remains to study the relationship between 2-layer k-quasi-planar and 2-layer 2-sided fbp graphs.

Theorem 7.91. *In the 2-layer setting, the following holds.*

(a) The classes $\mathcal{Q}_3^=$ and $\mathcal{B}_2^=$ are incomparable.

(b) The class $\mathcal{B}_2^=$ is a proper subclass of $\mathcal{Q}_k^=$ for all $k \geq 4$. In particular, every $\mathcal{B}_2^=$-drawing is 4-quasi-planar.

Proof. The graph $K_{2,9}$ is in $\mathcal{Q}_3^=$ but not in $\mathcal{B}_2^=$; the graph $K_{3,3}$ belongs to $\mathcal{B}_2^=$, but not to $\mathcal{Q}_3^=$. Hence $\mathcal{Q}_3^=$ and $\mathcal{B}_2^=$ are incomparable.

Consider a 2-layer 2-sided fanbundle-planar drawing Γ. Assume to the contrary that Γ contains 4 mutually crossing edges $(u_\ell, w_{r'})$, $(u_i, w_{j'})$, $(u_j, w_{i'})$ and $(u_r, w_{\ell'})$ for some $1 \leq \ell < i < j < r \leq a$ and $1 \leq \ell' < i' < j' < r' \leq b$ (refer to Fig. 7.75a).

Recall that a UW-bundle crossing is a crossing of bundles anchored at vertices belonging to different layers. Observe that, in the presence of the four mutually crossing edges, there cannot be a UW-bundle crossing between bundles anchored at $u \in \{u_\ell, u_i, u_j, u_r\}$ and $w \in \{w_{\ell'}, w_{i'}, w_{j'}, w_{r'}\}$, where $(u, w) \notin \{(u_\ell, w_{\ell'}), (u_r, w_{r'})\}$.

In order to realize the drawing Γ, there are basically three bundles and thus three terminals available for each vertex v: a left, a middle, and a right terminal (see Fig. 7.75b for an illustration). Consider the edge $e := (u_\ell, w_{r'})$. No matter which of the three terminals of u_ℓ and $w_{r'}$ are used to draw the planar part of e, the vertices u_j and $w_{i'}$ are separated by e; that is, the edge $(u_j, w_{i'})$ cannot be drawn anymore without violating the properties of a 2-layer 2-sided fbp drawing.

We conclude that Γ does not contain 4 mutually crossing edges, which yields a 4-quasi-planar drawing Γ. Since, $K_{2,9} \in \mathcal{Q}_k^= \setminus \mathcal{B}_2^=$ for every $k \geq 3$, we obtain $\mathcal{B}_2^= \subsetneq \mathcal{Q}_k^=$ for all $k \geq 4$. □

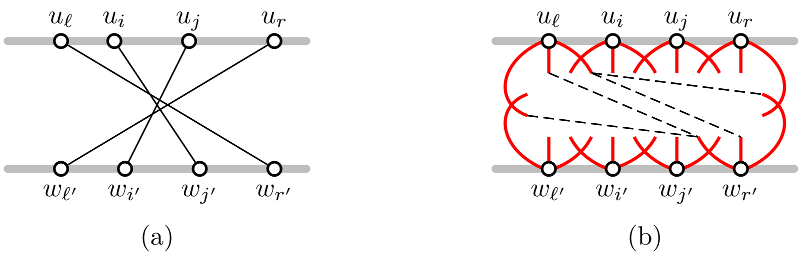

Fig. 7.75: Illustration for the proof of Thm. 7.91. (a) Four mutually crossing edges. (b) The dashed black edges show some possible routings for edge $(u_\ell, w_{r'})$.

7.8.17 Gap-planar and fanbundle-planar graphs

Since the graph $K_{2,4}$ is 2-layer 1-gap-planar, but not 2-layer 1-sided fbp, we have $\mathcal{G}_k^{=} \not\subset \mathcal{B}_1^{=}$ for all $k \geq 1$. However, we were not able to determine if $\mathcal{B}_1^{=} \subset \mathcal{G}_k^{=}$ for some $k \geq 1$.

In regard of the 2-sided fbp graphs, we first recall that neither $\mathcal{B}_2^{=}$ nor $\mathcal{B}_{2d}^{=}$ is a subclass of $\mathcal{G}_1^{=}$ (refer to Cor. 7.60). On the other hand, the graph $K_{3,4}$ is 2-layer 2-gap-planar (see Fig. 7.76), but not 2-layer 2-sided fanbundle-planar (refer to Thm. 7.59); thus we have $\mathcal{G}_k^{=} \not\subset \mathcal{B}_2^{=}$ and consequently $\mathcal{G}_k^{=} \not\subset \mathcal{B}_{2d}^{=}$ for $k \geq 2$. Note that the question if $\mathcal{G}_1^{=}$ is a subset of $\mathcal{B}_{2d}^{=}$, or – if not – if it is a subset of $\mathcal{B}_2^{=}$ is still open.

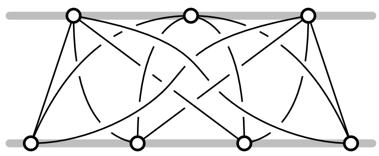

Fig. 7.76: A 2-layer 2-gap-planar drawing of $K_{3,4}$.

7.8.18 Overview

Oriented on Table 4 in *A Survey on Graph Drawing Beyond Planarity* by Didimo et al. [61] we present a corresponding table for 2-layer graphs in Fig. 7.77. In Fig. 7.78 we also provide an illustration which shows the relationships between the graph classes $\mathcal{P}_1^{=}$, $\mathcal{P}_2^{=}$, $\mathcal{Q}_3^{=}$, $\mathcal{Q}_4^{=}$, $\mathcal{F}^{=}$, $\mathcal{X}^{=}$, $\mathcal{B}_1^{=}$, $\mathcal{B}_{2d}^{=}$ and $\mathcal{B}_2^{=}$. Figure 7.78 does not include the classes $\mathcal{G}_k^{=}$, since we could not determine the relationship between them and the other graph classes well enough.

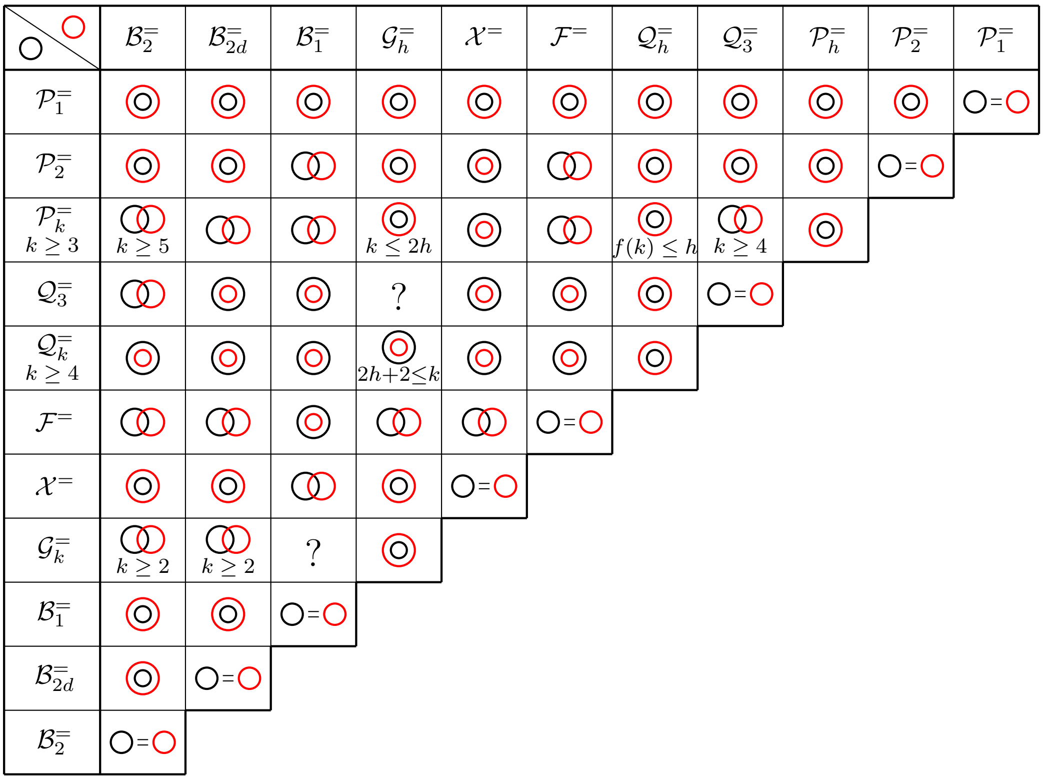

Fig. 7.77: Overview over the relationships between different 2-layer graph classes. If not specified otherwise, we assume $h \geq k$. The black and red circles represent the corresponding classes in the leftmost column and topmost row. The function f is defined by $f(k) = \frac{2}{3}k + 2$.

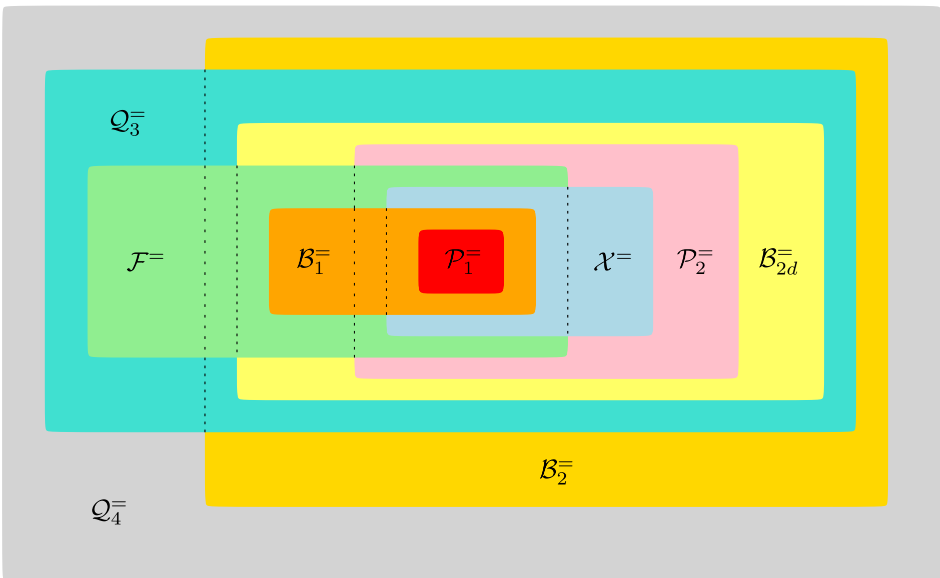

Fig. 7.78: Inclusion relationships between certain 2-layer graph classes. We also illustrate these relationships (in a different way) in Chapter 8; refer to Fig. 8.2.

7.9 Conclusion and Open Problems

In this chapter we proved tight edge density bounds for various 2-layer graph classes. Regarding 2-layer 2-sided fanbundle-planar graphs, we were able to improve the bound stated by Angelini et al. in [13].

Since our upper bound for 2-layer k-quasi-planar graphs is $(k-1)(n-3)+2$, while the lower bound construction consists of a graph family with n vertices and only $(k-1)n-(k-1)^2$ edges, the bound is not tight for $k > 3$. So we ask if it is possible to close the gap between the two values.

For 2-layer k-gap-planar graphs, where $k > 1$, we have no construction which provides a lower bound for the edge density; on the other hand, the upper bound is a consequence of the Crossing Lemma and cannot be expected to be tight. Therefore an interesting task for future research would be to prove better upper bounds for these graph classes and also find some lower bound construction.

In Sec. 7.4.1 we gave an example for a maximal 2-layer 2-planar drawing that has not the optimal number of edges. Namely, it only has $n+1$ edges, while the optimal number of edges is $\frac{5}{3}n-\frac{7}{3}$. We ask if this is the sparsest maximal drawing (or graph) in this graph class, that is, the maximal drawing (graph) with the smallest number of edges among all maximal drawings with n vertices. More general, we ask for sparsest maximal drawings (graphs) for all 2-layer graph classes.

As last point for the edge densities we remark that, if one can prove upper bounds for the number of edges in 2-layer 6-planar graphs, then at the same time the Crossing Lemma (refer to Cor. 7.33), as well as the general bounds for 2-layer k-planar and 2-layer k-gap-planar graphs (refer to Cors. 7.34 and 7.35), are improved.

We used the new edge density bounds to derive characterizations for complete bipartite graphs for several 2-layer graph classes. Thereby the characterization for k-gap-planar graphs, where $k \geq 2$, is missing. We suggest this problem as a future research direction.

With the help of the aforementioned results we derived inclusion relationships between various graph classes. However, there are still some questions open in this field. Especially we ask the following:

– Is every 2-layer 1-gap-planar graph also 2-layer 3-quasi-planar?

– Are 2-layer 3- and 4-planar graphs 2-layer 2-sided fanbundle-planar?

– Is the class of 2-layer k-gap-planar graphs a subclass of the 2-layer $(2k+1)$-quasi-planar graphs?

- Is every 2-layer 1-sided fanbundle-planar graph k-gap-planar for some $k \geq 1$?
- Is the class of 2-layer 1-gap-planar graphs $\mathcal{G}_1^=$ a subclass of the 2d-layer 2-sided fanbundle-planar graphs? And if not, is $\mathcal{G}_1^=$ a subclass of the 2-layer 2-sided fanbundle-planar graphs?

Answers to these questions will help in understanding better the relations between different graph classes, and are therefore of interest for the graph drawing community.

We conclude by the following observation. Beside the commonly studied classes of k-planar graphs (where $k \geq 1$), k-quasi-planar graphs (where $k \geq 3$) and k-gap-planar graphs (where $k \geq 1$), results have been proven for the general edge density of k-fan-crossing free graphs (where $k \geq 2$) [50].[14] Moreover, there exists the definition of k-fanbundle-planar graphs (for $k \geq 1$), where a fanbundle may cross at most k other fanbundles [13]. However, the k-fan-crossing free graphs have not been studied in the 2-layer setting for $k \geq 3$, and the k-fanbundle-planar graphs have not been studied at all for $k \geq 2$. Another generalization that never has been considered (as far as we know) is the one of k-fan-planar graphs (for $k \geq 2$), where an edge may cross at most k fans. All three families, the k-fan-crossing graphs, the k-fanbundle-planar graphs, and the k-fan-planar graphs, are interesting for future research – both, in the 2-layer and the general setting.

[14] A drawing is k-fan-crossing free, if no edge crosses a fan consisting of k edge, i. e. a set of k edges that all have a common end vertex.

Chapter 8

Conclusion and Open Problems

In this work we provided several new parameters for graphs and graph drawing, which are important indicators for the potential of graph classes, and measures regarding the human perception of drawn graphs.

In Chapter 4 we studied how the maximal vertex degree of a graph guarantees its membership in certain graph classes.

Namely, we showed that every graph with maximal vertex degree 3 is fan-crossing free by describing a corresponding drawing algorithm. On the other hand, not every graph of degree 5 is a member of the class of fan-crossing free graphs, since the complete bipartite graph $K_{5,5}$ does not belong to it. This leads immediately to the question whether all graphs of degree 4 are fan-crossing free.

With a lengthy proof using an enumeration technique, we not only showed that $K_{5,5}$ is not a member of the class of fan-crossing free graphs, but also that $K_{3,7}$ is not fan-crossing free. Together with the fact that $K_{2,b}$ (where $b > 0$) is planar and a corresponding certificate drawing of $K_{4,6}$, this yielded a characterization for complete bipartite fan-crossing free graphs.

We also showed that there are Hamiltonian bipartite graphs of degree 3 which are neither k-planar, nor fan-planar, nor k-gap-planar. To this end we considered the cube-connected cycles CCC_n which are 3-regular but do not belong to any of the three mentioned classes as their number of edges exceeds the number of edges allowed in these classes (for n large enough).

However, the question if a maximum degree d for all vertices of a graph guarantees its membership in a certain graph class remains open for $d > 2$ in most cases. In particular, it is unknown if all degree-3 graphs are RAC, even though degree-3 graphs are fan-crossing free and quasi-planar – both are necessary conditions for a graph to be RAC.

An overview of our findings and the state of the art can be found in Table 4.1, which is repeated in Table 8.1 for the readers convenience.

Table 8.1: The largest known value d_ℓ such that all graphs of degree $d \leq d_\ell$ belong to the indicated graph class $\mathcal{C}$, and the smallest value d_u where a graph is known that does not belong to $\mathcal{C}$ (refer to Chapter 4).

graph class $\mathcal{C}$	d_ℓ		d_u	
k-planar Hamiltonian bipartite	2		3	(CCC_n, Cor. 4.2)
fan-planar Hamiltonian bipartite	2		3	(CCC_n, Cor. 4.3)
k-gap-planar Hamiltonian bipartite	2		3	(CCC_n, Thm. 4.1)
quasi-planar	4	[8]	10	(K_{11}, ref. [4])
RAC (0-bend)	2		4	($K_{4,4}$, ref. [58])
RAC (0-bend) Hamiltonian	3	[22]	4	($K_{4,4}$, ref. [58])
RAC 1-bend	3	[18]	9	(K_{10}, ref. [10])
RAC 2-bends	6	[18]	148	(K_{149}, ref. [24])
fan-crossing free	3	(Thm. 4.4)	5	($K_{5,5}$, Thm. 4.5)

In Chapter 5 we addressed the question which complete and complete bipartite graphs belong to certain graph classes beyond-planarity. More precisely, given a graph class $\mathcal{C}$, our goal was it to find the largest n, such that K_n belongs to $\mathcal{C}$ and K_{n+1} does not, and to find values a, b, such that $K_{a,b}$ belongs to $\mathcal{C}$ while $K_{a,b+1}$ does not. This task usually involves large case analyses; therefore we developed an efficient algorithm to support the corresponding extensive analysis. The two main steps of the algorithm are the insertion of a new vertex – in all possible ways such that the properties of class $\mathcal{C}$ are respected – into every drawing of a complete or complete bipartite graph, and the elimination of isomorphic drawings.

We implemented our algorithm and applied it to several important graph classes, yielding characterizations for them, or at least certificate drawings, if very long running times did not allow for characterizations. We refer to Table 8.2 for an overview of the state of the art including our results. Corresponding references to the literature and to our results can be found in Tables 5.1 and 5.2 (note that the results for complete bipartite 6-planar graphs are a consequence of [13] and of the results for corresponding 5-planar graphs).

Our results also answered some questions stated in other works. Angelini et al. [14] conjectured that $K_{5,5}$ is not fan-planar, which we could answer in the positive (refer to Char. 5.9). Moreover, the graph $K_{5,5}$ is gap-planar (Obs. 5.13), but not fan-planar (Char. 5.9), while the graph $K_{4,9}$ is fan-planar but not gap-planar. This shows that the classes of fan-planar and gap-planar graphs are incomparable, answering a question posted in [30].

Table 8.2: Overview over the state of the art for (partial) characterizations regarding complete and complete bipartite graphs of several graph classes (refer to Chapter 5). We present the largest n (first entry in the tuple) such that K_n belongs to a class, and the smallest n (second entry in the tuple) such that K_n does not belong to the corresponding class. Moreover, for complete bipartite graphs $K_{a,b}$, where $a \leq b$ and $3 \leq a \leq 7$, we present the largest known value for b such that $K_{a,b}$ belongs to a graph class (first entry in the tuple), and the smallest known value for b such that $K_{a,b}$ does not belong to it (second entry in the tuple). If no drawing exists for $b \geq a$, the corresponding entry is "–". Question marks indicate that we don't know a value for b such that $K_{a,b}$ belongs to the considered class.

	complete	complete bipartite				
Class		$a = 3$	$a = 4$	$a = 5$	$a = 6$	$a = 7$
IC-planar	(5,6)	(3,4)	–	–	–	–
NIC-planar	(5,6)	(4,5)	–	–	–	–
1-planar	(6,7)	(6,7)	(4,5)	–	–	–
2-planar	(7,8)	(10,11)	(6,7)	–	–	–
3-planar	(8,9)	(14,15)	(9,10)	(6,7)	–	–
4-planar	(9,10)	(18,19)	(11,19)	(8,19)	(6,19)	(?,19)
5-planar	(9,10)	(22,23)	(11,23)	(8,23)	(7,23)	(?,23)
6-planar	(10,20)	(26,27)	(11,27)	(8,27)	(7,27)	(?,27)
fan-planar fan-crossing	(7,8)	(∞,$\emptyset$)	(∞,$\emptyset$)	–	–	–
fan-cr. free	(6,7)	(6,7)	(6,7)	–	–	–
gap-planar	(8,9)	(12,14)	(8,9)	(6,7)	–	–
RAC	(5,6)	(4,5)	–	–	–	–
quasi-planar	(10,11)	(∞,$\emptyset$)	(∞,$\emptyset$)	(18,?)	(10,?)	(7,52)

A main problem of our implementation is that it fails to derive characterizations e. g. for complete k-planar graphs if $k \geq 6$, and for complete bipartite k-planar graphs if $k \geq 4$. Using multi-threading might accelerate our implementation. However, we were not able to develop an idea in this direction, since with multi-threading it becomes very difficult to execute the isomorphism test efficiently. We pose the question if it is possible to overcome this difficulty. In general, is it possible to improve our algorithm or implementation, such that characterizations for more graph classes regarding complete and complete bipartite graphs can be obtained? Is it possible to also apply our algorithm to graphs which are less symmetric, e. g. to tripartite graphs, such that a result can be found within a reasonable time?

Regarding k-planar graphs, Angelini et al.[13] gave a characterization for $K_{3,b}$. Namely, the graph $K_{3,b}$ is k-planar if and only if $b \leq 4k + 2$. Inspired by this result, we state the question if there exist corresponding characterizations for $K_{a,b}$ when $a > 3$? In particular, are the graphs $K_{4,3k}$, $K_{5,2k}$ and $K_{6,k+2}$ k-planar for $k \geq 3$, and the graphs $K_{4,3k+1}$, $K_{5,2k+1}$ and $K_{6,k+3}$ not, as might be conjectured by Fig. 5.19?

In Chapter 6 we provided a generalized version of the well-known Crossing Lemma and used it to prove Meta Theorems for the maximal number of edges in k-planar and in k-gap-planar graphs. Using these theorems we showed that general outer-k-planar graphs (where $k \geq 2$) can have at most $2.924\sqrt{k}n$ edges, and that bipartite k-gap-planar graphs (where $k \geq 1$) have at most $4.25\sqrt{k}n$ edges. The latter implies that the number of edges in bipartite 1-gap-planar graphs is upper bounded by $4.25n$; we showed that this bound can be improved to $4n - 8$ under certain assumptions. On the other hand, we gave a lower bound construction for bipartite 1-gap-planar graphs containing $4n-16$ edges. We conjecture that the edge density of these graphs is between $4n - 8$ and $4n - 16$, even when dropping the special assumptions.

Further, outer-1-gap-planar graphs have at most $3n - 5$ edges (see Thm. 6.13), while our lower bound construction shows that the edge density of this class cannot be less then $3n - 6$. This gives rise to the question, which of the two formulas is the true edge density, either $3n - 5$ or $3n - 6$.

Our final question regarding the Meta Theorems is the following: Beside the applications mentioned above (and the one in Chapter 7), are there more cases where they, or similar Meta Theorems, are of interest?

The 2-layer setting, where vertices are placed on two parallel horizontal lines and the edges are (usually straight-line) y-monotonic curves, was studied in Chapter 7. This chapter consists of three main parts.

Table 8.3: Lower and upper bounds on the maximal number of edges in 2-layer drawings for several graph classes (refer to Chapter 7). The general bound for k-planar graphs is valid for $k \geq 6$. For quasi-planar graphs, the upper bound holds for $k \geq 3$ and $n \geq 3$, while the lower bound holds for $k \geq 3$ and sufficiently large n. For k-gap-planar drawings the general bound is valid for $k \geq 2$.

Class	Lower Bound	Reference	Upper Bound	Reference
planar	$n-1$	[77]	$n-1$	[77]
1-planar	$\frac{3}{2}n-2$	[57]	$\frac{3}{2}n-2$	[57]
2-planar	$\frac{5}{3}n-\frac{7}{3}$	Thm. 7.15	$\frac{5}{3}n-\frac{7}{3}$	Thm. 7.15
3-planar	$2n-4$	Thm. 7.17	$2n-4$	Thm. 7.19
4-planar	$2n-3$	Thm. 7.20	$2n-3$	Thm. 7.23
5-planar	$\frac{9}{4}n-\frac{9}{2}$	Thm. 7.25	$\frac{9}{4}n-\frac{9}{2}$	Thm. 7.31
6-planar	$\frac{5}{2}n-6$	Thm. 7.32	$3.19n$	Cor. 7.34
k-planar	$\frac{\lfloor\sqrt{k}\rfloor+2}{2}n-\mathcal{O}(\sqrt{k})$	Thm. 7.36	$\frac{125}{96}\sqrt{k}n$	Cor. 7.34
IC-planar	$\frac{5}{4}n-1$	Thm. 7.7	$\frac{5}{4}n-1$	Thm. 7.9
NIC-planar	$\frac{4}{3}n-\frac{4}{3}$	Thm. 7.7	$\frac{4}{3}n-\frac{4}{3}$	Thm. 7.10
k-quasi-planar	$(k-1)n-(k-1)^2$	Thm. 7.6	$(k-1)(n-3)+2$	Thm. 7.4
fan-planar	$2n-4$	[39]	$2n-4$	[39]
fan-crossing	$2n-4$	Obs. 7.2	$2n-4$	Obs. 7.2
fan-cr. free	$\frac{3}{2}n-2$	Obs. 7.1	$\frac{3}{2}n-2$	Obs. 7.1
gap-planar	$2n-4$	Thm. 7.37	$2n-4$	Thm. 7.41
k-gap-planar	$2n-4$	Thm. 7.37	$\frac{125}{48\sqrt{2}}\sqrt{k}n$	Cor. 7.35
1-sided 1-fbp	$\frac{5}{3}n-\frac{7}{3}$	[13]	$\frac{5}{3}n-\frac{7}{3}$	[13]
2d-layer 2-sided 1-fbp	$2n-4$	[13]	$2n-4$	Thm. 7.42
2-sided 1-fbp	$\frac{17}{8}n-\frac{13}{4}$	Thm. 7.44	$\frac{17}{8}n-\frac{13}{4}$	Thm. 7.47
RAC	$\frac{3}{2}n-2$	[56]	$\frac{3}{2}n-2$	[56]

In the first part, edge densities were proved for the classes of k-quasi-planar, IC-planar, NIC-planar, k-planar, gap-planar and fanbundle-planar graphs; refer to Table 7.1, which is, for the readers convenience, again shown in Table 8.3.

For k-quasi-planar graphs we improved the upper bound of $(k-1)(n-1)$ [137] edges to $(k-1)(n-3)+2$ and gave a lower bound construction with $(k-1)n-(k-1)^2$ edges. This yields a tight bound of $2n-4$ edges for $k=3$. We conjecture that $(k-1)n-(k-1)^2$ is in fact also an upper bound on the number of edges in 2-layer k-planar graphs.

We further remark that also our tight upper bounds on the number of edges in 2-layer 2-sided fanbundle-planar and 2d-layer 2-sided fanbundle-planar graphs present an improvement of known results; refer to Angelini et al. [13].

Since, in case of $k > 1$, the upper bound on the number of edges in 2-layer k-gap-planar graphs stems from the Meta Theorem of Chapter 6, it cannot be expected to be tight. Thus, an interesting problem is to find such a tight bound for general k.

Other consequences of the Meta Crossing Lemma were a Crossing Lemma tailored for 2-layer graphs, stating that every drawing of such a graph has at least $0.295\frac{m^3}{n^2}$ crossings, and a general upper bound of $\frac{125}{96}\sqrt{k}n$ edges for 2-layer k-planar graphs when $k \geq 6$. Both results can be improved if a tight edge density bound for 2-layer 6-planar graphs is found.

For 2-layer 2-planar graphs we provided a maximal drawing Γ with $n + 1$ edges. Since an optimal 2-layer 2-planar graph possesses $\frac{5}{3}n - 73$ edges, Γ is not optimal. An interesting question is if Γ is the sparsest maximal drawing, or if there exists a maximal 2-layer 2-planar planar with n edges or less.[1] More generally: How many edges do the sparsest maximal 2-layer drawings (or graphs) have for the different graph classes?

In the second part of Chapter 7, we characterized complete bipartite graphs in the 2-layer setting for the aforementioned graph classes (refer to Table 7.2, again shown in Table 8.4). However, for k-gap-planar graphs, where $k \geq 2$, we could not provide such a characterization. So this might be an interesting problem for future research.

In the final part of Chapter 7, the inclusion relationships between different 2-layer graph classes were studied extensively. To some extent using the results from the first two parts, we were able to reveal many such relations; refer to Figs. 7.77 and 7.78 in Chapter 7 and to Fig. 8.2.

An important result is that every 2-layer k-planar graph is 2-layer $f(k)$-quasi-planar, where $f(k) = \lceil \frac{2}{3}k + 2 \rceil$ is a function in k. The question if such a function f exists was asked in [11] for general graphs; by our result we can answer it in the positive at least for the 2-layer setting.

We were able to show that the 2-layer 1-planar graphs belong to all other graph classes discussed in Chapter 7, and that the 2-layer 2-planar graphs belong to almost all those classes, except three. Namely, the class of 2-layer 2-planar graphs is incomparable to the one of 2-layer 1-sided fanbundle-planar and to the one of 2-layer fan-planar graphs, while the 2-layer fan-crossing free graphs are contained in it. Hence, the class of 2-layer fan-crossing free graphs (which coincides with the class of 2-layer RAC graphs) lies "between" the 2-layer 1-planar and 2-layer 2-planar graphs.

[1] Note that 2-layer planar drawings have $n - 1$ edges, thus the number of edges of Γ is "close" the the number of edges 2-layer planar drawings have at most.

Table 8.4: Characterizations for complete bipartite graphs $K_{a,b}$ (where $a \leq b$) in 2-layer drawings for several graph classes (refer to Chapter 7). Stated are values for b, given $a = 2$, $a = 3$, and $a \geq 4$. If no drawing exists for $b \geq a$, the corresponding entry is "–" (in words: minus). Question marks indicate that the characterization is still open.

Class	$a = 2$	$a = 3$	$a \geq 4$
1-planar	$b \leq 2$	–	–
2-planar	$b \leq 3$	–	–
3-planar	$b \leq 4$	–	–
4-planar	$b \leq 5$	$b \leq 3$	–
5-planar	$b \leq 6$	$b \leq 3$	–
k-planar	$b \leq 1 + k$	$b \leq 1 + \frac{k}{2}$	$b \leq 1 + \frac{k}{a-1}$
IC-planar	$b \leq 2$	–	–
NIC-planar	$b \leq 2$	–	–
3-quasi-planar	all b	–	–
4-quasi-planar	all b	all b	–
fan-planar	all b	–	–
fan-cr. free	$b \leq 2$	–	–
1-gap-planar	$b \leq 4$	–	–
k-gap-planar	$b \leq 2k + 2$?	?	?
1-sided 1-fbp	$b \leq 3$	–	–
2-sided 1-fbp	$b \leq 8$	$b \leq 3$	–
2d-layer 2-sided 1-fbp	$b \leq 6$	–	–

By Bae et al. [30], the class of $(2k)$-planar graphs is a proper subclass of the k-gap-planar graphs, and the latter is a proper subclass of the $(2k + 2)$-quasi-planar. We proved that these inclusion relationships also hold for 2-layer graphs.

In general, the class of 2-layer quasi-planar graphs contains most of the classes studied in Chapter 7, except the classes of 2-layer 2-sided fanbundle-planar graphs and 2-layer k-planar graphs when $k > 2$ (and, of course, k-quasi-planar graphs for $k > 3$). Also the relationship between 2-layer quasi-planar and 2-layer gap-planar graphs is still open.

Regarding fanbundle-planar graphs, we realized that there are two different drawing styles in the 2-layer setting: One, where bundles anchored at vertices of different layers may cross, and one where this is not allowed (we called them 2d-layer 2-sided fan-bundle planar graphs). We showed that the former are incomparable to 2-layer quasi-planar graphs, while the latter are contained in the class of 2-layer quasi-

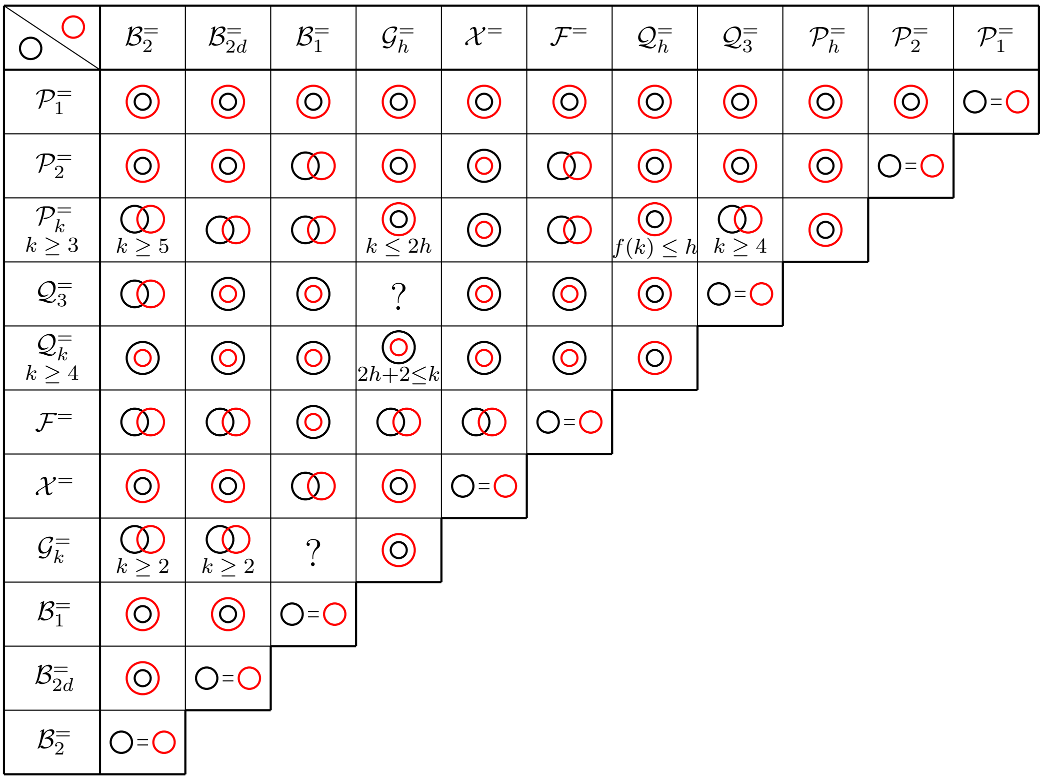

Fig. 8.1: Overview over the relationships between different 2-layer graph classes. If not specified otherwise, we assume $h \geq k$. The black circle symbolizes the classes of the left column in the table, while the red circle represents the classes of the top row in the table. The function $f(k)$ is defined by $f(k) = \lceil \frac{2}{3}k + 2 \rceil$.

planar graphs. Considering the relations between the different fanbundle-planar types, we recognized that 2-layer 1-sided fanbundle-planar graphs are a subclass of 2d-layer 2-sided fanbundle-planar graphs, and, on the other hand, 2d-layer 2-sided fanbundle-planar graphs are a subclass of 2-layer 2-sided fanbundle-planar graphs.

For our other results concerning the relationships between different 2-layer graph classes we refer to Figs. 8.1 and 8.2.

Open questions regarding these relationships are:

- Is every 2-layer 1-gap-planar graph also 2-layer 3-quasi-planar?
- Are 2-layer 3- and 4-planar graphs 2-layer 2-sided fanbundle-planar?
- Is the class of 2-layer k-gap-planar graphs a subclass of the 2-layer $(2k+1)$-quasi-planar graphs?
- Is every 2-layer 1-sided fanbundle-planar graph k-gap-planar for some $k \geq 1$?
- Is the class of 2-layer 1-gap-planar graphs a subclass of the 2d-layer 2-sided fanbundle-planar graphs? And if not, is the class of 2-layer 1-gap-planar graphs a subclass of the 2-layer 2-sided fanbundle-planar graphs?

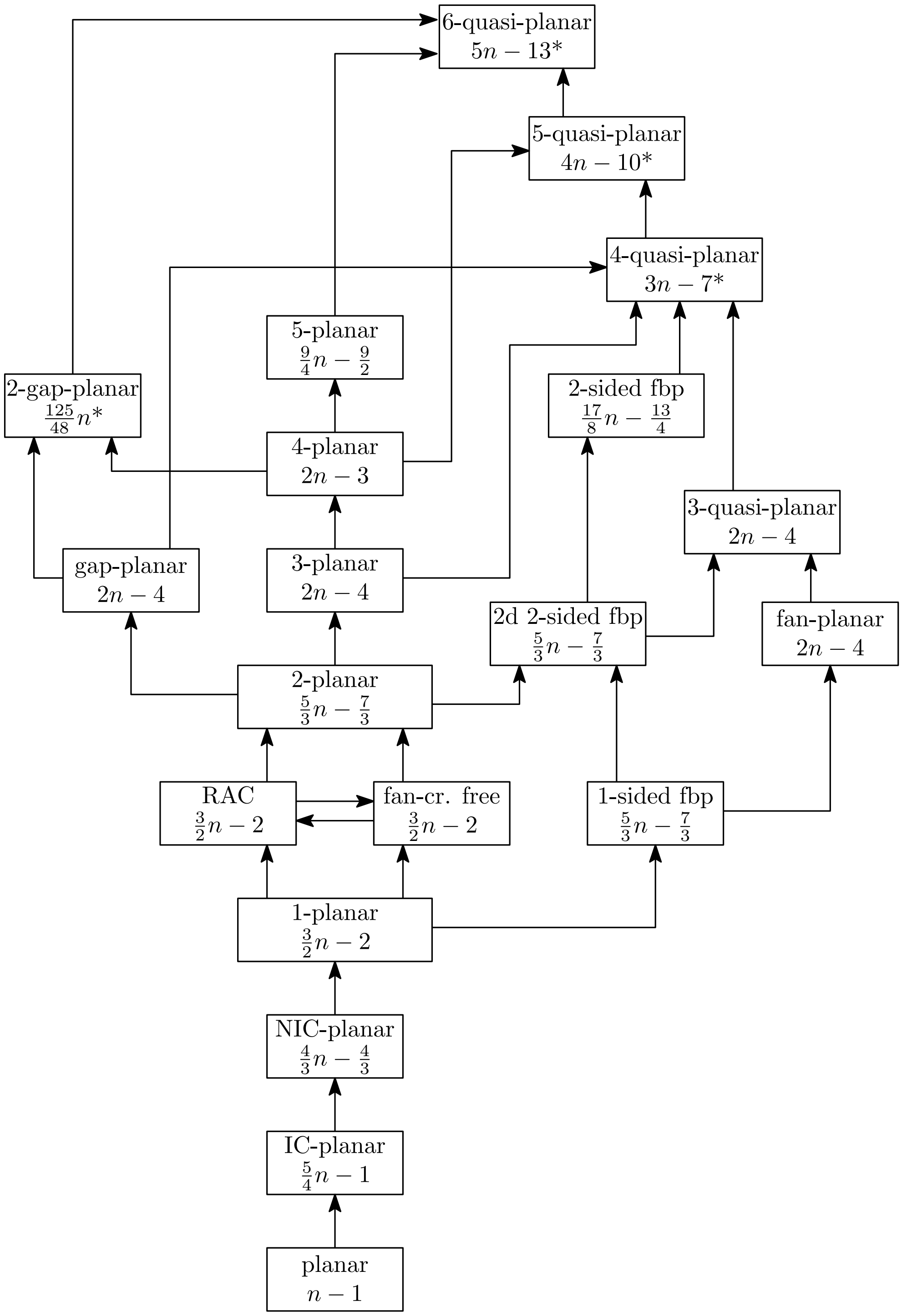

Fig. 8.2: The inclusion relationships between certain 2-layer graph classes. The edge densities are given as well. A star indicates that the bound might not be tight.

We conclude with our results from Chapter 3, where grid-drawings of trees with few segments were considered.

Hültenschmidt et al. [89] showed that every tree can be drawn on a grid of size $\mathcal{O}(n^{3.58})$ using at most $\frac{3}{4}n - 1$ segments. We improved the area requirement to $n \times n = \mathcal{O}(n^2)$, while preserving the upper bound on the number of segments. To this end, we described a linear-time algorithm which can solve this task. Our algorithm first reduces the given tree by contracting degree-2 vertices, and then removes the leaves of the resulting tree (refer to Fig. 8.3, which is a copy of Fig. 3.1). Finally the tree is drawn recursively, such that each subtree is placed inside a box and no vertex of the subtree is to the top left of its root – which is the key to draw the edge from the root to the parent vertex of the root.

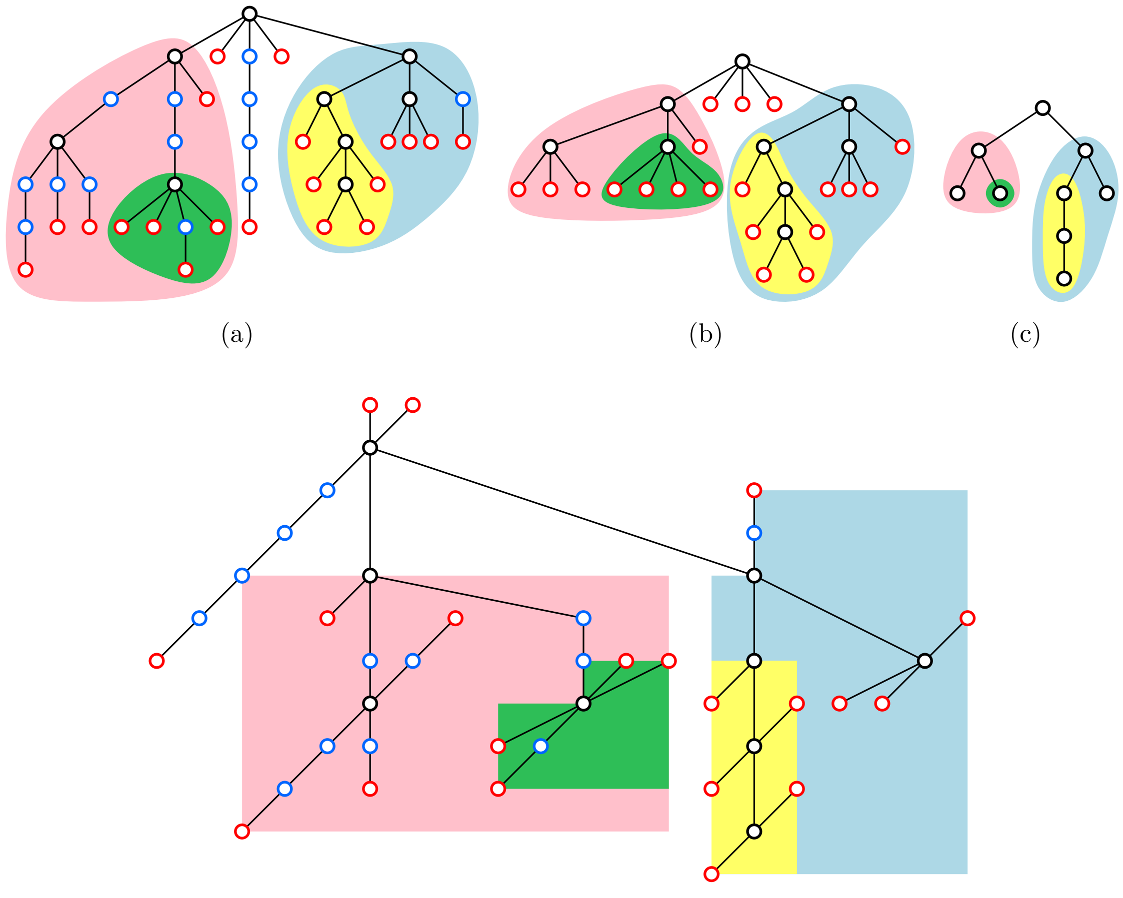

(a) (b) (c)

(d)

Fig. 8.3: Illustration for the different steps of our tree drawing algorithm. (a) A tree T. Degree-2 vertices are blue and leaves are red. (b) The tree T', where all degree-2 vertices from T are contracted. (c) The tree T'', where all leaves from T' are removed. (d) The drawing our algorithm produces.

The question remains open if the area of $n \times n$ is optimal for trees when using at most $\frac{3}{4}n - 1$ segments, or if a smaller grid size is possible. The latter would also be an interesting question if a slightly larger number of segments is allowed.

Altogether, we were able to provide many new parameters for various graph classes that help to understand better the properties and limitations of graphs belonging to these classes. However, the considerations above show that there are still many open problems, whose addressing might be interesting for future research.

Bibliography

[1] B. M. Ábrego, O. Aichholzer, S. Fernández-Merchant, T. Hackl, J. Pammer, A. Pilz, P. Ramos, G. Salazar, and B. Vogtenhuber. All good drawings of small complete graphs. In *EuroCG*, pages 57–60, 2015.

[2] E. Ackerman. On the maximum number of edges in topological graphs with no four pairwise crossing edges. *Disc. Comput. Geom.*, 41(3):365–375, 2009.

[3] E. Ackerman. On topological graphs with at most four crossings per edge. *CoRR*, abs/1509.01932, 2015.

[4] E. Ackerman and G. Tardos. On the maximum number of edges in quasi-planar graphs. *JCTA*, 114(3):563–571, 2007.

[5] P. K. Agarwal, B. Aronov, J. Pach, R. Pollack, and M. Sharir. Quasi-planar graphs have a linear number of edges. *Combinatorica*, 17(1):1–9, 1997.

[6] M. Aigner and G. M. Ziegler. *Proofs from THE BOOK (3rd. ed.)*. Springer, 2004.

[7] M. Ajtai, V. Chvátal, M. Newborn, and E. Szemerédi. Crossing-free subgraphs. In P. L. Hammer, A. Rosa, G. Sabidussi, and J. Turgeon, editors, *Theory and Practice of Combinatorics*, volume 60 of *North-Holland Mathematics Studies*, pages 9–12. North-Holland, 1982.

[8] M. J. Alam, K. Hanauer, S.-H. Hong, S. G. Kobourov, Q. Nguyen, S. Pupyrev, and M. S. Rahman. Working group B2: Beyond-planarity of graphs with bounded degree. In S.-H. Hong, M. Kaufmann, S. G. Kobourov, and J. Pach, editors, *Beyond-Planar Graphs: Algorithmics and Combinatorics (Dagstuhl Seminar 16452)*, volume 6 of *Dagstuhl Reports*, pages 55–56. Schloss Dagstuhl–Leibniz-Zentrum fuer Informatik, 2017.

[9] M. O. Albertson. Chromatic number, independence ratio, and crossing number. *Ars Math. Contemp.*, 1(1):1–6, 2008.

[10] P. Angelini, M. Bekos, H. Förster, and M. Kaufmann. On RAC drawings of graphs with one bend per edge. In *Graph Drawing and Network Visualization GD 2018*, 2018.

[11] P. Angelini, M. A. Bekos, F. J. Brandenburg, G. Da Lozzo, G. Di Battista, W. Didimo, M. Hoffmann, G. Liotta, F. Montecchiani, I. Rutter, and C. D. Tóth. Simple k-planar graphs are simple $(k + 1)$-quasiplanar. *Journal of Combinatorial Theory, Series B*, 142:1–35, 2020.

[12] P. Angelini, M. A. Bekos, F. J. Brandenburg, G. Da Lozzo, G. Di Battista, W. Didimo, G. Liotta, F. Montecchiani, and I. Rutter. On the relationship between k-planar and k-quasi planar graphs. In *WG*, volume 10520 of *LNCS*, pages 59–74. Springer, 2017.

[13] P. Angelini, M. A. Bekos, M. Kaufmann, P. Kindermann, and T. Schneck. 1-fan-bundle-planar drawings of graphs. *Theor. Comput. Sci.*, 723:23–50, 2018.

[14] P. Angelini, M. A. Bekos, M. Kaufmann, M. Pfister, and T. Ueckerdt. Beyond-planarity: Turán-type results for non-planar bipartite graphs. In *ISAAC*, volume 123 of *LIPIcs*, pages 28:1–28:13. Schloss Dagstuhl, 2018.

[15] P. Angelini, M. A. Bekos, M. Kaufmann, and T. Schneck. Low-degree graphs beyond planarity. In T. C. Biedl and A. Kerren, editors, *Graph Drawing and Network Visualization GD 2018*, volume 11282 of *Lecture Notes in Computer Science*, pages 630–632. Springer, 2018.

[16] P. Angelini, M. A. Bekos, M. Kaufmann, and T. Schneck. Efficient generation of different topological representations of graphs beyond-planarity. In D. Archambault and C. D. Tóth, editors, *Graph Drawing and Network Visualization GD 2019*, pages 253–267, Cham, 2019. Springer International Publishing.

[17] P. Angelini, M. A. Bekos, M. Kaufmann, and T. Schneck. Efficient generation of different topological representations of graphs beyond-planarity. *Journal of Graph Algorithms and Applications*, 2020.

[18] P. Angelini, L. Cittadini, W. Didimo, F. Frati, G. Di Battista, M. Kaufmann, and A. Symvonis. On the perspectives opened by right angle crossing drawings. *J. Graph Algorithms Appl.*, 15(1):53–78, 2011.

[19] P. Angelini, G. Da Lozzo, H. Förster, and T. Schneck. 2-layer k-planar graphs: Density, crossing lemma, relationships, and pathwidth. In *Graph Drawing and Network Visualization GD 2020*, Cham, 2020. Springer International Publishing. to appear.

[20] K. Appel and W. Haken. Every planar map is four colorable. part i: Discharging. *Illinois J. Math.*, 21(3):429–490, 09 1977.

[21] K. Appel, W. Haken, and J. Koch. Every planar map is four colorable. part ii: Reducibility. *Illinois J. Math.*, 21(3):491–567, 09 1977.

[22] E. N. Argyriou, M. A. Bekos, M. Kaufmann, and A. Symvonis. Geometric RAC simultaneous drawings of graphs. *J. Graph Algorithms Appl.*, 17(1):11–34, 2013.

[23] E. N. Argyriou, M. A. Bekos, and A. Symvonis. Maximizing the total resolution of graphs. *Comput. J.*, 56(7):887–900, 2013.

[24] K. Arikushi, R. Fulek, B. Keszegh, F. Moric, and C. D. Tóth. Graphs that admit right angle crossing drawings. *Comput. Geom.*, 45(4):169–177, 2012.

[25] A. Arleo, C. Binucci, E. Di Giacomo, W. S. Evans, L. Grilli, G. Liotta, H. Meijer, F. Montecchiani, S. Whitesides, and S. K. Wismath. Visibility representations of boxes in 2.5 dimensions. *Comput. Geom.*, 72:19–33, 2018.

[26] S. Aslan and B. Kaya. Time-aware link prediction based on strengthened projection in bipartite networks. *Information Sciences*, 506:217–233, 2020.

[27] A. S. Asratian, T. M. J. Denley, and R. Häggkvist. *Bipartite Graphs and their Applications*. Cambridge Tracts in Mathematics. Cambridge University Press, 1998.

[28] C. Auer, C. Bachmaier, F. J. Brandenburg, A. Gleißner, K. Hanauer, D. Neuwirth, and J. Reislhuber. Outer 1-planar graphs. *Algorithmica*, 74(4):1293–1320, 2016.

[29] C. Bachmaier, I. Rutter, and P. Stumpf. 1-gap planarity of complete bipartite graphs. In T. C. Biedl and A. Kerren, editors, *Graph Drawing and Network Visualization GD 2018*, volume 11282 of *LNCS*, pages 646–648. Springer, 2018.

[30] S. W. Bae, J. Baffier, J. Chun, P. Eades, K. Eickmeyer, L. Grilli, S. Hong, M. Korman, F. Montecchiani, I. Rutter, and C. D. Tóth. Gap-planar graphs. *TCS*, 745:36–52, 2018.

[31] F. Beck, R. Petkov, and S. Diehl. Visually exploring multi-dimensional code couplings. In *2011 6th International Workshop on Visualizing Software for Understanding and Analysis (VISSOFT)*, pages 1–8, 2011.

[32] M. A. Bekos, S. Cornelsen, L. Grilli, S. Hong, and M. Kaufmann. On the recognition of fan-planar and maximal outer-fan-planar graphs. *Algorithmica*, 79(2):401–427, 2017.

[33] M. A. Bekos, M. Kaufmann, and C. N. Raftopoulou. On Optimal 2- and 3-Planar Graphs. In B. Aronov and M. J. Katz, editors, *33rd International Symposium on Computational Geometry (SoCG 2017)*, volume 77 of *Leibniz*

International Proceedings in Informatics (LIPIcs), pages 16:1–16:16, Dagstuhl, Germany, 2017. Schloss Dagstuhl–Leibniz-Zentrum fuer Informatik.

[34] M. d. Berg, O. Cheong, M. v. Kreveld, and M. Overmars. *Computational Geometry: Algorithms and Applications.* Springer-Verlag TELOS, Santa Clara, CA, USA, 3rd ed. edition, 2008.

[35] S. Bhatt and F. Leighton. A framework for solving vlsi graph layout problems. *Journal of Computer and System Sciences*, 28:300–343, 02 2001.

[36] T. C. Biedl, S. Chaplick, J. Fiala, M. Kaufmann, F. Montecchiani, M. Nöllenburg, and C. N. Raftopoulou. On layered fan-planar graph drawings. *CoRR*, abs/2002.09597, 2020.

[37] N. Biggs, E. Lloyd, and R. Wilson. *Graph Theory, 1736-1936.* Clarendon Press, 1986.

[38] C. Binucci, M. Chimani, W. Didimo, M. Gronemann, K. Klein, J. Kratochvíl, F. Montecchiani, and I. G. Tollis. Algorithms and characterizations for 2-layer fan-planarity: From caterpillar to stegosaurus. *J. Graph Alg. Appl.*, 21(1):81–102, 2017.

[39] C. Binucci, E. Di Giacomo, W. Didimo, F. Montecchiani, M. Patrignani, A. Symvonis, and I. G. Tollis. Fan-planarity: Properties and complexity. *Theor. Comp. Sci.*, 589:76–86, 2015.

[40] R. Bodendiek, H. Schumacher, and K. Wagner. Über 1-optimale Graphen. *Math. Nachrichten*, 117(1):323–339, 1984.

[41] P. Bose, H. Everett, S. P. Fekete, M. E. Houle, A. Lubiw, H. Meijer, K. Romanik, G. Rote, T. C. Shermer, S. Whitesides, and C. Zelle. A visibility representation for graphs in three dimensions. *J. Graph Algorithms Appl.*, 2(2), 1998.

[42] F. J. Brandenburg. A simple quasi-planar drawing of K_{10}. In *Graph Drawing*, volume 9801 of *LNCS*, pages 603–604. Springer, 2016.

[43] F. J. Brandenburg. On fan-crossing graphs. *CoRR*, abs/1712.06840, 2017.

[44] F. J. Brandenburg. A first order logic definition of beyond-planar graphs. *J. Graph Algorithms Appl.*, 22(1):51–66, 2018.

[45] F. J. Brandenburg. On fan-crossing and fan-crossing free graphs. *Inf. Process. Lett.*, 138:67–71, 2018.

[46] G. Brinkmann, K. Coolsaet, J. Goedgebeur, and H. Mélot. House of graphs: A database of interesting graphs. *Discrete Applied Mathematics*, 161(1):311 – 314, 2013.

[47] T. Bruckdorfer, S. Cornelsen, C. Gutwenger, M. Kaufmann, F. Montecchiani, M. Nöllenburg, and A. Wolff. Progress on partial edge drawings. *J. Graph Algorithms Appl.*, 21(4):757–786, 2017.

[48] J. Cardinal and S. Felsner. Topological drawings of complete bipartite graphs. *JoCG*, 9(1):213–246, 2018.

[49] A. Cayley. On the theory of the analytical forms called trees. *The London, Edinburgh, and Dublin Philosophical Magazine and Journal of Science*, 13(85):172–176, 1857.

[50] O. Cheong, S. Har-Peled, H. Kim, and H. Kim. On the number of edges of fan-crossing free graphs. *Algorithmica*, 73(4):673–695, 2015.

[51] D. Constales, G. S. Yablonsky, D. R. D'hooge, J. W. Thybaut, and G. B. Marin. Chapter 3 - complex reactions: Kinetics and mechanisms - ordinary differential equations - graph theory. In D. Constales, G. S. Yablonsky, D. R. D'hooge, J. W. Thybaut, and G. B. Marin, editors, *Advanced Data Analysis & Modelling in Chemical Engineering*, pages 35–82. Elsevier, Amsterdam, 2017.

[52] T. H. Cormen, C. E. Leiserson, R. L. Rivest, and C. Stein. *Introduction To Algorithms.* MIT Press, 3 edition, 2009.

[53] J. Czap and D. Hudák. 1-planarity of complete multipartite graphs. *Disc. App. Math.*, 160(4-5):505–512, 2012.

[54] J. Czap, J. Przybyło, and E. Škrabul'áková. On an extremal problem in the class of bipartite 1-planar graphs. *Discussiones Mathematicae Graph Theory*, 36(1):141–151, 2016.

[55] E. Dekel and S. Sahni. A parallel matching algorithm for convex bipartite graphs and applications to scheduling. *Journal of Parallel and Distributed Computing*, 1(2):185–205, 1984.

[56] E. Di Giacomo, W. Didimo, P. Eades, and G. Liotta. 2-layer right angle crossing drawings. *Algorithmica*, 68(4):954–997, 2014.

[57] W. Didimo. Density of straight-line 1-planar graph drawings. *Inf. Process. Lett.*, 113(7):236–240, 2013.

[58] W. Didimo, P. Eades, and G. Liotta. A characterization of complete bipartite RAC graphs. *Inf. Process. Lett.*, 110(16):687–691, 2010.

[59] W. Didimo, P. Eades, and G. Liotta. Drawing graphs with right angle crossings. *Theor. Comp. Sci.*, 412(39):5156–5166, 2011.

[60] W. Didimo and G. Liotta. The crossing-angle resolution in graph drawing. In *Thirty Essays on Geometric Graph Theory*, pages 167–184. Springer, 2013.

[61] W. Didimo, G. Liotta, and F. Montecchiani. A survey on graph drawing beyond planarity. *ACM Comput. Surv.*, 52(1):4:1–4:37, Feb. 2019.

[62] V. Dujmović, D. Eppstein, M. Suderman, and D. R. Wood. Drawings of planar graphs with few slopes and segments. *Computational Geometry*, 38(3):194–212, 2007.

[63] S. Durocher and D. Mondal. Drawing plane triangulations with few segments. *Computational Geometry*, 77:27–39, 2019. Canadian Conference on Computational Geometry.

[64] P. Eades and G. Liotta. Right angle crossing graphs and 1-planarity. *Disc. Appl. Math.*, 161(7–8):961–969, 2013.

[65] P. Eades and N. C. Wormald. Edge crossings in drawings of bipartite graphs. *Algorithmica*, 11:379–403, 2005.

[66] D. Eppstein, P. Kindermann, S. G. Kobourov, G. Liotta, A. Lubiw, A. Maignan, D. Mondal, H. Vosoughpour, S. Whitesides, and S. K. Wismath. On the planar split thickness of graphs. *Algorithmica*, 80(3):977–994, 2018.

[67] P. Erdős and R. Guy. Crossing number problems. *The American Mathematical Monthly*, 80:52–58, 01 1973.

[68] L. Euler. *Solutio problematis ad geometriam situs pertinentis.* Comment. Acad. Sci. U. Petrop 8, 1736.

[69] W. Evans, M. Kaufmann, W. Lenhart, T. Mchedlidze, and S. K. Wismath. Bar 1-visibility graphs vs. other nearly planar graphs. *J. Graph Alg. Appl.*, 18(5):721–739, 2014.

[70] S. Even, A. Pnueli, and A. Lempel. Permutation graphs and transitive graphs. *Journal of the ACM (JACM)*, 19(3):400–410, 1972.

[71] J. Fox, J. Pach, and A. Suk. The number of edges in k-quasi-planar graphs. *SIAM J. Discrete Math.*, 27(1):550–561, 2013.

[72] E. Gioan. Complete graph drawings up to triangle mutations. In *WG*, volume 3787 of *LNCS*, pages 139–150. Springer, 2005.

[73] H.-D. O. Gronau and H. Harborth. Numbers of nonisomorphic drawings for small graphs. *Congressus Numerantium*, 71:105–114, 1990.

[74] R. Guy. *The Decline and Fall of Zarankiewicz's Theorem.* Research paper – University of Calgary, Department of Mathematics. University of Calgary, Department of Mathematics, 1968.

[75] R. K. Guy. A combinatorial problem. *Nabla (Bulletin of the Malayan Mathematical Society)*, 7:68–72, 1960.

[76] H. Hadwiger. Über eine Klassifikation der Streckenkomplexe. *Vierteljschr. Naturforsch. Ges. Zürich*, 88:133–143, 1943.

[77] F. Harary. A new crossing number for bipartite graphs. *Utilitas Math*, 1:203–209, 1972.

[78] F. Harary, J. P. Hayes, and H.-J. Wu. A survey of the theory of hypercube graphs. *Computers & Mathematics with Applications*, 15(4):277–289, 1988.

[79] F. Harary and E. M. Palmer. *Graphical enumeration.* Academic Press, 1973.

[80] F. Harary and I. C. Ross. A procedure for clique detection using the group matrix. *Sociometry*, 20(3):205–215, 1957.

[81] F. Harary and A. J. Schwenk. The number of caterpillars. *Discrete Mathematics*, 6(4):359 – 365, 1973.

[82] N. Hartsfield, B. Jackson, and G. Ringel. The splitting number of the complete graph. *Graphs and Combinatorics*, 1(1):311–329, 1985.

[83] P. J. Heawood. Map-colour theorem. *Quarterly Journal of Mathematics, Oxford*, 24:332–338, 1890.

[84] N. Henry Riche, A. Bezerianos, and J.-D. Fekete. Improving the readability of clustered social networks using node duplication. *IEEE Trans. Vis. Comput. Graph.*, 14:1317–1324, 01 2008.

[85] C. Hierholzer. Ueber die möglichkeit, einen linienzug ohne wiederholung und ohne unterbrechung zu umfahren. *Mathematische Annalen*, 6:30–32, 1873.

[86] M. Hoffmann and C. D. Tóth. Two-planar graphs are quasiplanar. In *MFCS*, volume 83 of *LIPIcs*, pages 47:1–47:14. Schloss Dagstuhl, 2017.

[87] S.-H. Hong, M. Kaufmann, S. G. Kobourov, and J. Pach. Beyond-Planar Graphs: Algorithmics and Combinatorics (Dagstuhl Seminar 16452). *Dagstuhl Reports*, 6(11):35–62, 2017.

[88] L. Hsu, T. Ho, Y. Ho, and C. Tsay. Cycles in cube-connected cycles graphs. *Discrete Applied Mathematics*, 167:163–171, 2014.

[89] G. Hültenschmidt, P. Kindermann, W. Meulemans, and A. Schulz. Drawing planar graphs with few geometric primitives. *Journal of Graph Algorithms and Applications*, 22(2):357–387, 2018.

[90] S. Irani and V. Leung. Scheduling with conflicts on bipartite and interval graphs. *J. Scheduling*, 6:287–307, 05 2003.

[91] M. Jünger and P. Mutzel. 2-layer straightline crossing minimization: Performance of exact and heuristic algorithms. *J. Graph Algorithms Appl.*, 1:1–25, 1997.

[92] S. Jänicke, J. Focht, and G. Scheuermann. Interactive visual profiling of musicians. *IEEE Transactions on Visualization and Computer Graphics*, 22(1):200–209, Jan 2016.

[93] M. Kaufmann and T. Ueckerdt. The density of fan-planar graphs. *CoRR*, 1403.6184, 2014.

[94] Z. Kehribar. $K_{5,5}$ kann nicht 2-planar gezeichnet werden: Analyse und Beweis, 2018. Bachelor Thesis, Universität Tübingen.

[95] P. Kindermann, T. Mchedlidze, T. Schneck, and A. Symvonis. Drawing planar graphs with few segments on a polynomial grid. In *Graph Drawing and Network Visualization GD 2019*, pages 416–429. Springer International Publishing, 2019.

[96] P. Kindermann, W. Meulemans, and A. Schulz. Experimental analysis of the accessibility of drawings with few segments. *Journal of Graph Algorithms and Applications*, 22(3):501–518, 2018.

[97] D. J. Kleitman. The crossing number of $k_{5,n}$. *Journal of Combinatorial Theory*, 9:315–323, 1971.

[98] S. G. Kobourov, T. Mchedlidze, and L. Vonessen. Gestalt principles in graph drawing. In *Graph Drawing and Network Visualization GD 2015*, pages 558–560. Springer International Publishing, 2015.

[99] J. Kynčl. Simple realizability of complete abstract topological graphs in P. *Disc. & Comp. Geom.*, 45(3):383–399, 2011.

[100] J. Kynčl. Improved enumeration of simple topological graphs. *Disc. & Comp. Geom.*, 50(3):727–770, 2013.

[101] F. Leighton. New lower bound techniques for vlsi. *NASA STI/Recon Technical Report N*, 83:19003, 07 1982.

[102] F. T. Leighton. *Complexity Issues in VLSI: Optimal Layouts for the Shuffle-exchange Graph and Other Networks.* MIT Press, Cambridge, MA, USA, 1983.

[103] R. D. Luce and A. D. Perry. A method of matrix analysis of group structure. *Psychometrika*, 14(2):95–116, 1949.

[104] D. MacKenzie. *Mechanizing Proof: Computing, Risk, and Trust.* Inside technology. MIT Press, 2004.

[105] J. Pach and P. K. Agarwal. *Computational Geometry*. John Wiley, New York, 1995.

[106] J. Pach, R. Radoičić, G. Tardos, and G. Tóth. Improving the crossing lemma by finding more crossings in sparse graphs. *DCG*, 36(4):527–552, 2006.

[107] J. Pach and M. Sharir. On the number of incidences between points and curves. *Combinatorics, Probability and Computing*, 7(1):121—127, 1998.

[108] J. Pach and G. Tóth. Graphs drawn with few crossings per edge. *Combinatorica*, 17(3):427–439, 1997.

[109] J. Pach and G. Tóth. How many ways can one draw a graph? *Combinatorica*, 26(5):559–576, 2006.

[110] H. E. Pence and A. Williams. ChemSpider: An Online Chemical Information Resource. *Journal of Chemical Education*, 87(11):1123–1124, Nov. 2010.

[111] J. Petersen. Die theorie der regulären graphs. *Acta Math.*, 15:193–220, 1891.

[112] M. Pfister. On the density of bipartite 3-planar graphs and its implications, 2020. Master Thesis, Universität Tübingen.

[113] A. Pnueli, A. Lempel, and S. Even. Transitive orientation of graphs and identification of permutation graphs. *Canadian Journal of Mathematics*, 23(1):160–175, 1971.

[114] G. Pólya. Kombinatorische anzahlbestimmungen für gruppen, graphen und chemische verbindungen. *Acta Math.*, 68:145–254, 1937.

[115] F. P. Preparata and J. Vuillemin. The cube-connected cycles: A versatile network for parallel computation. *Commun. ACM*, 24(5):300–309, 1981.

[116] H. C. Purchase. Which aesthetic has the greatest effect on human understanding? In *Proceedings of the 5th International Symposium on Graph Drawing*, GD '97, pages 248–261, Berlin, Heidelberg, 1997. Springer-Verlag.

[117] H. C. Purchase, R. F. Cohen, and M. James. Validating graph drawing aesthetics. In F. J. Brandenburg, editor, *Graph Drawing*, pages 435–446, Berlin, Heidelberg, 1996. Springer Berlin Heidelberg.

[118] N. H. Rafla. *The Good Drawings D_n of the Complete Graph K_n*. PhD thesis, McGill. University, Montreal, Quebec, 1988.

[119] J. H. Redfield. The theory of group-reduced distributions. *American Journal of Mathematics*, 49(3):433–455, 1927.

[120] J. H. Redfield. Enumeration by frame group and range groups. *Journal of Graph Theory*, 8(2):205–223, 1984.

[121] D. Richeson. *Euler's Gem: The Polyhedron Formula and the Birth of Topology.* Princeton University Press, 2012.

[122] G. Ringel. Ein Sechsfarbenproblem auf der Kugel. *Abh. Math. Sem. Univ. Hamb.*, 29:107–117, 1965.

[123] T. L. Saaty. The minimum number of intersections in complete graphs. *Proceedings of the National Academy of Sciences*, 52(3):688–690, 1964.

[124] N. Sangal, E. Jordan, V. Sinha, and D. Jackson. Using dependency models to manage software architecture. In *Companion to the 20th Annual ACM SIGPLAN Conference on Object-Oriented Programming, Systems, Languages, and Applications*, OOPSLA '05, pages 164–165, New York, NY, USA, 2005. Association for Computing Machinery.

[125] M. Schaefer. The graph crossing number and its variants: A survey (fourth edition. *Electr. J. Comb.*, 20:56–59, 04 2013.

[126] T. Schneck. Bundleplanar graphs, 2017. Master Thesis, Universität Tübingen.

[127] A. Schulz. Drawing graphs with few arcs. *Journal of Graph Algorithms and Applications*, 19(1):393–412, 2015.

[128] H. H. Seward. Information sorting in the application of electronic digital computers to business operations, 1954. Master Thesis, Report R-232, Massachusetts Institute of Technology.

[129] T. Spence. Ted spence's home page, 2020.

[130] J. Stola. 3d visibility representations of complete graphs. In *Graph Drawing*, volume 2912 of *LNCS*, pages 226–237. Springer, 2003.

[131] K. Sugiyama, S. Tagawa, and M. Toda. Methods for visual understanding of hierarchical system structures. *TSMC*, 11(2):109–125, 1981.

[132] O. Sýkora and I. Vrtó. On crossing numbers of hypercubes and cube connected cycles. *BIT*, 33:232–237, 1993.

[133] L. Székely. Crossing numbers and hard erdos problems in discrete geometry. *Combinatorics, Probability and Computing*, 6:353–358, 09 1997.

[134] R. Thomas. An update on the four-color theorem. *NOTICES AMER. MATH. SOC*, 45(7):848–859, 1998.

[135] A. Timmer and J. Jess. Exact scheduling strategies based on bipartite graph matching. In *Proceedings the European Design and Test Conference*, pages 42–47. IEEE Comput. Soc. Press, 04 1995.

[136] V. Valls, R. Marti, and P. Lino. A branch and bound algorithm for minimizing the number of crossing arcs in bipartite graphs. *European Journal of Operational Research*, 90:303–319, 02 1996.

[137] B. Walczak. Old and new challenges in coloring graphs with geometric representations. In D. Archambault and C. D. Tóth, editors, *Graph Drawing and Network Visualization GD 2019*, page xvi, Cham, 2019. Springer International Publishing.

[138] S. Wasserman, K. Faust, C. U. Press, M. Granovetter, U. of Cambridge, and D. Iacobucci. *Social Network Analysis: Methods and Applications*. Structural Analysis in the Social Sciences. Cambridge University Press, 1994.

[139] K. Zarankiewicz. On a problem of P. Turán concerning graphs. *Fundamenta Mathematicae*, 41:137–145, 1954.

[140] X. Zhang. Drawing complete multipartite graphs on the plane with restrictions on crossings. *Acta Mathematica Sinica, English Series*, 30(12):2045–2053, 2014.

[141] X. Zhang and G. Liu. The structure of plane graphs with independent crossings and its applications to coloring problems. *Central Eur. J. of Mathematics*, 11(2):308–321, 2013.